Composite Bridges

Innovative ways of achieving composite action

Robert Hällmark

Structural Engineering

LULEÅ
UNIVERSITY
OF TECHNOLOGY

Composite Bridges

Innovative ways of achieving composite action

ROBERT HÄLLMARK

Division of Structural and Fire Engineering – Structural Engineering
Department of Civil, Environmental and Natural Resources Engineering
Luleå University of Technology
971 87 Luleå, Sweden
www.ltu.se

Cover images: Photos of shear keys in a prefabricated deck element with dry joints and a Coiled Spring Pin (Robert Hällmark 2011 and 2017)

PREFACE

Inspired by Churchill, I would like to say that I really hope that this thesis is not the end and not even the beginning of the end, but perhaps the end of the beginning.

After a long and winding road, full of detours and different type of attractions along the roadside, I have finally reached the destination they call the dissertation. There have been moments of inspiration as well as perspiration, but now the thesis is written. A former professor at LTU once said that the outcome of the PhD studies is not a book, it is the development of an individual, who can go out in the industry and make use of the research. I believe he is right, and I hope that it is a better version of me that now returns to my ordinary work as a steel bridge specialist.

I would like to take the opportunity to thank the people who made this work come true.

First, I would like to thank my supervisor and friend Prof. Peter Collin, for giving me the opportunity to perform this research. It has been a pleasure to collaborate with you. A collaboration filled with fruitful discussions about bridges, stock market, philosophy and other important stuff. Your help, guidance and support have been very valuable to me. Thanks also to my assistant supervisors PhD Mikael Möller and Prof. Lennart Elfgren. The latter is basically the heart of the structural engineering group at LTU, a really big heart.

I would also like to thank my present colleagues at LTU and Trafikverket, and my former colleagues at Ramboll. Special thanks to my co-authors PhD Paul Jackson, Harry White, PhD Martin Nilsson and PhD Stephen Hicks, who has contributed with external input and ideas to improve the research. The project partners in the two European R&D-projects ELEM and PROLIFE should also be mentioned. I have really enjoyed our cooperation and I am looking forward to see you in future projects and alliances.

The staff at the MCE-Lab, especially Erik Andersson and Mats Petersson, deserve a big thanks for their work and for their positive attitude and friendly reception every time

you visit the lab. The tests campaigns had been impossible to perform without your expertise and assistance.

My great thanks to my family and friends for their support, help and belief in me. The list will be endless if I try to name every one of you that fill my life with joy and fruitful discussions.

Last but definitely not least, I would like to thank my beloved Alexandra for her love, patience and support, as well as our children Olivia and Oscar for bringing fun, warmth and happiness to my life.

To Olivia and Oscar:

This book is just a bunch of paper that daddy has written, and soon it will stand in a bookshelf collecting dust. You two are the total opposite, in constant development and always on the run, driven by curiosity to find out more about how things work. I hope your curiosity remains the same even when you are adults, and I truly wish that more adults had retained their curiosity as well. Primarily, since I believe that the world would be a better place if that were the case. Secondly, since I am of the opinion that research should be performed based on internal driving forces such as curiosity, not by external driving forces such as money, funding or academic titles.

Luleå, October 2018

Robert Hällmark

ACKNOWLEDGEMENT

SUMMARY

The topic of this thesis is steel-concrete composite bridges and innovative ways of achieving composite action. The typical superstructure consists of three main components: the steel girders, the concrete deck slab and the shear connectors. The latter connects the steel and the concrete parts to each other, which enables a design where the parts are assumed to act as one structural member, the composite beam.

The research presented in this thesis is primarily focused on different construction- and strengthening-methods, developed to reduce the impact on the road users, mainly by reducing the time spent on the construction site and the need of traffic restrictions.

The prefabricated steel girders give composite bridges some advantages in the construction stage, in comparison to the more common in-situ cast concrete bridges, since the girders can be launched or lifted into their final positions. Such an installation procedure is often favourable in case of crossings over roads, railways, rivers etc., since it minimizes the impact on the citizens using the infrastructure below the bridges and the need of temporary supports. In order to shorten the time spent on the construction site and to reduce the impact on the road users even more, prefabrication of the concrete deck can also be considered.

In this thesis, a review of different prefabrication techniques for composite bridges is presented, along with a study of one specific prefabrication concept that reduces the need of in-situ cast deck joints. This concept, with prefabricated concrete deck elements with dry joints, utilizes concrete shear keys to transfer shear forces over the transverse deck joints, while in-situ cast joints are used for the longitudinal connection between the steel girders and the concrete deck slab.

The structural behaviour of composite bridges with dry deck joints has been investigated by large scale beam tests, along with field measurements on a composite bridge built with this prefabrication concept. The load capacity of the shear keys has also been investigated by laboratory tests. The test results have been compared to numerical analyses and different design models, with the aim of developing design recommendations.

The results indicate that this type of bridges do not behave as conventional composite bridges with in-situ cast deck slabs. For single span bridges, which only experience positive bending moments, the structural behaviour in the ultimate limit state is close to the structural behaviour of conventional composite bridges. However, the degree of composite action is strongly reduced at lower load levels. This should be taken into account in the design in the fatigue- and the serviceability-limit states. Sections under negative bending moments behave in general as non-composite sections, which was expected due to the dry deck joints.

Based on the evaluation of the test results and the state-of-the-art review, design recommendations and design criteria are presented, along with production and execution recommendations for this type of prefabricated bridges.

Strengthening of existing bridges is another activity that often leads to traffic restrictions, which causes costs and troubles for the road users and the society. One method for strengthening non-composite steel-concrete bridges is post-installation of shear connectors, to create composite action. The composite cross-section has a larger stiffness and bending capacity, implying that a larger traffic load often can be allowed. It must however also be assured that other structural parts do not limit the load capacity of the structure.

There are several different types of shear connectors that can be used for post-installation, and some are more suitable than others. This thesis presents a state-of-the-art review on post-installed shear connectors in general and Coiled Spring Pins in particular. The latter is an interference fit connector that can be installed from below the bridge, with no or minor impact on the traffic on the bridge.

The behaviour of Coiled Spring Pins, used as shear connectors in composite bridges, has been investigated by experimental methods. Push-out tests have been used to study the static strength and the fatigue lifetime, while field monitoring of a real bridge structure has been used to study the behaviour on a structural level. The tests results have been evaluated and design criteria and design recommendations have been suggested.

The static tests and the following analysis show that Coiled Spring Pins are a very ductile type of shear connector, with a slightly different load-deformation behaviour than headed shear studs. The static strength of the shear connection shows a quite small spread even when different parameters are varied quite a lot. The performed fatigue tests indicate a fatigue strength that are somewhat lower than headed studs, in terms of detail category, while previous test series by other researchers indicate a higher fatigue strength than headed studs. It can be noted that there is a large scatter between the results from different test series, performed by different researchers. The reasons to this scatter are discussed in the thesis and a conservative fatigue design criterion is presented.

The results from the field monitoring indicate that a bridge strengthened with Coiled Spring Pins behaves as a composite structure and that the Coiled Spring Pins reduce the slip significantly. The analysis of the test results shows that a design assuming full composite action, with rigid shear connection, describes the measured behaviour in a good way.

Based on the state–of–the–art review and the different tests performed, design recommendations and criteria are presented, along with production and execution recommendations for post-installation of Coiled Spring Pins.

SAMMANFATTNING

Ämnet för denna avhandling är samverkansbroar och innovativa sätt att skapa samverkan. Broöverbyggnaden består i regel av tre huvudkomponenter: stålbalkarna, betongfarbanan samt skjuvförbindarna. De sistnämnda binder samman stål- och betong-delarna, vilket möjliggör en dimensionering där de ingående delarna antas agera som en konstruktionsenhet, samverkansbalken.

Forskningen som presenteras i denna avhandling är framförallt fokuserad på olika konstruktions- och förstärknings-metoder, utvecklade för att minska påverkan på trafikanterna, huvudsakligen genom att reducera den tid som tillbringas på byggarbetsplatsen och därmed behovet av restriktioner för trafikanterna.

De prefabricerade stålbalkarna ger samverkansbroar en del fördelar i byggskedet, i jämförelse med de mer vanliga platsgjutna betongbroarna, eftersom stålbalkarna kan lanseras eller lyftas på plats. En sådan installationsprocedur är ofta fördelaktig för broar över vägar, järnvägar, älvar etc., eftersom den minimerar påverkan på de trafikanter som nyttjar infrastrukturen under bron samt behovet av temporära stöd. För att ytterligare reducera tiden på byggarbetsplatsen och påverkan på trafikanterna, kan även prefabricering av betongfarbanan övervägas.

I denna avhandling presenteras en genomgång av olika typer av prefabriceringstekniker för samverkansbroar, tillsammans med en studie av ett specifikt prefabriceringskoncept som reducerar behovet av platsgjutna fogar i farbanan. Detta koncept, med prefabricerade betongelement med torra fogar, nyttjar sig av betongklackar för att överföra skjuvkrafter i de tvärgående fogarna i brofarbanan, medan platsgjutna fogar används för den längsgående förbindningen mellan stålbalkarna och betongfarbanan.

Det statiska beteendet för samverkansbroar med torra farbanefogar har undersökts via storskaliga balktester, tillsammans med fältmätningar på en prefabricerad samverkansbro. Betongklackarnas lastkapacitet har också undersökts genom provning. Testresultaten har jämförts med numeriska analyser samt olika dimensioneringsmodeller, med målet att ta fram dimensionerings-rekommendationer.

Resultaten indikerar att denna typ av broar inte helt beter sig som konventionella samverkansbroar med platsgjutna farbanor. För enspanns-broar, som endast utsätts för positiva böjmoment, är beteendet i brottgränstillståndet snarlikt beteendet för en konventionell samverkansbro. Graden av samverkan är dock kraftigt reducerad vid lägre belastningsnivåer, vilket måste tas i beaktande vid dimensionering i bruksgränstillståndet respektive vid dimensionering för utmattning. Tvärsnitt utsatta för negativt böjmoment beter sig i allmänhet som icke-samverkans tvärsnitt, vilket var förväntat med tanke på de torra fogarna i farbanan.

Baserat på utvärderingen av testresultaten och litteraturstudien, presenteras dimensionerings-rekommendationer och -kriterier, tillsammans med produktions- och utförande-rekommendationer för denna typ av prefabriceringskoncept.

Förstärkning av befintliga broar är en annan aktivitet som ofta leder till trafikstörningar, vilket medför kostnader och problem för både trafikanterna och samhället i stort. En metod för att förstärka stål-betong balkbroar, som ursprungligen byggts utan samverkan, är att skapa samverkan genom efterinstallation av skjuvförbindare. Samverkanstvärsnittet har större styvhet och böjmotstånd, vilket innebär att högre trafiklaster ofta kan tillåtas. Det måste emellertid även säkerställas att andra konstruktionsdelar inte begränsar konstruktionens lastkapacitet.

Flertalet olika typer av skjuvförbindare kan användas för efterinstallation, vissa är dock mer lämpliga för detta än andra. Denna avhandling presenterar en litteraturstudie över efterinstallerade skjuvförbindare i allmänhet och spiralbultar (Coiled Spring Pins) i synnerhet. Den sistnämnda är en mekanisk presspassnings-förbindare som kan installeras underifrån bron, med ingen eller liten påverkan på trafiken uppe på bron.

Spiralbultarnas beteende, då de används som skjuvförbindare i samverkansbroar, har undersökts med experimentella metoder. Push-out-tester har använts för att studera den statiska lastkapaciteten och utmattningslivlängden, medan fältmätningar på en bro har använts för att studera konstruktionsbeteendet i större skala. Testresultaten har utvärderats och dimensionerings-kriterier och -rekommendationer har föreslagits.

De statiska testerna och den efterföljande analysen visar att spiralbultar är en väldigt duktil typ av skjuvförbindare, med ett något annorlunda last-deformations-samband än svetsbultar. Den statiska lastkapaciteten visar en ganska liten spridning även när olika parametrar varieras tämligen mycket. De utförda utmattningstesterna indikerar en utmattningskapacitet som är något lägre än den för svetsbultar, med avseende på detaljkategori, medan tidigare testserier av andra forskare indikerar en högre utmattningskapacitet än svetsbultar. Det kan noteras att det råder en stor spridning mellan resultaten från olika testserier, utförda av olika forskare. Anledningen till denna spridning diskuteras i avhandlingen och ett konservativt dimensioneringkriterium för utmattning presenteras.

Resultaten från fältmätningarna indikerar att en bro som förstärkts med spiralbultar beter sig som en samverkanskonstruktion och att spiralbultarna avsevärt reducerar glidningen i övergångsytan mellan stål och betong. Analysen av testresultaten visar att ett

dimensioneringsantagande om full samverkan, med styv skjuvförbindning, beskriver det uppmätta beteendet på ett bra sätt.

Baserat på litteraturstudien och de utförda testerna, presenteras dimensionerings-rekommendationer och- kriterier, tillsammans med produktions- och utförande-rekommendationer för efterinstallation av spiralbultar.

Nyckelord: Samverkan; bro; stål; betong; skjuvförbindare; prefabricering; spiralbult; svetsbultar; installation i efterhand; push-out test; utmattning

PUBLICATIONS

Appended publications

This thesis is based on the work described in the nine papers that are listed below and referred to in the text by the associated roman numbers:

I.   Hällmark, R., White, H., & Collin, P. (2012). Prefabricated bridge construction across Europe and America. *Practice Periodical on Structural Design and Construction*, *17*(3), 82-92.

II. Hällmark, R., Collin, P., & Stoltz, A. (2009). Innovative prefabricated composite bridges. *Structural Engineering International*, *19*(1), 69-78.

III. Hällmark, R., Collin, P., & Nilsson, M. (2011). Concrete shear keys in prefabricated bridges with dry deck joints. *Nordic Concrete Research*, *44*(2), 109-122.

IV. Hällmark, R., Collin, P., & Möller, M. (2013). The behaviour of a prefabricated composite bridge with dry deck joints. *Structural Engineering International*, *23*(1), 47-54.

V.   Hällmark, R., Collin, P., & Nilsson, M. (2013). Large-scale tests on a composite bridge with prefabricated concrete deck and dry deck joints. *Stahlbau*, *82*(2), 122-133.

VI. Hällmark, R., Jackson, P., Collin, P. & White, H. (2018). Strengthening Bridges with Postinstalled Coiled Spring Pin Shear Connectors: State-of-the-Art Review. Accepted for publication in: *Practice Periodical on Structural Design and Construction*.

VII. Hällmark, R. & Collin, P. (2018). Post-Installed Shear Connectors: Monitoring a Bridge Strengthened with Coiled Spring Pins. Scheduled for publishing in: *Structural Engineering International*, *28*(4), pre-published on-line July 2018.

VIII. Hällmark, R., Collin, P. & Hicks J. S. (2018). Post-Installed Shear Connectors: Push-out tests of coiled spring pins vs. headed studs. Submitted to: *Journal of Constructional Steel Research*, August 2018.

IX. Hällmark, R., Collin, P. & Hicks J. S. (2018). Post-Installed Shear Connectors: Fatigue push-out tests of coiled spring pins. Submitted to: *Journal of Constructional Steel Research*, September 2018.

The papers above were planned and written by Robert Hällmark, who also designed and evaluated the associated experiments and numerical analysis, with one exception in Paper II. In this paper, the third author (Stoltz, A.) planned and performed the laboratory test, which is a part of the paper. The other co-authors provided guidance throughout the work and reviewed the manuscripts before submission. Among the co-authors, the contributions from Peter Collin, who has contributed as a supervisor during the entire work, must be highlighted.

Additional publications

The author has also contributed to the following publications that are related to the topic of the thesis, but not appended:

Licentiate thesis

– Hällmark, R. (2012). *Prefabricated Composite Bridges – a Study of Dry Deck Joints*. (Licentiate thesis, Luleå University of Technology, Luleå, Sweden).

Journal papers

– Thulstrup, M., Nielsen J. P., Nilsson, M. & Hällmark, R. (2011). Railway bridge over Södertälje Canal, Sweden. *Proceedings of the Institution of Civil Engineers – Bridge Engineering, 164*(3), 123-132.

– Hällmark, R., Collin, P. & Nilsson, M. (2010). Prefabricated composite bridges. *AMOST - World Bridge Construction*, 2:2010, 71-80. (in Russian)

Conference papers

– Hällmark, R., Collin, P., Petersson, M., & Andersson, E. (2017). Monitoring of a bridge strengthened with post-installed coiled spring pins. *Proceedings of the 39th IABSE Symposium – Engineering the Future, Vancouver, Canada, September 21-23, 2017*. (p. 1193-1200).

– Hällmark, R., Collin, P. & Möller, M. (2017). Testing of coiled spring pins as shear connectors. *Proceedings of the 39th IABSE Symposium – Engineering the Future, Vancouver, Canada, September 21-23, 2017*. (p. 1201-1208).

– Hällmark, R., Jackson, P. and Collin, P. (2016). Post-installed shear connectors–coiled spring pins. *Proceedings of the 19th IABSE Congress, Stockholm, Sweden, September 21-23, 2016*. (p. 1227-1234).

– Lundmark, T., Hällmark, R. & Collin, P. (2016). Upgrading of an old railway bridge – the Old Årsta Bridge. *Proceedings of the 19th IABSE Congress, Stockholm, Sweden, September 21-23, 2016*. (p. 624-631).

– Hällmark, R., Nilsson, M. & Collin, P. (2011). Concrete shear keys in prefabricated bridges with dry joints. *Proceedings of the XXI Symposium on Nordic Concrete Research & Development, Hämeenlinna, Finland, May 30 – June 1, 2011.*

– Hällmark, R., Collin, P. & Nilsson, M. (2009). Prefabricated composite bridges. *Proceedings of the IABSE Symposium – Sustainable Infrastructure, Bangkok, Thailand, September 9-11, 2009*. (p. 107-117).

– Thulstrup, M., Nilsson, M., Hällmark, R. & Nielsen, J. P. (2009). Design, fabrication and construction of railway bridge over Södertälje Canal. *Proceedings of the Nordic Steel Construction Conference, Malmö, Sweden, September 2-4, 2009*. (p. 128-137).

– Hällmark, R., Collin, P., Pétursson, H. & Johansson, B. (2007). Simulation of low-cycle fatigue in integral abutment piles. *Proceedings of the IABSE Symposium – Improving Infrastructure Worldwide, Weimar, Germany, September 19-21, 2007*. (p. 41-48).

Other type of publications

– Breisand, S. & Hällmark, R. (2012). Tidig samverkan gav bättre samverkansbroar. *Samhällsbyggaren, No:3, 2012.* (p. 12-15). (in Swedish)

– Möller, F., Collin, P., Haarju, T., Hällmark R., Hehne, T., Hoyer, O., et al. (2012a). *Final Report – ELEM - Composite Bridges with Prefabricated Decks*. Research project of the Research Fund for Coal and Steel RFSR-CT-2008-00039, Final Report.

– Möller, F., Collin, P., Haarju, T., Hällmark R., Hehne, T., Hoyer, O., et al. (2012b). *Design Guide – ELEM - Composite Bridges with Prefabricated Decks*. Research project of the Research Fund for Coal and Steel RFSR-CT-2008-00039, Design Guidance.

– Hällmark, R. (2011). Swedish experience from EC4-2. *Proceedings from International Workshop on Eurocode 4-2 – Composite Bridges, Stockholm, Sweden, March 17th, 2011*. (p. 133-144).

– Collin, P., Häggström, J. & Hällmark, R. (Editors). (2011). *International workshop on strengthening of steel/composite bridges* (Technical Report). Luleå, Sweden: Luleå University of Technology.

– Collin, P., Hällmark, R. & Nilsson, M. (Editors). (2009). *International Workshop on prefabricated composite bridges* (Technical Report). Luleå, Sweden: Luleå University of Technology.

NOTATION

Roman upper case letters

A	Area
A_{conc}	Cross-sectional area of the concrete deck slab
A_{sc}	The cross-sectional area of a shear connector
$A_{sc,CSP}$	The cross-sectional area of a Coiled Spring Pin shear connector
A_{sw}	Cross-sectional area of the shear reinforcement
E	Modulus of elasticity
E_a	Modulus of elasticity of structural steel
E_{cm}	Secant modulus of elasticity of concrete
I	Moment of inertia
I_2	Moment of inertia of the effective equivalent steel section neglecting concrete in tension but including reinforcement
L	Length
L_e	Equivalent span length
L_{elem}	Element length
M	Bending moment
M_{mean}	Mean value of the moment distributed over the length of one element
N	Number of cycles
N_c	Number of cycles used for the fatigue strength reference values: $2 \cdot 10^6$
N_f	Number of fatigue load cycles until failure

N_R	Design lifetime expressed as number of cycles at a constant stress range
P	Force, load
P_{calc}	Ultimate load capacity of a composite bridge cross-section
P_{ini}	Initial load prior to the fatigue load cycles
$P_{max,f}$	Maximum load in the fatigue load cycle
$P_{min,f}$	Minimum load in the fatigue load cycle
P_R	Shear resistance of a single connector
$P_{Rd,c}$	Design value of the shear connector resistance in case of a concrete failure
$P_{Rd,s}$	Design value of the shear connector resistance in case of a steel failure
P_{Rk}	Characteristic value of the shear resistance of a single connector
$P_{Rk,EC0}$	Characteristic value of the shear resistance, based on the method in EC0
$P_{Rk,EC4}$	Characteristic value of the shear resistance, based on the method in EC4
P_u	Maximum load in the push-out tests
$P_{u,m}$	Mean value of the maximum load for specimens of the same type
R	The ratio between the minimum and the maximum load in the load cycle
R^2	The coefficient of determination
S	Stress
V	Shear force
V_{max}	Measured shear strength of the shear keys
$V_{Rd,s}$	Shear resistance
W	Elastic section modulus
W_{tf}	Elastic section modulus at the upper side of the top flange
$\varnothing$	Diameter

Roman lower case letters

a	The intercept of the N-axis in a S-N (P-N) diagram
d	Diameter
e	Eccentricity
e_{CG}	Vertical position of the neutral bending axis
f_c	Compressive strength of the concrete
f_{ck}	Characteristic value of the concrete cylinder compressive strength at 28 days

$f_{cm,cube}$	Mean value of concrete cube compressive strength
f_{sk}	Characteristic value of the yield strength of reinforcing steel
f_u	Specified ultimate tensile strength
f_{ywd}	Design yield strength of the shear reinforcement
h_{conc}	Concrete deck thickness
h_{sc}	Overall nominal height of a stud connector
k	Initial stiffness of a shear connector
k_x	Linear spring stiffness in the horizontal x-direction
k_y	Linear spring stiffness in the horizontal y-direction
m	The slope of a linear regression line
t	Thickness
w	Deflection
z	Distance measured in the vertical direction

Greek letters

α	Inclination of the shear reinforcement; Factor
β	Inclination of the compression strut
γ_v	Partial factor for the design shear resistance of a shear connector
δ	Slip at the steel-concrete interface
δ_j	Estimated joint opening
$\delta_{j,meas}$	Measured joint opening
δ_{Pu}	Slip at the maximum load
δ_u	Slip capacity
δ_{uk}	Characteristic value of slip capacity
ΔP_f	Fatigue load range
$\Delta \tau_c$	Reference value of the fatigue shear strength at N_C = 2 million cycles
$\Delta \tau_R$	Fatigue shear strength
ρ	Ratio between the reinforcement- and the concrete-area in a cross-section
σ	Stress
τ	Shear stress

Abbreviations

AASHTO	American Association of State Highway and Transportation Officials
ABC	Accelerated Bridge Construction
BIM	Building Information Modelling
CRC	Compact Reinforced Composite
CSP	Coiled Spring Pin
DLR	Docklands Light Railway (in London)
EC0	Eurocode 0
EC4	Eurocode 4
EN	European Standard
FE	Finite Element
FEM	Finite Element Model
FHWA	The Federal Highway Administration
FLM	Fatigue Load Model
FLS	Fatigue Limit State
ISO	International Organization for Standardization
KTH	The Royal Institute of Technology in Stockholm
LC	Load Case
LCC	Life Cycle Cost
LTU	Luleå University of Technology
LVDT	Linear Variable Differential Transformer
MCE-Lab	Mining and Civil Engineering Lab (at LTU)
NCHRP	National Cooperative Highway Research Program
RFCS	The European Union's Research Fund for Coal and Steel
RQ	Research Question
RWTH	Rheinisch-Westfaelische Technische Hochschule (Aachen University)
SCC	Self Compacting Concrete
SLS	Serviceability Limit State
UHPC	Ultra High Performance Concrete
ULS	Ultimate Limit State
WHS	Welded Headed Studs

TABLE OF CONTENTS

Chapter 1

INTRODUCTION

1.1 Background

The popular quote "time is money" has been a guiding star in the research presented in this thesis.

Nowadays, the total cost of a bridge is no longer limited to the money spent on labour and material. In an urban environment, there are several other factors that should be taken into account when new bridges are constructed or when existing bridges are replaced, widened, strengthened or repaired. Construction activities that disrupt the ordinary traffic flow will result in increased road user costs, since the road users have to wait in queues or taking detours around the construction site. Finding ways to shorten the time spent on construction sites and minimizing the impact on the road users will give positive effects for contractors, bridge owners and the road users.

Prefabrication, lean-thinking and production planning through BIM (Building Information Modelling) have all become everyday tasks in the house building industry, but are still rare exceptions in bridge constructions. Actors in the bridge industry, in Sweden and Europe, have tried to implement prefabrication during the recent decades and there are several examples of successful projects involving prefabrication of both steel and concrete parts. Still, the bridge industry always seems to fall back into old habits and conventional construction methods. In order to get an impact of new building technologies there must be a change in the behaviour of contractors, designers and last but not least the bridge owners.

The research presented in this thesis, limited to steel-concrete composite bridges, was initiated with the aim to contribute to a progress towards the use of new and innovative bridge design solutions to minimize the traffic disturbance.

Throughout the remainder of the thesis, "composite bridge" is used as a shorter synonym for the more complete "steel-concrete composite bridge" and should not be mistaken as bridges made out of composites, which are out of scope for this thesis.

1.2 Objectives

The overall objective of the performed research was to achieve more time and cost efficient use of composite bridges, by further development of suitable design procedures for new composite bridges and strengthening methods based on the creation of composite action.

The research has been focused on two different applications:

(A) Further development of design methods for prefabricated concrete deck elements with dry deck joints, used in new composite structures.

(B) Further development of strengthening methods based on post-installation of shear connectors in general and Coiled Spring Pins (CSPs) in particular, used in existing structures.

For both cases, the aim has been to develop practical design guidelines for the studied methods and to eliminate the need of future project specific tests as far as possible, in order to remove some of the barriers for the use of the specific methods.

1.3 Hypotheses and research questions

The research presented in this thesis deals with the shear force transfer at the steel–concrete interface in composite bridges and partially also the force transfer at the dry concrete–concrete interfaces in prefabricated composite bridges with dry deck joints.

Two separate hypotheses were stated in the beginning, followed by two different sets of research questions, which have been used to guide the scientific work:

A − Prefabricated composite bridges with dry deck joints

Hypothesis:

"If reliable and practical design guidelines are developed, composite bridges with prefabricated concrete deck elements with dry deck joints would be a competitive design approach when it is essential to reduce the construction time on site, to minimize the impact on the traffic."

Research questions (RQ):

A-RQ1. *What is the state-of-the-art within this field?*

A-RQ2. *How does a superstructure with dry deck joints behave under positive and negative bending moments?*

A-RQ3. *How do the shear keys fail under an increased static load and how should a rational design calculation of the shear keys be done?*

A-RQ4. *What is the long-term behaviour of a bridge with dry deck joints, compared to a composite bridge with a conventional in-situ cast deck slab?*

A-RQ5. *Which aspects need to be covered in a detailed design of this type of bridges?*

B – Post-installed Coiled Spring Pins

Hypothesis:

"Strengthening non-composite steel–concrete bridges by post-installation of CSP shear connectors would be a more competitive approach if reliable and practical design guidelines are developed."

Research questions:

B-RQ1. *What is the state-of-the-art within this field?*

B-RQ2. *In what way does a CSP fail under static loading and which parameters are influencing the behaviour?*

B-RQ3. *In what way does a CSP fail under fatigue loading and which parameters are influencing the behaviour?*

B-RQ4. *What is the structural behaviour of a bridge strengthened with Coiled Spring Pins?*

B-RQ5. *Which aspects need to be covered in a detailed design of this type of strengthening?*

1.4   Limitations

Since the two research topics are wide, the research presented in this thesis has the following limitations:

Case A – Prefabricated composite bridges with dry deck joints

-   The research is limited to the bridge superstructure and its structural behaviour.

-   The type of superstructure is limited to a composite superstructure, consisting of two steel I-girders and a bridge deck made of prefabricated concrete elements.

-   The transverse joints between the prefabricated deck elements are limited to dry joints, implying that forces are transferred from one concrete surface to another by contact pressure only. However, the longitudinal connections between the steel girders and the prefabricated concrete elements is created by in-situ cast concrete. Figure 1.1 illustrates a typical cross-section of such a superstructure.
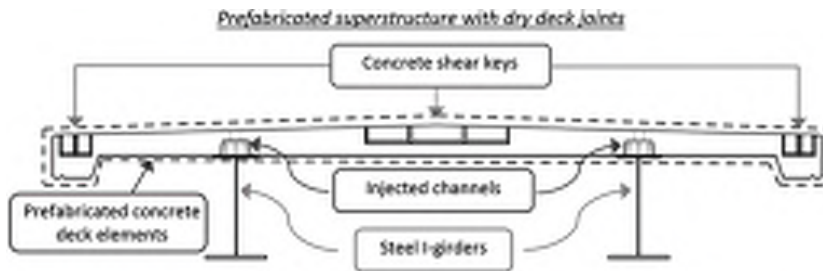
Figure 1.1 *The studied type of superstructure*

<u>*Case B − Post-installed Coiled Spring Pins*</u>

- The research is limited to strengthening of non-composite steel-concrete structures by post-installation of CSPs.

- The studied degree of composite action is limited to full composite action.

- Only one type and dimension of the CSP is studied. This implies that the presented results and conclusions are valid only for Heavy-duty CSPs with a nominal diameter of 20 mm and produced in line with ISO 8748 (2007).

1.5 Scientific approach

The general approach adopted for scientific studies at the Division of Structural and Fire Engineering at Luleå University of Technology (LTU) is a straightforward procedure comprised of the following four steps: (1) state hypothesis, (2) literature review, (3) formulate research questions and (4) address research questions using an appropriate theoretical and experimental framework.

The research presented in this thesis follows the general approach presented above, but with some minor modifications. The first three steps were conducted as a part of the application process for research funding, implying that they initially were performed on a basic level and under time pressure. Later, when the research projects were realized there was a need to return back to step (2) and (3) in order to extend the literature review and to modify the research questions based on the new knowledge. After the update of step (2) and (3) the research questions were addressed in step (4) by experimental tests performed on small- and large-scale specimens as well as full scale structures, followed by evaluations of the test results and comparisons to theoretical design models as well as numerical analysis.

1.6   Outline of the thesis

The thesis consists of five chapters presenting a summary of the scientific work that is further described in the nine appended papers. Seven papers (*Paper I-VII*) have been published or scheduled for publishing in scientific journals, while the eighth and ninth paper (*Paper VIII and IX*) have been submitted and are both under review.

The contents of the chapters and papers are briefly described below:

Chapter 1 introduces the background and the research objectives. The content of the thesis and the scientific approach are also summarised.

Chapter 2 describes, on a general level, the basic concept of composite action, composite bridge design and the competitiveness of composite structures.

Chapter 3 presents, together with Paper I-V, the research performed within the field of prefabricated composite bridges. This research has previously been reported in a Licentiate thesis (Hällmark 2012a) and is covered more briefly in this thesis.

Chapter 4 describes the research performed on post-installed shear connectors and particular the use of Coiled Spring Pins. Paper VI-IX complements this chapter.

Chapter 5 presents and discuss the results and conclusions from the research presented in this thesis, together with proposals for further research.

Appendix A is a complement to Chapter 3 and presents a design guidance for *Composite bridges with prefabricated concrete deck elements with dry joints*.

Appendix B is a complement to Chapter 4 and presents a design guidance for *Strengthening by post-installation of Coiled Spring Pins as shear connectors*.

Paper I summarises the state of the art in the field of prefabricated bridge design. The paper is based on experiences from researchers and bridge designers. The information has been gathered by a literature review and by arranging an international Workshop in Stockholm, March 4th 2009.

Paper II summarises the previously performed research in Sweden on prefabricated concrete deck elements with dry joins. The paper presents the results from laboratory tests of shear keys as well as shear studs. Experiences from the construction process of a Swedish pilot bridge are also presented, together with an economic analysis of prefabricated concrete decks in comparison to conventional in-situ cast concrete decks.

Paper III describes an evaluation of the load capacity of the shear keys in the dry deck joints. Laboratory tests on full-scale shear keys have been performed. This paper presents the tests, the results and an analysis aiming for a rational way to design the shear keys.

Paper IV presents the results from a field monitoring of a single span bridge with a prefabricated concrete deck with dry joints. The field monitoring performed in 2011 is compared to a similar monitoring performed in 2001, shortly after the opening of the monitored bridge. This is done in order to study the long-term behaviour of the bridge, and if there are some deterioration of the joints.

Paper V describes large-scale laboratory tests of a composite bridge with prefabricated deck elements with dry joints. The structural behaviour of such a cross-section has been studied in case of both positive and negative bending moments. The effective width of the interacting concrete, which corresponds to the test results, has been compared to the model given in EN 1994-2 (2005). Recommendations of how this type of bridges should be modelled in global analysis are given, together with recommendations for cross-sectional design.

Paper VI presents a state of the art study of post-installed shear connectors in general and Coiled Spring Pins in particular. The strengthening method is described together with experiences from bridge strengthening projects, along with a study of load capacity and structural behaviour.

Paper VII presents a study of a steel-concrete bridge, the Pitsund Bridge, which has been strengthened with post-installed Coiled Spring Pins. The strengthening method and design procedure are presented, along with the results from a field monitoring performed in 2016, to evaluate the behaviour of the strengthened structure.

Paper VIII describes an experimental study of the static capacity and stiffness of Coiled Spring Pins used as shear connectors at steel-concrete interfaces. Six push-out test series are presented, with a total of 28 tests, together with an evaluation of an alternative type of test set-up for push-out tests.

Paper IX describes an experimental study of the fatigue strength of Coiled Spring Pins and a compilation of previously performed fatigue tests on this type of shear connector. The new test series, with nine specimens, are evaluated statistically and a fatigue strength design criterion is proposed.

How the different papers fit into the major research topic, and how they relates to the research questions, are illustrated by the graphical scheme in Figure 1.2.

A - Prefabricated composite bridges with dry deck joints

Prefabricated composite bridges

A-RQ1

Paper I
Prefabricated Bridge Construction across Europe and America

Prefabricated concrete deck elements

Paper II
Innovative Prefabricated Composite Bridges

A-RQ2

Performed tests

Shear keys
A-RQ3

Paper III
Concrete shear keys in prefabricated bridges with dry deck joints

Field monitoring
A-RQ2 | A-RQ4

Paper IV
Field monitoring of a bridge with prefabricated concrete deck elements

Structural behavior
A-RQ2

Paper V
Large scale test of a superstructure with dry deck joints

Design recommendations

Design and production issues
Ch. 3
A-RQ5

Conclusions, discussion and further research

Ch. 5 | A-RQ1 | A-RQ2 | A-RQ3 | A-RQ4 | A-RQ5 | B-RQ1 | B-RQ2 | B-RQ3 | B-RQ4 | B-RQ5

B – Post installed Coiled Spring Pins

Strengthening by post-installation of shear connectors

Paper VI
Strengthening Bridges with Postinstalled Coiled Spring Pin Shear Connectors: State-of-the-Art Review

B-RQ1

Structural behaviour

Paper VII
Post-Installed Shear Connectors: Monitoring a Bridge Strengthened with Coiled Spring Pins

B-RQ4

Shear connection

Paper VIII
Post-installed Shear Connectors: Push-out Tests of Coiled Spring Pins vs. Headed Studs

B-RQ2

Paper IX
Post-installed Shear Connectors: Fatigue Push-out Tests of Coiled Spring Pins

B-RQ3

Design recommendations

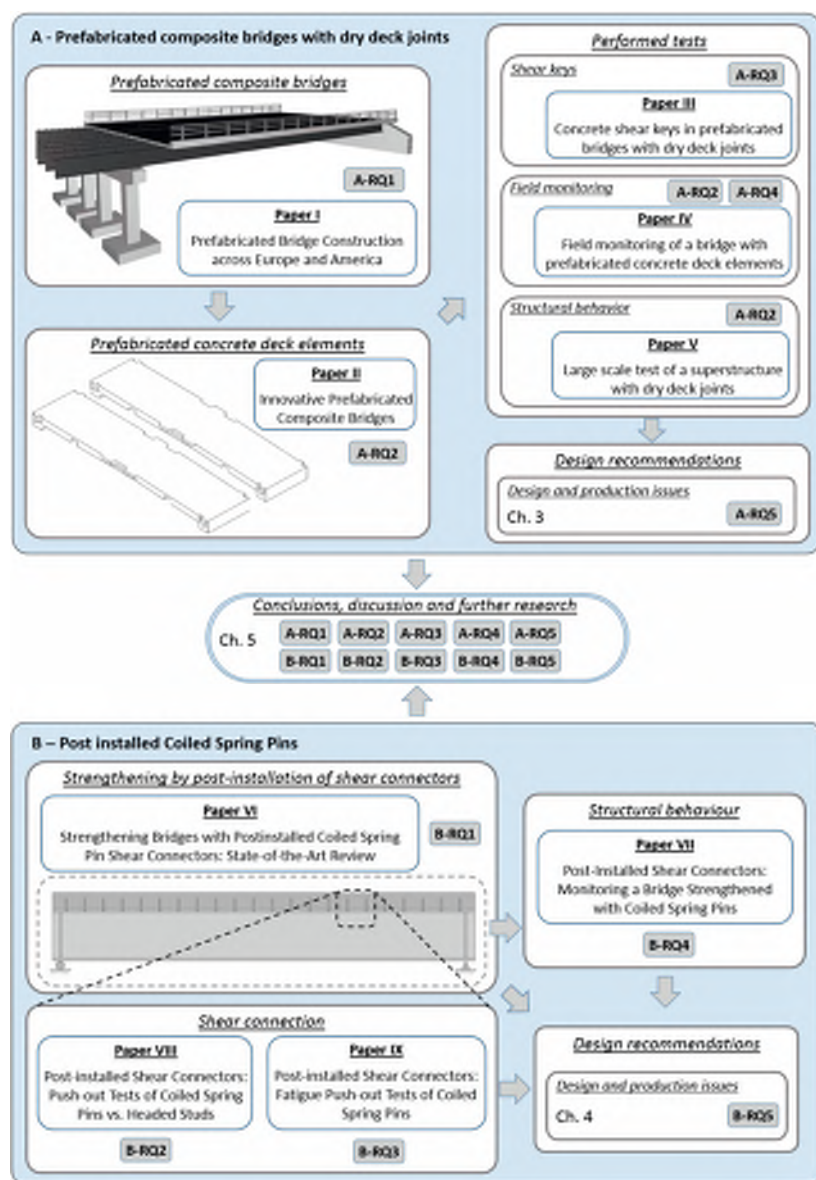*Design and production issues*
Ch. 4
B-RQ5

Figure 1.2 *Schematic illustration of how the content of this thesis is organised*

Chapter 2

COMPOSITE STRUCTURES

Steel-concrete composite bridges are structures, primary subjected to bending, with components of both steel and concrete that are connected to each other by shear connectors, to prevent slips and separation at the steel-concrete interface. A properly designed full composite shear connection will make the steel- and the concrete-parts act as a single structural member, a composite beam. A schematic illustration of a composite beam and its main components is shown in Figure 2.1.
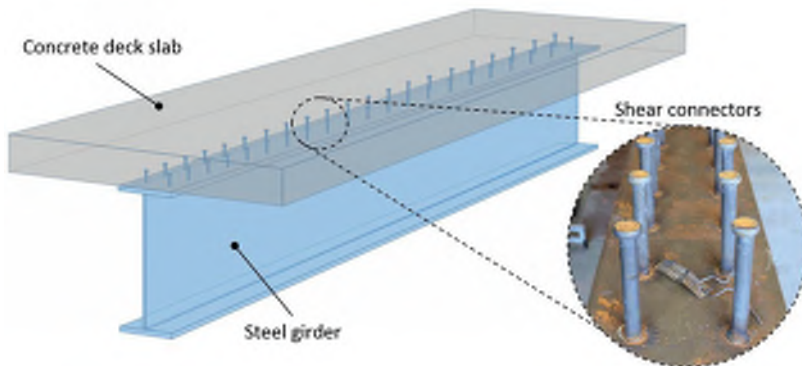
***Figure 2.1** Schematic illustration of a composite beam*

Composite bridges are an efficient and cost effective type of bridge construction. By utilizing the high tensile strength of the steel girders and the compressive strength of the concrete deck slab, the load capacity of the composite cross-section is significantly increased in comparison to a non-composite cross-section. This enables longer spans and more slender structures. (El Sarraf et al. 2013, Hanswille 2011a)

Today, a composite design is more or less a requirement in the design of steel-concrete bridges, but as late as the 1980's Swedish steel-concrete bridges were still built without composite action. The development of steel-concrete composite construction started however already in the mid of the 19th century, but it took until the first half of the 20th century before this type of structure started to become established in the construction industry. Pelke & Kurrer (2015), Hicks et al. (2016) and Lam (1998) present brief historical reviews on the evolution of steel-concrete composite construction.

This chapter gives an introduction to composite bridges, by a brief presentation of the basic concept of composite action, followed by a short summary of composite bridge design and a presentation of the advantages of composite bridges.

2.1   Composite action

Composite action means that parts of different materials are connected to each other in a way that they act as one single structural member. The components that are connecting the parts, the shear connectors, are essential for the behaviour of the construction. The connectors must have sufficient strength, stiffness and ductility to enable a design procedure where the different components are designed as parts of a single structural member, the composite beam. (EN 1994-2 2005)

The difference between composite action and no composite action is schematically illustrated in Figure 2.2.

Figure 2.2 *No composite action vs. composite action*
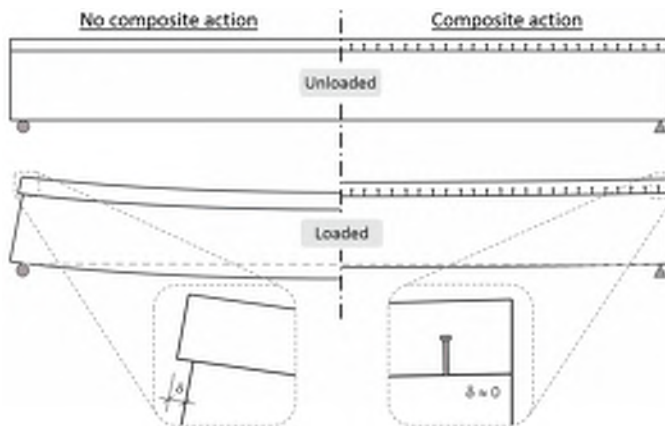
The left part of Figure 2.2 shows a beam without shear connectors, i.e. a non-composite steel-concrete beam. In this case, when the beam is loaded there will be a slip (δ) at the steel concrete interface, implying that plane sections will not remain plane after bending. The steel and the concrete parts will share the load, in relation to their individual flexural

stiffness (EI). The opposite case is illustrated in the right part of Figure 2.2, where rigid shear connectors provide full composite action without any slips at the steel-concrete interface. In this case, the steel and the concrete parts will act as one structural member and it can be assumed that plane sections remain plane under bending moments, in line with the assumptions in the Euler-Bernoulli beam theory.

The difference in the structural response, in terms of strains, between a non-composite section and a full composite section is illustrated in Figure 2.3a-b. Figure 2.3a shows a steel beam with a concrete slab on top, without any shear connectors. These parts are acting as two individual sections, if frictional forces at the steel-concrete interface are neglected, which is illustrated by the corresponding strain (ε) diagram. The slip, δ, is defined as the difference between the steel strain, ε_s, and the concrete strain, ε_c, at the steel-concrete interface. Figure 2.3b shows a composite beam with the same structural parts as in (a), but with shear connectors that make the parts acting as one section without any slip at the steel-concrete interface, illustrated by the corresponding strain diagram. A composite beam is considered to have full composite action if the shear connection provides a sufficient strength, to enable the development of the full strength of the cross-section. This implies that the strength of the composite beam will not be governed by the shear connection, but instead by the steel girder or the concrete deck slab.
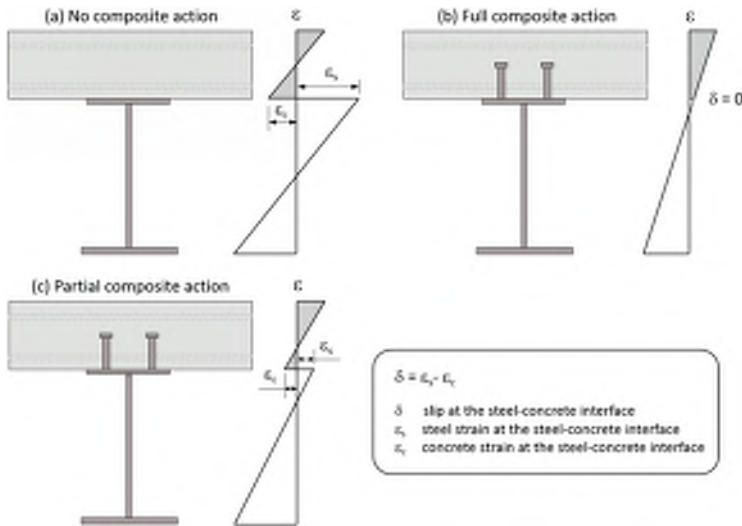
Figure 2.3 Schematic illustration of the vertical strain distribution for cross-sections with (a) no composite action, (b) full composite action and (c) partial composite action.

The non-composite and the full-composite behaviour presented above are the two extremes, while the real behaviour of a structure often is somewhere in between. In case of the non-composite beam, there is always frictional forces or other interlocking phenomenon providing limited transfer of shear forces. Natural bonds are however

neglected in the design procedure, by requirements in EN 1994-2 (2005), to ensure a robust behaviour without brittle failure modes. In the opposite case with full composite action, there will always be a degree of slip in real structures, caused by concrete crushing and bending of the shear connectors, in line with the headed shear stud behaviour presented by Nellinger et al. (2017) and originally by Lungershausen (1988). However, as long as the shear connectors provide sufficient strength, stiffness and ductility, EN 1994-2 (2005) allows the sections to be designed assuming full composite action.

Between the two extremes, cross-sections with partial composite action can be found, see Figure 2.3c. These cross-sections are characterized by the fact that the shear connection is the weakest part, and that the limited number of shear connectors will cause a degree of slip. In the design of new composite bridges, EN 1994-2 (2005) requires a design based on full composite action, while other types of structures often can be designed based on partial shear connection, as long as the requirements in EN 1994-1-1 (2005) are fulfilled.

The research presented in this thesis is limited to cross-sections with full composite action. However, in the strengthening of existing bridges, partial composite action has been proven to be a cost effective alternative, since the number of post-installed shear connectors can be reduced significantly in many cases (Kwon 2008, Kwon et al. 2011).

2.2 Composite bridge design

In Europe, the design of composite bridges is mainly governed by the European standard EN 1994-2 (2005). This is however not a stand-alone document, implying that it must be supported by additional parts of the Eurocodes. Figure 2.4 illustrates the relationships between the different parts of the Eurocodes needed for the composite bridge design.

The first five parts of the Eurocodes (EN 1990-1994) acts as the reference standards for the research presented in this thesis.
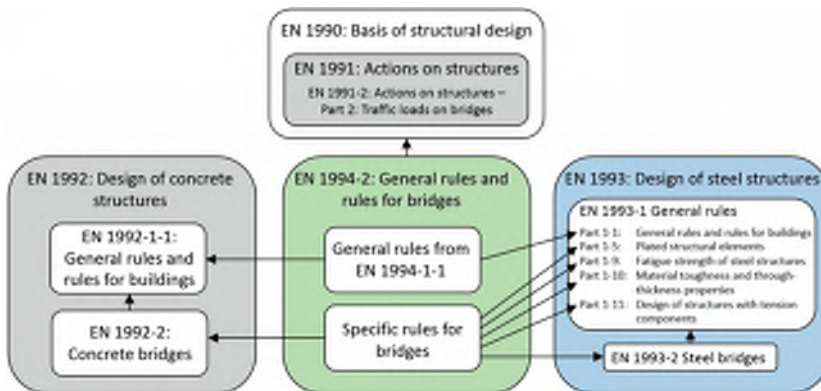

Figure 2.4 *Eurocode 4-2 and its references standards*

The structural analysis of composite bridges is, among other things, characterized by the influence of the sequences of construction, shear lag effects, effects of cracking of concrete, internal forces caused by creep and shrinkage, degree of composite action and by non-linear material behaviour (Hanswille 2011b).

It is however impossible to cover all design issues in this compilation thesis. In this chapter, the author has chosen to focus on the shear connection design, which is essential for composite structures and the reason behind the composite action. The shear connection design is also essential for the research tasks presented further in this thesis. Other important design issues are presented together with the research tasks related to these issues, in Chapter 3 and 4.

Comprehensive guidelines for the design of composite bridges, in line with EN 1994-2 (2005), are provided by several authors, for instance Johnson & Hendy (2006) and Kuhlmann et al. (2008a), among others.

2.3   Shear connection design

Several different types of shear connectors have been tested and used over the years. Figure 2.5 illustrates some examples, from welded shear connectors such as: (a) headed studs, (b) channel connectors, (c) T-connectors, (d) perfobond strips and (e) looped bars, to different types of bolted shear connectors, (f), and continuous shear connectors, (g), integrated as a part of the steel web-plate. (Hicks et al. 2016, Xie & Valente 2011, Hechler et al. 2011)

(a)-(e) Examples of welded shear connectors

(f) Examples of bolted connectors   (g) Continuous connectors, composite dowels
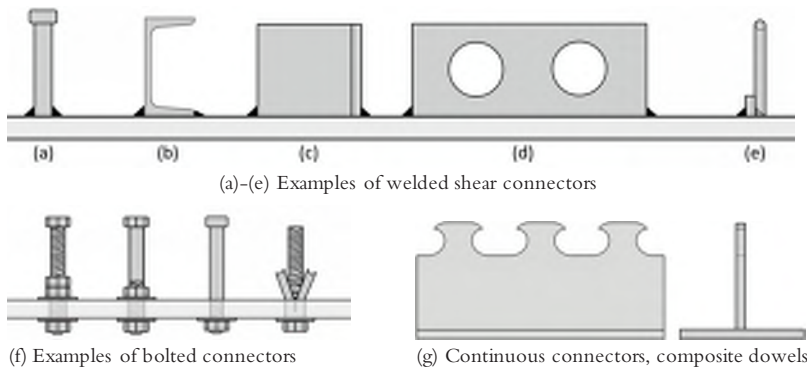
Figure 2.5 *Examples of different types of shear connectors*

Today, the welded headed shear stud is by far the most common type of shear connector in new bridge structures, see Figure 2.5a. The design of shear connections with headed studs are covered by international design codes, such as the European EN 1994-2 (2005) and the US AASHTO (2017), while the components and the installation procedures are covered by international product- and execution-standards such as ISO 13918 (2008) and ISO 14555 (2014).

In Europe, the design rules for shear connections in bridges are presented in EN 1994-2 (2005) section 6.6. These rules state that the connection shall be designed to transfer the shear forces between the steel and the concrete parts, ignoring natural bond.

The code also states that the shear connection should be capable of preventing separation at the steel–concrete interface, if separation is not prevented by other means. Headed studs, which meet the requirements in EN 1994-2 (2005), may be assumed to provide sufficient resistant to uplift. This requirement might however be an important issue for other types of shear connectors, which is discussed in Chapter 4 of this thesis.

The design rules for the static resistance of headed studs, in EN 1994-2 (2005), are based on empirical examinations over the years (Hicks 2017, Roik et al. 1989). The design requires a double verification of the shear connection resistance, where equation (2.1) gives the shear resistance in case of a failure in the shear stud, while equations (2.2) and (2.3) give the shear resistance in case of a failure in the concrete.

$$P_{Rd,s} = \frac{0.8 f_u \pi d^2 / 4}{\gamma_V} \tag{2.1}$$

$$P_{Rd,c} = \frac{0.29 \alpha d^2 \sqrt{f_{ck} E_{cm}}}{\gamma_V} \tag{2.2}$$

$$\alpha = \begin{cases} 0.2\left(\frac{h_{sc}}{d} + 1\right) & for \ 3 \leq h_{sc}/d \leq 4 \\ 1 & for \ h_{sc}/d > 4 \end{cases} \tag{2.3}$$

where γ_V is the partial factor, d is the diameter of the shank of the studs, f_u is the ultimate tensile strength of the stud material (limited to 500 MPa), f_{ck} is the characteristic cylinder compressive strength, E_{cm} the secant modulus of elasticity of concrete and h_{sc} is the overall nominal height of the stud connector.

To enable an assumption of ideal plastic behaviour of the shear connection, there is an additional ductility requirement of a characteristic slip capacity of at least 6 mm,

The design fatigue lifetime of a shear connection is governed by the design rules given in EN 1994-2 (2005) and EN 1993-1-9 (2005). The fatigue strength curve for headed studs, in normal weight concrete, is described by equation (2.4).

$$\Delta \tau_R^m N_R = \Delta \tau_c^m N_c \tag{2.4}$$

where $\Delta \tau_R$ is the fatigue shear strength related to the cross-sectional area of the headed stud using the nominal diameter, $\Delta \tau_c$ is the reference value at $N_c = 2 \cdot 10^6$ cycles (i.e. the detail category 90 MPa), m is the slope of the fatigue strength curve (m = 8) and N_R is the number of stress cycles.

If another type of shear connector is used, than headed studs, the design should be based on tests and supported by a conceptual model. Annex B in EN 1994-1-1 (2005) provides a standard method for testing different types of shear connectors, by defining a standard test specimen (see Figure 2.6) along with recommendations covering the manufacturing of the specimens, the testing procedure and also the evaluation of the test results. This

Annex is of particular interest for the study of an alternative type of shear connector, presented in Chapter 4 of this thesis.
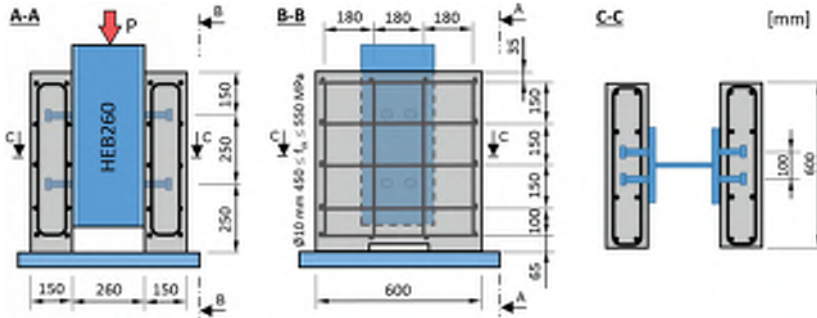

Figure 2.6 *Test specimen for standard push-out tests, from EN 1994-1-1 (2005)*

The brief presentation of the shear connection design, within this section, is far from complete. It is a selection of requirements and issues, which are considered to be of interest for the research presented later in this thesis. The complete set of requirements is provided by EN 1994-2 (2005) and its reference standards.

2.4   Advantages of composite bridges

As highlighted in the introduction of this chapter, steel-concrete composite bridges are characterized by an efficient use of the ingoing materials, utilizing the high tensile strength of the steel and the high compressive strength of the concrete (El Sarraf et al. 2013, Hanswille 2011a). Hanswille (2011a) also highlights the high durability and the robustness of this type of bridges.

A combination of high-strength steel and composite action enables slender and aesthetic structures, which might have increased the competitiveness of composite bridges (Collin & Lundmark 2002, Hanswille 2011a). The normal span to depth ratio is often within the range of 20-30 m, if there are no project specific restrictions on the girder depth (Kuhlmann et al. 2008b).

In comparison to in-situ cast concrete bridges, composite bridges have a large benefit concerning the degree of prefabrication. The prefabricated steel girders can carry the weight of the formwork and the fresh concrete and also be launched, or lifted, into the final position with minimum or no impact on the activities on the ground below. This makes this type of bridge competitive especially in situations where it is hard, or even impossible, to find space for temporary supports (Collin & Lundmark 2002, Hanswille 2011a). Examples of such situations are bridges over water, roads, railways etc., see Figure 2.7a–c.

(a) Composite bridge over railway

(b) Composite bridge over water

(c) Composite bridge over motorway

(d) Scaffolding for concrete bridge

Figure 2.7 (a)-(c) Examples of composite bridges, (d) In-situ cast concrete bridge under construction

Figure 2.7d illustrates the differences in comparison to an in-situ cast concrete bridge, where a lot of temporary scaffolding often are used to carry the weight of the formwork and the fresh concrete, prior to the hardening. However, it should be noted that also concrete bridge girders can be prefabricated, partly or totally, and that movable scaffolding systems or incremental launching techniques can enable concrete bridge construction without access to the ground below. A comparison of these two techniques are presented by El Hamad & Tanhan (2018).

Short span bridges, with spans up to 30 m, are often built as concrete bridges, while the benefits of composite bridges increase for longer spans. The significantly lower weight enables longer spans, limited by the strength of the superstructure or the strength of the foundation and the corresponding settlements (Hanswille 2011a). El Sarraf et al. (2013) presents potential span ranges for different types of road bridge superstructures, combined with information about economic span lengths as well, see Figure 2.8. The numbers are from New Zealand and might be affected by local requirements and traditions, but can be used as a general indication of suitable types of superstructures for road bridges in different span ranges.
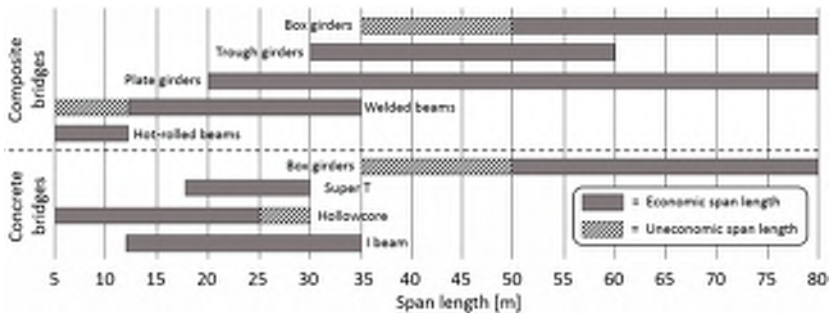
Figure 2.8 Suitable road bridge superstructures for different span ranges (after El Sarraf et al. 2013)

Traditionally, the bridge alternative with the lowest initial cost has often been the one that has been built. Nowadays, there are several other factors that should be taken into account when a proper structure, or strengthening method, is chosen, Example of such factors are CO_2-emission, impact on road users, working environment, social environment, maintenance aspects etc. There are different approaches of how to deal with the different type of factors. One holistic approach that considers the sustainability of steel-composite bridges during the entire life-cycle has been presented by Kuhlmann et al. (2013). This approach is primary based on three different components: Life-cycle Assessment (LCA), Life-cycle Costs (LCC) and Functionality analyses. Where LCA represents the environmental quality, LCC the economic quality and Functionality analysis the social and functional quality.

As highlighted above, there are many factors and aspects that need to be taken into account when choosing, or designing, an appropriate bridge structure. In the end, the optimal structure for the society is often a compromise between different aspects, strongly dependent on how these aspects are weighted. In the remainder of the thesis, the author has investigated two different methods to reduce the impact on the road users, when new bridges are built or existing bridges strengthened. Chapter 3 is focused on prefabricated composite bridges in general, and particular on a prefabrication concept with prefabricated concrete deck elements with dry joint. While Chapter 4 is focused on strengthening by post-installation of shear connector in general and Coiled Spring Pins in particular.

Chapter 3

PREFABRICATED COMPOSITE BRIDGES

In order to shorten the time spent on the construction sites, different prefabrication techniques can be used. The degree of prefabrication spans from single elements to entire structures, fabricated off-site and then transported to the site and erected in a matter of hours or days, instead of months. This chapter deals with prefabrication of composite bridges in general and concrete deck elements in particular.

The chapter is complemented by the appended Paper I-V, which give more detailed information about the research. Additional information is also provided in the previously presented licentiate thesis by the present author (Hällmark 2012a).

3.1   Introduction

The time spent on a bridge site can often be shortened by using a more industrial approach to the construction process. The definition of the term "industrial", in the construction industry, seems to vary from one author to another. Simonsson (2008) gives some examples of different interpretations, and defines also his own definition as: "a modernisation process of the construction industry for a smarter and more sustainable production". One philosophy that often is mentioned together with industrialised construction is lean production.

Lean production is an approach that was started by Toyota in the middle of the 20th century. Womack et al. (2003) describes the lean thinking concept in detail. Briefly, it is all about eliminating waste (Muda) from the production process, and to do "more and more with less and less" as Womack et al. (2003) writes.

If lean production is applied on a bridge construction process, the aim is to minimize the waste activities. The first step might be to prefabricate reinforcement cages to the supports or to use reinforcement carpets, which are rolled out on site as deck reinforcement.

Another waste activity is the concrete compaction work task. If traditional vibrated concrete is replaced by self-compacting concrete (SCC), it would be possible to eliminate this work task. These examples can all be classified as industrial in-situ construction.

In order to shorten the time spent on the construction site even more, industrial prefabrication can be applied. This means that construction elements are produced off-site in a controlled workshop environment, under strict environmental- and quality-controls.

Prefabrication offers several advantages but also some disadvantages. Some of the main advantages and disadvantages are presented in Paper II and briefly listed below (Culmo 2009, Hällmark et al. 2009, NCHRP 2003).

Advantages: Reduction of the construction time on-site; reduced impact on the traffic and the environment; lower road user costs; production performed in a controlled indoor climate; improved working environment and safety.

Disadvantages: Tighter tolerances; increased need of control programs; lack of experience among designers and contractors; non-standardized details.

Traditionally, the road user costs have often been neglected when different design alternatives have been compared. A study done in the US, shows that the initial monetary costs of prefabricated bridges are often a bit higher, or comparable, with the costs of bridges constructed with traditional on-site techniques (NCHRP 2003). However, Culmo (2009) indicates that the state traffic agencies in the US that use prefabrication more frequently have lowered the initial costs significantly. If the road user costs are taken into account, the traditional construction technique tends to be more expensive. Similar conclusions have also been presented by Nilsson (2001) and Degerman (2002), based on two Swedish case studies. In recent years, the Swedish Transport Administration (Trafikverket) has introduced a mandatory requirement to perform life cycle cost analysis (LCC) including the road user costs, in the early stage of the design process before choosing the appropriate type of structure. Such a change can promote the use of prefabricated structures, when it is appropriate. Paper I and II are both dealing with economic issues concerning prefabricated bridge construction. This issue is also discussed in the Final Report from the RFCS-project *ELEM* (Möller et al. 2012a).

Although prefabrication is possible for all structural parts of a bridge structure, the superstructure tends to be the bridge component that is most suitable for prefabrication, according to a survey performed in the US (NCHRP 2003). This thesis is also limited to the bridge superstructure.

3.2   Prefabricated superstructures of composite bridges

There are different degrees of prefabrication for composite bridge superstructures. From a low degree of prefabrication, where only the steel girders are prefabricated, up to prefabrication of the entire bridge structure. The author has defined five levels of prefabrication illustrated in Figure 3.1.
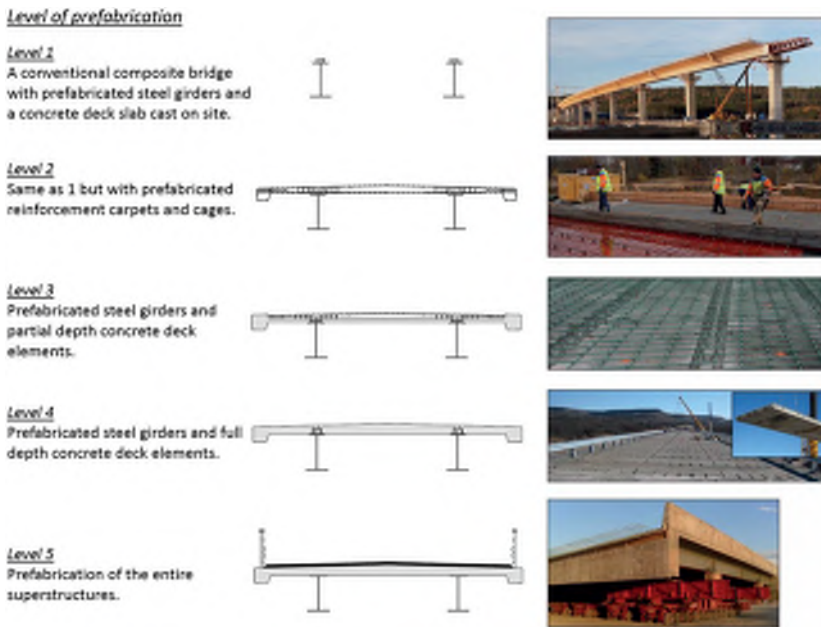
Figure 3.1 *Different levels of prefabrication for composite bridge structures.*

As a part of the research, a state-of-the-art review was performed on prefabricated bridge construction. This study is presented in Paper I and complemented by additional examples in Hällmark (2012a). Similar studies have been presented by Collin et al. (1998), Ralls et al. (2005) and Gordon & May (2007) among others.

From the US, the Accelerated Bridge Construction (ABC) approach should be highlighted, where prefabrication of bridge components is a vital part. Several ABC-projects and different design solutions are presented by FHWA (2018a, 2018b), NCHRP (2009), Culmo (2011) and Culmo et al. (2017), among others. There are, however, numerous examples of prefabricated composite bridge superstructures from all over the world. A few examples from Asia are given by Shim et al. (2010), while Berthellemy (2009), Seidl et al. (2009a,b) and Möller et al. (2012a) presents some European examples.

3.3   Prefabricated concrete deck elements

Roughly speaking, there are two types of prefabricated concrete deck elements, partial depth elements and full depth elements.

Partial depth elements are used as collaborating formwork, requiring on-site reinforcement work and in-situ concreting of the upper part of the deck slab.

In contrast to partial depth elements, full depth elements only requires in-situ concreting of the longitudinal joints between the steel girders and the concrete deck elements, and in most cases also in the transverse joints between the elements. Some reinforcement work is also often needed in the transverse joints between the elements.

The research presented in the remainder of this chapter is limited to a prefabrication level corresponding to Level 4 in Figure 3.1, i.e. prefabricated steel girders and full depth concrete deck elements. In the two following sections, the different types of joints will be in focus.

3.3.1 Longitudinal joints

A literature review performed by the author indicates that the design of the longitudinal joints varies a lot between different project and countries. The author has chosen to divide the type of longitudinal joints into four different groups, depending on the design of the recesses for the in-situ cast concrete, see Figure 3.2.
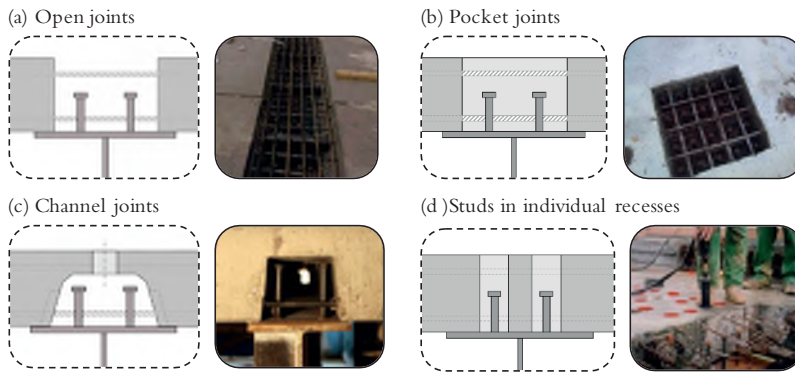
(a) Open joints

(b) Pocket joints

(c) Channel joints

(d) Studs in individual recesses

Figure 3.2 *Different types of longitudinal joints in prefabricated concrete deck elements*

Open joints (a) seems to be the most common solution, examples can be found from Sweden, Finland, USA, France etc. (Collin et al. 1998, Hällmark et al. 2012b, Culmo 2011). The pocket joints (b), with grouped shear connectors, are also quite common and experiences from this type of joints is presented by Collin et al. (1998), Ralls et al. (2005) and Shim et al. (2010) among others. The injection channel joints (c), have been used successfully in several countries (Stoltz 2001, Hällmark et al. 2009, 2012b), while experiences from the on-site welding of studs in individual recesses (d) only have been found in France (Berthellemy 2009, Ralls et al. 2005).

A more detailed review of the different type of longitudinal joints, and their pros and cons, is presented in (Hällmark 2012a) and (Möller et al. 2012a).

3.3.2 Transverse joints

The literature review indicate that an in-situ cast joint is, by far, the most common type of joint between two prefabricated concrete deck elements, the transverse joint. This

type of joint is denoted "wet joint" in this thesis and covers a huge amount of different types of detailing. Some examples of wet joints are shown in Figure 3.3 and are presented more detailed in (Hällmark 2012a).
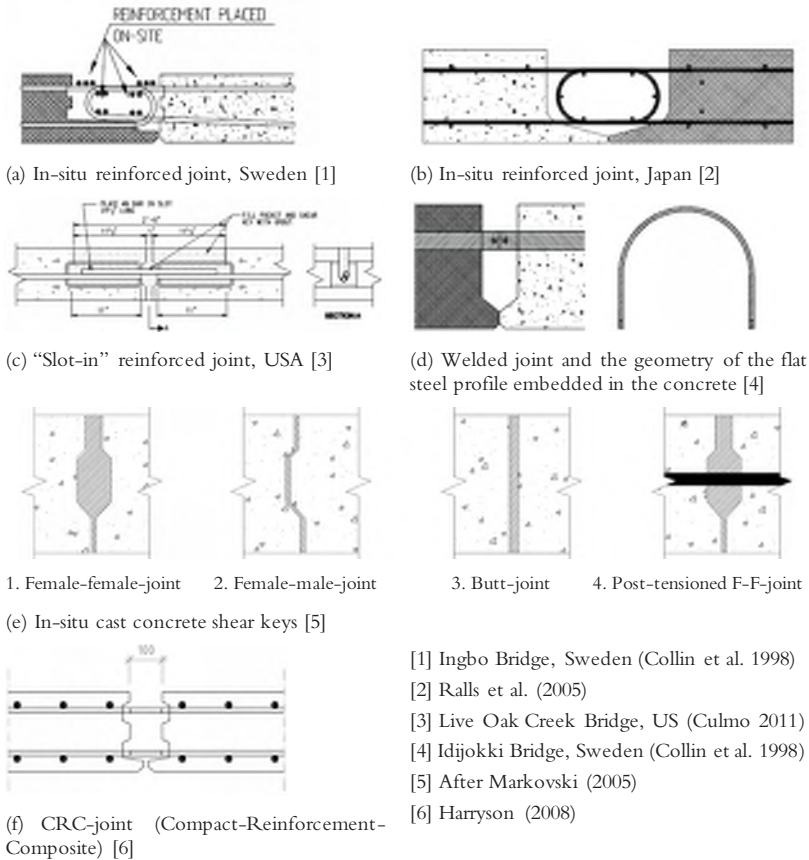
(a) In-situ reinforced joint, Sweden [1]

(b) In-situ reinforced joint, Japan [2]

(c) "Slot-in" reinforced joint, USA [3]

(d) Welded joint and the geometry of the flat steel profile embedded in the concrete [4]

1. Female-female-joint   2. Female-male-joint

3. Butt-joint   4. Post-tensioned F-F-joint

(e) In-situ cast concrete shear keys [5]

[1] Ingbo Bridge, Sweden (Collin et al. 1998)
[2] Ralls et al. (2005)
[3] Live Oak Creek Bridge, US (Culmo 2011)
[4] Idijokki Bridge, Sweden (Collin et al. 1998)
[5] After Markovski (2005)
[6] Harryson (2008)

(f) CRC-joint (Compact-Reinforcement–Composite) [6]

Figure 3.3 *Examples of wet joints*

To shorten the time spent on the construction sites even more, a prefabricated concrete deck system with dry joints can be used. A transverse joint must be capable of transferring the vertical and the horizontal shear forces from one side of the joint to the other. If the deck elements are pre-stressed by a clamping force, it would be possible to make use of the friction between the elements to create a dry joint. However, creep and shrinkage must be considered during the lifetime of the bridge. Another possible solution is to use overlapping concrete shear keys to transfer the shear forces. The research presented in this chapter is focused on the latter one.

Dry joints with shear keys have been used in different type of superstructures, from pre-tensioned segmental concrete bridges to composite bridges with and without pre-stressing tendons. Hewson (2003) presents some examples of different designs of dry joints with shear keys in pre-tensioned segmental bridges, while Berthellemy (2009), Möller et al. (2012a) and Collin et al. (1998) reports about some French, German and Swedish experiences from composite bridges with pre-tensioned prefabricated concrete deck elements with dry joints, see Figure 3.4a–b.

(a) Prefabricated bridge deck element with dry joints, France (Berthellemy 2009)

(b) Dry joints with linear shear keys, Germany (Möller et al. 2012a)
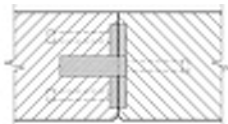

(c) Dry joints with overlapping conrete shear keys, Sweden (Hällmark 2012a)

Figure 3.4 *Examples of different types of dry joints in prefabricated concrete deck elements*

In contrast to the other examples, there are some Swedish experiences from single span composite bridges without any pre-stressing tendons (Collin et al. 1998, Stoltz 2001), see Figure 3.4c. The deck elements have, however, been clamped together by bolting the prefabricated back walls to the end plate on the steel girders. This results in an initial compressive force in the concrete deck, which might be regarded as a form of pre-stressing, but it is mainly used to minimise the gaps in the dry joints, prior to the in-situ concreting of the longitudinal joints.
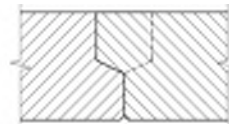
The Swedish design of the shear keys has varied from stainless steel rods to concrete shear keys, see Figure 3.5a–c, where alternative (c) is the latest design.

(a) Stainless steel stud   (b)Internal shear key   (c) Overlapping shear keys

Figure 3.5 *Swedish examples of different shear keys used in concrete deck elements with dry joints*

Although there are many interesting research questions among both wet- and dry-joints, the research on prefabricated bridge deck elements, performed by the author, has been limited to prefabricated elements with dry-joints with overlapping shear keys of the type shown in Figure 3.5c.

3.4   Prefabricated concrete deck elements with dry joints

The type of prefabricated concrete deck elements that has been in focus, in the research conducted by the present author, is briefly presented in this section by describing the prefabrication concept from the manufacturing process to the final assembly. Paper II gives a more detailed overview of the design, manufacturing and erection procedure, together with a summary of experiences from bridge projects in which this type of prefabrication concept has been used.

The design of this concept is characterised by a high degree of prefabrication, utilizing longitudinal channel joints and dry transverse joints (see Figure 3.2c and Figure 3.4c) to get a cured concrete deck surface directly after the installation, excluding the local injection holes (Ø100 mm) for the casting of the longitudinal joints.

This type of prefabricated concrete elements deviates from other concepts in that sense that they have totally dry transverse joints between the elements, in combination with no external or internal pre-stressing tendons. The shear forces are transferred from one element to another by overlapping concrete shear keys. The design of the joints can be seen in Figure 3.6, which shows pictures from the erection of two Swedish bridges that have been built with this concept (Hällmark et al. 2009).

Figure 3.6 Erection of elements at the Norrfors Bridge (left) and the Rokån bridge (right)

The overlapping shear keys imply that the elements must be erected with a longitudinal displacement larger than the depth of the shear keys. The assembly tolerances, between the reinforcement bars in the bottom of the elements and the shear studs at the steel girder top flanges, are tight and crucial for the installation process, as illustrated in Figure 3.7.
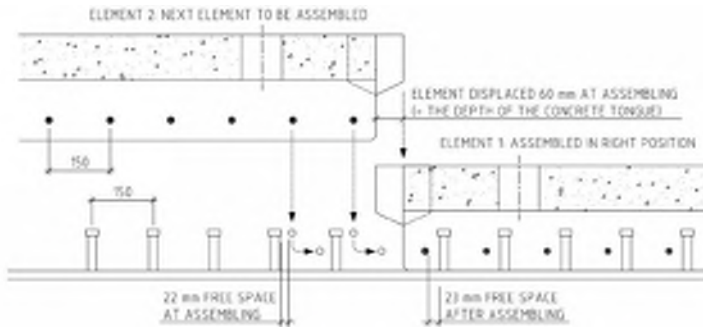
Figure 3.7 *Illustration of the tight tolerances during installation (Hällmark et al. 2009)*

The concrete elements must be manufactured with very tight tolerances, both regarding the geometry of the elements and the positions of the reinforcement bars. The elements are always match-cast, with the previous cast element as formwork on one side and a steel formwork on the other sides. To assure that the elements will fit into each other, it is necessary to cast the elements in the same order as they will be erected on-site. So far, the described concept has been implemented successfully on bridges with lengths up to 30 m. By using additional control programs, at the bridge site and in the steel- and concrete-workshops, it should be possible to implement the concept on bridges up to ~40 m without using wet-joints. For longer bridges, the tight tolerances will probably make it necessary to use some wet joints in order to reset the cumulative errors in relation to the ideal geometry. (Hällmark et al. 2009)

When all elements are in their final positions, the joint gaps can be reduced by pushing the elements together. This can be done by pulling the prefabricated end-screen elements against the deck elements, by using pre-stressed threaded bars between the steel girder end-plate and the end-screen element, see Figure 3.8.
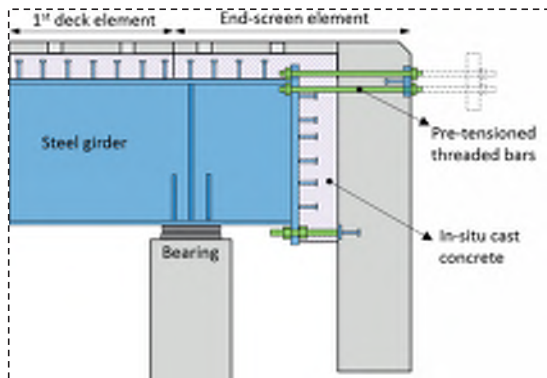

Figure 3.8 *Illustration of how a clamping force can be applied prior to the injection of the channels*

After the elements have been pushed together, the channels are injected with a suitable concrete through the injection holes at the top surface, see Figure 3.9. In order to avoid air entrapment, air release holes (Ø16 mm) have been used every 300–400 mm.
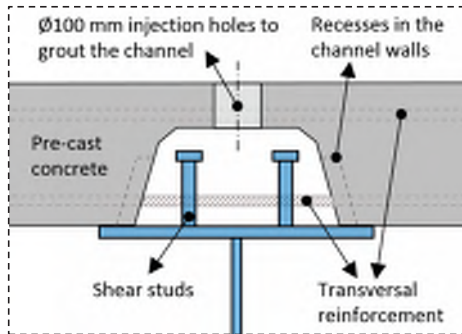

Figure 3.9 *Illustration of the design of the longitudinal joint*

After the channels have been injected, the waterproofing can be installed almost immediately, since the concrete top surface is made of prefabricated concrete, with the exception of the injection holes. The next step is to add pavement to the bridge surface and then take it into service.

The prefabrication concept described in this section has been investigated by the author, in order to get a better understanding of the structural behaviour and to contribute to a progress towards general design guidelines for this type of bridges. The research has been focused on three aspects; structural behaviour, shear keys and design and production issues. These three aspects are in focus in the following sections.

3.4.1 Structural behaviour

The structural behaviour has been investigated through large-scale tests, performed in the MCE-Lab at LTU, and by field monitoring performed on a single span bridge constructed in line with the studied concept, see Figure 3.10. The results from the tests have been evaluated and compared to FE-models as well as suggested design models.

Figure 3.10 *Large-scale laboratory test (left) and field monitoring of the Rokån Bridge (right)*

This section gives a brief summary of the tests and the outcome, while more details are presented in the appended Paper IV and V. Paper IV describes the field monitoring of the Rokån Bridge, while Paper V presents the large-scale laboratory tests. The author's licentiate thesis (Hällmark 2012a) provides additional results and detailed drawings of the specimens and the test set-ups.

Field monitoring test set–up and test program

In year 2000, the Rokån Bridge was built in the northern part of Sweden. This 16.2 m long single span bridge was designed and constructed in line with the prefabrication concept presented in this thesis. In 2001, the bridge was monitored in order to study the structural behaviour. This field monitoring and the conducted laboratory tests have all been focused on the short-term behaviour, except the fatigue test presented in Paper II. In order to study the long-term behaviour of this type of bridge, a second field monitoring was performed on the same bridge, in year 2011. Paper IV describes the new field monitoring in detail, while this section gives a brief summary of the test set-up and the test program.

The monitoring was focused on the steel girder strains and the deflection of the steel girders. In order to make it easier to compare the test results from year 2001 and 2011, the measuring sensors were all placed in the same positions in both tests. The deflections were measured at the supports and in midspan on both steel girders, while the steel strains were measured in three sections in one of the girders and in two sections in the other. Figure 3.11 shows a schematic illustration of how the bridge was monitored.
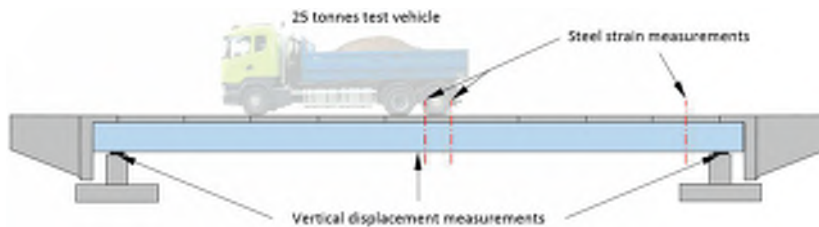
Figure 3.11 *Schematic illustration of the monitoring of the Rokån Bridge*

Before the tests started, the truck was weighted and the aimed load positions were marked on the pavement in both the longitudinal and the transversal directions. The truck was driven over the bridge along three longitudinal lines: the centre line of the bridge and the centre lines of each girder. The test vehicle was stopped at two designated positions along each line. The first stop was when the front axle was in the middle of the span, and the second stop was when the bogie was centred at midspan. A similar load pattern was used in year 2001.

**Large–scale test set–up, specimen and test program**

The non–destructive large-scale tests were performed on one single specimen, which was designed to enable two different test set-ups. The first test set-up simulated an internal support with negative bending moment, while the second test set-up simulated a midspan section under positive bending moment, as illustrated in Figure 3.12.

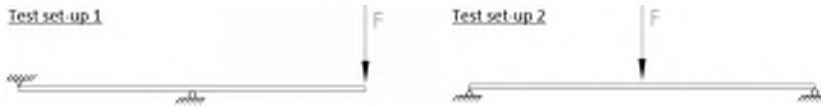**Figure 3.12** *Schematic illustration of test set-up 1 and 2*

The specimen consisted of four prefabricated concrete deck elements and two steel I-girders. The transverse deck joints were designed as dry joints with overlapping shear keys, while composite action was achieved by in-situ casting of the longitudinal joints. The concrete deck elements were designed with shear keys in scale 1:1, in comparison to the previously used shear keys in real structures. The lengths of the concrete elements were 1.8 m, i.e. the distance between the dry joints, which corresponds well to the dimensions used in real bridges. The outer dimensions of the complete large-scale specimen were 7.2 x 3.5 x 1.1 m.

Five different types of measurements, excluding the measured force and stroke in the hydraulic actuator, were conducted during the tests: steel girder strains, concrete strains, reinforcement bar strains, vertical displacements and joint openings. A schematic illustration of the instrumentation of the specimen is shown in Figure 3.13.

Thirteen tests were performed on the specimen, in line with the test program presented in Table 3.1.

Table 3.1 *Test program for the large-scale laboratory tests*

| Test no:	Type of load situation	F [kN]	Load cycles
Test 1	Set-up 1 – one point load	100	–
Test 2	Set-up 1 – one point load	280	–
Test 3	Set-up 1 – two point loads	310	–
Test 4	Set-up 1 – two point loads	430	–
Test 5	Set-up 1 – two point loads	5-250	50
Test 6	Set-up 1 – one point load	250	–
Test 7	Set-up 1 – two point loads	400	–
Test 8	Set-up 1 – two point loads	5-250	50
Test 9	Set-up 2 – two point loads	500	–
Test 10	Set-up 2 – two point loads	5-450	100
Test 11	Set-up 2 – one point loads	300	–
Test 12	Set-up 2 – one point loads	450	–
Test 13	Set-up 2 – one point loads	5-400	100
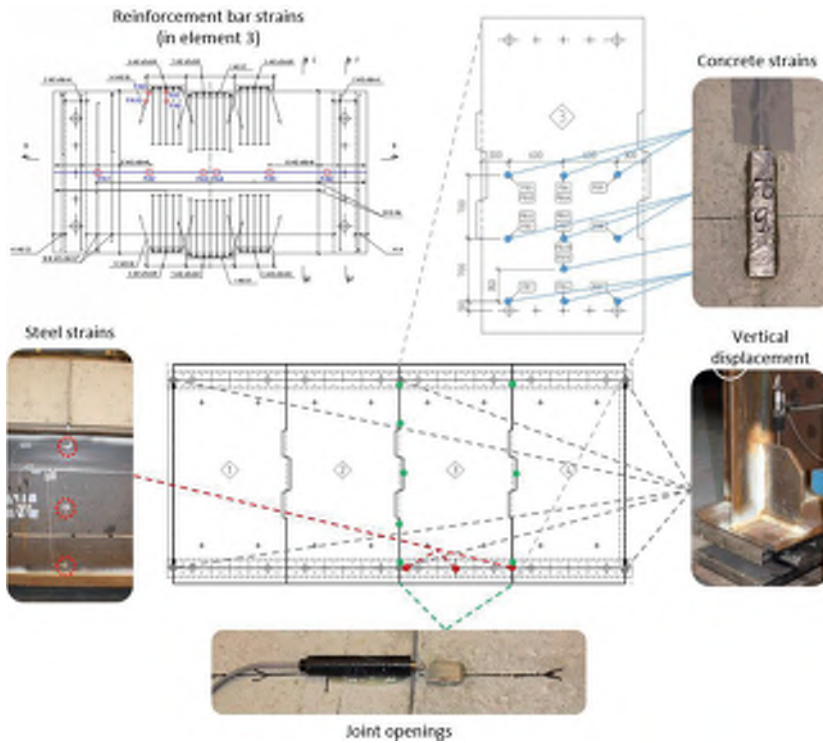
Figure 3.13 *Schematic illustration of the instrumentation of the large-scale test specimen*

<u>*Test results and analysis*</u>

The test results from the large-scale tests and the bridge monitoring are briefly presented and analysed in this section. A complete presentation of all results is provided in Hällmark (2012a).

Composite action – interacting concrete area

The results, from the laboratory tests and the field monitoring, indicate that a cross-section in a prefabricated composite bridge with dry deck joints has a lower stiffness than a corresponding cross-section in a composite bridge with an in-situ cast bridge deck (Hällmark et al. 2012a, 2013a, 2013b).

In regions with negative bending moments, near internal supports, the results from the tests and the FE-analysis show that the global stiffness contribution from the concrete deck is negligible. The measured strains in the steel, concrete and reinforcement bars, as well as the measured deflections, are all indicating the same (Hällmark et al. 2012a, 2013b). The limited contribution from the concrete deck was expected, since the forces

carried by the composite section must enter and leave the concrete deck every 1.5 m, which corresponds to the distance between the outmost shear studs within an element.

In regions with positive bending moments, midspan regions, the concrete in compression will contribute to the global stiffness. However, results from laboratory tests and field monitoring indicate that the interacting concrete area is less than the interacting area in a corresponding cross-section with an in-situ cast concrete deck slab (Hällmark et al. 2013a, 2013b). The strain measurements, and the comparative calculations, indicate an effective width of the concrete deck slab, in SLS (Serviceability Limit State) and FLS (Fatigue Limit State), which on the safe side can be estimated by assuming an equivalent span (L_e) equal to the longitudinal distance between the outmost shear studs within an element (Hällmark et al. 2012a, 2013b). This observation is also verified by similar tests performed at Rheinisch-Westfaelische Technische Hochschule (RWTH), reported by Möller et al. (2012a).

The magnitude of the initial joint gaps are differing a lot between the Swedish and the German tests. In the tests reported by Hällmark et al. (2013b), the initial joint gaps were all less than 0.5 mm, while joint gaps with magnitudes of 1-5 mm were reported by Möller et al. (2012a). The deflection measurements in the latter tests indicated an initial effective concrete width corresponding to the width on the in-situ cast channels. These results, all together, indicate that the combination of intermittent joint gaps and continuous in-situ cast channels will influence the initial stiffness, even if the gaps are very small. The reason to the large differences in the initial joint gaps, between the tests reported by Hällmark et al. (2013b) and Möller et al. (2012a), can be explained by differences in the manufacturing of the concrete deck elements. The Swedish tests utilized match-casting, with the previous cast element as formwork on one side of the next element, while a steel formwork was used for the German elements. The measurements show that the initial gap of the match-cast joints were about ten times smaller than the initial gaps between elements cast in steel formwork.

The tests reported in (Hällmark et al. 2013a, 2013b) were all non-destructive tests performed to study the behaviour in SLS and FLS. The research project partners at RWTH performed tests on a similar type of large-scale specimens, but loaded the beams until failure. These tests were performed to study the behaviour in the Ultimate Limit State (ULS) and are reported in (Möller et al. 2012a). The latter tests indicate that the magnitude of the initial joint gaps will influence the ultimate capacity of the composite section, since the stress concentrations in the concrete contact areas will increase with an increasing initial gap, governing the initial concrete failure. Figure 3.14 shows the load-displacement curves from the tests, where the specimens VT1 − VT3 had prefabricated concrete deck elements, while specimen VT4 was a reference test with an in-situ cast deck slab. The test results indicate that the stiffness, as well as the ultimate capacity, of a composite section with dry deck joints is somewhat lower in comparison to a corresponding composite section with an in-situ cast deck. The test results also indicate that the load capacity is affected by the magnitude of the initial joint gaps. However, the tested capacity still reaches, or almost reaches, the calculated ultimate limit capacity (P_{calc}) according to EN 1994-2 (2005). The latter is calculated with tested values of the material parameters and without partial safety factors (Möller et al. 2012a). These observations

indicate that there is no large reduction of the effective width of the interacting concrete in the ULS, in comparison to the model suggested by EN 1994-2 (2005), even though the initial joint gaps are far larger than the recommended tolerances, see section 3.4.3. However, due to the limited number of test results available, it might be appropriate with some reduction of the interacting concrete area.
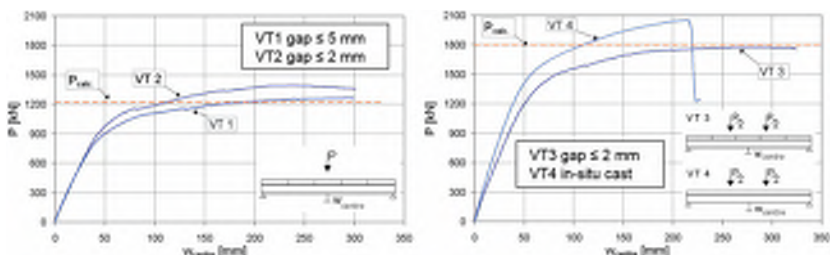

Figure 3.14 *Load-displacement curves for the large-scale tests reported in Möller et al. (2012a)*

Joint openings

To protect the concrete top surface from degradation due to water, chlorides etc., waterproofing layers are often used. A negative bending moment, resulting in tensile stresses in the concrete deck, will cause an elongation of the waterproofing over a very short distance near the joints. This may result in a rupture of the waterproofing layers and lead to leakage through the joints. Therefore, it is important to distribute the elongation of the waterproofing over a longer distance, which implies that the waterproofing layers cannot be completely fixed to the concrete deck slab near an opening joint. Fatigue tests of the waterproofing and the pavement have been performed, at KTH (The Royal Institute of Technology in Stockholm), to investigate the durability of different waterproofing solutions. The results and conclusions from these tests are presented by Möller et al. (2012a) and briefly summarised in (Hällmark 2012a).

The detailed design of the waterproofing is out of scope for this thesis. However, the magnitude of the joint opening, due to negative bending moments, is of interest as a design criterion for the waterproofing and for the pavement. Based on the large-scale test results reported in (Hällmark et al. 2013b, Hällmark 2012a), a design model to estimate the joint openings (δ_j) has been suggested, see (3.1).

$$\delta_j = \frac{M_{mean}/W_{tf}}{E_a} \cdot \frac{(e_{CG}+h_{conc})}{e_{CG}} \cdot L_{elem} \qquad (3.1)$$

M_{mean} = mean value of the moment distributed over the length of one element

W_{tf} = elastic section modulus at the upper side of the top flange

e_{CG} = vertical position of the neutral bending axis with the origin at the steel concrete interface, with positive values downwards (0.400 m)

h_{conc} = concrete deck thickness (0.290 m)

L_{elem} = concrete deck element length (1.800 m)

E_a = elastic modulus for the structural steel (210 GPa)

The previously presented results, regarding the degree of composite action, for a section under negative bending moment indicate that it is reasonable to assume no composite action at all in such sections. Therefore, the joint openings are estimated based on the stiffness of the steel girder alone. Table 3.2 shows a comparison between the estimated joint opening (δ_j) and the measured joints opening ($\delta_{j,meas}$) above an internal support, tested at different load levels (P) in the large scale tests reported in (Hällmark 2012a). The measured joint openings are ~10-20% lower than the openings calculated in line with equation (3.1), with an absolute difference less than 0.2 mm. This comparison indicate that equation (3.1) gives conservative results and that it can be used to establish the design criterion for the elongation of the waterproofing.

Table 3.2 *Theoretical joint openings vs. measured joint openings*

	P [kN]	M_{mean} [kNm]	δ_j [mm]	$\delta_{j,meas.}$ [mm]
Test 1	100	147	−0.38	−0.30
Test 2	280	412	−1.08	−0.95
Test 3	310	456	−1.19	−1.02
Test 4	430	633	−1.65	−1.49
Test 5	250	368	−0.96	−0.80
Test 6	250	368	−0.96	−0.83
Test 7	400	589	−1.54	−1.33
Test 8	250	368	−0.96	−0.81

Long-term behaviour

The long-term behaviour, of a prefabricated bridge of this type, has been studied by a comparison of the results from two field-monitoring occasions at the Rokån Bridge, performed in 2001 and 2011, respectively.

From the test results for the eccentric load cases, it can be noted that the distribution of the deflection between the loaded girder and the passive girder has changed from year 2001 to 2011. The relative deflection of the passive girder in relation to the active girder, was 0.4 in the previous test and 0.3 in the latter test, with a magnitude of the scatter as low as +/- 0.01. This difference might indicate that there were larger joint gaps in 2001, which might have been closed or partly closed during the time elapsed between the tests (10 years). One possible explanation is that there has been an abrasion of irregularities at the concrete contact surfaces, giving a better distribution of forces over the joint. If this was the case, the deflection of the bridge due to the weight of the structure should have increased over time. However, since the absolute vertical positions of the girders were not measured in 2001, it was hard to verify this effect ten years later. Even if the data had been available, it would have been hard to identify this effect among the effects of the concrete creep and shrinkage.

It can also be noted that the studied bridge was inspected in 2014, by the Swedish Transport Administration, and no comments related to the dry joints were made in the subsequent report.

Recommendations for the structural design

Based on the test results presented above, and in Paper IV-V, design recommendations for the structural analysis and the cross-sectional design are presented below.

Global analysis

EN 1994-2 5.4.1.2 - Effective width of flanges for shear lag:

Positive bending moment (concrete in compression):

ULS   A fairly similar behaviour as for in-situ cast concrete decks has been verified by (Möller et al. 2012a). Due to a limited amount of tests, and results somewhat lower than the results from a corresponding test with an in-situ cast deck, it is recommended to use only 80% of the interacting concrete area according to EN 1994-2 (2005).

SLS/FLS   It is recommended to use an equivalent span length (L_e) equal to the longitudinal distance between the outermost shear studs within an element.

Negative bending moment (concrete in tension):

ULS/SLS/FLS   It is recommended to use the bending stiffness of the steel cross-section alone, since the degree of composite action is very limited.

EN 1994-2. 5.4.2.3 (3) – Effects of cracking of concrete

Since there are no reinforcement bars crossing the dry joints, the moment of inertia (I_2) should be based on the equivalent effective steel cross-section without including the longitudinal reinforcement.

Resistance of cross-sections

If the concrete deck is in compression, both bending moments and normal forces taken into consideration, then the resistance can be checked according to the common rules given in EN 1994-2 (2005), but with 20% reduction of the interacting concrete area (factor 0.8). The reduction is due to the limited number of tests loaded until failure.

If the concrete deck is in tension, both bending moments and normal forces taken into consideration, the steel section should be designed to carry the entire load.

Concrete element design

The concrete element design can be performed according to EN 1992-1-1 (2004), EN 1992-2 (2005) and EN 1994-2 (2005). Specific recommendations for the shear key design are presented in next section.

Steel design

The steel girders are designed according to the general requirements in EN 1994-2 (2005) and the relevant parts of EN 1993, mainly EN 1993-1-1 (2005) and EN 1993-1-5 (2006). No specific recommendations are given for the studied type of structure. It should, however, be noted that the shear stud spacing can result in problems if it is not done in a proper way. More about this in section 3.4.3, about production issues.

3.4.2   Shear keys – shear strength

Shear keys are used to transfer vertical and lateral shear forces through the transverse joints, and to prevent vertical displacements between the adjacent deck elements. In the studied concept, the shear keys are designed as a series of overlapping male-female connections along the transverse joint, see Figure 3.15.
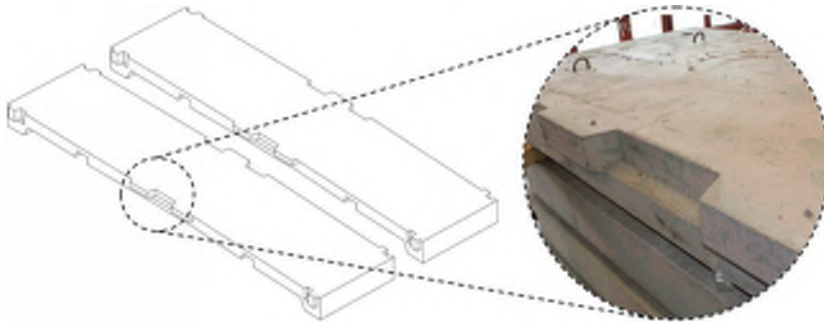

Figure 3.15 *Shear keys in prefabricated deck elements with dry joints*

The research concerning the shear keys is deviating a bit from the rest of the thesis, since it is focused on a concrete detail that can be used in different types of structures, not only composite bridges. However, the study of *prefabricated composite bridges with dry deck joints* would be somehow incomplete, if the shear keys would have been totally put aside from the study.

Laboratory tests of the shear key strength have primarily been performed to demonstrate that the shear key concept works, but also in order to get a better understanding of the static failure mode, to be able to predict the static strength with a rational design criterion. The tested shear keys were designed with a similar reinforcement layout as those previously used in real structures. It should be noted that no attempts have been made to optimize the layout of the reinforcement, since this is more a question of an optimization of a concrete detail.

The outcome of the laboratory tests are briefly presented in this section, while Paper III describes the tests in detail. The fatigue capacity of the shear keys has not been in focus in the research performed by the present author. However, the results from previously performed fatigue tests, by Stoltz (2001), are summarised in Paper II.

Test set–up, specimens and test program

A test series, focused on the vertical load transfer capacity of the studied shear keys, was conducted in 2010 at the MCE-Lab at LTU. The test specimens were designed to be representative to the design and behaviour of shear keys in real bridge decks. Different types of small push-out tests were initially considered, but later rejected to avoid situations where the applied load could be transferred directly into the supports, by inclined compressive struts. Focus was instead shifted to beam specimens, representing a strip of a real deck element. To avoid underestimations of the load distribution effects,

the specimens were given a width of 1300 mm, which can be compared to the 540 mm wide shear keys. Figure 3.16a–b presents the general geometry of the specimens, together with the reinforcement drawing for the Type 1 specimens, while Figure 3.17 shows as picture of the test set-up.
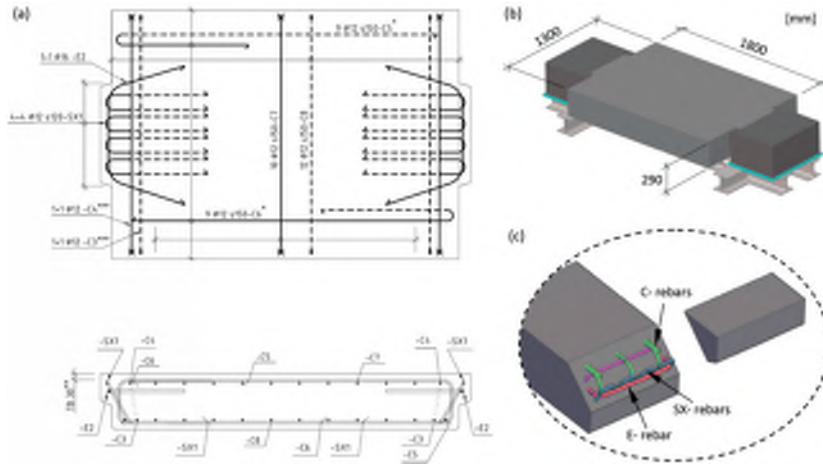

Figure 3.16 *General geometry of the test specimens and reinforcement layout for specimen Type 1*

Figure 3.17 *The shear key test set-up*

Each of the six specimens had two shear keys and the test set-up was designed to enable individual testing of both shear keys within an element, which implies that 12 shear keys were tested. All tests were performed with a displacement-controlled load that was increased until a failure occurred in the loaded shear key.

Three different layouts of the shear key reinforcement were studied, while the other parameters were kept constant. The reinforcement bars crossing the expected crack plane are schematically illustrated in Figure 3.16c. Four specimens were tested with Ø12 mm SX-rebars (SK1), four with Ø8 mm SX-rebars (SK2) and the last four without SX-rebars (SK3).

Prior to the tests, the forces transferred by the shear keys in a bridge deck were estimated by a FE-model representing a part of a typical superstructure for the bridges built, so far, with this prefabrication concept. The model, which is presented more in detail in Appendix A section A.3.1, indicate a required shear key strength of 180 kN and 120 kN for the large and the small shear keys, respectively.

Test results

In Table 3.3 the measured shear strength (V_{max}) is presented for the twelve tests, while Figure 3.18 shows the load-displacement curves. The plotted displacements (δ) are the vertical displacements at the position of the applied load.

Table 3.3 *Ultimate shear strength for the tested shear keys*

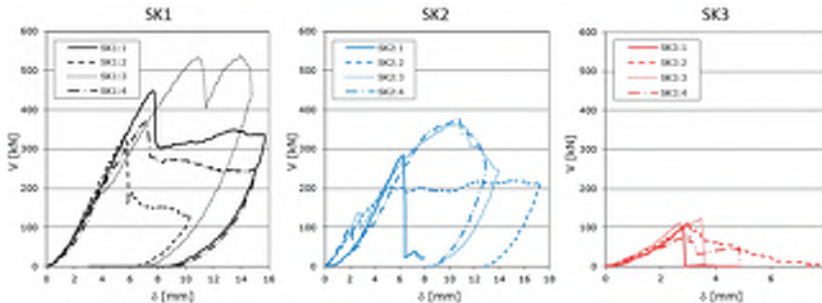|	V_{max} [kN]		V_{max} [kN]		V_{max} [kN]
SK1:1	449	SK2:1	285	SK3:1	104
SK1:2	337	SK2:2	222	SK3:2	114
SK1:3	532	SK2:3	363	SK3:3	123
SK1:4	370	SK2:4	376	SK3:4	82

Figure 3.18 *Load-displacement curves for the tested shear key specimens*

From the tests of the unreinforced shear keys, it can be noted that two out of four tests indicated a ductile post failure capacity, while the two other shear keys failed in a very brittle mode. Figure 3.19a shows a typical failure of the unreinforced shear keys. As expected, the unreinforced shear keys all failed to reach the capacity needed to resist the traffic loads given by EN 1991-2 (2005).

For the reinforced shear keys, two different kinds of failures were observed in the tests. The first type of failure was a ductile failure, observed in five out of eight tests, with crack planes that crossed the shear reinforcement (SX-bars), see Figure 3.19b. The second

type of failure occurred in three shear keys and was caused by crack planes developed outside the shear key reinforcement, see Figure 3.19c, resulting in a separation of the concrete cover layer. This type of failure occurred at lower load levels than the previously describe failure mode, but still at loads ~2-3 times higher than the failure load for the unreinforced shear keys. This gives an indication that there is a significant contribution from the reinforcement bars to the shear key strength, even if the final failure occurs outside the reinforcement bars.
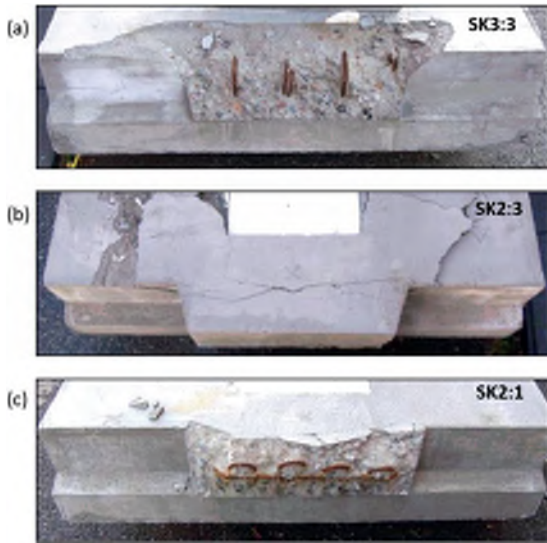

Figure 3.19 *Different types of shear key failures*

Analysis

One of the aims of the tests was to find a rational design model for the shear keys. In Paper III, four different design models have been compared to the test results:

    Model 1.   Classic beam linear elastic analysis (Betonghandboken 1990)
    Model 2.   Concrete capacity (EN 1992-1-1 2004)
    Model 3.   Reinforcement capacity (EN 1992-1-1 2004)
    Model 4.   Force equilibrium model

The comparison shows that:
    –   Model 1 and 2 can be useful for estimating the strength of the shear keys without reinforcement
    –   Model 3 gives results on the safe side, except when the failure occurs in the concrete cover layer

–   Model 4 gives to high estimations of the shear key strength. This indicates that the vertical reinforcement bars do not influence the strength at much as assumed in the model.

The test results show a considerable scatter, with different type of failure modes, which makes it hard to establish a general design criterion. Still there are some interesting observations that should be highlighted.

All reinforced shear keys showed a sufficient capacity compared to the design load, also the shear keys that failed in the concrete cover layer. However, it is important for the robustness that failures in the concrete cover layers can be avoided. To ensure the robustness, the shear reinforcement bars need to be positioned correctly. If the concrete cover layer is too large, it might result in a shear failure outside the shear reinforcement. Bad positioning of the reinforcement bars are believed to be a part of the reason why failures occurred in the concrete cover layers. Figure 3.20 illustrates the difference in the accuracy of the positioning of the reinforcement bars between the specimens presented in this section and the large-scale specimen presented in Paper V. It should be noted that similar tolerances were prescribed in both cases. These differences illustrate how important it is that the manufacturer strictly follows the established control program, in order to achieve the desired tolerances. It can be noted that the prior specimen (a) was manufactured in a local concrete workshop, while the latter specimen (b) was manufactured by a company specialized on prefabrication of concrete structures.
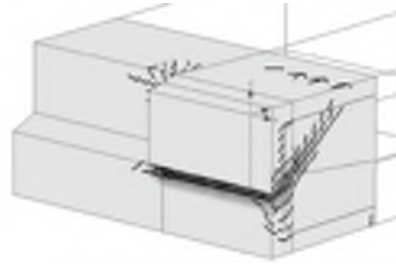

(a)   Shear key test specimen   (b)   Large-scale test specimen

Figure 3.20 *Differences in the accuracy of the shear key reinforcement positions*

When shear keys have been tested as a part of a complete superstructure, with steel girders and prefabricated concrete deck elements on top, failure in the concrete cover layer has not been observed (Stoltz 2001, Hällmark et al. 2009). After the non-destructive large-scale tests presented in Paper V, one of the joints was loaded until failure of the shear keys. Also in this test, there was no sign of cracking in the concrete cover layer. The cracks have instead been developed from the bottom of the shear keys and up to the concrete surface, activating the reinforcement, as shown in Figure 3.21a. This is the expected failure mode and also the failure mode predicted by FEM-modelling of the tests, performed by Mikael Hallgren (KTH), see Figure 3.21b.

(a) Photo of the expected type of failure   (b) Failure predicted by the FE-analysis

Figure 3.21 *Illustration of the expected failure mode*

Based on the observations presented above, the author's hypothesis is that the strength of the shear keys, within a structure, will be higher than the presented laboratory test results indicate, at least for single span bridges. This hypothesis is based on the fact that, in a real structure the surrounding elements will deflect together with the loaded element. This behaviour should result in larger contact surfaces that transfers the forces and also longitudinal compressive stresses in the upper part of the deck slab, which counteract the tensile stresses that occur due to the shear forces.

The results, from the previously performed fatigue tests and the static tests presented in this section, show that the previously used design of the shear keys (SK1) has a sufficient capacity to transfer the forces caused by the traffic loads in EN 1991-2 (2005), on the studied type of superstructure. The static tests also indicate that it would be possible do decrease the amount of shear reinforcement in the shear keys. However, if the shear reinforcement bars are changed from Ø12 mm to Ø8 mm, the reduced amount of steel will only be less than 20 kg/element, assuming the type of element previously used in Swedish bridges. The author recommends that further development of the shear keys should be focused on optimizing the layout of the shear reinforcement.

Recommended design criterion

With the available knowledge, it is recommended to design shear keys according to the formula for inclined shear reinforcement in EN 1992-1-1 (2004) equation (6.13), i.e. Model 3 presented in Paper III. This formula can be simplified for shear keys with inclined shear reinforcement bars in one single line,

$$V_{Rd,s} = A_{sw} f_{ywd} \sin \alpha \tag{3.2}$$

Where: $V_{Rd,s}$ is the shear strength

         A_{sw} is the cross-sectional area of the shear reinforcement

         f_{ywd} is the design yield strength of the shear reinforcement

         α is the inclination of the shear reinforcement related to the longitudinal axis of the superstructure

3.4.3 Production issues

This section summarizes the experiences from the production of test specimens as well as the experiences from the design and construction of three Swedish single span bridges in which the studied prefabrication concept has been used. Suggestions how to deal with the different production issues are briefly presented below, while a more detailed overview of the production issues are given in the attached design guidance in Appendix A. The latter is the present author's contribution to a public available design guide on composite bridges with prefabricated decks (Möller et al. 2012b), which was an outcome of the European research project ELEM, RFSR-CT-2008-00039.

It should be highlighted that the recommendations presented below are based on important production aspects and design details identified by the author. However, these examples do not claim to be comprehensive. It is likely that other bridge designers will identify additional critical aspects and encounter design problems that have been overlooked in this study.

Concrete elements

- Match-casting, together with an individual numbering of each element, is essential to ensure as small joint gaps as possible.

- The positions of the transversal reinforcement bars, in the bottom layer, are crucial to avoid collisions with the shear studs at installation. The formwork used to create the longitudinal recesses, the in-situ cast channels, can be used as templates for the positioning of the transversal reinforcement bars. Additional controls are needed to assure that the bars, or the templates, are in the right positions.

- It is recommended to measure the gaps in each joint by doing a test assembly in the concrete workshop. At this stage, without applying a clamping force, the mean values of the joint gaps have been allowed to be up to 1.0 mm, in the bridges built so far.

- To avoid damages, especially on the shear keys and the joint surfaces, the elements should be handled carefully during the transport and the erection.

- The bridge designer should prescribe lifting anchors and their positions, to ensure that the elements are lifted only in the pre-determined positions that have been designed for lifting.

- The in-situ cast channels, the injection holes and the air release holes should be designed to avoid air entrapment.

Steel girders

- The positions of the shear studs, in relation to the transverse bottom reinforcement bars, are crucial to avoid collisions under the erection of the elements. Additional control programs are needed, both in the steel- and the concrete-workshop as well as on the bridge site.

- It is strongly recommended to use 3D-models for the design drawings, to ensure that there are no collisions between the reinforcement bars and the shear studs, in any stage of the installation process.
- The recommended tolerances for the positioning of the shear studs is ± 5 mm. To avoid repetitions of the same type of error, the absolute position of the first and the last shear stud within an element should be checked.
- Prior to the erection of the first concrete element, it is recommended that the alignment of the steel girders is checked, to ensure that all elements can be installed without collisions.

Installation

- The concrete elements should be pushed against each other to minimize the joint gaps.
- After the elements have been pushed together, the mean value of the joint gap should be ≤ 0.40 mm. In Sweden, so far, a maximum gap of 1.5 mm has been allowed locally over a length of less than 1.0 m.
- For the in-situ cast channels, it is recommended to use a concrete suitable for injection, together with a full-scale test of the filling ability.
- It should be ensured that the air-release holes are open prior to the injection.

Waterproofing

The installation of the waterproofing is a bit off topic for this thesis. However, for multi-span continuous bridges it is very important that the waterproofing is properly designed, to avoid future maintenance problems due to water leakages in the joints. Within the RFCS-project ELEM, the project partners at KTH have performed some studies on the waterproofing, the results are briefly presented in Appendix A.

- For single-span bridges, conventional waterproofing systems can be used.
- For multi-span bridges, the durability of the standard waterproofing system must be improved to ensure that it can withstand the opening of the dry joints (Möller et al. 2012a).

Chapter 4

POST-INSTALLED SHEAR CONNECTORS

There are numerous types of strengthening techniques to keep existing structures in service and to enable higher loads or additional load cycles. This chapter deals with one specific method for one specific type of structure, which is post-installation of shear connectors in non-composite steel-concrete bridges. The research has been focused on a specific type of shear connector called Coiled Spring Pin.

The appended Paper VI-IX complement this chapter by providing additional and more detailed information about the research.

4.1 Introduction

The traffic density and the vehicle weight have been increasing over time and the tendency seems to continue (Lumsden 2004). This implies that many existing bridges experience higher traffic loads and higher number of load cycles than they originally were designed for. Finland and Sweden are two examples of countries that recently have increased the maximum allowed truck weight. In 2013, the maximum truck weight in Finland was increased in one step from 60 tonnes to 76 tonnes (Blanquart et al 2016). Sweden have performed a similar change but in two steps from 60 tonnes to 64 tonnes in 2015, and later up to 74 tonnes in 2018. The latter results in a need to assess approximately one thousand bridges in Sweden, according to an analysis presented by Trafikverket (2016).

To keep the existing bridges in service, despite the increased loads and number of load cycles, bridge assessment is often the first and the most cost effective method. If the assessment fails to confirm the required load capacity, an effective and well-designed strengthening method is often a very competitive alternative, both in economical and environmental terms, in comparison to a bridge replacement. The appropriate

strengthening methods vary between different types of bridges, but also from one bridge to another, since object specific conditions often need to be taken into account.

This thesis is limited to composite bridges, which is the commonly used method to design steel-concrete bridge structures nowadays. However, as late as the 1980s, many Swedish steel-concrete bridges were still designed as non-composite structures. This implies that there are quite a lot of bridges designed this way, which should have many years left of their technical lifetime. A survey within the Nordic countries, based on data from the National Transport Administrations bridge managing systems in Sweden, Finland and Norway, indicates that there are at least 2 000 bridges of this type only in these three countries.

One way of strengthening these bridges, is by creating composite action at the steel-concrete interface. The new composite cross-section will carry the traffic loads more efficiently than the non-composite section (see Figure 4.1 and Chapter 2), implying that the maximum allowed bending moment due to traffic loads often can be increased. Examples of bridges strengthened this way are reported by Peiris & Harik (2014), Kwon et al. (2009) and Olsson (2017).
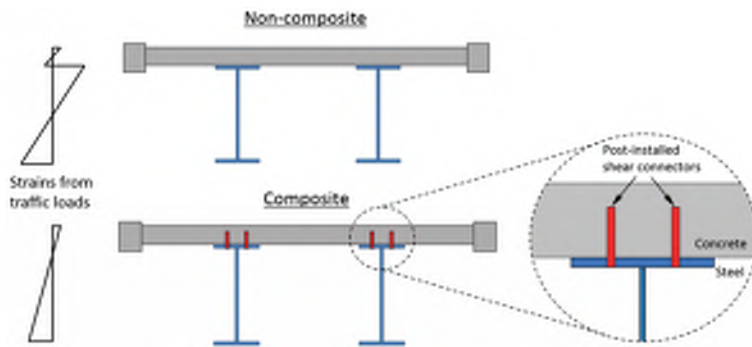

Figure 4.1 *Impact of post-installed shear connectors on the strains caused by the traffic loads*

The research presented in this thesis is focused on the shear connection, but it should be highlighted that there are several other structural details that need to be checked, to assure that the load capacity can be increased when a bridge is strengthened in this way. A few examples of details that need to be assessed are the transverse- and the longitudinal-reinforcement of the deck slab and the shear capacity of the steel girder web-plates. The assessment and strengthening of such details are out of scope for this thesis, but important issues that must be handled in the design of the bridge strengthening.

4.2   Post-installed shear connectors

Different types of shear connectors can be used to create composite action at the steel-concrete interfaces. For new composite structures, welded headed studs (WHS) are undoubtedly the most common type of shear connector. The welded studs offer an

effective installation procedure, with the drawn arch stud welding, which can be performed in a controlled environment in a steel workshop, with good access to the steel top flanges.

For an existing bridge, the benefits of using welded studs are fewer. The post-installation procedure requires access to the steel top flanges from above, which implies that any pavement, waterproofing and concrete above the steel flanges have to be removed. Such an operation would in most cases require the bridge to be closed or at least partly closed. If the bridge deck is in good condition, there are other types of shear connectors more suitable for post-installation than welded studs. The author has been particularly interested in connectors that can be installed from below the bridge, with no or minor impact on the traffic on the bridge.

Paper VI presents a review of different kinds of post-installed shear connectors, while a short summary is given below.

Even if the installation procedure for welded headed shear studs (Figure 4.2a) is a bit impractical in existing structures, they are still used and offer a well-known design and installation procedure covered by international design-, product- and installation-standards such as EN 1994-2 (2005), AASHTO (2017), ISO 13918 (2008) and ISO 14555 (2014).

Comprehensive research on different types of post-installed shear connectors has been performed at the University of Texas at Austin, among which the latter studies has been focused on High-Tension Friction Grip Bolts, Adhesive Anchors and Double-Nut Bolts, see Figure 4.2b-d (Schaap 2004, Hungerford 2004, Kayir 2006, Kwon 2008, Kwon et al. 2009, 2010a, 2010b, 2011). Additional studies on friction grip bolts have been reported by Chen et al. (2014) and Liu et al. (2016), while Pavlovic et al. (2013) present as comparison between bolted shear connectors (Figure 4.2f) and headed studs.
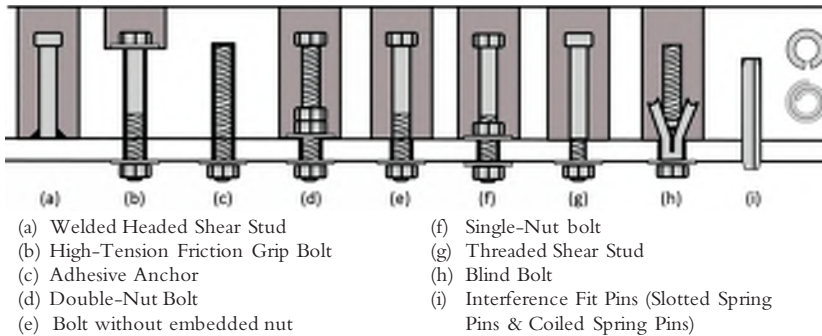

(a) Welded Headed Shear Stud
(b) High-Tension Friction Grip Bolt
(c) Adhesive Anchor
(d) Double-Nut Bolt
(e) Bolt without embedded nut

(f) Single-Nut bolt
(g) Threaded Shear Stud
(h) Blind Bolt
(i) Interference Fit Pins (Slotted Spring Pins & Coiled Spring Pins)

Figure 4.2 *Examples of different types of post-installed shear connectors*

In recent years, research has also been performed on demountable studs and different type of blind bolts, see Figure 4.2g and Figure 4.2h, respectively (Wang et al. 2017, Moynihan & Allwood 2014, Pathirana et al. 2015, 2016a, 2016b). Interference fit connectors can also be used to create composite action, two such examples are Slotted

Spring Pins and Coiled Spring Pins, see Figure 4.2i, where the latter is of most interest (Pritchard 1992, Buckby et al. 1997). This type of connector, consisting of just one component, relies on the spring force created by the compressed pin itself.

The research presented in this thesis is focused on Coiled Spring Pins (CSPs), primary due to two reasons: (1) This type of connector offers an installation procedure from below the bridge deck, relying only on the mechanical spring force. The latter implies that the connectors can be installed during traffic, since there is no need of welding, grouting, adhesives etc. (Pritchard 1992, Buckby et al. 1997, Olsson 2017). The minimum impact on the traffic is believed to be the main advantage of using CPSs. (2) Compared to other types of shear connectors suited for post installation from below the bridge deck, such as adhesive anchors, expansion bolts etc., only limited research has been performed and presented in the literature. A knowledge and information gap has been identified concerning the structural behaviour of a bridge strengthened with CSPs, but also concerning the static- and fatigue-strength of the shear connection.

The remainder of this chapter is focused on CSPs and the research performed by the present author.

4.3   Coiled Spring Pins

The CSP, also known as a type of tension pin or roll pin, is a standard component used as a connector in different types of industries and available in diameters from parts of a millimetre up to 20 mm (ISO 8748 2007). The pins are manufactured from steel plates that are spirally wound 2.25 times around the central axis of the pin, see Figure 4.3.
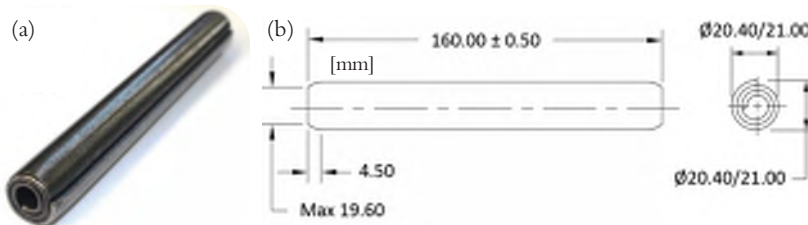

Figure 4.3 (a) Photo of a CSP, (b) CSP 20x160 dimensions

The interference fit is created by installing the oversized pin into an undersized hole. The pins are manufactured with chamfered ends, to make the installation easier. At installation, the spring is compressed when it is jacked into the smaller hole to achieve the interference fit. After the installation, the pin will be connected to the surrounding parts by the radial spring force provided by the pin itself.

4.3.1   Civil engineering application

Although the CSPs are frequently used in other type of industries, they are not common as shear connectors in civil engineering structures, implying that their behaviour in steel-concrete connections is not that well documented (Pritchard 1992, Buckby et al. 1997).

The type of CSP that is best suited as shear connectors in bridges is the "Heavy Duty" type, with the highest shear strength, covered by the international standard ISO 8748 (2007). The largest standard dimension, Ø20 mm with a plate thickness of 2.2 mm (see Figure 4.3b), has been used in all bridge strengthening projects and research studies presented so far (Pritchard 1992, Buckby et al. 1997, Fahleson 2005, Hällmark et al. 2016, Olsson 2017). It is also the most likely one to be used in future civil engineering applications, since it is the strongest CSP among the standardized types and dimensions. The results, analysis and recommendations within this thesis are also all limited to this specific dimension and type of CSP.

As mentioned above, the largest advantage of CSPs is the installation procedure, which can be done from below the bridge deck while the traffic is running on the bridge. The typical installation procedure for CSPs in a bridge deck is illustrated in Figure 4.4. First, holes are drilled through the steel flange (Step 1). Followed by the drilling into the concrete (Step 2). Normally, the drill is changed between Step 1 and 2, from a cutting drill to a diamond core drill. After the drilling, the tolerances are measured to ensure that the desired interference fit is obtained (Step 3). If the tolerances are fulfilled, a CSP is jacked into the hole (Step 4). The installation procedure is ended by sealing the hole and restoring the corrosion protection (Step 5).
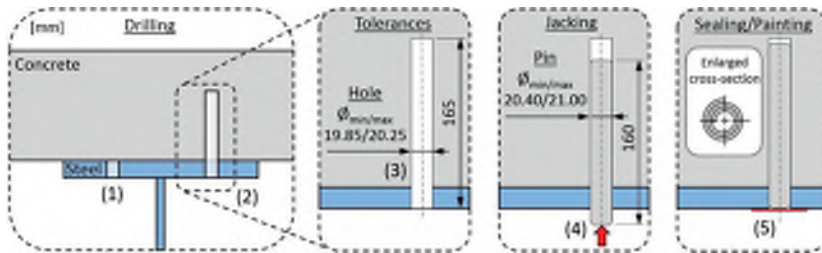

Figure 4.4 *General installation procedure for CSPs in steel-concrete bridges*

Experiences from CSPs used as shear connectors in steel–concrete bridges and the research conducted within this field, so far, are briefly summarised below and presented more in detail in Paper VI.

Only a few bridge strengthening projects, using CSPs, have been identified by the author. The first bridge application that has been found in the literature is the upgrade of Docklands Light Railway (DLR) in London 1988 (Pritchard 1992), see Figure 4.5a. Due to heavier traffic, an existing shear connection was strengthened with CSPs to increase the fatigue lifetime of the connection. In 2008, the bridge was further strengthened due to even heavier traffic (Jackson et al. 2012).

There is at least one more bridge in the UK that has been strengthened with CSPs, the Tinsley Viaduct. Unfortunately, the strengthening and the project specific tests have not been documented in any public available reports. This is also the case for a couple of bridge strengthening projects that never were realized, but for which pre-studies and tests were performed on post-installation of CSPs.

In 1995, the existing shear connections in two bridges on a light railway system in Vancouver (Canada) were strengthened by installing CSPs, see Figure 4.5b. During a period of six months, 2 500 CSPs were installed without traffic interruptions. (Buckby et al. 1997)

One bridge project is also reported from Sweden, the Pitsund Bridge shown in Figure 4.5c. In 2006, composite action was created in a part of the structure originally constructed as a non-composite steel-concrete structure in 1984. In this case, the primary reason for strengthening was not to increase the load capacity, but to counteract sudden slips at the steel-concrete interface resulting in loud bangs, up to 105 dB. After the installation of 1 200 CSPs, the loud bangs disappeared. Also in this case, the installation was performed while the bridge was still in service. Only short distances of the outer lanes were closed, one part at a time, during the installation work. (Olsson 2017)

(a)　Docklands Light Railway bridge in London (UK)

(b)　North approach spans (to the left) for the Skybridge in Vancouver (Canada)

(c) The Pitsund Bridge in Piteå (Sweden)

Figure 4.5 Example of bridges strengthened with CSPs

So far, the research reported in the literature has been focused on specific bridge strengthening projects (Pritchard 1992, Buckby et al. 1997, Fahleson 2005, Olsson 2017). In most cases the static strength of the CSP is reported, and in some cases also the fatigue

strength, but often related to one specific steel flange thickness and one specific concrete grade.

One of the aims of the research presented in this thesis was to bring the knowledge about CSPs further, by contributing to a progress towards the development of more general design guidelines for the use of CSPs as shear connectors at steel-concrete interfaces. Such guidelines could eliminate the need of future project specific tests, thereby removing some of the barriers for this strengthening method.

The first step in the progress towards more general design guidelines, was a compilation of the available information and research presented on CSPs, so far. The outcome is presented as a state-of-the art review in Paper VI. The literature survey was followed by two push-out test campaigns, studying the static- and the fatigue-strength of the shear connectors. Paper VIII presents a summary of the static tests, while Paper IX presents the fatigue tests. These tests, which focused on the local behaviour of the shear connection, were supplemented by field monitoring of a strengthened bridge, to obtain information about the behaviour on a structural level. Paper VII summarises the outcome of the bridge monitoring.

The information gained from the research activities have been analysed, evaluated and processed into design recommendations, which are briefly summarised in the following sections and presented more in detail in Appendix B.

4.3.2 Static strength and load-slip behaviour

This section is complemented by Paper VIII, which presents the detailed results and analysis from the static tests.

In 2016-2017, an experimental investigation of the static strength of CSPs was conducted in the MCE-Lab at LTU. The tests were primarily performed in order to investigate the influence of the concrete strength and the steel plate thickness on the strength and the ductility of a shear connection created by CSPs.

The preferred method to establish the static capacity and the load-slip behaviour of a steel-concrete shear connection is push-out tests. It is also possible to perform tests on composite beams. However, the latter is more expensive to perform and harder to evaluate, since the forces acting on the shear connectors must be calculated from the measured strain distribution, which results in a need for extensive measurements and a knowledge of the stress-strain behaviour of the materials used in the tests. Therefore, the static tests and the fatigue tests presented in this thesis have all been performed as push-out tests.

The standard push-out test specimen recommended in EN 1994-1-1 (2005) is not suitable for testing of post-installed shear connectors. The limited space between the flanges in the steel section makes it difficult to perform the drilling through the steel flanges and into the concrete, see Figure 2.6. Hence, before the push-out test set-up was designed, a review of different kinds of test specimens and test set-ups was conducted.

There are several different types of alternative push-out test set-ups presented in the literature. Horizontal test set-ups are interesting alternatives, which have been used by Kwon (2010a), Ernst (2010) and Lam (2007), among others. The present author found the test set-up developed at the University of Texas at Austin, presented by Kwon (2010a), best suited for testing post-installed shear connectors. This test set-up provides good access to the steel flange, enabling an easy installation, and has successfully been used by Schaap (2004), Hungerford (2004), Kayir (2006) and Kwon (2010a). For CSP testing, different kinds of inverted test set-ups have been used so far (Pritchard 1992, Buckby et al. 1997, Fahleson 2005). The test specimens are inverted by the means that the steel and the concrete parts have changed positions, implying that there is one single concrete block in the middle surrounded by two steel plates. Such a design simplifies the post-installation of shear connectors.

Some type of clamping has been used in all inverted test specimens. This is necessary to avoid too conservative results due to separation at the steel-concrete interface during the tests. This separation is mainly driven by the geometry of the test set-up, and does not correspond to the behaviour in a real structure with a continuous shear connection. Since the CSPs have no heads, the test results become even more sensitive to separation. The differences between the assumed behaviour of CSPs and headed studs, in terms of force components, are schematically illustrated in Figure 4.6.
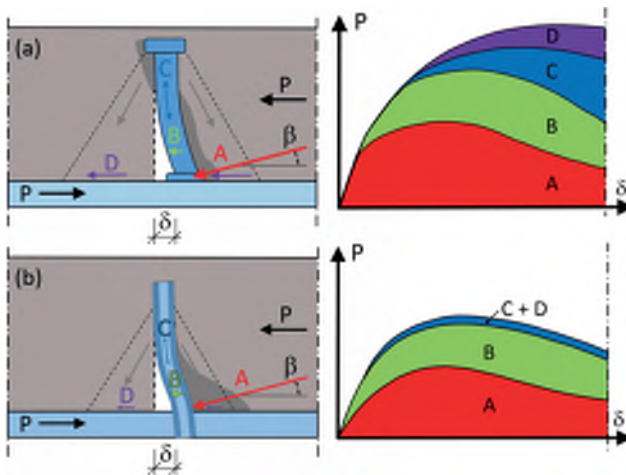

Figure 4.6 *(a) Load transfer model for headed studs, (b) suggested load transfer model for CSPs*

The force components involved in the shear behaviour of welded studs, embedded in solid concrete slabs, are often described by the illustration in Figure 4.6a, originally presented by Lungershausen (1988). Initially, the external shear force (P) is predominantly acting on the lowest part of the shear connector by a compression strut

(A), which is inclined with an angle β. When the load increases, concrete crushing will occur near the weld collar, which implies that the additional shear force (B) is shifted higher up in the stud shank. The shift of the force results in increased shear deformations and bending of the stud. Since the ends are restrained from vertical movements by the head and the weld collar, a tension force (C) will be developed in the stud shank. The tension force is balanced by a compression force in the concrete, which gives an additional contribution to the frictional capacity at the steel-concrete interface, through the force component D. The final failure is expected directly above the weld collar as a result of the combination of shear and tensile stresses (Roik et al. 1989, Nellinger et al. 2017).
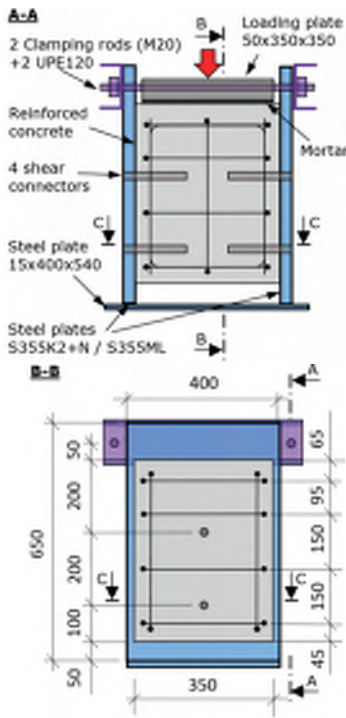
If the failure of the CSPs is considered instead, it seems reasonable to assume that the force components A and B will contribute in a similar way as for the shear studs. However, since the CSPs have no heads, there will be no restraint from vertical movement in the top of the connectors, except the assumed minor contribution from the vertical frictional forces acting on the pin. This should imply that the force components C and D only give negligible contributions to the total shear capacity of a CSP. A schematic illustration of the suggested load transfer model is shown in Figure 4.6b.

The previously reported tests conducted on CSPs have all been undertaken on non-standardized test specimens with externally applied clamping forces. However, the test results have not been verified by similar tests on welded headed studs with known shear resistance and load-slip behaviour. To verify the previous test results on CSPs and to ensure that the results can be considered comparable to those obtained from standard push-out tests, the author chose to use an almost identical design of the specimens as Buckby et al. (1997) and Fahleson (2005), with some modification of the clamping. In the new tests performed by the author, clamping rods were used in the upper part of the specimen, while welded steel strips were used in the previous tests. The clamping was measured continuously during the tests, by tension load cells in the clamping rods, to be able to evaluate the effect of the clamping force. The type of test specimen and the test set-up, used by the author, is illustrated in Figure 4.7.

This set-up was used to investigate the behaviour of three different combinations of shear connectors: (a) four welded headed shear studs; (b) four Coiled Spring Pins; and (c) two welded headed shear studs (WHS) in the upper positions combined with two Coiled Spring Pins in the lower positions. The latter was tested in order to study the behaviour of an existing shear connection strengthened with CSPs, which can be of interest if a bridge with an existing shear connection is strengthened. The total test program consisted of 28 test specimens divided into six test series. The first two test series were reference tests performed to obtain comparable results for welded headed studs (Type RW) and CSPs (Type RC). In the four following test series, three different parameters were varied: the concrete strength; steel plate thickness; and the shear connector configuration. Table 4.1 summarises the test program and the varied parameters.

Table 4.1 *Static test program*

Type	No.	Shear connectors	Concrete strength class	Steel plates	
				t [mm]	Grade
RW	5	4 CSP	C30/37	30	S355K2+N
RC	5	4 WHS	C30/37	30	S355K2+N
A	5	4 CSP	C20/25	30	S355K2+N
B	5	4 CSP	C40/50	30	S355K2+N
D	5	4 CSP	C30/37	45	S355ML
E	3	2 CSP + 2 WHS	C30/37	30	S355K2+N

(a) Test specimen   (b) Test set-up

Figure 4.7 *Type of test specimen and test set-up used in the static tests*

The tests were performed in line with the recommendations in EN 1994-1-1 (2005), with a minor change of the lower load in the cyclic pre-loading, from 5% to 10% of the expected failure load, due to a limitation of the hydraulic actuator that was used. Prior to the testing, some material parameters were tested for the steel plates, the concrete, the headed studs and the CSPs. A detailed description of the test procedure along with the results from the material testing are presented in Paper VIII.

Test results

The test results regarding the load–slip behaviour are summarized in Table 4.2 together with the test results from the concrete testing. The presented parameters are the maximum load (P_u), the characteristic resistance of the shear connectors (P_{Rk}), the slip at the maximum load (δ_{Pu}) and the slip capacity (δ_u) measured at the characteristic load level. The characteristic resistances have been evaluated both according to the simplified method given in Annex B in EN 1994-1-1 (2005) and according to the more general statistical method in Annex D in EN 1990 (2002), $P_{Rk,EC4}$ and $P_{Rk,EC0}$, respectively.

Table 4.2 *Load-slip test results*

Series/ specimens		$f_{cm,cube}$ [MPa]	P_u [kN]	$P_{u,m}$ [kN]	$P_u / P_{u,m}$ [-]	$P_{Rk,EC4}$	$P_{Rk,EC0}$ [kN/SC]	δ_{Pu} [mm]	δ_u [mm]	δ_{uk} [mm]
Type RC	RC1	47.0	598		0.98	132	138	13.7	17.4	14.3
	RC2		625	611	1.02			12.0	20.8	
	RC3	Min: 44.7	586		0.96			21.3	>22.0	
	RC4	Max: 48.8	633		1.04			13.5	15.9	
	RCX		530	–	–	–	–	11.6	–	–
Type RW	RW1	52.9	811		1.01	165	163	14.8	>22.0	12.1
	RW2		800	805	0.99			16.3	>22.0	
	RW3	Min: 51.4	733		0.91			12.8	13.4	
	RW4	Max: 55.8	876		1.09			>22.0	>22.0	
	RWX		659	–	–	–	–	17.0		–
Type A	A1	30.3	619		1.04	128	138	21.1	> 22.0	17.9
	A2		586		0.98			20.7	> 21.0	
	A3	Min: 27.8	606	597	1.01			18.8	> 22.0	
	A4	Max: 32.7	571		0.96			21.3	> 22.0	
	A5		605		1.01			17.9	19.9	
Type B	B1	47.0	654		1.02	141	154	19.0	> 22.0	16.0
	B2		636		0.99			15.5	17.8	
	B3	Min: 44.0	625	640	0.98			18.8	20.3	
	B4	Max: 48.4	643		1.00			18.8	18.9	
	B5		642		1.00			18.8	22.0	
Type D	D1	50.2	659		1.03	137	146	14.2	14.6	9.2
	D2	Min: 48.8	607		0.94			8.7	10.4	
	D3	Max: 51.8	626	643	0.97			11.6	16.2	
	D4		656		1.02			9.1	10.2	
	D5		666		1.04			11.2	15.4	
Type E	E1	46.3	682		0.99	153	165	11.9	13.1	8.7
	E2	Min: 45.2	686	689	1.00			8.9	9.7	
	E3	Max: 46.8	698		1.01			10.0	11.4	

The concrete classes by type: RC: C30/37; RW: C30/37; A: C20/25; B: C40/50; D: C30/37; E: C30/37.

The load–slip diagrams for the test series RC and RW are presented in Figure 4.8, illustrating the typical load–slip behaviour for the tested CSPs and WHSs. All specimens show a ductile behaviour and exceed by far the ductility criterion of a characteristic slip (δ_{uk}) of at least 6 mm, in accordance with EN 1994-1-1 (2005). Some of the curves end

abruptly in a vertical line. This does not correspond to the real behaviour but can be explained by the fact that the measuring LVDTs (Linear Variable Differential Transformer), with a maximum stroke of 25 mm, run out of stroke at these levels. If the stroke of the hydraulic jack was plotted instead, this phenomenon would not be observed. It can also be noted that the specimens with CSPs have an S-shape in the beginning of the load-slip curves, while the specimens with WHSs have a more linear behaviour in this part of the curve.

(a)Type RC   (b)Type RW
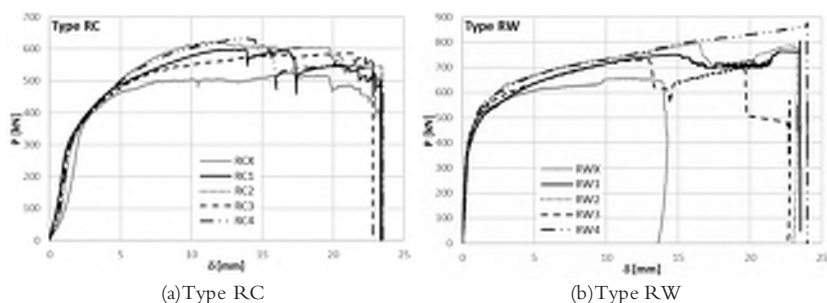
Figure 4.8 *Load-slip diagrams for the Type RC and RW test series*

Different failure mechanisms were observed for the different types of specimens. The Type RW specimens with WHSs failed by shear failures near or through the weld collar of the studs, see Figure 4.9a. The failures were preceded by large deformations due to concrete crushing near the bottom part of the studs and yielding in the steel stud shank. Vertical and diagonal cracking of the concrete were also observed, see Figure 4.9b.
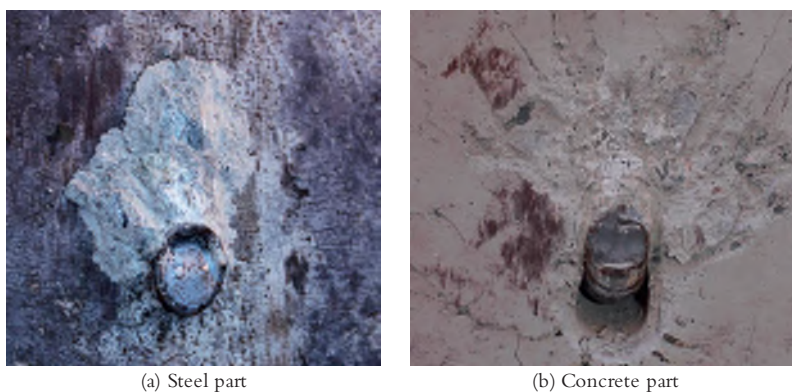

(a) Steel part   (b) Concrete part

Figure 4.9 *WHS test specimens after finalised test*

The failures of the CSP specimens were very ductile. In many cases, slips exceeding 20 mm were registered without shear failures of the shear connectors. The large slips are caused by concrete crushing and yielding of the connectors as well as the hole-edges in the bearing steel plate. Two distinct plastic hinges were developed in the CSPs, one at

the interface between the steel and the concrete and the other a few centimetres into the concrete, see Figure 4.10a and d. In comparison to the studs, the largest difference of the failure mode is that the CSP in most cases remains in one piece even at very large slips. It should also be noted that the typical failure of the CSPs involves yielding at the edge of the bearing steel plate, which is shown in Figure 4.10b. In some cases, as for specimens of Type D, a shear failure occurred in the CSPs, see Figure 4.10e. A reverse movement of the end of the failed CSP followed such a failure. This implies that the ends of the failed pins were sticking out, as shown in Figure 4.10c, indicating a failure.
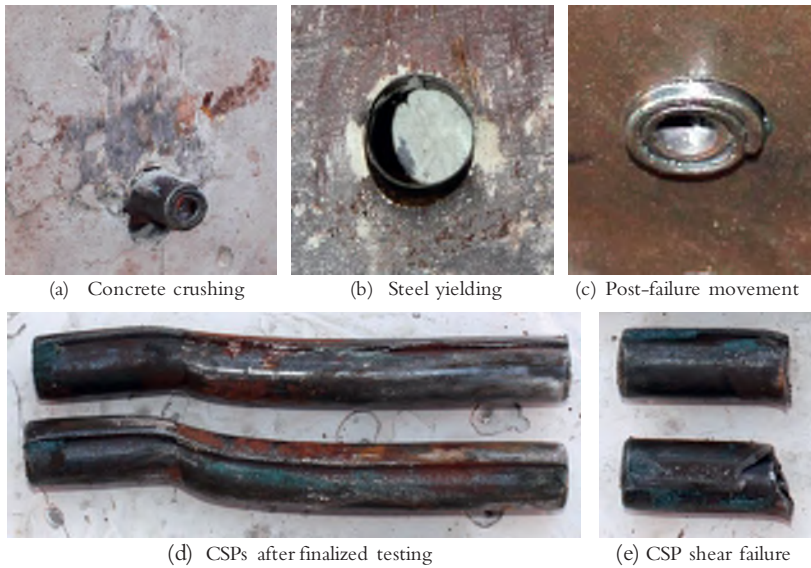
(a) Concrete crushing	(b) Steel yielding	(c) Post-failure movement

(d) CSPs after finalized testing	(e) CSP shear failure

Figure 4.10 *CSP test specimens after finalised tests*

Analysis

As a part of the evaluation, the test results for the CSPs have been compared against the design rules for headed studs, presented in equation (2.1) and (2.2), by plotting the relationship between the shear resistance (P_R) and the concrete compressive strength (f_c), see Figure 4.11. The dependency of the stud diameter in equation (2.1) has been rewritten as a dependency of the connector shear area, A_{sc}, to enable a comparison to the CSPs. The partial factors have also been excluded and mean measured values of the variables are used within the equations.

From Figure 4.11, it can be noted that all test results are on the safe side compared to the lowest design capacity given by equations (2.1) and (2.2). Also the characteristic values, presented in Table 4.2, are all clearly on the safe side if the EC0 model is used, while the EC4 model gives characteristic values that are almost equal to the design criteria for the Type RC and D specimens and on the safe side for the others. As shown in Figure 4.11,

there seems to be a dependency between the measured shear resistance and the concrete compressive strength, but not as strong as in equation (2.2).
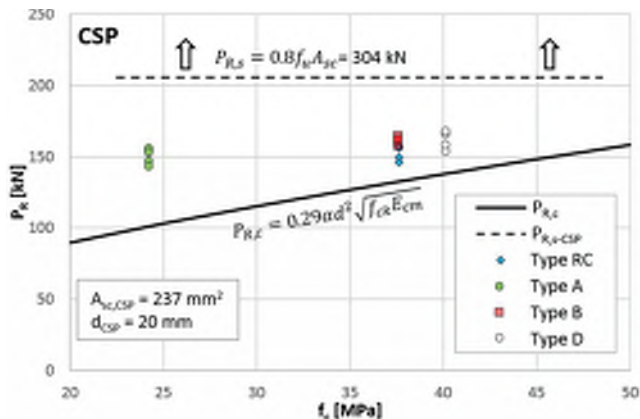

Figure 4.11 Test results compared to the shear resistance criteria in EN 1994-2 (2005)

A study of the impact of different steel flange thicknesses has been done by a comparison between the specimens of Type RC, B and D, which have comparable concrete compressive strength and steel flange thicknesses of 30 mm and 45 mm, respectively. The test results indicate no significant difference in the failure load between the two tested steel flange thicknesses. However, there is a difference in the ductility of the shear connection and in the stiffness. The specimens with thinner steel plates show a more ductile behaviour with longer yielding plateaus on the load-slip curves. The specimens with the thicker steel plates have a more distinct and earlier failure, in terms of slip. The characteristic slip capacity (δ_{uk}) is 55% and 75% bigger (Type RC and B) for the 30 mm plates in comparison to the 45 mm plates.

In the development of a design criterion for the static strength of CSPs, the author's test results have been complemented by test results from tests performed by other researchers. Figure 4.11 presents a graphical summary of the available test results. The tested shear resistance (P_{Rk}) is presented in terms of kN/CSP and is plotted in relation to the cylinder compressive strength of the concrete (f_c).

For the tests performed by the author, there is only a weak correlation between an increased concrete compressive strength and an increased shear capacity of the shear connection. The test results reported by others are few, but indicate a stronger correlation between the concrete compressive strength and the shear capacity of the connection. This observation is also valid even if the Tinsley test results, which deviates a lot from the others, are excluded. The main reason for the large variations in test results between different test series are believed to be the different types of test set-ups that have been used and the different degree of clamping of the specimens. Tests on standardized specimens would be preferable.
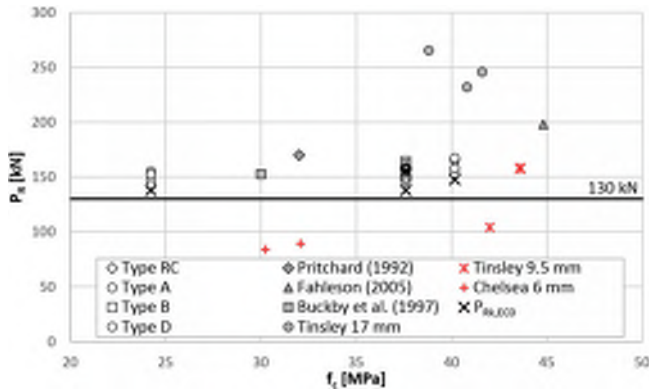
Figure 4.12 *Compilation of the available static push-out test results on CSPs*

Based on three static push-out tests, Bucky et al. (1997) recommended that a nominal strength of 130 kN can be used for CSPs installed in C30/37 concrete and for steel plate thicknesses between 25-35 mm. It turns out that the characteristic static capacity of 130 kN/CSP suggested by Buckby et al. (1997) fits quite well to the new test results and are also on the safe side compared to the other test results available, if the tests with steel plate thicknesses smaller than 17 mm are excluded, see Figure 4.12. The test specimens with steel plate thicknesses below 10 mm have a completely different failure mode, with a bearing failure in the steel plate. These thin dimensions are generally not relevant for the top flanges in steel girder bridges.

The evaluation of the test set-up in (Hällmark et al. 2018c) indicate that it is necessary to apply a clamping force on this type of push-out test specimen, in order to avoid separations driven by the geometry of the specimen. The clamping used in the test series will not give any positive constraint effects in the ultimate state, since visual gaps are developed at the steel-concrete interfaces. The magnitude of the clamping forces are also small in comparison to the corresponding forces recommended by Hicks & Smith (2014) for push-out tests. However, the evaluation of the previously used test set-ups indicate that higher degrees of constraint might give non-conservative test results.

Even though the evaluation of the test set-up indicates that the test results should be comparable to those from standard specimens, future push-out tests are considered to be performed on standard specimens. In such a case, the steel section could be cut into two halves prior to the installation of the CSPs and then welded back into one unit after the installation of the shear connectors.

Recommended design criterion

The analysis presented briefly above, and more detailed in (Hällmark et al. 2018c), indicates that the static strength of a shear connection created with CSPs can be estimated as 130 kN/CSP, if the minimum steel plate thickness is limited to 20 mm and if the compressive cylinder strength of the concrete is within the interval of 24-45 MPa.

4.3.3 Fatigue strength

This section is complemented by Paper IX, which presents the detailed results and analysis from the fatigue tests.

In 2017-2018, a fatigue test campaign on CSPs was conducted in the MCE-Lab at LTU. The tests were performed in order to investigate the fatigue strength of CSPs used as shear connectors in steel–concrete bridges.

Roik & Hanswille (1990) highlight some important factors that are affecting the fatigue lifetime of headed studs. From the author's perspective, it is likely that the majority of these factors are the same for CSPs. The most important factor is the fatigue stress range, which is defined as the difference between the maximum and the minimum shear stresses within the fatigue load cycle. The magnitude of the peak load, within the fatigue load cycle, is another parameter that will affect the fatigue lifetime. A high peak load will result in an earlier, and more widely spread, concrete crushing near the root of the shear connectors. This will result in additional bending stresses in the shear connectors, which reduce the fatigue lifetime. The same effects will be obtained if the concrete strength is lowered, resulting in concrete crushing at lower load levels.

Test set–up, specimens and test program

The test specimens were almost identical to those used in the static tests presented in the previous section. The major difference is that the tension load cells in the clamping rods have been removed to avoid fatigue of the load cells. This implies that the clamping forces have not been measured in the fatigue tests. Instead the nuts were tightened with a similar torque as in the static tests, where the initial clamping force was about 1 kN/rod.

Figure 4.13 presents the two types of test specimens used in the fatigue tests. In six out of nine tests, the four CSPs were located at two different heights within the specimen, like in the previously performed static tests, see Type F1 in Figure 4.13a. The three remaining tests were performed on specimens with the four shear connectors all positioned at the same height, see Type F2 in Figure 4.13b.

The fatigue tests were performed with a hydraulic jack applying a unidirectional force-controlled load, varying between the predetermined load levels. After an initial period with a lower frequency, to ensure that the specimens were stable, the frequency was increased to the desired level of 4 Hz. The testing procedure started with an initial loading (P_{ini}) up to 0-22.5 kN/CSP above the maximum load in the fatigue load cycle ($P_{max,f}$). This overload was used in order to break the bonds between the steel and the concrete and to simulate the impact of loads higher than the fatigue loads. After the initial loading, the fatigue load cycles were started with the load range ΔP_f. The minimum load ($P_{min,f}$) was kept constant at 5 kN/CSP in all tests, while different $P_{max,f}$ where tested within the interval of 35-55 kN/CSP. This gives an R–ratio ($P_{min,f}/P_{max,f}$) between 0.09-0.14.

Prior to the fatigue tests, some of the important material parameters were tested. A detailed description of the test procedure along with the results from the material tests are presented in (Hällmark et al. 2018d).
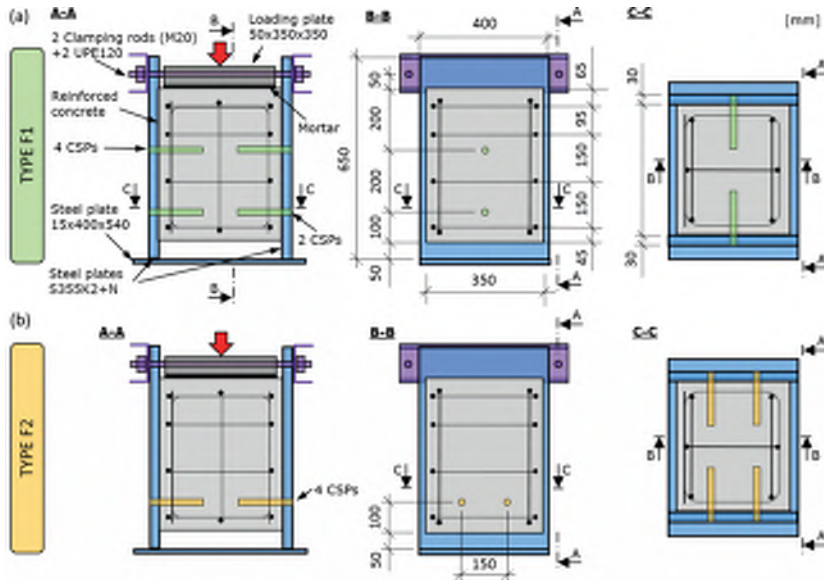
Figure 4.13 *Fatigue test specimens, (a) Type F1 and (b) Type F2*

<u>**Test results**</u>

The fatigue tests were run until a fatigue failure was observed, at N_f load cycles, in at least one of the connectors. Table 4.3 summarizes the fatigue test results and presents the detailed information about the applied load cycles.

Table 4.3 *Fatigue and concrete test results*

Specimen		Concrete	$f_{cm,cube}$ [MPa]	E_{cm} [GPa]	P_{ini} [kN]	$P_{max,f}$ [kN]	$P_{min,f}$ [kN]	ΔP_f [kN]	R [-]	$P_{max,f}/P_u$ [-]	N_f [10^6]
Type F1	F1:1	C30/37	48.5 Max: 49.6 Min: 46.3	33.0	50	50	5	45	0.10	0.38	0.086
	F1:2				62.5	55	5	50	0.09	0.42	0.066
	F1:3				62.5	40	5	35	0.13	0.31	0.367
	F1:4				62.5	40	5	35	0.13	0.31	0.267
	F1:5				50	40	5	35	0.13	0.31	0.306
	F1:6				50	40	5	35	0.13	0.31	0.447
Type F2	F2:1	C30/37	59.4 Max: 61.1 Min: 57.6	35.1	45	35	5	30	0.14	0.27	2.813
	F2:2				50	40	5	35	0.13	0.31	0.438
	F2:3				45	35	5	30	0.14	0.27	0.760

After the tests were finalized, the concrete parts and the steel plates were separated, to enable a visual inspection of the failure. The failed CSPs had in many cases separated into small pieces, which made it hard to identify the initiation points of the fatigue cracks and the propagation directions. The typical fatigue failure of the CSPs, shown in Figure 4.14,

seems to occur at a section a few millimetres into the steel plate. The corrosion, visible in some of the pictures, has not affected the test results, since it arose during the storage of the already tested specimens. It should also be noted that some damages might have been caused by the removal of the external steel plates after the tests were completed, or by the last load cycles before the displacement limits were reached and the tests automatically stopped. In line with the observations made on the static push-out tests, the end of the failed CSPs started to move out from the steel plates after failure had occurred. The movements had magnitudes of a few millimetres and could easily be observed.
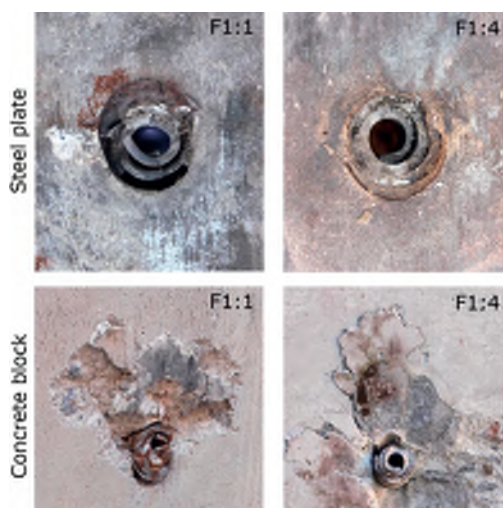
Figure 4.14 *Pictures of failed CSPs, and the surrounding concrete and steel, after the fatigue tests*

Analysis

The new fatigue test results have been analysed first separately and then together with previous test results. The evaluation is based on the assumption that there is a linear relationship between *log S* and the *log P*, as for the fatigue strength curves in EN 1993-1-9 (2005),

$$\log N_i = \log a + m \cdot \log \Delta P_i \qquad (4.1)$$

where m is the slope and *log a* is the intercept of the *log N*-axis. In contradiction to the design of shear studs, the author have chosen to present the fatigue strength in terms of shear forces (P) instead of shear stresses (τ), i.e. in a P–N curve instead of an S–N curve (see Figure 4.15). This implies that the presented analysis is valid only for the tested type of CSPs, i.e. a Heavy-duty CSP with a nominal diameter of 20 mm and manufactured in line with ISO 8748 (2007).
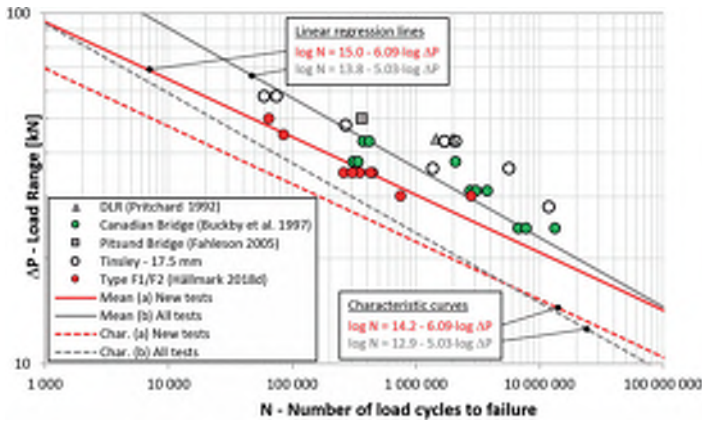
Figure 4.15 *Fatigue strength test results and their associated regression lines and characteristic curves*

A linear regression analysis, based on the least square method, for the new test results gives the following formula for the regression line,

$$\log N = 15.0 - 6.09 \log \Delta P. \tag{4.2}$$

The coeffcient of determination, R^2, indicate that there is a good agreeement between the linear regression line an the test results, since 85% of the variance of *log N* can be explained by *log P*.

From the test results and the linear regression line, a characteristic fatigue curve has also been established. The curve is representing 95% probability of survival, like the fatigue curves in EN 1993-1-9 (2005), and has been developed in line with a method presented by Schneider & Maddox (2003),

$$\log N = 14.2 - 6.09 \; log\Delta P. \tag{4.3}$$

The new test results have also been compared to previous test results presented by Pritchard (1992), Buckby et al. (1997), Fahleson (2005) and Hällmark et al. (2018a). The test results are illustrated by the points in Figure 4.15. If a linear regression line is created based on all available test results, the agreement is not so good with R^2 equal to 59%. However, if the two other large test series by Bucky et al. (1997) and the Tinsley project are analysed separately, they both indicate a good agreement with R^2 equal to 84% and 89%, respectively. There are several factors that might explain why the linear regression lines give a better agreement on single test series, rather than all test series analysed as one sample. Example of such factors are the different types of test specimens, varying material parameters and dimensions, differences in the definition of the fatigue failure and deviating testing procedures.

The specimens used, so far, in the fatigue tests on CSPs, have had different layouts and different degrees of clamping and clamping methods. In line with one of the conclusions from the static tests, it would be beneficial if one standardized type of specimen could be

used in the future, to remove the uncertainties about the different degrees of clamping and the varying eccentricities between the load position and the support points.

The different definitions of the fatigue failure, between the different test series, make it difficult to use all available test results in the development of a fatigue design criterion. Some researchers have defined the fatigue failure as when the first CSP failed, while others have defined the failure as a limitation of the accumulated slip.

If the CSPs are installed in a structure in order to create composite action, not to strengthen an already existing shear connection, the author suggests that the failure is defined as when the first CSP fails or when the accumulated mean slip reaches 5 mm.

The recent tests by the present author deviate most from the other test series, and this deviation cannot be explained by a different fatigue definition or different material parameters. The type of specimen is also similar, in some cases almost identical, to those used by Pritchard (1992), Buckby et al. (1997) and Fahleson (2005). Instead, the initial overload prior to the start of the fatigue tests could be the reason for the difference in the fatigue test results. Future FE-modelling and research might be able to give an estimation of the impact of the initial overload and show whether the fatigue strength of the CSPs are more dependent on overloads than headed studs are.

Recommended design criterion

Based on the test results, a recommended characteristic fatigue strength curve is presented in equation (4.3) and rewritten in (4.4), using the equation format adopted in EN 1993-1-9 (2005),

$$\Delta\tau_R^{6.09} N_R = 84.4^{6.09} \cdot 2 \cdot 10^6 \quad \text{(from } \Delta\tau_R^m N_R = \Delta\tau_c^m N_c\text{)} \tag{4.4}$$

where $\Delta\tau_R$ is the fatigue shear strength (in MPa) of the Ø20 mm CSP, using the nominal area of 237 mm², $\Delta\tau_c$ is the reference value at $N_c = 2 \cdot 10^6$ cycles (i.e. the detail category), m is the slope of the fatigue strength curve and N_R is the number of stress cycles.

This is a conservative design recommendation compared to the previous recommendation by Buckby et al. (1997). Future research might provide additional information about the CSP fatigue strength, which makes it possible to develop the fatigue design criterion further.

4.3.4 *Structural behaviour and modelling*

This section is complemented by Paper VII, which presents the detailed results and analysis from the monitoring of a bridge strengthened with post-installed CSPs.

The definition of a shear connection in EN 1994-2 (2005) section 1.5.2.2, is:

"An interconnection between the concrete and steel components of a composite member that has sufficient strength and stiffness to enable the two components to be designed as parts of a single structural member."

The performed push-out tests on CSPs indicate a very ductile behaviour and the ductility criterion in EN 1994-2 (2005) 6.6.1.1 (3)-(5) is by far fulfilled. However, the tests also

showed that there is a significant difference in the load-slip behaviour between the studied CSPs and the studied WHSs, as shown in Figure 4.16. The latter is about four times stiffer than the tested CSPs. One question that was raised was whether the CSPs have "sufficient stiffness" related to the definition of a shear connection, presented above. This has been investigated by field monitoring of a bridge strengthened with CPSs, and associated FE-models, presented in this section and more detailed in (Hällmark 2018b).
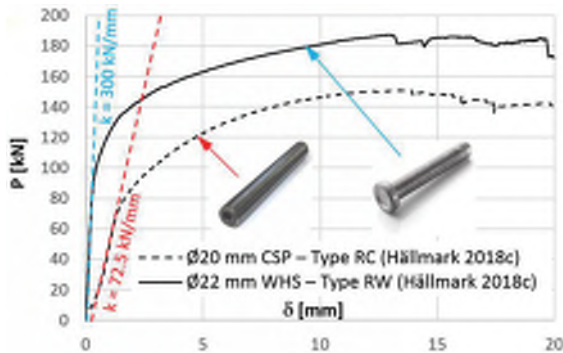
Figure 4.16 *Load-slip diagrams for the studied CSPs and headed studs*

The Pitsund Bridge

As far as the author knows, there are only a few bridges in the world that have been strengthened by post-installation of CSPs. One of these bridges is the Pitsund Bridge, located in the northern part of Sweden. This bridge offered a unique possibility to monitor bridge spans strengthened with CPSs and spans without shear connectors.

The Pitsund Bridge is a seven span bridge with a total length of almost 400 m. The superstructure is divided into three separate parts, see Figure 4.17. The first four and last two spans consist of continuous steel girders with a concrete deck slab on top, whereas the fifth span is movable. The latter is an independent structure and outside the scope of the field monitoring.
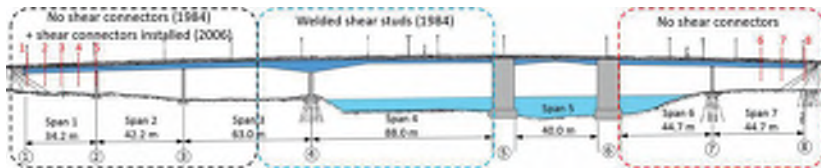

Figure 4.17 *Elevation drawing of the Pitsund Bridge*

The bridge was designed and built in the early 1980s, a time when composite steel-concrete bridges were rare structures in Sweden, and had in its original design spans both with and without composite action. In Figure 4.17, the different types of shear connections are illustrated by the coloured boxes. In the red part, there are no shear

connectors. In the blue part, the bridge was designed as a composite structure with welded headed studs. The black part was originally designed with no composite action, but has been strengthened in year 2006 by post-installation of CSPs. The two parts of the bridge that were of most interest for the author, was the black and the red parts, since they offered the possibility to compare measurements on a strengthened cross-section with measurements on a similar non-strengthened cross-section. Therefore, it was decided to monitor both Span 1 and 7. The monitored sections are illustrated as red lines in Figure 4.17, while the cross-sectional geometry of the monitored sections is illustrated in Figure 4.18.
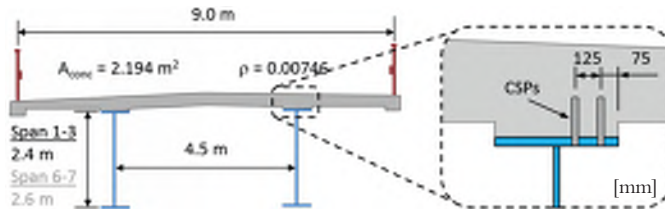

Figure 4.18 *Cross-sectional geometry of the measured sections*

<u>*Monitoring*</u>

The monitoring performed in 2016 was focused on four topics: (a) the vertical distribution of the longitudinal strains in the steel main girders, (b) the horizontal slip at the steel-concrete interface, (c) the vertical separation (uplift) at the steel-concrete interface, and (d) the vertical displacements of the main girders (deflection).

The typical instrumentation consisted of three strain gauges, measuring the longitudinal strains at different heights in the steel web plate, and two LVDTs measuring the relative vertical displacement (uplift) and the horizontal displacement (slip) at the steel-concrete interface, see Figure 4.19. The deflections were however only measured in the middle of span 1, i.e. in section 3 in Figure 4.17.
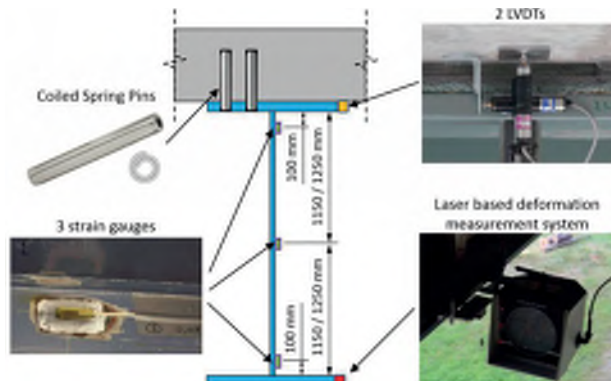

Figure 4.19 *Schematic illustration of the instrumentation*

During the monitoring, a test vehicle was positioned in predetermined positions on the bridge, in the mid of span 1 and 7, while the bridge was temporary closed for other vehicles. The dimensions and axle loads of the test vehicle are presented in Figure 4.20, together with the different load cases (LC), i.e. the different positions of the test vehicle in the transversal direction. It can be noted that the difference between LC1 and LC2 is the driving direction of the vehicle.
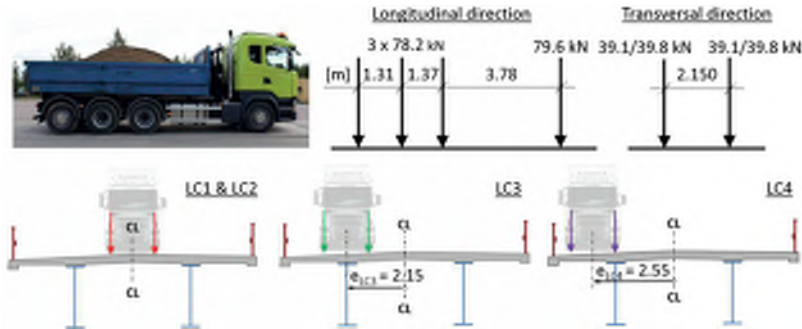

Figure 4.20 *Test vehicle loads and load positions in the transverse direction*

The FE-models

Prior to the field monitoring, a FE-model of the bridge was created in order to study the correspondence between different design models and the measured behaviour. Focus was set on the modelling of the shear connection and its stiffness. The shear connection was modelled by rigid connection elements, connecting the concrete deck slab and the upper flanges of the steel girders. In the lower end of the connection elements, linear springs were used to model the horizontal stiffness, see Figure 4.21. Three different stiffnesses (k) were investigated in the study: FEM 1 simulated a rigid shear connection ($k_{x,y} = \infty$), FEM 2 simulated no composite action ($k_{x,y} = 0$), while the linear springs in FEM 3 were given stiffnesses corresponding to the results from the static push-out tests performed on CSPs ($k_{x,y} = 72.5$ MN/m per CSP).
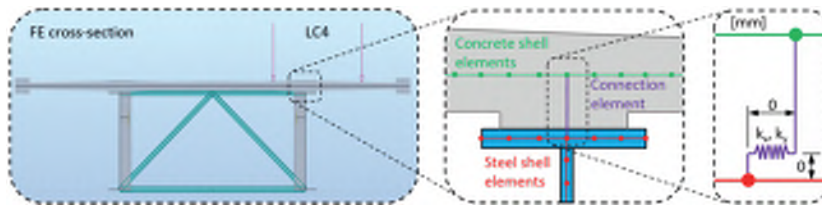

Figure 4.21 *Schematic illustration of the connection elements and the FE cross-section*

The material models were all linear-elastic, since the studied load levels generate stresses far below the yielding point of the steel and the concrete compression strength. Regarding the concrete parts in tension, cracking was assumed over the internal supports.

However, since this is an existing structure with an unknown load history, there is no point in trying to capture the cracking of the concrete related to the test vehicle. Therefore, the model is based on the simplified design approach according to 5.4.2.3 (3) in EN 1994-2 (2005), which is a likely design model in a real situation.

Test results and analysis

For the strengthened cross-sections in regions with positive bending moments (Section 3 and 4), the steel strain measurements indicate a neutral bending axis located close, or even above, the theoretical position assuming full composite action. This is illustrated by the test results for LC1 shown in Figure 4.22a, where the measured steel strains have been transformed to stresses by Hooke´s law assuming a linear elastic material.
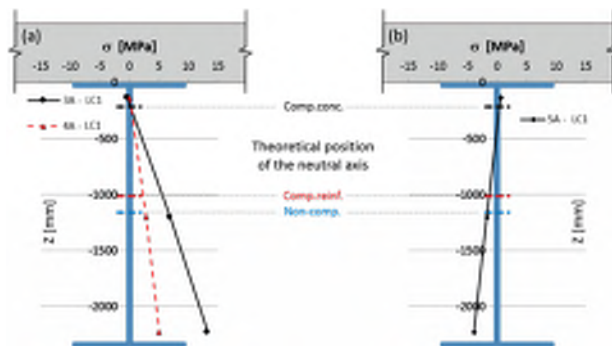

Figure 4.22 *Measured steel stresses for LC1, in section 3-5 of span 1.*

The steel strain measurements indicate composite action also in strengthened regions that experience negative bending moments, see Figure 4.22b. The position of the neutral bending axis is far above the neutral axis representing interaction with only the longitudinal reinforcement bars. This indicates significant stiffness contributions from the concrete deck itself. This could be explained either by tension stiffening between the cracks or the fact that the concrete section might be non-cracked. However, these effects are believed to be unrelated to the type of shear connectors. The impact of an increased stiffness contribution from the concrete in tension has been studied in a modified FE-model, in which the concrete elastic modulus and the longitudinal distribution of the cracked concrete at an internal support has been varied. These modifications are not related to the CSPs or the post-installation, but are derived from uncertainties of material parameters and the global behaviour. Therefore, the modified FE-model is not within the focus of the research presented in this thesis. However, the modified FE-model shows that it is possible to get a good agreement between a FE-model and the test results in all sections.

Regarding the stiffness of the shear connection, a comparison between the measured steel stresses and the FE-stresses is shown in Figure 4.23, for Span 1 and LC1. It can be observed that the FE-model with a rigid shear connection (FEM 1) gives a good

prediction of the steel stresses in the areas where the concrete deck slab is in compression, while all models fails to predict the steel stresses when the concrete is in tension near an internal support (Section 5). This is an expected result since the measurements show that the concrete parts in tension contributes to the flexural stiffness, while the FE-models only consider the contribution from the longitudinal reinforcement area, in line with the simplified design approach according to 5.4.2.3 (3) in EN 1994-2 (2005).
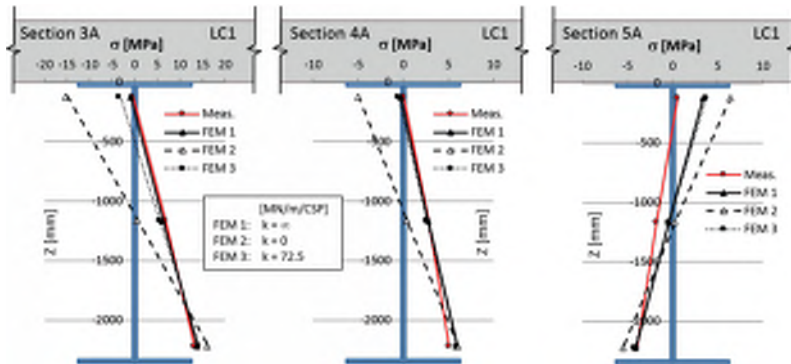

Figure 4.23 *Measured steel stresses vs. FE-stresses for LC1*

A comparison based on the measured deflections, instead of steel strains, also indicates that a rigid connection seems to be the best estimate of the shear connection stiffness at the tested load levels.

Regarding the slip measurements, very small slips were measured in the strengthened sections in comparison to the non-strengthened sections. The slips varied within an interval of 0.00-0.04 mm in the sections with CSPs, while slips up to 0.26 mm were registered in the non-strengthened sections. This comparison indicates that the CSPs are reducing the slip significantly. However, the small slips in Span 1 can hardly be explained by the stiffness of the shear connectors alone, but are believed to be a consequence of large contributions from frictional forces or other interlocking phenomena at the steel-concrete interface. These contributions can also be observed in the test results from the non-strengthened cross-sections in Span 7. In these sections, the neutral bending axis is located lower than in a corresponding composite section, as expected, but the measurements indicate still a rather high degree of composite action. The measured vertical position of the neutral bending axis, in relation to the steel-concrete interface, is varying between 460-500 mm. This can be compared to the theoretical positions for a full composite section and a non-composite section, which is 320 mm and 1140 mm, respectively.

Regarding the relative vertical movement at the steel-concrete interface, the measurements in the strengthened span show no clear indications of uplift of the concrete deck, with registered separations less than 0.03 mm. This is an expected result, since the forces acting on the shear connectors are rather low. Partly since the tested load levels

are a lot smaller than the ultimate load, for obvious reasons, and partly since the frictional forces seem to contribute a lot at the tested load levels. It can also be noted that the measured vertical separations in the non-strengthened sections are comparable to those in the strengthened sections, with one exception. At the end-support of the non-strengthened Span 7, an uplift has been registered that are about ten times bigger than the maximum uplifts in the other sections.

The results from the monitoring gives an indication that the installation of CSPs will not cause a concrete uplift at the studied load levels. However, according to EN 1994-2 (2005) all types of shear connectors must be able to prevent separation of the concrete deck from the steel girders. The uplift forces are generally not considered in the design of the shear connection in new structures, since the WHSs may be assumed to provide sufficient resistance to uplift, in line with EN 1994-2 (2005). This is not the case for the CSPs, where only frictional forces at the surface of the pins will counteract the uplift, together with the gravity forces from dead weight and traffic. The potential problem with the uplift is one issue that will be investigated further, which might affect the final design of a shear connection with CSPs.

Design recommendations

The following design recommendations are based on the evaluation of the test results presented above, but also based on input from the research presented in the previous sections within this chapter. It should, however, be noted that there are additional research questions that have been identified by the author, which need to be investigated further before utilizing the full potential capacity of the CSPs.

At the tested load levels, the shear connection created by post-installed CSPs show a sufficient stiffness to be modelled as a rigid connection. Therefore, the author recommends a design model based on an assumption of a rigid shear connection.

There are, however, some cases when it might be necessary to model the stiffness of the shear connection more accurate, or at least to consider the stiffness. For instance, if there are any SLS design criteria that are crucial in the design, such as a strict deflection criterion with almost 100% utilization ratio, it might be necessary to create a structural model that takes into account the stiffness of the shear connectors.

The potential problem with an uplift of the concrete deck slab, should be dependent on the slip and the inclination of the shear connector and the concrete compressive strut, see Figure 4.6b. If the slip is kept at moderate levels, the uplift forces would also be kept low. Thus, before the potential uplift has been investigated further, the recommendation is to utilize only the elastic capacity of a composite beam with post-installed CSPs and to design the shear connection for full composite action. This restriction is on a general level and aims to increase the safety margin of the strengthened structure, until the potential uplift has been investigated further.

More detailed design recommendations are presented in the design guidance, written by the present author, provided in Appendix B.

4.3.5 Installation of CSPs

The focus of the research presented in this chapter has been on the design of CSP shear connections rather than the post-installation procedure. However, since there is limited information available about the installation procedure, the author has summarised the knowledge obtained from installing CSPs in steel-concrete structures, in Appendix B. This section gives a brief summary of the different stages in the installation procedure.

As previously presented, the installation procedure includes generally five steps: (1) drilling through the steel top flanges, (2) drilling into the concrete, (3) tolerances measurements, (4) jacking of the CSP into the hole, and (5) sealing of the hole and restoring the corrosion protection. These steps are illustrated in Figure 4.4 and will be presented more in detail below, together with a summary of some of the important decisions that must be made prior to the installation. Such examples are how to deal with the risk of collisions with reinforcement bars and the risk of exceeding the hole tolerances etc.

CSP positions

The positions of the post-installed CSPs have to be adapted to the conditions in the existing bridge. Typical factors that need to be considered are the location of the transversal reinforcement, the location of the longitudinal reinforcement and the design requirements in EN 1993-1-8 (2005) and EN 1994-2 (2005).

To perform the post-installation of the CSPs, it is necessary to drill into the existing reinforced concrete deck slab. The holes need to pass the horizontal bottom layers of reinforcement, both the transversal and the longitudinal, but will in the general case be ended before the reinforcement bars in the top layers are reached. If no actions are taken to locate the reinforcement bars, the drilling will most likely cut some of the transversal reinforcement bars apart. These bars are mainly needed to distribute the shear forces to the concrete deck slab, since the main transversal moments are negative above the steel girder, implying that the bottom part of the deck slab is in compression in the transversal direction. However, since there are positive transversal moments between the girders, it must be assured that sufficient anchorage lengths are provided if the reinforcement bars are utilized in the design.

Two different approaches to deal with this problem have been found in the literature, both used in bridge strengthening projects. In the Pitsund Bridge strengthening project, in Sweden, no detection of the reinforcement bars was performed (Olsson 2017), while Peiris & Harik (2014) reports about an installation procedure where ground penetrating radar was used to determine the positions of the reinforcement bars. The latter strengthening project was not with CSPs, but with adhesive anchors used as post-installed shear connectors. The detection procedure is however not dependent on the type of connector.

Based on the available knowledge about these two approaches, a flow chart has been created for the CSP-positioning in relation to the transversal reinforcement bars, see Figure 4.24. The tasks within the flow chart are described more in detail in the design guidance in Appendix B.
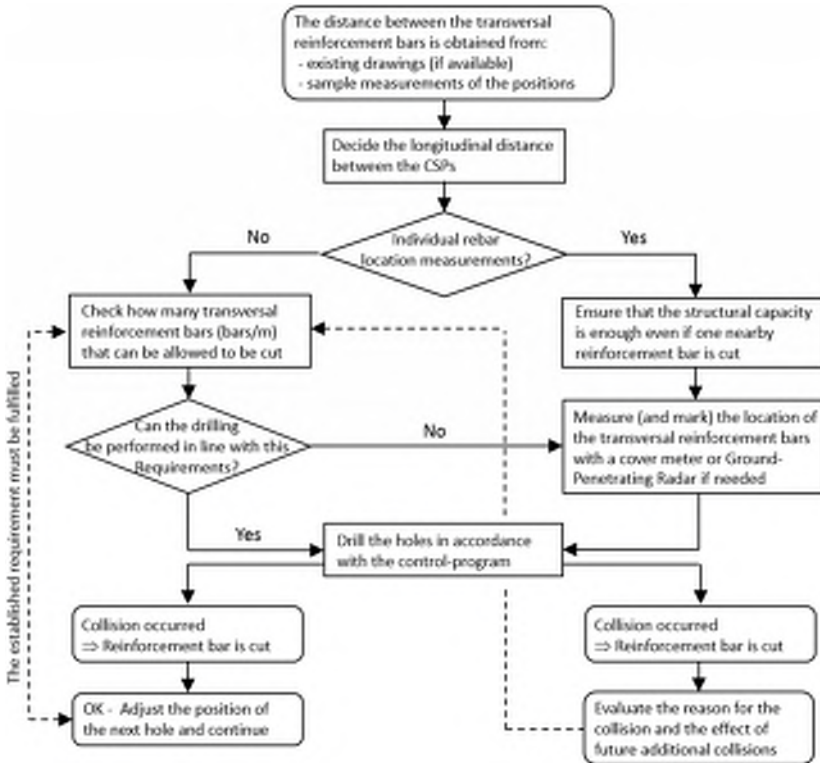
Figure 4.24 *Flow chart for the CSP-positions in relation to the transversal reinforcement*

Concerning the risk of collisions between CSPs and longitudinal reinforcement bars, it is harder to detect the positions of the longitudinal reinforcement bars by measurements. As a first assumption when the positions of the post-installed CSPs are decided, the theoretical positions of the reinforcement bars can be taken from the drawings of the existing bridge, if available. However, the bridge designer must either establish at least a second alternative position of the connectors in the transversal direction, or ensure that the structural capacity will not be affected by the loss of the affected reinforcement bars.

The European design code for composite bridges EN 1994-2 (2005) specifies the general design requirements for the location of the shear connectors. These requirements must be complemented by the requirements for positioning of holes for bolts and rivets, given by EN 1993-1-8 (2005). This is necessary since the CSP connection is quite similar to riveted- or bearing type bolt-connections, in the aspect of potential failures in the connecting steel plate. However, as presented in Appendix B, the requirement in EN 1994-2 (2005) will be governing the CSP-positions in the general case.

In addition to the design requirements, the locations of the CSPs are also governed by project specific execution requirements. These requirements are often related to the space needed for the drilling equipment.

From an installation point of view, it is often preferable to locate all post-installed connectors on one side of the steel web-plate, if possible. This unsymmetrical shear transfer will cause a bending moment acting of the steel girder in the week direction. However, this moment will be counteracted by transversal force couples in the CSPs, over a long distance, which often are negligible.

Precision drilling

To be able to install the CSPs from below the bridge, holes must be drilled through the steel top flange and into the concrete deck. This drilling can either be done by using different drill bits for the steel and concrete drilling, or by using one diamond core drill for the whole drilling operation. The wearing down of the bits can be a significant cost factor since the required tolerances are very tight.

The product data sheet provided by the manufacturer of the CSPs gives the tolerances of the pins, prior to installation. The studied CSP, with a nominal diameter of 20 mm, has a tolerance interval of 20.40-21.00 mm for the outer diameter, as illustrated in Figure 4.3. The tolerances of the holes must be tight to ensure proper field performance of the CSPs (Pritchard 1992, Buckby et al. 1997). For the two bridge projects presented by Pritchard (1992) and Buckby et al. (1997), the DLR-bridge in London and a Canadian light railway bridge in Vancouver, the hole diameters were allowed to vary between 19.85 mm and 20.25 mm. This interval was also reported as the manufacturer's tolerances in these cases. For the Canadian Bridge, an additional requirement was used, limiting the relative differences in hole diameters between the hole in the steel and the concrete to 0.1 mm. During the installation of approximately 2 500 pins, only fourteen holes failed to meet these criteria. Holes that did not meet the tolerance requirements were abandoned and new holes drilled nearby (Buckby et al. 1997). The same hole tolerances, 19.85 mm to 20.25 mm, were used in the Pitsund Bridge strengthening project in Sweden reported by Olsson (2017) and in the manufacturing of the push-out test specimens presented in (Hällmark et al. 2018c, 2018d).

Based on the experiences presented above, it is recommended to use hole tolerances of 19.85 − 20.25 mm, combined with a requirement of a relative hole diameter difference of maximum 0.1 mm between the hole in the steel- and the concrete-part, respectively. These tolerances might be demanding for the drilling operator, but have been proven feasible.

The drilling should be followed by control measurements of the hole diameter, in both the steel- and the concrete-part, to ensure that the holes are within the tolerances. If the tolerances are exceeded, the hole should be abandoned and a new nearby hole should be drilled in an alternative position provided by the designer of the strengthening.

To enable an installation of the oversized CSPs (20.40-21.00 mm) into the undersized holes (19.85-20.25 mm), the CSPs are chamfered in both ends to an outer diameter less than 19.6 mm, see Figure 4.3b. This makes it easier to push the CSPs into the holes, using a hydraulic jack, to create an interference fit. Figure 4.25 shows the installation of CSPs in the DLR-bridge strengthening project in London 2008, presented by Jackson (2015).

Figure 4.25 _Installation of CSPs in the DLR-bridge_

Lubricants have often been used to lower the jacking force required for the installation of the pins (Pritchard 1992, Buckby et al. 1997, Olsson 2017). Laboratory tests indicate that the use of lubricants have a negligible effect on the ultimate load capacity, although the measured slip increases slightly (Buckby et al. 1997). These conclusions are supported by the push-out tests with and without lubrication presented by Hällmark et al. (2018c).

The jacking force required to press the CSPs into the holes varied between 62-205 kN in the installation of the approximately 2 500 Coiled Spring Pins in the Canadian Bridge (Buckby et al. 1997). In the manufacturing of the test specimens presented in (Hällmark et al. 2018c, 2018d), jacking forces between 50-130 kN were registered when lubricated pins were pressed into holes with diameters between 19.95-20.31 mm.

Based on the experiences from real strengthening projects and the manufacturing of test specimens, it is recommended to start the installation of the CSPs without using lubricants. However, if the magnitude of the installation force becomes too big, for the jack or for the supporting bottom flange, tests have shown that lubricants can be used without jeopardizing the load capacity of the connectors. Suitable lubricants can be chosen on a case-to-case basis, depending on the requirements for the sealing and corrosion protection products.

Corrosion protection

After the installation is complete, it is important to seal the holes to prevent air and moisture from entering and corroding the CSPs. In the case with the Pitsund Bridge, a penetrating corrosion protection system was applied on the new steel surfaces after drilling. The coating system had a drying time of 24 hours, which implied that it also had a lubricating effect since the installation of the pins were done directly after the drilling (Olsson 2017). The holes were however not sealed in this bridge and the CSPs were only electrogalvanized with a minimum zinc thickness of 5 μm, which is not enough to provide a long term protection against atmospheric corrosion in an outdoor climate. As a consequence of this, after slightly more than ten years there is some corrosion in the end of the pins, see Figure 4.26. This is more of a cosmetic problem, but can easily be avoided in future projects by sealing the holes properly.
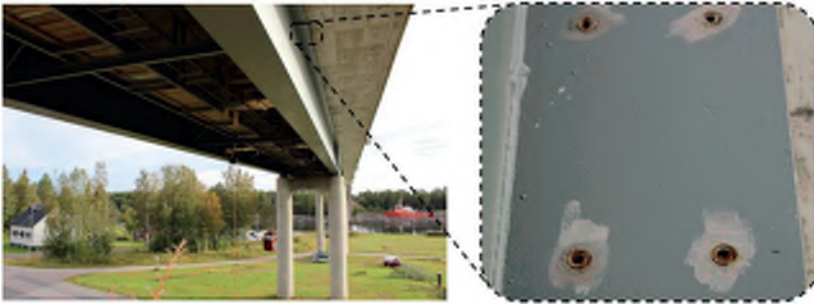

Figure 4.26 *Picture of the CSPs in the Pitsund Bridge, ten years after the installation*

In other projects involving post-installation of CSPs, different types of sealing techniques have been used. Buckby et al. (1997) reports about a sealing of the end of the CSPs in order to prevent air and moisture ingress. In another case, the Coiled Spring Pins were recessed 2 mm into the steel flanges and those recesses were filled by sealant before local repainting (Pritchard 1992). It should be noted that any reduction in the contact area between the steel flange and the Coiled Spring Pin due to the pin chamfer or any recess must be considered in the design. This effect can be significant for thinner steel flanges where the chamfer and recess may represent a large percentage of the available contact area.

Even if the holes are sealed, they can still be opened in order to perform sample inspections of the pins from the inside. By inspecting the inside of the pins, fatigue cracks or already occurred failures can be detected. This is an advantage compared to other types of embedded connectors, which often cannot be inspected.

Based on the experiences so far, it is recommended to seal the holes to prevent air and moisture ingress, and to apply a suitable corrosion protection at the top of the sealing.

Installation methods

The suitable installation method can vary a lot between different bridges, depending on the traffic condition on the bridge, the access from below the bridge, the width of the superstructure, the number of girders etc.

As highlighted in previous sections, it is often preferable if the post-installed CSPs are located only on one side of the web plates. This enables an installation procedure where access to the steel top-flange is needed from just one side of the web plate. Two examples of such installation procedures, alternative (a) and (b), are illustrated in Figure 4.27. If the traffic volume enables a close down of the outer lanes, one at the time, the alternative (a) can be considered with an installation from a truck based boom lift. Such an installation procedure was used for the installation of 1 200 CSPs in the Pitsund Bridge strengthening project in Sweden, see Figure 4.27b. During the installation of CSPs, the bridge was open for traffic, with the exception of the outer lane where the boom lift was located. Alternative (b), in Figure 4.27a, with a temporary working platform between the bottom flanges enables an installation procedure without affecting the traffic at all. If there is a need to install CSPs from both sides of the web plates, alternative (c) in Figure 4.27a can be considered. If it is possible to get access to the ground below the bridge, it can also be considered to perform the installation works from the ground, in a boom lift or on temporary working platforms.
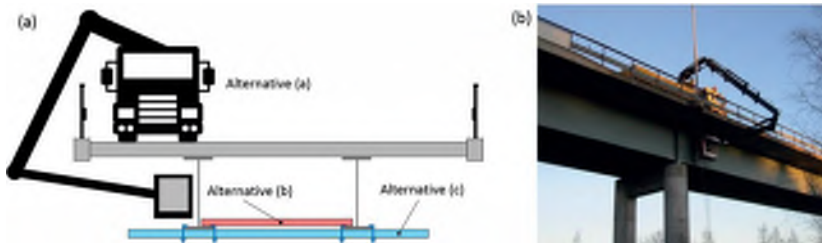

Figure 4.27 *Examples of possible installation methods*

It can be worth to spend some time on the choice of the installation method, and an optimization of it, since the strengthening technique with CSPs is labour intensive and the majority of the costs are related to the hours spent on the on-site installation. For the Pitsund Bridge, two persons installed 20-30 CSPs each working shift (eight hours). This installation method resulted in a cost of approximately 60 €/CSP, in year 2006. The material costs for the CSPs were less than 10% of the total costs, while the labour costs were more than 50%.

Chapter 5

DISCUSSION AND CONCLUSIONS

This chapter summarises the conclusions of the research presented in this thesis and presents a discussion of the outcome together with suggestions for future research.

5.1   Introduction

The overall objective of this thesis was to achieve more time and cost efficient use of composite bridges, by further development of suitable design procedures for new composite bridges and strengthening methods based on the creation of composite action.

When a bridge is constructed, strengthened or rehabilitated, the impact on the road users can be reduced if a proper design, production or installation method is chosen. Prefabrication is one method to reduce the time spent on-site, choosing an appropriate strengthening method is another.

This thesis deals with two specific methods, *Prefabricated composite bridges with dry deck joints* and *Post-installed Coiled Spring Pins*, both focused on minimizing the impact on the road users. A part of the hypothesis was that the methods would be more competitive if reliable and practical design guidelines were developed. In the beginning of the research process, the identified key issues were formulated and later compiled into two sets of research questions, presented in Chapter 1. The main findings related to these questions are summarised and discussed in this chapter. The two methods are first discussed separately, followed by a section with a common discussion about composite bridges and innovative ways of achieving composite action.

5.2   Prefabricated composite bridges with dry deck joints

The conclusions from the research within the topic *Prefabricated composite bridges with dry deck joints* are presented below, followed by a discussion section and recommendations for further research.

5.2.1   Research questions and findings related to these

A-RQ1.   What is the state-of-the-art within this field?

The ever increasing number of vehicles in urban areas has contributed to the development of new production methods and structural designs, to reduce the time spent on the construction sites when new bridges are built or old bridges replaced. Thus, accelerated bridge construction techniques are gaining ground around the world. Procedures for prefabricating bridge elements have been intensively developed and researched, and numerous ways of using prefabricated deck elements have been described. This thesis has focused on elements with dry transverse joints, which so far is a very rare design solution. Currently, prefabricated decks are generally constructed using transverse joints with in-situ cast concrete surrounding overlapping reinforcement bars from the adjacent deck elements.

This research question has been handled by performing a literature state-of-the-art review. The outcome is presented in Paper I and section 3.1-3.3 of this thesis.

A-RQ2.   How does a superstructure with dry deck joints behave under positive and negative bending moments?

The structural behaviour of a composite superstructure with dry deck joints has been investigated through large-scale laboratory tests, in combination with field monitoring of a single span bridge constructed using the studied prefabrication system.

In case of positive bending moments, i.e. with the concrete deck in compression, the test results indicate that this type of bridge behave almost as a corresponding bridge with an in-situ cast concrete deck, in the ULS. However, there is still a difference in load capacity between the reference test with an in-situ cast deck and the specimens with prefabricated deck elements with dry joints. Therefore, it is suggested that the effective width of the concrete flanges are reduced with a factor 0.8 in the ULS. The statement above is only valid in the ULS, which often is the most important limit state in the design of this type of bridge. Under moderate positive bending moments, in SLS and FLS, the test results indicate that the stiffness is significantly reduced. This reduction is mainly caused by a combination of the initial joint gaps and the continuous in-situ cast channels, which have to be compressed before the rest of the joint starts to transfer forces. This has to be taken into consideration in SLS- and FLS-design, for instance, when the steel parts are designed for fatigue or the deflection criterion is checked. Recommendations how to perform the global analysis in the different limit states, and the cross-sectional design, have been presented in section 3.4.1 and also in Appendix A.

In case of negative bending moments, there will be gaps in the joints, implying that longitudinal forces cannot be transferred over the joints. Thus, the shear forces transferred to the concrete by the shear connectors have to enter and leave the concrete elements between every joint. This results in a huge shear-lag, since the equivalent length is reduced to the longitudinal distance between the outermost shear studs within an

element. Therefore, when a bridge deck of this type is in tension, the stiffness as well as the cross-sectional resistance should be based on the steel section only.

This research question is covered by Paper IV, V and section 3.4.1 of this thesis.

A-RQ3.   How do the shear keys fail under an increased static load and how should a rational design calculation of the shear keys be done?

The shear keys are vital parts of the construction, since they ensure that vertical forces can be distributed between the elements. The ultimate load capacity and the failure mode of the shear keys have been studied by laboratory tests.

From the eight tests on reinforced shear keys, two different failure modes were observed.

In the first failure mode, cracks were developed in the bottom of the shear keys. Under an increasing load, the cracks propagated with inclinations of ~45° until they reached the upper surface of the deck element. These cracks passed the shear reinforcement, the SX-bars, and the dimension of the reinforcement bars governed the ultimate capacity of the shear keys.

In the second failure mode, cracks were developed in the concrete cover layer. If the shear keys are properly reinforced, with overlapping reinforcement in the male-female concrete tongues, this type of failure should not govern their ultimate load capacity. The shear keys would continue to transfer forces even if the concrete cover layer separates from the rest of the shear key. However, this type of failure is still undesirable, since it might affect the long-term sustainability of the bridge.

The second type of failure has only been observed in the shear-key laboratory tests with stiff supporting elements. When large-scale joints have been tested, only the first failure mode has been observed. In section 3.4.2, possible reasons why this failure occurred only in the small-scale tests have been discussed.

The scatter of the test results was quite high, which makes it difficult to establish any general design criterion. The scatter was mainly a consequence of the occurrence of two different failure modes, as presented above.

With current knowledge, based on the observations and measurements presented in section 3.4.2 and Paper III, it is recommended to design the shear keys according to the formulas for inclined shear reinforcement in EN 1992-1-1 (2005), presented in equation (3.2) in this thesis.

A-RQ4. What is the long-term behaviour of a bridge with dry deck joints, compared to a composite bridge with a conventional in-situ cast deck slab?

The long-term behaviour of the studied concept with prefabricated deck elements with dry joints has mainly been investigated by field monitoring of a single span bridge built in 2000. This bridge has been monitored two times, in 2001 and 2011, which made it possible to investigate if there were any significant differences between the test results.

From the comparison of the test results, one possible long-term effect was observed. When the bridge was loaded with an eccentric load, the distribution of the deflection between the loaded girder and the passive girder has changed over time. The relative deflection of the passive girder, in relation to the active girder, has decreased from 40% to 30%. This change might be a consequence of reduced joint gaps, during the time elapsed between the tests, caused by abrasion of irregularities at the concrete contact surfaces, resulting in more evenly distribution of forces over the joints.

The study of the long-term effects is presented in Paper IV and also briefly in section 3.4.1 of this thesis.

A-RQ5. Which aspects need to be covered in a detailed design of this type of bridges?

Composite bridges with prefabricated concrete deck elements with dry joints can generally be designed according to the same design procedures as conventional composite bridges, with in-situ cast concrete deck slabs. However, the author has identified some important differences, which makes it necessary to modify some of the design assumptions. These differences have been highlighted in section 3.4.1-3 and in Appendix A.

5.2.2 Discussion and further research

The prefabricated bridge concept studied within this thesis is generally best suited for short single span bridges. If the concept would be applied on longer bridges, it might be necessary to use some in-situ cast joints to zero the cumulative tolerance errors. In order to design longer bridges without in-situ cast joints, it would be beneficial if the tolerances could be increased, or the deck element system redesigned to avoid collisions between shear connectors and reinforcement bars. One example of a possible way to increase the tolerances is presented in Figure 3 in Paper I. This innovative connection detail, from the US, utilizes UHPC (Ultra High Performance Concrete) to avoid an intersection between the shear connectors and the reinforcement bars in the prefabricated concrete elements.

A competitive alternative to prefabricated deck elements with dry-joints is prefabricated deck elements with in-situ cast joints (wet-joints). If elements with wet-joints are used, it will not be possible to install the waterproofing almost immediately after the erection, since the concrete needs to dry out. Hence, the bridge cannot be opened for traffic as fast as a bridge with dry joints. However, if the geometry of the bridge is complex, with varying curvature, deck widths etc., in-situ cast joints offer the valuable opportunity to make small adjustments at each joint.

Continuous multi-span composite bridges with dry deck joints will require more steel in the superstructure than a corresponding bridge with prefabricated deck elements with in-situ cast joints or with a totally in-situ cast deck slab. Therefore, a design solution with prefabricated deck elements with dry joints will not be the optimal choice for a new bridge that can be built without disturbing the traffic or the environment. However, if the work at the bridge site will result in a huge impact on the traffic, the neighbours, the environment etc., or if the client and the contractor would benefit significantly from a shorter construction time, prefabricated deck elements with dry deck joints can be competitive.

One critical factor in continuous multi-span bridges, built with the studied concept, is the durability of the waterproofing. The waterproofing has to be designed to withstand cyclic variations of the joint opening, to avoid damages caused by water penetration and leakage in the joints. This is beyond the scope of this thesis, but an important issue to address in further research. It is also strongly recommended to involve the manufacturers of the waterproofing systems in the further research.

The shear connection is also an area that would require further research. The outermost shear studs within an element will probably transfer higher shear forces than those in the middle of an element. Previous tests have shown that the fatigue resistance of shear studs at internal supports is sufficient, if they are designed for composite action. Further research would be beneficial to investigate how the shear forces are distributed between the shear connectors within an element and to evaluate the consequences in FLS and ULS.

5.3 Post-installed Coiled Spring Pins

The conclusions from the research within the topic *Post-installed Coiled Spring Pins* are presented below, followed by a discussion section and recommendations for further research.

5.3.1 Research questions and findings related to these

B-RQ1. What is the state-of-the-art within this field?

Post-installation of shear connectors in non-composite steel-concrete bridges, is a strengthening method that has been used in several countries. Welded headed studs, the most well-known and well documented shear connector today, are probably the most common choice when a bridge is strengthened by post-installation of shear connectors, although the installation process requires a rather large intervention in the structure. However, there are bridge designers and researchers from all over the world that have tried to use and develop alternative types of shear connectors to simplify the installation procedure, reduce the traffic disturbance, improve the fatigue lifetime etc. Research has been performed on several types of shear connectors suitable for post-installation, such as: different types of bolted connections, adhesive anchors, mechanical anchors and interference fit connectors.

The shear connector that has been in focus in this thesis, the interference fit Coiled Spring Pin, is not a well-documented shear connector in steel-concrete connections, even though it has been used in other industries for several decades. The author has been able to identify a few bridge strengthening project, in Europe and Canada, through a literature review followed by personal contacts to some of the bridge designers involved in the projects. However, the available literature references from the use of CSPs in bridge strengthening can be counted on one hand.

The author has tried to contribute to the dissemination of the use of CSPs as shear connectors in composite bridges, by performing a state-of-the-art review presented in Paper VI and briefly summarized in section 4.1-4.3.

B-RQ2.   In what way does a CSP fail under static loading and which parameters are influencing the behaviour?

The static strength and the load-slip behaviour of the CSPs have been investigated by a test series of 28 push-out tests. An alternative push-out test set-up was used, to enable an easier post-installation procedure in comparison to the standard test specimen presented in the European design codes. This test set-up has been evaluated and validated by a comparative test series on headed shear studs.

The test results show that the failure mode of the CSPs is very ductile, exceeding the shear connector ductility criterion in the Eurocodes, by far. The large slip prior to the failure is a consequence of concrete crushing around the lower parts of the CSPs, near the steel-concrete interface, and plastic deformations of the CSPs as well as the edges of the holes in the bearing steel plates. Two plastic hinges were developed in the CSPs, one at the interface between the steel and the concrete and another one a few centimetres into the concrete. In comparison to welded headed studs, the CSP is in general more ductile and remains often in one piece even at slips exceeding 20 mm. In case of a failure, the end of the failed CSP starts to move out of the steel plate indicating a failure.

The influence of different parameters on the static strength and the stiffness has been studied. The two parameters in focus were the concrete compressive strength and the steel plate thickness. The test results indicate a dependency between the concrete compressive strength and the static strength of the shear connection, but not at all as strong dependency as in the dimension criterion for headed shear studs. Concerning the steel plate thickness, no significant difference in the static strength of the shear connection has been identified between the two tested steel plate thicknesses (30-45 mm), whereas a difference in the ductility and in the stiffness have been verified. Specimens with thinner steel plates show a more ductile behaviour, while specimens with thicker steel plates have more distinct and earlier failures, in terms of slip.

Based on the presented research, the author suggests that the static strength of the studied CSP is estimated as 130 kN/CSP, if the minimum steel plate thickness is limited to 20 mm and if the compressive cylinder strength of the concrete is within the interval of 24-45 MPa.

This research question is covered by the study of the static strength of CSPs presented in Paper VIII and briefly summarized in section 4.3.2.

B-RQ3.   *In what way does a CSP fail under fatigue loading and which parameters are influencing the behaviour?*

The fatigue strength of CSPs has been investigated by a test series of nine fatigue push-out tests and by evaluating previously performed tests by other researchers.

The most important factor for the fatigue lifetime is the fatigue stress range. In the tests performed by the author, the stress range and the initial load have been varied, while the other parameters have been kept constant. The initial load cycle was higher than the other load cycles, to simulate the impact of loads higher than the fatigue loads.

The fatigue tests were run until failure occurred in at least one CSP and the number of cycles until failure were registered. After the tests were ended, the steel plates were removed from the concrete blocks and the failures visually inspected. The inspection showed that the failed CSPs, in many cases, had separated into small pieces near the fatigue failure, which made it hard to identify the crack initiation points and the crack propagation directions. The typical fatigue failure of the CSPs seems to occur a few millimetres into the steel plate, in the same position where the first plastic hinge is developed in the static tests and where the stresses in the CSPs are expected to be highest. After a fatigue failure of a CSP, the end of the failed pin starts to move out from the steel plate indicating a failure, like in the static tests.

The test results have been summarised and evaluated, together with previous test results presented by other researchers. Linear regression analyses for the S-N (or P-N) curves, assuming a linear relationship in a double logarithmic scale, indicate good agreement within the different test series, while comparisons between different test series indicate clear differences. Some of the factors that can explain the differences are: different types of test specimens, varying material parameters and dimensions, differences in the definition of the fatigue failure and deviating testing procedures. The last two are the ones that the author believes are the major reason for the large scatter between the test series.

Based on the new test results, the author recommends that the characteristic fatigue strength curve presented in equation (4.3) is used for the studied type of CSPs.

This research question is covered by the study of the fatigue strength of CSPs presented in Paper IX and briefly summarized in section 4.3.3.

B-RQ4.   *What is the structural behaviour of a bridge strengthened with Coiled Spring Pins?*

In order to answer this research question, the author has planned and conducted a field monitoring of one of the few bridges strengthened with CSPs, the Pitsund Bridge. The results from the field monitoring have been compared to different design assumptions regarding the stiffness of the shear connection.

The steel strain measurements indicate that the strengthened cross-sections behave as composite cross-sections. In the strengthened span, the registered slips are all very small in comparison to the slips registered in the non-strengthened span. This comparison indicates that the CSPs are reducing the slip significantly.

If the test results, both steel strains and deflections, are compared to FE-models with varying shear connection stiffness, an assumption of a rigid shear connection gives the best agreement.

Regarding the relative vertical movement at the steel-concrete interface, the potential uplift, the measurements show no indications of uplift in the parts with CPSs. This is an expected result, since the forces acting on the shear connectors, during the monitoring, are rather low and since the potential separation is expected to occur in the ultimate limit state.

The results and conclusions presented above are only verified at the tested load levels, which is comparable to the load caused by the fatigue load model three (FLM 3) in Eurocode.

Paper VII contributes with additional information about the structural behaviour, while section 4.3.4 gives a brief summary of this topic.

B-RQ5.   Which aspects need to be covered in a detailed design of this type of strengthening?

Previous research and the research performed by the author, show that there are several important aspects that need to be taken into account in the design procedure of a bridge strengthening by post-installation of CSPs.

Experiences from laboratory tests and bridge strengthening projects have been gathered and used to develop design recommendations based on the author's best knowledge. These recommendations span from the early design stage to the end of the installation procedure.

The recommendations are summarized in a design guidance that is attached to this thesis as Appendix B. This guidance is based on the essence of the information presented in Chapter 4 and the appended Paper VI-IX.

5.3.2   Discussion and further research

The research presented in this thesis is a first step in the development towards general design criteria for post-installed CSPs. Several interesting conclusions have been drawn, observations have been made, improvements have been identified and additional research questions have been raised. Among all, the author would like to highlight the following interesting areas for further research.

There is no doubt that there is a need for large-scale beam tests with CSPs as shear connectors. So far, there are no tests performed in the ultimate limit state on a structural level, only push-out tests on a local shear connection level. There are several reasons why it is important to complete the present knowledge with results from steel-concrete beams

strengthened with CSPs and loaded to failure. Firstly, it is important to prove that the results from the push-out tests are conservative and that the results can be used on a structural level. Secondly, it is also important to study the risk of a potential uplift of the concrete deck slab, to find out if such a behaviour would affect the load capacity in the ultimate limit state or not. The latter is very important, since the European code for new composite bridges, EN 1994-2 (2005), requires that *"Shear connectors shall be capable of preventing separation of the concrete element from the steel element, except where separation is prevented by other means"*. If future beam tests indicate that there is a risk of an uplift that affects the structural load capacity, then it might be necessary to complement the CSPs with additional anchoring devices, which take care of the vertical forces.

As a result of the conclusions from the static and the fatigue push-out tests, the author recommends that future push-out tests are performed on the type of standard push-out test specimen recommended by EN 1994-1-1 (2005). This implies that the steel section needs to be split into two halves prior to the installation of the CSPs and then welded back into one unit after the installation of shear connectors. It should be noted that the HE260B section in the standard test has to be replaced, since the steel flange thickness is a parameter that will affect the test results. By using a standard specimen, it would be easier to compare the results to other types of shear connectors.

It is recommended that the results from the static- and the fatigue-push-out tests are analysed further by comparisons to FE-models. The FE-models should be calibrated to the tests results, followed by parametric studies of the important parameters.

For bridge strengthening projects with CSPs, a large part of the strengthening costs are related to the installation work. Therefore, it would be of interest to reduce the amount of shear connectors by using partial composite action instead of full composite action. This would imply that only the necessary amount of connectors would be installed, in order to achieve the desired strengthening effect. However, before the focus is shifted towards partial composite action, the structural behaviour of a full composite section in the ultimate limit state and the potential risk of uplift should be investigated.

5.4   Concluding discussion

This thesis has been focused on two different ways of reducing the time spent on the construction site and the impact on the road users. None of these methods are mainstream solutions that can, nor should, be used as standard solutions.

The prefabricated concrete deck elements with dry joints, is an example of a possible design solution that can be used if it is crucial to reduce the time spent on the bridge site. However, there are drawbacks and limitations of the concept, which limits the possibilities and the competitiveness. One drawback is the limited tolerances in all stages, from the manufacturing of the steel and the concrete parts to the installation on site. Another drawback, in continuous multi-span bridges, is the need of additional detailing of the waterproofing and the pavement in regions with negative bending moments, due to the varying gap of the dry joints. However, prefabricated bridge deck elements with in-situ cast joints do not have these drawbacks, but they are still rare exceptions in

Sweden. There seems to be a consensus that prefabrication is a good tool to reduce the time spent on the construction site and the impact on the road users. Still the in-situ cast and reinforced concrete deck, which needs both formwork and scaffolding installed on site, is the standard design solution in the quite conservative bridge construction industry.

The strengthening method with post-installed CSPs offers the possibility to strengthen non-composite steel-concrete bridges with no or minimum traffic disturbance. The CSP connector will not be a competitor to the welded headed studs, rather a complement. In new structures, welded headed studs offers an effective installation procedure under controlled conditions in a steel workshop, while CSPs are inappropriate and should not even be considered as an alternative at all. In strengthening of existing structures, welded headed studs will probably be the bridge designers' first choice even in the future, especially if there is a need of additional rehabilitation work on the concrete deck, or if it is not a problem to close the bridge, partly or completely, during the strengthening work. If this is not the case, implying that the concrete deck slab is in good condition and that it is important to minimize the impact on the traffic, then CSPs can be really competitive.

To increase the use of CSPs as shear connectors in composite bridges, the author believes that there is a need of general guidelines, describing the different criteria from the early design process to the end of the installation procedure. This thesis has been a kind of take-off in that direction, but there are still several research questions left to answer before a general design guidance can be written, and additional questions will probably be identified along the way. This is basically what research is about for me, to identify questions that neither you, your colleagues nor the available literature can provide answers to, and then making your own way to the answers through empirical and analytical investigations.

REFERENCES

AASHTO. (2017). *AASHTO LRFD bridge design specifications 8th edition.* Washington DC. USA.

Berthellemy, J. (2009). French bridge experiences from prefabricated deck elements. *Proceedings from Workshop on Composite Bridges with Prefabricated Deck Elements, Stockholm, Sweden, March 4th, 2009.*

Betonghandoken. (1990). *Betonghandboken konstruktion – utg. 2.* Stockholm: Svensk Byggtjänst. (in Swedish)

Blanquart, C., Clausen, U., & Jacob, B. (2016). *Towards Innovative Freight and Logistics.* Hoboken, NJ, USA: John Wiley & Sons.

Buckby, R., Ogle, M., Johnson, R. P., and Harvey, D. (1997). The performance of coiled spring pin connectors under static and fatigue loading. *Proceedings of the International IABSE Conference: Composite construction - conventional and innovative, Innsbruck, Austria, September, 1997.* (p. 669-674). Zürich: IABSE.

Chen Y-T., Zhao Y., West J.S. & Walbridge S. (2014). Behaviour of steel–precast composite girders with through-bolt shear connectors under static loading. *Journal of Constructional Steel Research, 103*, 168-178.

Collin, P., Johansson, B. & Pétursson, H. (1998). S*amverkansbroar med elementbyggda farbanor* (SBI - Publication 165). Stockholm, Sweden: Swedish Institute of Steel Construction.

Collin, P., & Lundmark, T. (2002). Competitive Swedish composite bridges, *IABSE Symposium Report, Melbourne, Australia, September 8-13, 2002.* (p. 94–104). Zürich: IABSE.

Culmo, M.P. (2009). Prefabricated Composite Bridges in the United States – including total bridge prefabrication. *Proceedings from Workshop on Composite Bridges with Prefabricated Deck Elements, Stockholm, Sweden, March 4th, 2009.*

Culmo, M. P. (2011). *Accelerated bridge construction-experience in design, fabrication and erection of prefabricated bridge elements and systems* (Federal Highway Administration Report No. FHWA-HIF-12-013). Washington DC: FHWA.

Culmo, M. P., Marsh, L., Stanton, J., & Mertz, D. (2017). *Recommended AASHTO Guide Specifications for ABC Design and Construction* (Transportation Research Board No. NCHRP Project 12-102). Washington DC: NCHRP, TRB.

Degerman, H. (2002). *Samhällsekonomisk analys av hastighetsnedsättning vid bro söder om Norrfors* (Banverket - Internal Report). Borlänge: Banverket. (in Swedish)

El Hamad, H. & Tanhan, F. (2018). *Analysis of post-tensioned concrete box-girder bridges.* (Master's thesis, KTH Royal Institute of Technology, Stockholm, Sweden). Retrieved from: https://kth.diva-portal.org/smash/get/diva2:1238157/FULLTEXT01.pdf

El Sarraf, R., Iles, D., Momtahan, A., Easey, D., & Hicks, S. (2013). *Steel-concrete composite bridge design guide* (New Zealand Transport Agency research report: 525). Wellington, New Zealand: NZ Transport Agency.

EN 1990 (2002). *Eurocode – Basis of structural design.* European Committee for Standardization; Brussels. Belgium.

EN 1991-2 (2005). *Eurocode 1: Actions on structures – Part 2: Traffic Loads on Bridges.* CEN – European Committee for Standardization, Brussel, Belgium

EN 1992-1-1 (2004). *Eurocode 2: Design of concrete structures – Part 1: General rules and rules for buildings.* Brussels, CEN – European Committee for Standardization.

EN 1992-2 (2005). *Eurocode 2: Design of concrete structures – Part 2: Concrete bridges – Design and detailing rules.* Brussels, CEN – European Committee for Standardization.

EN 1993-1-1 (2005). *Eurocode 3: Design of steel structures – Part 1-1: General rules and rules for buildings.* Brussels, CEN – European Committee for Standardization.

EN 1993-1-5 (2006). *Eurocode 3: Design of steel structures – Part 1-5: Plated structural elements.* Brussels, CEN – European Committee for Standardization.

EN 1993-1-8 (2005). *Eurocode 3: Design of steel structures – Part 1-8: Design of joints.* Brussels, CEN – European Committee for Standardization.

EN 1993-1-9 (2005). *Eurocode 3: Design of steel structures – Part 1-9: Fatigue.* Brussels, CEN – European Committee for Standardization.

EN 1994-1-1 (2005). *Eurocode 4 - Design of composite steel and concrete structures – Part 1-1: General rules and rules for buildings.* Brussels, CEN – European Committee for Standardization.

EN 1994-2 (2005). *Eurocode 4: Design of composite steel and concrete structures – Part 2: General rules and rules for bridges.* Brussels, CEN – European Committee for Standardization.

Ernst, S., Bridge, R. Q., & Wheeler, A. (2010). Correlation of beam tests with pushout tests in steel-concrete composite beams. *Journal of structural engineering, 136*(2), 183-192.

Fahleson, C. (2005). *Provning av skjuvförbindare* (LTU Laboratory Report No: 05035). Luleå, Sweden: Luleå University of Technology. Retrieved from: http://www.diva-portal.org/smash/get/diva2:1172860/FULLTEXT01.pdf (in Swedish)

FHWA (2018a). Highways for Life, Federal Highway Administration. Retrieved 2018 August 17 from https://www.fhwa.dot.gov/hfl/

FHWA (2018b). Accelerated Bridge Construction, Federal Highway Administration. Retrieved 2018 August 17 from https://www.fhwa.dot.gov/bridge/abc/

Gordon, S. & May, I. (2007). Precast deck systems for steel-concrete composite bridges. *Proceedings of the ICE – Bridge Engineering, 160*(1), 25-35.

Hällmark, R., Collin, P. & Stoltz, A. (2009). Innovative Prefabricated Composite Bridges. *Structural Engineering International, 19*(1), 69-78.

Hällmark, R., Collin, P., & Nilsson, M. (2011). Concrete shear keys in prefabricated bridges with dry deck joints. *Nordic Concrete Research*, *44*(2), 109-122.

Hällmark, R. (2012a). *Prefabricated Composite Bridges – a Study of Dry Deck Joints*. (Licentiate thesis, Luleå University of Technology, Luleå, Sweden). Retrieved from: http://www.diva-portal.org/smash/get/diva2:991279/FULLTEXT01.pdf

Hällmark, R., White, H., & Collin, P. (2012b). Prefabricated bridge construction across Europe and America. *Practice Periodical on Structural Design and Construction*, *17*(3), 82-92.

Hällmark, R., Collin, P., & Möller, M. (2013a). The behaviour of a prefabricated composite bridge with dry deck joints. *Structural Engineering International*, *23*(1), 47-54.

Hällmark, R., Collin, P., & Nilsson, M. (2013b). Large-scale tests on a composite bridge with prefabricated concrete deck and dry deck joints. *Stahlbau*, *82*(2), 122-133.

Hällmark, R., Jackson, P., & Collin, P. (2016). Post-installed shear connectors: coiled spring pins. *Proceedings of the 19th IABSE Congress, Stockholm, Sweden, September 21-23, 2016.* (p. 1227-1234). Zürich: IABSE.

Hällmark, R., Jackson, P., Collin, P. & White, H. (2018a). Bridge Strengthening by Post-Installation of Coiled Spring Pin Shear Connectors – a State-of-the-Art Review. *Practice Periodical on Structural Design and Construction*. (in press).

Hällmark, R. & Collin, P. (2018b). Post-Installed Shear Connectors: Monitoring a Bridge Strengthened with Coiled Spring Pins. *Structural Engineering International*. DOI: 10.1080/10168664.2018.1456893 (in press)

Hällmark, R., Collin, P. & Hicks J. S. (2018c). *Post-Installed Shear Connectors: Push-out Tests of Coiled Spring Pins vs. Headed Studs*. Unpublished manuscript (Submitted in August 2018).

Hällmark, R., Collin, P. & Hicks J. S. (2018d). *Post-Installed Shear Connectors: Fatigue Push-out Tests of Coiled Spring Pins*. Unpublished manuscript (Submitted in September 2018).

Hanswille, G. (2011a). Composite bridges in Germany designed according to Eurocode 4-2. *Proceedings of the Sixth International Conference on Composite Construction in Steel and Concrete, Taernash, USA, July 20-24, 2008*. (p. 391-405). Washington DC: ASCE.

Hanswille, G. (2011b). EC 4-2 Background and rules. *Proceedings from International Workshop on Eurocode 4-2 − Composite Bridges, Stockholm, Sweden, March 17th, 2011*. (p. 13-46).

Harryson, P. (2008). *Industrial Bridge Engineering − Structural developments for more efficient bridge construction*. (Doctoral thesis, Chalmers University of Technology, Göteborg). Retrieved from: http://publications.lib.chalmers.se/records/fulltext/70808.pdf

Hechler, O., Berthellemy, J., Lorenc, W., Seidl, G., & Viefhues, E. (2011). Continuous shear connectors in bridge construction. *Proceedings of the Sixth International Conference on Composite Construction in Steel and Concrete, Taernash, USA, July 20-24, 2008*. (p. 78-491). Washington DC: ASCE.

Hewson, N. R. (2003). *Prestressed Concrete Bridges: design and construction*. London, UK: Tomas Telford.

Hicks, S. J., & Smith, A. L. (2014). Stud shear connectors in composite beams that support slabs with profiled steel sheeting. *Structural Engineering International, 24*(2), 246-253.

Hicks, S., Cao, J., McKenzie, C., Chowdhury, M., & Kaufusi, R. (2016). *Evaluation of shear connectors in composite bridges* (NZ Transport Agency research report No. 602). Wellington, New Zealand: NZ Transport Agency.

Hicks, S. J. (2017). Design shear resistance of headed studs embedded in solid slabs and encasements. *Journal of Constructional Steel Research, 139*, 339-352.

Hungerford, B. (2004). *Methods to Develop Composite Action in Non-Composite Bridge Floor Systems: Part II*. (Master's thesis, The University of Texas at Austin, USA). Retrieved from: https://fsel.engr.utexas.edu/pdfs/Hungerford%20Thesis%20May%202004.pdf

ISO 13918 (2008). *Studs and Ceramic ferrules for arc stud welding*. Geneva, ISO − the International Organization for Standardization.

ISO 14555 (2014). *Welding − Arc stud welding of metallic materials*. Geneva, ISO − the International Organization for Standardization.

ISO 8748 (2007). *Spring-type straight pins − Coiled. Heavy duty*. Geneva, ISO − the International Organization for Standardization.

Jackson, P. A., Duckett, W. G., & Spencer, W. A. (2012). Fatigue assessment of structures on the Docklands Light Railway, London, UK. *Proceedings of the Institution of Civil Engineers-Bridge Engineering, 165*(4), 207-214.

Jackson, P. (2015). UK Examples, *Proceedings of the International workshop on strengthening of steel/composite bridges, Stockholm, Sweden, September 28th, 2015.* (p. 28-45).

Johnson, R. P., & Hendy, C. R. (2006). *Designers' Guide to EN 1994-2: Eurocode 4: Design of Steel and Composite Structures: Part 2: General Rules and Rules for Bridges.* London, UK: Thomas Telford.

Kayir, H. (2006). *Methods to develop composite action in non-composite bridge floor systems: Fatigue behavior of post-installed shear connectors.* (Master's thesis, The University of Texas at Austin, USA). Retrieved from: http://fsel.engr.utexas.edu/pdfs/ Kayir_THESIS_May%202006.pdf

Kuhlmann, U., Braun, B., Feldmann, M., Naumes, J. Martin, P-O., Galea, Y., et al. (2008a). *COMBRI Design Manual. Part I: Application of Eurocode Rules.* Research Fund for Coal and Steel and University of Stuttgart Institute of Structural Design.

Kuhlmann, U., Braun, B., Feldmann, M., Naumes, J. Martin, P-O., Galea, Y., (2008b). *COMBRI Design Manual. Part II: State-of-the-Art and Conceptual Design of Steel and Composite Bridge*s. Research Fund for Coal and Steel and University of Stuttgart Institute of Structural Design

Kuhlmann, U., Maier, P., da Silva, L., Gervásio, H., Brett, C., Schröter, F. et al., (2013). *Sustainable Steel-Composite Bridges in Built Environment (SBRI).* Research project of the Research Fund for Coal and Steel RFSR-CT-2009-00020. Final Report.

Kwon, G. (2008). *Strengthening Existing Steel Bridge Girders by the Use of Post-Installed Shear Connectors.* (Doctoral thesis, The University of Texas at Austin, USA). Retrieved from: https://repositories.lib.utexas.edu/bitstream/handle/2152/18079/kwond74300.pdf?seq uence=2&isAllowed=y

Kwon, G., Engelhardt, M. D., & Klingner, R. E. (2009). Strengthening bridges by developing composite action in existing non-composite bridge girders. *Structural Engineering International, 19*(4), 432-437.

Kwon, G., Engelhardt, M. D., & Klingner, R. E. (2010a). Behavior of post-installed shear connectors under static and fatigue loading. *Journal of Constructional Steel Research, 66*(4), 532-541.

Kwon, G., Engelhardt, M. D., & Klingner, R. E. (2010b). Experimental behavior of bridge beams retrofitted with postinstalled shear connectors. *Journal of Bridge Engineering, 16*(4), 536-545.

Kwon, G., Engelhardt, M. D., & Klingner, R. E. (2011). Parametric studies and preliminary design recommendations on the use of postinstalled shear connectors for strengthening noncomposite steel bridges. *Journal of Bridge Engineering, 17*(2), 310-317.

Lam, D. (1998). *Composite steel beams using precast concrete hollow core floor slabs.* (Doctoral thesis, University of Nottingham, UK). Retrieved from: http://eprints.nottingham.ac.uk/11350/1/243351.pdf

Lam, D. (2007). Capacities of headed stud shear connectors in composite steel beams with precast hollowcore slabs. *Journal of Constructional Steel Research, 63*, 1160-1174.

Liu X., Bradford M.A., Chen Q-J. & Ban H. (2016). Finite element modelling of steel–concrete composite beams with high-strength friction-grip bolt shear connectors. *Finite Elements in Analysis and Design, 108*, 54-65.

Lumsden, K. (2004). *Truck masses and dimensions - impact on transport efficiency* (Research Report; Department of Logistics and Transportation, Chalmers University of Technology). Gothenburg, Sweden: Chalmers University of Technology

Lungershausen, H. (1988). *Zur Schubtragfähigkeit von Kopfbolzendübeln*. (Doctoral thesis, Ruhr Universität Bochum, Germany).

Markowski, S. (2005). *Experimental and Analytical Study of Full-Depth Precast/Prestressed Concrete Deck Panels for Highway Bridges*. (Master's thesis, University of Wisconsin-Madison, USA).

Möller F., Collin, P., Haarju, T., Hällmark R., Hehne, T., Hoyer, O., et al. (2012a). *Final Report − ELEM - Composite Bridges with Prefabricated Decks*. Research project of the Research Fund for Coal and Steel RFSR–CT–2008-00039, Final Report.

Möller F., Collin, P., Haarju, T., Hällmark R., Hehne, T., Hoyer, O., et al. (2012b). *Design Guide − ELEM - Composite Bridges with Prefabricated Decks*. Research project of the Research Fund for Coal and Steel RFSR–CT–2008-00039, Design Guidance.

Moynihan M.C. & Allwood J.M. (2014). Viability and performance of demountable composite connectors, *Journal of Constructional Steel Research, 99*, 47-56.

NCHRP (2003). *NCHRP Synthesis 324 − Prefabricated Bridge Elements and Systems to Limit Traffic Disruption During Construction*. Washington DC, USA: Transportation Research Board.

NCHRP (2009). *NCHRP Project 20-68A − Best Practice in Accelerated Construction Techniques* (Scan Team Report). Lawrenceville, USA: Scan Management.

Nellinger, S., Odenbreit, C., Obiala, R., & Lawson, M. (2017). Influence of transverse loading onto push-out tests with deep steel decking. *Journal of Constructional Steel Research, 128*, 335-353.

Nilsson, M. (2001). *Samverkansbroar ur ett samhällsekonomiskt perspektiv* (Master's thesis, Luleå University of Technology, Sweden). Retrieved from: http://www.diva-portal.org/smash/get/diva2:1019240/FULLTEXT01.pdf (in Swedish)

Olsson, D. (2017). *Achieving Composite Action in Existing Bridges − With post-installed shear connectors*. (Master's thesis, Luleå University of Technology, Sweden). Retrieved from: http://www.diva-portal.org/smash/get/diva2:1066328/FULLTEXT02

Pathirana, S. W., Uy, B., Mirza, O., & Zhu, X. (2015). Strengthening of existing composite steel-concrete beams utilising bolted shear connectors and welded studs. *Journal of Constructional Steel Research, 114*, 417-430.

Pathirana, S. W., Uy, B., Mirza, O., & Zhu, X. (2016a). Flexural behaviour of composite steel–concrete beams utilising blind bolt shear connectors. *Engineering Structures, 114*, 181-194.

Pathirana, S. W., Uy, B., Mirza, O., & Zhu, X. (2016b). Bolted and welded connectors for the rehabilitation of composite beams. *Journal of Constructional Steel Research, 125*, 61-73.

Pavlovic M., Markovic Z., Veljkovic M. & Budevac D. (2013). Bolted shear connectors vs. headed studs behavior in push-out tests. *Journal of Constructional Steel Research, 88*, 134-149.

Peiris, A. & Harik, I. (2014). Steel bridge girder strengthening using postinstalled shear connectors and UHM CFRP laminates. *Journal of Performance of Constructed Facilities, 29*(5).

Pelke, E., & Kurrer, K. E. (2015). On the evolution of steel-concrete composite construction. *Proceedings of the 5th International Congress on Construction History Chicago, USA, June 3-7, 2015*. (p. 107-116).

Pritchard, B. (1992). *Bridge Design for Economy and Durability: Concepts for New, Strengthened and Replacement Bridges*. London, UK: Thomas Telford.

Ralls, M.L, Tang, B. Bhidé, S., Brecto, B. et al. (2005). *Prefabricated Bridge Elements and Systems in Japan and Europe* (FHWA Publication No: FHWA-PL-05-003). Washington DC, USA: FHWA.

Roik, K., Hanswille, G. Cunze, A. & Lanna, O. (1989). *Harmonisation of the European Construction Codes – Report on EUROCODE 4 Clause 6.3.2: Stud Connectors* (Research Report No: EC4/8/88). Bochum, Germany.

Roik, K. & Hanswille, G. (1990). *Harmonization of the European Construction Codes – Background Report on EUROCODE 4 – Limit state of fatigue for headed studs*. (Research Report No: EC4/11/90). Bochum, Germany.

Schaap, B. (2004). *Methods to Develop Composite Action in Non-Composite Bridge Floor Systems*. (Master's thesis, The University of Texas at Austin, USA).

Schneider, C. R. A. & Maddox, S. J. (2003). *Best practice guide on statistical analysis of fatigue data*. (International Institute of Welding Doc: IIW-XIII-WG1-114-03). Cambridge, UK: The Welding Institute

Seidl, G. (2009a). Composite Element Bridges. *Proceedings from Workshop on Composite Bridges with Prefabricated Deck Elements, Stockholm, Sweden, March 4ᵗʰ, 2009*.

Seidl, G. & Braun, A. (2009b). VFT-WIB-Brücke bei Vigaun – Verbundsbrück mit externer Bewehrung. *Stahlbau, 78*(2), 86-93. (in German)

Shim, C.S., Chung, C.H., Kim, I.K., & Kim, Y.J. (2010). Development and application of precast decks for composite bridges. *Structural Engineering International, 20*(2), 126-133.

Simonsson, P. (2008). *Industrial Bridge Construction with Cast in Place Concrete*. (Licentiate thesis, Luleå University of Technology, Sweden). Retrieved from: https://www.diva-portal.org/smash/get/diva2:991640/FULLTEXT01.pdf

Stoltz, A. (2001). *Effektivare samverkansbroar – Prefabricerade farbanor med torra fogar*. (Licentiate thesis, Luleå University of Technology, Sweden). Retrieved from: http://www.diva-portal.org/smash/get/diva2:991667/FULLTEXT01.pdf (in Swedish)

Trafikverket (2016). *Statliga vägar som kan anses lämpade för en ny bärighetsklass 4*. Borlänge, Sweden: Trafikverket. (in Swedish)

Wang, J. Y., Guo, J. Y., Jia, L. J., Chen, S. M., & Dong, Y. (2017). Push-out tests of demountable headed stud shear connectors in steel-UHPC composite structures. *Composite Structures*, *170*, 69-79.

Womack, J. & Jone, D. (2003). *Lean Thinking – Banish waste and create wealth in your corporation*. New York, USA: Simon and Schuster

Xie, E. & Valente, I. (2011). F*atigue strength of shear connectors* (Research report, University of Minho). Guimarães, Portugal: University of Minho

DOCTORAL AND LICENTIATE THESES

Division of Structural Engineering

Luleå University of Technology

Doctoral theses

1980   Ulf Arne Girhammar: *Dynamic fail-safe behaviour of steel structures*. Doctoral Thesis 1980:060D. 309 pp.

1983   Kent Gylltoft: *Fracture mechanics models for fatigue in concrete structures*. Doctoral Thesis 1983:25D. 210 pp.

1985   Thomas Olofsson: *Mathematical modelling of jointed rock masses*. Doctoral Thesis 1985:42D. 143 pp. (In collaboration with the Division of Rock Mechanics).

1988   Lennart Fransson: *Thermal ice pressure on structures in ice covers*. Doctoral Thesis 1988:67D. 161 pp.

1989   Mats Emborg: *Thermal stresses in concrete structures at early ages*. Doctoral Thesis 1989:73D. 285 pp.

1993   Lars Stehn: *Tensile fracture of ice. Test methods and fracture mechanics analysis*. Doctoral Thesis 1993:129D, September 1993. 136 pp.

1994   Björn Täljsten: *Plate bonding. Strengthening of existing concrete structures with epoxy bonded plates of steel or fibre reinforced plastics*. Doctoral Thesis 1994:152D, August 1994. 283 pp.

1994   Jan-Erik Jonasson: *Modelling of temperature, moisture and stresses in young concrete*. Doctoral Thesis 1994:153D, August 1994. 227 pp.

1994   Anders Sundin: *High performance hybrid mixed elements using orthogonal stress interpolants and scaling of the higher order stiffness*. Doctoral Thesis 1986:156D, 184 pp. Structural Mechanics

1995   Ulf Ohlsson: *Fracture mechanics analysis of concrete structures*. Doctoral Thesis 1995:179D, December 1995. 98 pp.

1995   Annika Moström: *Search for efficient time integration methods in structural dynamics for finite element meshes with large variations of properties*. Doctoral Thesis 1995:181D, 202 pp. Structural Mechanics.

1998   Keivan Noghabai: *Effect of tension softening on the performance of concrete structures*. Doctoral Thesis 1998:21, August 1998. 150 pp.

1998   Ireneusz Czmoch: *Influence of structural timber variability on reliability and damage tolerance of timber beams*. Doctoral Thesis 1998:30D, 297 pp. Structural Mechanics.

1999   Gustaf Westman: *Concrete creep and thermal stresses. New creep models and their effects on stress development*. Doctoral Thesis 1999:10, May 1999. 301 pp.

1999   Henrik Gabrielsson: *Ductility in high performance concrete structures. An experimental investigation and a theoretical study of prestressed hollow core slabs and prestressed cylindrical pole elements*. Doctoral Thesis 1999:15, May 1999. 283 pp.

2000   Patrik Groth: Fibre r*einforced concrete − Fracture mechanics methods applied on self-compacting concrete and energetically modified binders*. Doctoral Thesis 2000:04, January 2000. 214 pp. ISBN 978-91-85685-00-4.

2000   Hans Hedlund: *Hardening concrete. Measurements and evaluation of non-elastic deformation and associated restraint stresses*. Doctoral Thesis 2000:25, December 2000. 394 pp. ISBN 91-89580-00-1.

2001   Robert Tano: *Modelling of localized failure with emphasis on band paths*. Doctoral Thesis 2001:08D, 200 pp. Structural Mechanics.

2003   Anders Carolin: *Carbon fibre reinforced polymers for strengthening of structural members*. Doctoral Thesis 2003:18, June 2003. 190 pp. ISBN 91-89580-04-4.

2003   Martin Nilsson: *Restraint factors and partial coefficients for crack risk analyses of early age concrete structures*. Doctoral Thesis 2003:19, June 2003. 170 pp. ISBN: 91-89580-05-2.

2003   Mårten Larson: *Thermal crack estimation in early age concrete − Models and methods for practical application*. Doctoral Thesis 2003:20, June 2003. 190 pp. ISBN 91-86580-06-0.

2004   Chouping Luo: *Finite elements based on the piece-wise linear weight functions in contact problems*. Doctoral Thesis 2004:46D, 122 pp. Structural Mechanics.

2005   Erik Nordström: *Durability of sprayed concrete. Steel fibre corrosion in cracks*. Doctoral Thesis 2005:02, January 2005. 151 pp. ISBN 978-91-85685-01-1.

2006   Rogier Jongeling: *A process model for work-flow management in construction. Combined use of location-based scheduling and 4D CAD*. Doctoral Thesis 2006:47, October 2006. 191 pp. ISBN 978-91-85685-02-8.

2006   Jonas Carlswärd: *Shrinkage cracking of steel fibre reinforced self compacting concrete overlays – Test methods and theoretical modelling*. Doctoral Thesis 2006:55, December 2006. 250 pp. ISBN 978-91-85685-04-2.

2006   Håkan Thun: *Assessment of fatigue resistance and strength in existing concrete structures*. Doctoral Thesis 2006:65, December 2006. 169 pp. ISBN 978-91-85685-03-5.

2007   Lundqvist Joakim: *Numerical analysis of concrete elements strengthened with carbon fiber reinforced polymers*. Doctoral Thesis 2007:07, March 2007. 50 pp. ISBN 978-91-85685-06-6.

2007   Arvid Hejll: *Civil structural health monitoring – Strategies, methods and applications*. Doctoral Thesis 2007:10, March 2007. 189 pp. ISBN 978-91-85685-08-0.

2007   Stefan Woksepp: *Virtual reality in construction: Tools, methods and processes*. Doctoral Thesis 2007:49, November 2007. 191 pp. ISBN 978-91-85685-09-7.

2007   Romuald Rwamamara: *Planning the healthy construction workplace through risk assessment and design methods*. Doctoral Thesis 2007:74, November 2007. 179 pp. ISBN 978-91-85685-11-0.

2008   Björnar Sand: *Nonlinear finite element simulations of ice forces on offshore structures*. Doctoral Thesis 2008:39, September 2008. 241 pp.

2008   Bengt Toolanen: *Lean contracting: relational contracting influenced by lean thinking*. Doctoral Thesis 2008:41, October 2008. 190 pp.

2008   Sofia Utsi: *Performance based concrete mix-design: Aggregate and micro mortar optimization applied on self-compacting concrete containing fly ash*. Doctoral Thesis 2008:49, November 2008. 190 pp.

2009   Markus Bergström: *Assessment of existing concrete bridges: Bending stiffness as a performance indicator*. Doctoral Thesis, March 2009. 241 pp. ISBN 978-91-86233-11-2.

2009   Tobias Larsson: *Fatigue assessment of riveted bridges*. Doctoral Thesis, March 2009. 165 pp. ISBN 978-91-86233-13-6.

2009   Thomas Blanksvärd: *Strengthening of concrete structures by the use of mineral based composites: System and design models for flexure and shear*. Doctoral Thesis, April 2009. 156 pp. ISBN 978-91-86233-23-5.

2011   Anders Bennitz: *Externally unbonded post-tensioned CFRP tendons – A system solution*. Doctoral Thesis, February 2011. 68 pp. ISBN 978-91-7439-206-7.

2011   Gabriel Sas: *FRP shear strengthening of reinforced concrete beams*. Doctoral Thesis, April 2011. 97 pp. ISBN 978-91-7439-239-5.

2011   Peter Simonsson: *Buildability of concrete structures: processes, methods and material*. Doctoral Thesis, April 2011. 64 pp. ISBN 978-91-7439-243-2.

2011   Stig Bernander: *Progressive landslides in long natural slopes. Formation, potential extension and configuration of finished slides in strain-softening soils*. Doctoral Thesis, May 2011, rev. August 2011 and April 2012. 250 pp. ISBN 978-91-7439-238-8. (In collaboration with the Division of Soil Mechanics and Foundation Engineering).

2012   Arto Puurula: *Load carrying capacity of a strengthened reinforced concrete bridge: non-linear finite element modeling of a test to failure. Assessment of train load capacity of a two span railway trough bridge in Örnsköldsvik strengthened with bars of carbon fibre reinforced polymers (CFRP)*. Doctoral Thesis, May 2012. 100 pp. ISBN 978-91-7439-433-7.

2015   Mohammed Salih Mohammed Mahal: *Fatigue behaviour of RC beams strengthened with CFRP. Analytical and experimental investigations*. Doctoral Thesis, March 2015. 138 pp. ISBN 978-91-7583-234-0.

2015   Jonny Nilimaa: *Concrete bridges: Improved load capacity*. Doctoral Thesis, June 2015. 180 pp. ISBN 978-91-7583-344-6.

2015   Tarek Edrees Saaed: *Structural control and identification of civil engineering structures*. Doctoral Thesis, June 2015. 314 pp. ISBN 978-91-7583-241-8.

2015   Majid Al-Gburi: *Restraint effect in early age concrete structures*. Doctoral Thesis, September 2015. 190 pp. ISBN 978-91-7583-374-3.

2017   Cosmin Popescu: *CFRP strengthening of cut-out openings in concrete walls – Analysis and laboratory tests*. Doctoral Thesis, February 2017, 159 pp. ISBN 978-91-7583-794-9.

2017   Katalin Orosz: *Early age autogenous deformation and cracking of cementitious materials – Implications on strengthening of concrete*. Doctoral Thesis, June 2017, 226 pp. ISBN 978-91-7583-908-0.

2017   Niklas Bagge: *Structural assessment procedures for existing concrete bridges: Experiences from failure tests of the Kiruna Bridge*. Doctoral Thesis, June 2017, 310 pp. ISBN 978-91-7583-878-6.

2017   Rasoul Nilforoush: *Anchorage in Concrete Structures: Numerical and Experimental Evaluations of Load-Carrying Capacity of Cast-in-Place Headed Anchors and Post-Installed Adhesive Anchors*. Doctoral Thesis, November 2017, 352 pp. ISBN 978-91-7790-002-3.

Licentiate theses

1984   Lennart Fransson: *Bärförmåga hos ett flytande istäcke. Beräkningsmodeller och experimentella studier av naturlig is och av is förstärkt med armering*. Licentiate Thesis 1984:012L. 137 pp. (In Swedish).

1985   Mats Emborg: *Temperature stresses in massive concrete structures. Viscoelastic models and laboratory tests*. Licentiate Thesis 1985:011L, May 1985. rev. November 1985. 163 pp.

1987   Christer Hjalmarsson: *Effektbehov i bostadshus. Experimentell bestämning av effektbehov i små- och flerbostadshus*. Licentiate Thesis 1987:009L, October 1987. 72 pp. (In Swedish).

1990   Björn Täljsten: *Förstärkning av betongkonstruktioner genom pålimning av stålplåtar*. Licentiate Thesis 1990:06L, May 1990. 205 pp. (In Swedish).

1990   Ulf Ohlsson: *Fracture mechanics studies of concrete structures*. Licentiate Thesis 1990:07L, May 1990. 66 pp.

1990   Lars Stehn: *Fracture toughness of sea ice. Development of a test system based on chevron notched specimens*. Licentiate Thesis 1990:11L, September 1990. 88 pp.

1991   Anders Sundin: *Accuracy and reliability of plane hybrid mixed elements for two-dimensional elasticity*. Licentiate Thesis 1991:02L. 118 pp. Structural Mechanics

1991   Annika Vallgren: *Self-adaptive solution algorithms for non-linear structural problems*. Licentiate Thesis 1991:03L. 124 pp. Structural Mechanics

1992   Mikael Nyström: *Numerical modelling of floating ice covers including anisotropy and inhomogeneity*. Licentiate Thesis 1992:03L. 78 pp. Structural Mechanics

1992   Per Anders Daerga: *Some experimental fracture mechanics studies in mode I of concrete and wood*. Licentiate Thesis 1992:12L, April 1992, rev. June 1992. 81 pp.

1993   Henrik Gabrielsson: *Shear capacity of beams of reinforced high performance concrete*. Licentiate Thesis 1993:21L, May 1993. 109 pp.

1995   Keivan Noghabai: *Splitting of concrete in the anchoring zone of deformed bars. A fracture mechanics approach to bond*. Licentiate Thesis 1995:26L, May 1995. 123 pp.

1995   Gustaf Westman: *Thermal cracking in high performance concrete. Viscoelastic models and laboratory tests*. Licentiate Thesis 1995:27L, May 1995. 125 pp.

1995   Katarina Ekerfors: *Mognadsutveckling i ung betong. Temperaturkänslighet, hållfasthet och värmeutveckling*. Licentiate Thesis 1995:34L, October 1995. 137 pp. (In Swedish).

1996   Patrik Groth: *Cracking in concrete. Crack prevention with air-cooling and crack distribution with steel fibre reinforcement*. Licentiate Thesis 1996:37L, October 1996. 128 pp.

1996   Hans Hedlund: *Stresses in high performance concrete due to temperature and moisture variations at early ages*. Licentiate Thesis 1996:38L, October 1996. 240 pp.

1996   Tomas Karlsson: *Finite element simulation of flow in granular materials*. Licentiate Thesis 1996:08L. 139 pp. Structural Mechanics

1997   Robert Tano: *Localization modelling with inner softening band finite elements*. Licentiate Thesis 1997:26L. 110 pp. Structural Mechanics

2000   Mårten Larson: *Estimation of crack risk in early age concrete. Simplified methods for practical use*. Licentiate Thesis 2000:10, April 2000. 170 pp.

2000   Stig Bernander: *Progressive landslides in long natural slopes. Formation, potential extension and configuration of finished slides in strain-softening soils*. Licentiate Thesis 2000:16, May 2000. 137 pp. (In collaboration with the Division of Soil Mechanics and Foundation Engineering).

2000   Martin Nilsson: *Thermal cracking of young concrete. Partial coefficients, restraint effects and influences of casting joints*. Licentiate Thesis 2000:27, October 2000. 267 pp.

2000   Erik Nordström: *Steel fibre corrosion in cracks. Durability of sprayed concrete*. Licentiate Thesis 2000:49, December 2000. 103 pp.

2001   Anders Carolin: *Strengthening of concrete structures with CFRP – Shear strengthening and full-scale applications*. Licentiate thesis 2001:01, June 2001. 120 pp. ISBN 91–89580–01–X.

2001   Håkan Thun: *Evaluation of concrete structures. Strength development and fatigue capacity*. Licentiate Thesis 2001:25, June 2001. 164 pp. ISBN 91–89580–08–2.

2002   Patrice Godonue: *Preliminary design and analysis of pedestrian FRP bridge deck*. Licentiate Thesis 2002:18. 203 pp.

2002   Jonas Carlswärd: *Steel fibre reinforced concrete toppings exposed to shrinkage and temperature deformations*. Licentiate Thesis 2002:33, August 2002. 112 pp.

2003   Sofia Utsi: *Self-compacting concrete – Properties of fresh and hardening concrete for civil engineering applications*. Licentiate Thesis 2003:19, June 2003. 185 pp.

2003   Anders Rönneblad: *Product models for concrete structures – Standards, applications and implementations*. Licentiate Thesis 2003:22, June 2003. 104 pp.

2003   Håkan Nordin: *Strengthening of concrete structures with pre-stressed CFRP*. Licentiate Thesis 2003:25, June 2003. 125 pp.

2004   Arto Puurula: *Assessment of prestressed concrete bridges loaded in combined shear, torsion and bending*. Licentiate Thesis 2004:43, November 2004. 212 pp.

2004   Arvid Hejll: *Structural health monitoring of bridges. Monitor, assess and retrofit*. Licentiate Thesis 2004:46, November 2004. 128 pp.

2004   Joakim Lundqvist: *Numerical simulation of tube hydroforming: adaptive loading paths*. Licentiate Thesis 2004:26L. 101 pp. Structural Mechanics

2005   Ola Enochsson: *CFRP strengthening of concrete slabs, with and without openings. Experiment, analysis, design and field application*. Licentiate Thesis 2005:87, November 2005. 154 pp.

2006   Markus Bergström: *Life cycle behaviour of concrete structures − Laboratory test and probabilistic evaluation*. Licentiate Thesis 2006:59, December 2006. 173 pp. ISBN 978-91-85685-05-9.

2007   Thomas Blanksvärd: *Strengthening of concrete structures by mineral based composites*. Licentiate Thesis 2007:15, March 2007. 300 pp. ISBN 978-91-85685-07-3.

2008   Peter Simonsson: *Industrial bridge construction with cast in place concrete: New production methods and lean construction philosophies*. Licentiate Thesis 2008:17, May 2008. 164 pp. ISBN 978-91-85685-12-7.

2008   Anders Stenlund: *Load carrying capacity of bridges: Three case studies of bridges in northern Sweden where probabilistic methods have been used to study effects of monitoring and strengthening*. Licentiate Thesis 2008:18, May 2008. 306 pp. ISBN 978-91-85685-13-4.

2008   Anders Bennitz: *Mechanical anchorage of prestressed CFRP tendons − Theory and tests*. Licentiate Thesis 2008:32, November 2008. 319 pp.

2008   Gabriel Sas: *FRP shear strengthening of RC beams and walls*. Licentiate Thesis 2008:39, December 2008. 107 pp.

2010   Tomas Sandström: *Durability of concrete hydropower structures when repaired with concrete overlays*. Licentiate Thesis, February 2010. 179 pp. ISBN 978-91-7439-074-2.

2013   Johan Larsson: *Mapping the concept of industrialized bridge construction: Potentials and obstacles*. Licentiate Thesis, January 2013. 66 pp. ISBN 978-91-7439-543-3.

2013   Jonny Nilimaa: *Upgrading concrete bridges: Post-tensioning for higher loads*. Licentiate Thesis, January 2013. 300 pp. ISBN 978-91-7439-546-4.

2013   Katalin Orosz: *Tensile behaviour of mineral-based composites*. Licentiate Thesis, May 2013. 92 pp. ISBN 978-91-7439-663-8.

2013   Peter Fjellström: *Measurement and modelling of young concrete properties*. Licentiate Thesis, May 2013. 121 pp. ISBN 978-91-7439-644-7.

2014   Majid Al-Gburi: *Restraint in structures with young concrete: Tools and estimations for practical use*. Licentiate Thesis, September 2014. 106 pp. ISBN 978-91-7439-977-6.

2014   Tarek Edrees Saaed: *Structural identification of civil engineering structures*. Licentiate Thesis, November 2014. 135 pp. ISBN 978-91-7583-053-7.

2014   Niklas Bagge: *Assessment of concrete bridges: Models and tests for refined capacity estimates*. Licentiate Thesis, December 2014. 132 pp. ISBN 978–91–7583–163–0.

2015   Cosmin Popescu: *FRP strengthening of concrete walls with openings*. Licentiate Thesis, December 2015. 134 pp. ISBN 978–91–7583–453–5.

2016   Faez Sayahi: *Plastic Shrinkage Cracking in Concrete*. Licentiate Thesis, December 2015. 134 pp. ISBN: 978–91–7583–678–2.

2016   Jens Häggström: *Evaluation of the load carrying capacity of a steel truss railway bridge: testing, theory and evaluation*. Licentiate Thesis, December 2016. 139 pp. ISBN: 978–91–7583–739–0.

2017   Yahya Ghasemi: *Aggregates in concrete mix design*. Licentiate Thesis, March 2017. 60 pp. ISBN: 978–91–7583–801–4.

2017   Anders Hösthagen: *Thermal Crack Risk Estimation and Material Properties of Young Concrete*. Licentiate Thesis, October 2017. 85 pp. ISBN: 978–91–7583–951–6.

Appendix A

DESIGN GUIDANCE

COMPOSITE BRIDGES WITH PREFABRICATED CONCRETE DECK ELEMENTS WITH DRY JOINTS

This appendix summarises the knowledge and research on composite bridges with prefabricated concrete deck elements with dry joints, by presenting a design guidance along with a design example.

The recommendations are limited to steel–concrete composite bridges designed with prefabricated concrete deck elements, with dry joints between the concrete elements and with in-situ cast longitudinal connections between the steel girders and the concrete deck. The latter is created by injecting concrete into a closed channel, to get a dry deck surface as soon as possible, see Figure A.1a. Overlapping concrete tongues, shear keys, are used to transfer shear forces over the dry joints, see Figure A.1b.

(a) Illustration of the longitudinal joint   (b) Dry deck joint with shear keys
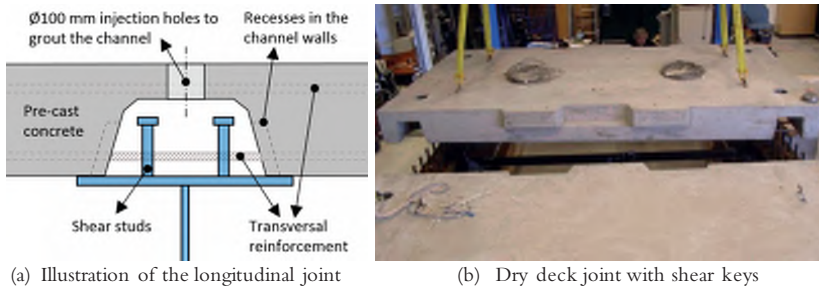
Figure A.1 Illustration of the longitudinal and transversal joints in the studied concept

The suggestions and advices presented in this appendix are based on results from laboratory tests, field monitoring of a bridge and the experiences from the design of three single span bridges of this type. It should be highlighted that the presented

recommendations are examples of important aspects and details that have been identified by the author. However, these examples do not claim to be comprehensive. It is likely that bridge designers will identify additional critical aspects and encounter design problems that have been overlooked in this study.

The design methods are generally identical as those used for conventional composite bridges, with in-situ cast concrete decks, designed according to EN 1994-2 (2005). Therefore, only the design steps where differences have been identified are presented in this appendix.

A.1 Global analysis

For the studied type of bridge, the global analysis can generally be performed in accordance with the requirement of EN 1994-2 (2005). There are however some parts of the design process that need to be modified. Some of the most important modifications are presented below.

It should be mentioned that the structural behaviour are affected by the magnitude of the joint gaps. The design recommendations below require that the specified production tolerances of the joint gaps are fulfilled, see section A.5.

EN 1994-2 (2005) 5.4.1.2 – Effective width of flanges for shear lag

ULS – positive bending moment (concrete in compression)

Large-scale tests reported by (Möller et al. 2012a) indicate that the stiffness of a composite section with prefabricated deck elements with dry joints is a bit lower than the stiffness of an in-situ cast deck. The tested ultimate capacities are also lower in comparison to the result from the reference test, with an in-situ cast concrete deck, but still higher or equal to the load capacity calculated according to EN 1994-2 (2005). It would be preferable if this behaviour had been verified by additional tests.

In the ULS it is suggested to use the formulas given in EN 1994-2 (2005) for calculating the effective width of the interacting concrete and the equivalent span length, L_e, see Figure A.2. In lack of additional test results, the author suggests that the effective concrete flange area, calculated in line with EN 1994-2 (2005), is reduced by a factor of 0.8.

1. $L_e = 0.85L_1$ for $b_{eff,1}$
2. $L_e = 0.25(L_1+L_2)$ for $b_{eff,2}$
3. $L_e = 0.70L_2$ for $b_{eff,1}$
4. $L_e = 2L_3$ for $b_{eff,2}$
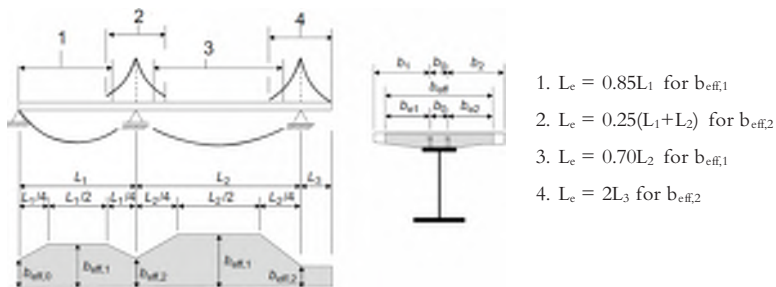
Figure A.2 *Equivalent length for calculation of effective width of the concrete, EN 1994-2 (2005)*

SLS and FLS – positive bending moment (concrete in compression)

Under moderate loading, results from laboratory tests, field monitoring and FE-analyses all indicate a lower stiffness of this kind of bridge deck, i.e. a reduced effective width of the concrete flanges, in comparison to a corresponding in-situ cast bridge deck. Under the same load, the steel stresses will be higher in this type of structure in comparison to the steel stresses in a corresponding bridge with an in-situ cast deck. This behaviour is a consequence of the combination of initial joint gaps, that need to be closed, and the existences of the continuous in-situ cast concrete channels that need to be compressed in order to close the joint. This leads altogether to a significant reduction of the effective concrete width for a beam model in SLS and FLS.

It is suggested that the effective concrete width is calculated according to EN 1994-2 5.4.1.2, assuming an equivalent span length (L_e) equal to the maximum longitudinal distance between the outermost shear studs within an element.

ULS, SLS and FLS – negative bending moment (concrete in tension)

In case of negative bending moments, the model described in EN 1994-2 (2005) is not suitable for defining the effective width of the concrete flanges. The distance between the points of zero bending moment, the equivalent span (L_e), cannot be approximated in the same way. L_e can never be longer than the maximum longitudinal distance between the outermost shear studs within the element, since the concrete elements cannot transfer any longitudinal tensional forces over a joint. Laboratory tests, as well as FE-analyses, indicate that the structural stiffness over an internal support (negative bending moment) is rather close to the stiffness of the steel section itself. Therefore, in the global analysis it is recommended to use the stiffness of the steel cross-section alone. If there are doubts whether this approximation can be used on a specific bridge or not, it is recommended to perform a quick sensitivity analysis studying the impact, on the moment distribution, of an increased interacting concrete area.

EN 1994-2 (2005) 5.4.2.3 (3) – Effects of cracking of concrete

The simplified method that is described in this paragraph should be good enough also for a global analysis of multi span composite bridges with dry deck joints. However, the stiffness in the support regions (15% of the span length at each side of an internal support) has to be modified. EN 1994-2 (2005) provides a stiffness for composite sections with cracked concrete, which is based on the moment of inertia for the equivalent effective steel cross-section (I_2) including reinforcement bars but excluding concrete in tension. Since there are no longitudinal reinforcement bars that cross the joints, only the cross-section of the steel girder should be used to model the support regions of the superstructure in the global analysis.

A.2   Resistance of cross-sections

The following approach is suggested to determine the cross-sectional resistance of the superstructure.

If the concrete deck is in tension, bending moments and normal forces taken into consideration, the steel cross-section should be designed to take the entire load. In comparison to an in-situ cast bridge deck, this design will result in some extra steel in the upper flanges in the support sections, approximately replacing the area of the longitudinal reinforcement, with a minor addition due to the shorter distance to the neutral bending axis.

If the concrete deck is in compression, bending moments and normal forces taken into consideration, the cross-sectional resistance can be determined according to the rules given in EN 1994-2 (2005) but with 20% reduction of the interacting concrete area (factor 0.8). The reduction is due to a limited number of beam tests loaded until failure and due to tested load capacities that are somewhat lower than the capacity of the reference test with an in-situ cast deck. This assumption is reasonable in the ULS, according to the tests presented by Möller et al. (2012a). However, under moderate loading, in the SLS and FLS, the effective width of the interacting concrete is smaller. Tests have shown that an equivalent span length (L_e) equal to the distance between the outermost shear studs within an element, gives a good approximation of the interacting concrete area.

If the mean value of the gaps between the elements are assumed to be large (>1.0 mm), one should consider doing a non-linear FE-analysis simulating joint gaps that are closing under an increased load. Such an analysis will give an estimation of the impact, from the joints gaps, on the stress distribution in the composite cross-section.

In most cases, the neutral bending axis will be located close to the upper flange in cross-sections experiencing positive bending moments. Therefore, the bottom flange will often be the critical part of the steel girder, together with the details attached to the bottom flanges that have to be checked for fatigue. The relative influence on the stress level, from the joint gaps, is small in the bottom flange and high in the upper flange, which is beneficial from this point of view.

A.3   Concrete element design

The concrete element design is performed in line with EN 1992-1-1 (2004), EN 1992-2 (2005) and EN 1994-2 (2005). This section presents some examples of design solutions and procedures used so far.

The shear keys are critical details in the design of the elements. This guidance describes one type of shear key, which has been tested and evaluated with varying reinforcement layouts. This type of shear key, shown in Figure A.3a, has been proven suitable for bridges with girder spacing ≤ 5.0 m. The shear keys are designed as a series of overlapping male-female connections, always with one large shear key distributing the load in one direction, and two smaller shear keys distributing the load in the other direction, see Figure A.3b.
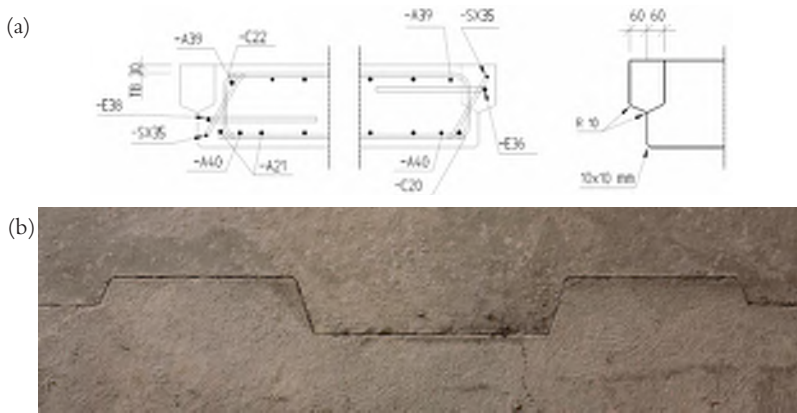
(a)

(b)

Figure A.3 *Tested type of shear key, (a) reinforcement and geometry, (b) photo of a dry joint*

The dimensions of the elements will vary due to different: road profiles, design traditions in different countries, distance between the girders, reinforcement layout in the elements etc. This implies that the shear key design will vary as well. This section should be treated as a summary of recommendations and advices of how shear keys can be designed, rather than rules.

The presented recommendations are valid for the type of shear key and reinforcement layout shown in Figure A.3. It should be noted that an optimization of the reinforcement layout has not been within the scope of the study that this design guidance is based on.

A.3.1 Shear key design loads

The forces transferred by the shear keys, from one element to another, have to be determined in the design process. Since the design of the deck slab will vary from one bridge to another, it is strongly recommended to perform an individual FE-analysis for each bridge, giving the information needed to design the shear keys, the transverse- and the longitudinal-reinforcement etc. In an early design stage, a simple model is often accurate enough to investigate the force distribution between the elements.

An example of such a model is presented below for a superstructure with a typical cross-section of the one-span bridges built so far with this type of prefabricated concrete deck elements, see Figure A.4a. The FE-model consists of a series of concrete deck elements, modelled as simply supported by the steel girders in the transversal direction, see Figure A.4b. In the transverse joints, the elements are connected only in the positions of the shear keys, by rigid connection elements. Figure A.4c shows the worst load case for the large shear keys, while Table A.1 presents the maximum shear forces transferred by the shear keys, when the central element is loaded with the characteristic values ($\alpha_i = 1.0$) of the traffic loads LM1 and LM2 from EN 1991-2 (2005). The model indicate a required shear key capacity of 180 kN and 120 kN for the large- and the small shear keys, respectively.
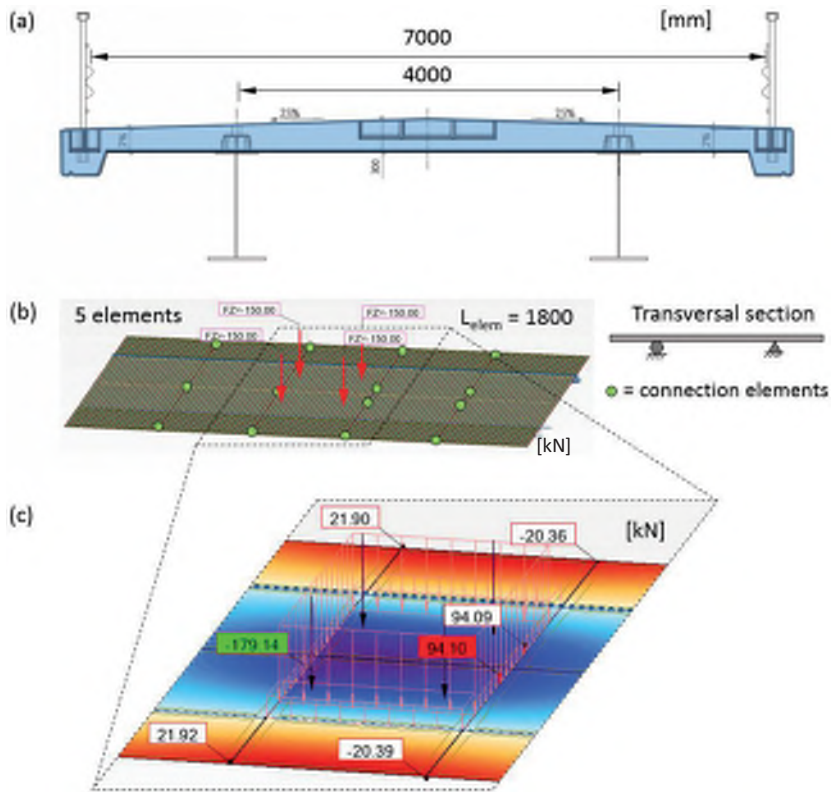
Figure A.4 *(a) Modelled cross-section, (b) FE-model, (c) worst load case for the large shear key*

Table A.1 *Maximum shear forces transferred by the shear keys*

[kN]		Large shear key		Small shear keys	
		LM1	LM2	LM1	LM2
Axle loads	2x300 kN	109.8	–	73.6	–
Axle load	400 kN	–	104.2	–	75,4
Lane load 1	9.0 kPa	9.5	–	5.5	–
Lane load n	2.5 kPa	0.2	–	0.1	–
	$V_{Sd} = 1.5 \times \Sigma =$	**179.1**	156.3	**118.8**	113.0

A.3.2 Shear key strength

Tests have shown that a design model in which the inclined shear reinforcement bars are assumed to take the entire load gives results on the safe side. The shear key strength is suggested to be estimated in line with equation (A.1), which is a simplified version of the formula for inclined shear reinforcement presented in EN 1992-1-1 (2005), equation (6.13).

$$V_{Rd,s} = A_{sw} f_{ywd} \sin \alpha \qquad (A.1)$$

Where: $V_{Rd,s}$ is the shear strength

A_{sw} is the cross-sectional area of the shear reinforcement

f_{ywd} is the design yield strength of the shear reinforcement

α is the inclination of the shear reinforcement related to the longitudinal axis of the superstructure

It is important to assure that the reinforcement bars in the shear keys are positioned correctly, to ensure the robustness of the shear transfer. If the shear reinforcement bars are positioned with too large concrete cover layers, there is a risk of failures outside the shear reinforcement in the concrete cover layer. This risk can be reduced if the work tasks within the prefabrication workshop follow a proper control program. It is also recommended that the shear reinforcement in the male-female connection are overlapping to ensure the robustness.

A.4   Steel design

The steel girders are designed according to the general requirements in EN 1994-2 (2005) and the relevant parts of EN 1993, mainly EN 1993-1-1 (2005) and EN 1993-1-5 (2006). No specific recommendations are given for the studied type of structure. However, it should be noted that the shear stud spacing can results in problems if it is not done in a proper way. More about this in the section A.5.2, about production issues.

A.5   Production and installation issues

This section summarises the experiences from the manufacturing of test specimens and the design and construction of three Swedish single span bridges in which the studied prefabrication concept has been utilized.

A.5.1 Concrete elements

When dry joints are used, it is essential to ensure that the joint gaps are as tight as possible. This is preferably done by using a match-casting technique, where one side of the previously cast element is used as formwork for the next element. Figure A.5 shows a picture from the production of a deck element to a large-scale test specimen, in which the match-casting technique can be seen.

Figure A.5 *Production of a match-cast concrete deck element for a large-scale test specimen*

Match-casting in combination with individual numbering of the elements, to ensure that they are erected in the correct order, has proven to be a successful production technique in the bridges built so far.

In order to assure that the chosen production technique is capable of fulfilling the required tolerances, it is recommended to perform a test assembly of the elements in the concrete workshop and to measure the initial joint gaps. At this stage, without any clamping forces on the elements, the mean values of the gaps have been allowed to be 1.0 mm, in the bridges built in Sweden so far. The gaps can be measured by using feeler gauges. If a feeler gauge of 0.30 mm cannot be pushed into the joint, the joint gap has been considered as 0.0 mm. The gaps should be measured at several positions along the joint, both from the top and the bottom side. Figure A.6 presents the measurements points used in one of the single span bridges that has been built in Sweden.
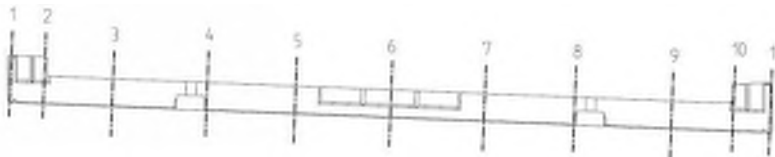
Figure A.6 *Measurement positions for joint gaps*

The positions of the transversal reinforcement bars, in the bottom layer, are crucial to avoid collisions with the shear studs at installation. The formwork used to create the longitudinal recesses, the in-situ cast channels, can be used as templates for the positioning of the transversal reinforcement bars. Additional controls are needed to assure that the bars, or the templates, are in the right positions.

To avoid damages, especially on the shear keys and the joint surfaces, the concrete elements should be handled carefully during the transport and the erection. It is strongly

recommended to avoid right-angled corners if possible. This can be done by using triangular strips (45°) in the corners of the formwork.

During the erection, the elements are often handled by a crane, see Figure A.7. To ensure that the elements are lifted in the pre-determined positions, it is recommended that the bridge designer prescribe properly located lifting anchors on the workshop drawings.

Figure A.7 Erection of a prefabricated concrete deck element

To assure that the joint gaps are as tight as possible, it is recommended that the elements are pushed together after the erection of every new element. Different techniques for pushing the element together have been tested. Small portable jacks can be supported by the shear studs and be used to push the elements together. In short bridges, where the steel girders often are cast into the back-walls at the abutment, bolts can be used to pull the prefabricated back-walls against the deck elements. This results in a clamping of the deck elements, prior to the injection of the in-situ cast channels.

The joint gaps should also be measured after the prefabricated elements have been pushed against each other. At this stage, the gaps can often only be measured from above, since it is generally hard to get access to the bottom of the joints under the bridge. After the elements have been pushed together, the mean values of the joint gaps are recommended to be limited to ≤ 0.40 mm. So far, the maximum gap has been allowed to be 1.5 mm locally over a maximum distance of 1.0 m.

It is hard to perform a good compaction of the concrete in the in-situ cast channels, by using concrete vibrators. Therefore, it is recommended to use Self-Compacting Concrete (SCC) or other types of concrete suitable for injection in the in-situ cast channels, which are filled from above through injection holes. In the real bridges built so far, and also in the test specimens, Ø100 mm injection holes have been used with a spacing of 0.6 – 1.2 m. When the channels are injected it is important to avoid air entrapment. Therefore, in addition to the injection holes, air release holes with smaller diameters are recommended, Ø16 mm with a spacing of 300 mm have been used successfully. The filling ability of the injected concrete should also be established by full-scale tests, prior to the injection of the in-situ cast channels.

A.5.2 Steel girders

The distance between the shear studs is governed by the spacing of the transverse reinforcement bars in the bottom of the prefabricated elements, or vice versa. In the bridges constructed so far, the stud spacing has been 150 mm and the shear key depth has been 60 mm. In the assembly phase, the new element must be longitudinally displaced ≥ 60 mm, to pass the shear keys on the former element, see Figure A.8. If the shear stud spacing is 150 mm, as well as the spacing of the transverse reinforcement bars (Ø12 mm), the tolerances will be about ±22 mm (the rebar ribs taken into account). If possible, it is strongly recommended to increase the shear studs spacing and the spacing of the transverse reinforcement bars, to increase the tolerances.
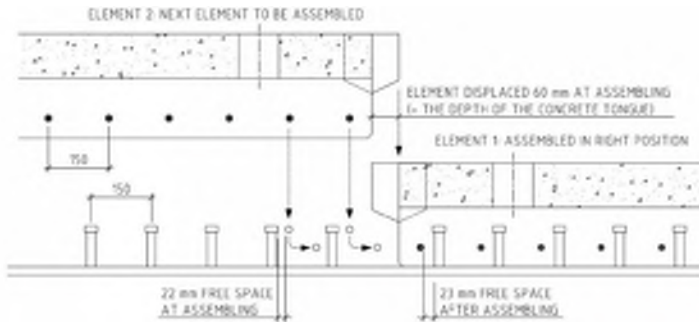
Figure A.8 *Illustration of the tolerances during the assembly procedure of the deck elements*

The tolerance for the positioning of a single shear stud is recommended to ± 5 mm. However, it is also important that the same mistake is not repeated again and again. Therefore, the absolute position of the first shear stud in each element should be checked, as well as the distance between the first and the last shear stud within an element, see Figure A.9.
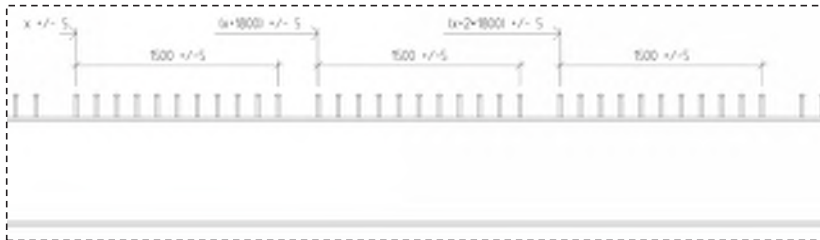
Figure A.9 *Tolerances for the positioning of the shear connectors*

It is strongly recommended to use 3D-models for the design drawings. This enables the possibility to perform a virtual preassembly of the structure, to ensure that there are no theoretical collisions between the reinforcement bars and the shear studs, in any stage of the installation process.

The alignment of the steel girders is also very important. However, experiences from real bridge projects have shown that there is no idea focusing on the alignment before the steel girders are in their final position (after launching/lifting). Laterally adjustable cross stays can be used to adjust the positions of the girders. Attachment points for such cross stays should be considered in the design stage. To make it easier to align the girders, measurement points can be marked already in the workshop. One the bridge site, the distances between these points can be measured and used to adjust the girders into the right positions. Figure A.10 shows an example of an alignment control program. Theoretical distances and a formula to calculate the necessary displacement of Girder B is presented. It should be noted that the formula is not general and valid only for the specific bridge.
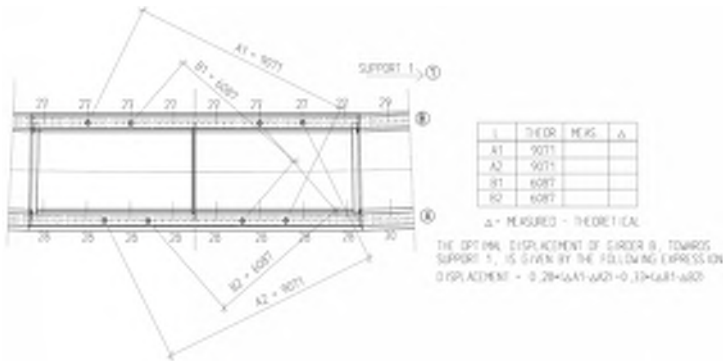
Figure A.10 *Example of a control program for the steel girder alignment*

A.6 Waterproofing

In multi-span bridges, the joint gaps in areas with negative bending moments will increase when the bending moment increases. The waterproofing must be capable of withstand the local elongation it will be subjected to, without cracking. The joint openings can be quite big (1-2 mm) especially near internal supports.

Based on large-scale test results it is suggested that the joint opening (δ_j) is estimated by equation (A.2).

$$\delta_j = \frac{M_{mean}/W_{tf}}{E_a} \cdot \frac{(e_{CG}+h_{conc})}{e_{CG}} \cdot L_{elem} \tag{A.2}$$

M_{mean} = mean value of the moment distributed over the length of one element

W_{tf} = elastic section modulus at the upper side of the top flange

e_{CG} = vertical position of the neutral bending axis with the origin at the steel concrete interface, with positive values downwards

h_{conc} = concrete deck thickness

L_{elem} = concrete deck element length

E_a = elastic modulus for the structural steel

Research on the durability of the waterproofing, at opening deck joints, has been performed by researchers at KTH (Stockholm, Sweden), under the lead of Bert Norlin. Since the waterproofing is essential for the sustainability of a multi-span bridge of this kind, the outcome of the research performed at KTH is summarised in this section. The waterproofing durability tests are described in detail in (Möller et al. 2012a). The outcomes from these tests resulted in the recommendations presented below. These recommendations are directly cited from a section written by Bert Norlin, in Möller et al. (2012b).

"If just one single waterproofing membrane is used, some kind of artificial de-bonding between the membrane and concrete as well as between the membrane and asphalt must be present to substantially improve the fatigue resistance. The total width of such regions must be about 20 cm. For this solution to work it is probably also necessary to artificially control the cracking of the asphalt layer such that it is more or less located over the deck joint opening rather than over the edge of the de-bonded region. Otherwise, the de-bonding strip cannot prevent the crack from growing into the membrane.

If two or more water proofing membranes are used the above statement holds but the de-bonded regions must increase in width when going from the top towards the concrete surface. Otherwise, the de-bonded region will not be able to stop a crack in an upper layer from growing into an underlying one. This reasoning holds as long as the cracks are formed and propagates from the top and downwards, which is the most likely scenario over an intermediate support of a bridge deck. The width increase should not be less than 5 cm, even if these regions can be placed with great accuracy.

One cannot rely on natural de-bonding between the material layers. De-bonding will not occur, not even between the concrete and the membrane, before the asphalt layer cracks right through at the deck-to-deck joint. Best practice is to artificially ensure that the asphalt cracks in line with the deck-to-deck joint such that the already de-bonded region below can stop the crack from propagating into the membrane. This can, for instance, be achieved by putting some kind of rubber based product in the asphalt layer right above the joint and towards the top membrane, see Figure A.11. In combination with mastic asphalt, which in itself is water tight, this rubber can act as a fist seal preventing water an dust from penetrating into the de-bonded region below.
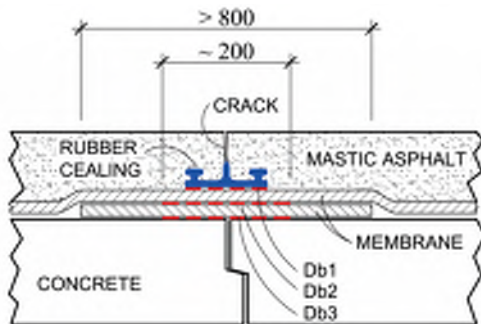

Figure A.11   *Arrangement of water proofing membranes and de-bonded regions (denoted Db1, Db2 and Db3) over a deck-to-deck joint at an intermediate support.*

The actual de-bonding can be achieved by any practical means. But in order to promote rapid assembly and sufficient quality it should preferably be built into the membranes themselves. Here, product development in collaboration with some membrane manufacturer might be needed. The means used for de-bonding must in all cases ensure that the materials does not stick or bond to each other as time passes.

Mastic asphalt is preferred in contrast to traditional asphalts, as this product in itself is water tight, which will effectively localise the water proofing problem to each deck joint. This will also make it easier to protect the de-bonded regions as stated above.

For a joint, produced following the above recommendations, the expected lifetime is more than 2 million cycles of 2.0 mm joint displacement at -20°C. If the temperature is higher than -20°C, the traffic induced joint opening is smaller than 2 mm and/or the de-bonded regions are longer than 20 cm the number of cycles to failure will be much greater.

There are two major drawbacks with the above solution. The first is that deliberate de-bonding is not allowed in the present regulations of some European countries. It is suspected that the de-bonded region may grow in size when for instance passed by heavy vehicles. The second is that water, dust and all kinds of pollutions may penetrate down to the membrane as soon as the asphalt cracks. Especially the water may increase the de-bonded region if it repeatedly freezes to ice. The first problem can be counteracted by using a thicker asphalt layer than usual, and the second by using some kind of rubber sealing as described above."

The tests indicate that it is possible to design a waterproofing solution that can resists the expected joint openings even in low temperatures. The tests also show that this is an area for further research and product development.

A.7 Design example

To summarise this design guidance, a brief design example is presented. In order to cover most of the design issues that this guidance deals with, a cross-section over an internal support is studied.

Two comparative calculations are briefly presented, to illustrate the differences between a bridge with an in-situ cast deck and a corresponding bridge with prefabricated deck elements with dry joints.

Example – Design of a bridge section under negative bending moment

In this example the Forssjösjön Bridge, a 265 m long five span bridge in Sweden, is studied. The bridge was constructed in year 2011 as a conventional composite bridge, with an in-situ cast concrete deck. The steel cross-section, illustrated in Figure A.12, is a hybrid girder with S460/S420 in the flanges and S355 in the web plates,
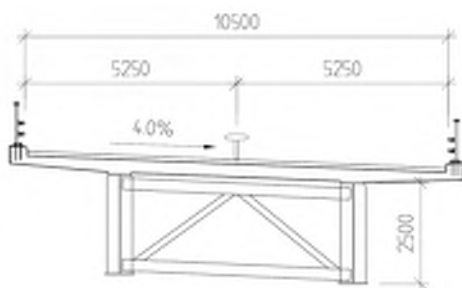
Figure A.12 *Typical cross-section of the superstructure*

Global analysis

The stiffness of the superstructure in the support sections (15% out in the spans) are modelled as the steel section only. This implies that the support moment will decrease in comparison to an in-situ cast deck (~5% in this case), in which the reinforcement area is included in the stiffness of the support cross-sections. However, the sectional modulus will also decrease (~25% for the upper flange). This results in steel stresses that are far higher than the comparable stresses in a bridge with an in-situ cast deck, which implies that the bending moment resistance of the steel girders must be increased.

Cross-sectional resistance

In the case with the in-situ cast concrete deck, the deck is cast in nine stages, resulting in a stepwise-introduced composite action. In the case with a prefabricated deck, the total load from the prefabricated deck elements is acting on the non-composite cross-sections. Since no composite action is assumed in the support sections, moments and normal forces from the different loads can just be summed up. In Table A.2 the cross-sectional forces are summarised for the prefabricated alternative at the internal support 3.

Table A.2 Cross-sectional forces at the internal support 3, for the prefabricated alternative

| Section | Characteristic loads | | ULS | | Dim. Loads |
x = 103.169 m	M [MNm]	N [MN]	LF	M_{dim} [MNm]	N_{dim} [MN]
Steel	-2.43	0	1.2	-2.92	0
Conc. deck	-14.23	0	1.2	-17.08	0
Railing+ walkway	-0.40	0	1.2	-0.49	0
Pavement	-3.28	0	1.32	-4.33	0
Shrinkage	-2.74	0	1.2	-3.29	0
Temp. grad –	-2.22	0	0.9	-2.00	0
Support settl.	-0.72	0	1.1	-0.79	0
LM1	-12.84	0	0	0	0
Special vehicle	-14.44	0	1.5	-21.66	0
Breaking load	-0.01	1.2	0.68	-0.01	0.81
				-52.6	**0.81**

In the in-situ cast alternative, 1% longitudinal reinforcement is assumed in the concrete deck slab. In order to get a similar utilization ratio in both alternatives, the thickness of the steel top-flanges have been increased from 50 mm to 64 mm, in the case with a prefabricated deck. Below, the cross-sections in the two alternatives are compared.

| Section | ELEM- | | Section | In-situ cast |
x = 103.169 m	Bridge		x = 103.169 m	deck
web t [mm]	22		web t [mm]	22
web h [mm]	2386		web h [mm]	2400
b.flange t [mm]	50		b.flange t [mm]	50
b.flange w [mm]	1000		b.flange w [mm]	1000
t.flange t [mm]	64		t.flange t [mm]	50
t.flange w [mm]	750		t.flange w [mm]	750
web.red.			*web.red.*	
A [mm²]	-1543		A [mm²]	-595
I [mm⁴]	-6.3E+05		I [mm⁴]	-3.6E+04
CG [mm]	1967		CG [mm]	1990
conc.			*conc.*	
n_L or n_0			n_L or n_0	100.0
A_{conc} [m²]			A_{conc} [m²]	1.565
I [m⁴]			I [m⁴]	0.0120
CG [mm]			CG [mm]	-195
e_{CG} [mm]	1264		e_{CG} [mm]	1200
Area [mm²]	0.1489		Area [mm²]	0.1554
I_x [mm⁴]	0.17035		I_x [mm⁴]	0.18875
W_{tfl} [m³]	-0.1348		W_{tfl} [m³]	-0.1573
$W_{w.t}$ [m³]	-0.1420		$W_{w.t}$ [m³]	-0.1641
$W_{w.b}$ [m³]	0.1436		$W_{w.b}$ [m³]	0.1510
W_{bfl} [m³]	0.1378		W_{bfl} [m³]	0.1452

$\Rightarrow$ σ_{tfl} = 396 MPa $\Rightarrow$ σ_{tfl} = 395 MPa
      σ_{bfl} = 387 MPa σ_{bfl} = 379 MPa

Joint openings

In theory, if the concrete deck elements are pushed together after the installation, there will be no joint openings due to the weight of the concrete and the steel, since the steel girders are pre-cambered for these loads. The loads applied after the injection of the channels will however affect the joint openings.

The joint opening at the internal support 3 are estimated by equation (A.2) in this appendix. In the ULS, the maximum joint opening is calculated based on the sum of all bending moments, with the exception of the moments caused by the weight of the steel and concrete. In the FLS, only the bending moment caused by the fatigue load model (FLM) is taken into account. In this case FLM 3 from EN 1991-2 (2005) has been used.

With the highest point of the concrete surface 350 mm above the top-flange of the steel girder, and with an element length of 1.8 m, the following joint openings are calculated.

Maximum joint opening – ULS

$$\delta_{j,ULS} = \frac{-32.6/0.1348}{210\cdot10^3} \cdot \frac{(1264+350)}{1264} \cdot 1800 \quad = 2.7 \text{ mm}$$

Maximum joint opening – SLS

$$\delta_{j,SLS} = \frac{-21.8/0.1348}{210\cdot10^3} \cdot \frac{(1264+350)}{1264} \cdot 1800 \quad = 1.8 \text{ mm}$$

Maximum joint opening – FLS

$$\delta_{j,FLS} = \frac{-4.7/0.1348}{210\cdot10^3} \cdot \frac{(1264+350)}{1264} \cdot 1800 \quad = 0.4 \text{ mm}$$

The magnitude of the joint openings are of most interest as design criteria for the water insulation and the pavement. Fatigue tests, performed at KTH, indicate that the waterproofing can be designed to resist at least 2 million cycles, in -20°C, with a displacement amplitude of 2.0 mm. If the recommendations presented in section A.6 are followed, it should definitely be possible to design a waterproofing that resists the fatigue it will be exposed to, during its technical lifetime of approximately 40 years. However, it is probably also necessary to define a ULS and SLS criterion, which has not been done in the study at KTH.

Additional steel weight

If a multi-span composite bridge is designed with prefabricated deck elements with dry joints, instead of an in-situ cast deck, it will be necessary to add additional steel to the top flanges near the internal supports. For this specific bridge, the total steel weight is 465 tonnes for the alternative with an in-situ cast deck. This weight has to be increased with approximately 21 tonnes if the alternative with prefabricated deck elements with dry joints is used instead.

The positions of the assembly joints in the steel girders are in this example optimized for an in-situ cast bridge. A minor reduction of the additional steel, for the prefabricated alternative, can be achieved if the joints instead were optimized for the prefabricated alternative.

Appendix B

DESIGN GUIDANCE

STRENGTHENING BY POST-INSTALLATION OF COILED SPRING PINS AS SHEAR CONNECTORS

This appendix summarises the knowledge and research on strengthening by post-installation of Coiled Spring Pins as shear connectors, by presenting a design guidance. The design guidance has been developed by the author within the frame of the European RFCS-project PROLIFE, implying that parts of this guidance will also be published in future public reports from the PROLIFE-project.

In the absence of a common European standard for existing bridges, the European design codes for new steel and steel-concrete composite structures, Eurocode 3 and 4, have been used as the reference codes in this guidance. The author is aware that there might be national codes and guidelines that cover this topic on a national level.

The recommendations in this guidance are limited to strengthening of non-composite steel-concrete bridges and to Coiled Spring Pins (CSP) of standard type ISO 8748 – 20 x 160 – HWK. The letters indicate that the pin is of the type Heavy Duty (H) and made out of AISI 6150 Alloy Steel (W) with no surface treatment (K), while the digits represent the nominal outer diameter of 20 mm and the length of 160 mm, see Figure B.1.
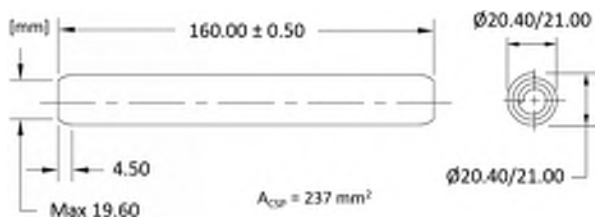
Figure B.1 *Dimensions of the CSP covered by this guidance*

The design guidance is focused on the shear connection, but it should be highlighted that there are several other structural details that need to be checked, to assure that the load capacity can be increased when a bridge is strengthened in this way.

The guidance has been divided into two main subsections: Design issues and Installation issues.

B.1   Design issues

The suggested design approach, presented below, is based on the research performed so far. However, additional research questions have been identified, which implies that additional research is needed before utilizing the full potential capacity of the CSPs. The areas where further research is needed are highlighted in the text.

B.1.1 Structural modelling

Based on the results from a field monitoring and the subsequent analyses, it is recommended that the CSP shear connection is modelled as being rigid (Hällmark et al. 2018b).

There are, however, some cases when it might be necessary to model the stiffness of the shear connection more accurate. Two examples of such cases are presented below.

Strengthening of a non-composite bridge:
If CSPs are installed in a non-composite bridge, i.e. in a bridge without connectors designed to primary transfer longitudinal shear forces, the connectors can be treated as rigid in the ULS, FLS and in many cases also the SLS. However, if there are any SLS design criterion that are crucial in the design, for instance a strict deflection criterion with almost 100% utilization ratio, it might be necessary to create a structural model that takes into account the stiffness of the connectors. This recommendation is given since there are no test results available from beam tests at these load levels and since only elastic steel strains are allowed in the SLS. Future beam tests can hopefully provide additional information about the loads-slip behaviour, showing if this kind of restriction is necessary or not.

Strengthening of an existing shear connection in a composite bridge:
In the global analysis, the shear connection can be modelled as rigid. However, when combining different types of shear connectors, differences in their load-slip properties needs to be taken into account, in line with EN 1994-2 (2005) 6.6.1.1 (6).

If CSPs are installed in order to strengthen an existing shear connection, for instance due to insufficient fatigue capacity of the existing welded headed studs, the relative stiffness of the different connectors will be essential for the detailed design in SLS and FLS. The distribution of the shear force between the CSPs and the existing shear connectors must be evaluated on a project specific basis. As an input to such an evaluation, the load-slip curves presented in (Hällmark et al. 2018c) can be used for the CSPs.

B.1.2 Static strength

Based on the results from a new push-out-test series by Hällmark et al. (2018c) and from previous push-out tests performed by other researchers (Pritchard 1992, Buckby et al. 1997, Fahleson 2005, Hällmark et al. 2018a), the following recommendation is given for estimating the characteristic static strength (P_{Rk}) of the studied type of CSP.

$$P_{Rk} = 130 \text{ kN/CSP}$$

if $\quad 24 \le f_c \le 45 \text{ MPa}$

and $\quad 20 \text{ mm} \le t_s$

The recommendation above is limited to a minimum steel flange thickness (t_s) of 20 mm and to a compressive cylinder strength of the concrete within the interval of 24–45 MPa.

For thinner steel flanges, or lower compressive strength of the concrete, it is recommended to perform additional project specific tests, since different types of failure modes are expected if the steel flanges become too thin or the concrete to weak. For higher concrete strengths, the value presented above should be on the safe side and possible to use, even if there are no tests confirming this.

B.1.3 Fatigue strength

Based on the results from a new fatigue push-out-test series by Hällmark et al. (2018d) and from previous fatigue tests performed by other researchers (Pritchard 1992, Buckby et al. 1997, Fahleson 2005, Hällmark et al. 2018a), the author recommends that the characteristic fatigue strength of the CSPs are estimated as,

$$\log N = 14.2 - 6.09 \cdot log \Delta P. \tag{B.1}$$

or

$$\Delta \tau_R^{6.09} N_R = 84.4^{6.09} \cdot 2 \cdot 10^6 \quad (\text{from} \quad \Delta \tau_R^m N_R = \Delta \tau_c^m N_c) \tag{B.2}$$

where N is the design life time expressed as number of cycles related to a constant load range, ΔP. In (B.2), the denotation has been adapted to the format used in EN 1993-1-9 (2005), implying that the load range has been transformed into a shear stress range, $\Delta \tau$, using the CSP shear area $A_{CSP} = 237 \text{ mm}^2$.

This is a conservative design recommendation compared to the previous recommendation by Buckby et al. (1997), presented below.

$$\log N = 14.767 - 6.1 \cdot log \Delta P \tag{B.3}$$

Future research, containing additional tests and FE-modelling of the tests presented in (Hällmark 2018d), might provide additional information about the CSP fatigue strength, which makes it possible to develop the fatigue design criterion further.

B.1.4   Vertical separation – uplift

A vertical separation, uplift of the concrete deck slab, at the steel-concrete interface is prevented by frictional forces developed at the surfaces between the CSPs and the surrounding concrete and steel, and also by permanent vertical forces from the weight of the bridge deck and temporary vertical forces from the traffic loads. The curvature of the beam will also have a positive influence to reduce separation. However, clause 6.6.1.1 (7) in EN 1994-2 (2005) might not be regarded as fulfilled if not frictional forces and/or external forces are taken into account. However, as shown in push-out tests, the CSPs are very ductile even after a separation has occurred (Hällmark et al. 2018c). If this fact is combined with the observation, presented in (Hällmark et al. 2018b), that there are no uplift of importance in the monitored structure at moderate load levels (FLS level), the author strongly believe that CSPs can be used without jeopardizing the robustness of the strengthened structure. The potential separation problem should be dependent on the slip and the inclination of the shear connector and the concrete compressive strut, see Hällmark et al. (2018c). If the slips are kept at moderate levels, the uplift forces would also be kept low. But until the potential uplift has been investigated further, the recommendation is to utilize only the elastic capacity of a composite beam with post-installed CSPs and to design the shear connection for full composite action. This restriction is on a general level and aims to increase the safety margin of the strengthened structure, until the potential separation has been investigated more deeply.

Future beam tests are planned to be performed, to investigate if uplift will be a problem in the ULS. Alternatively, just an irreversible but harmless deformation that occurs when other parts are yielding and crushing, i.e. when the structure is loaded to a point where it has to be replaced or undergo extensive repairs.

B.1.5   Design recommendations vs. EN 1994–2

In this section, recommendations for the design of CSP-shear-connections are presented as comments to the general "Basis of design" for shear connectors presented in EN 1994-2 (2005) 6.6.1.1. If there are no specific recommendation given for CSPs in this guidance, the general requirements are assumed valid also for the CSPs.

Comments – design of CSP-shear-connections in line with EN 1994-2 section 6.6.1.1:

   6.6 Shear Connection

      6.6.1 General

      6.6.1.1Basis of design

      (1)   –

      (2)   –

      (3)   Sufficient deformation capacity has been verified by push-out tests.

      (4)   CSPs can be treated as ductile connectors.

      (5)   The characteristic slip capacity exceeds 6 mm.

(6) This clause is very important if a bridge with an already existing shear connection is strengthened with additional shear connectors (CSPs). The load-slip curves for CSPs presented in (Hällmark et al. 2018c) can be used as input to the project specific comparison to the existing shear connectors.

(7) Separation of the concrete element from the steel element is prevented by frictional forces developed at the surfaces between the CSPs and the surrounding concrete and steel. The permanent vertical forces from the weight of the bridge deck and temporary vertical forces from the traffic loads are also contributing to the forces that counteracts the uplift. The curvature of the beam will also have a positive influence to reduce separation. However, this clause cannot be treated as fulfilled if not frictional forces and/or external forces are taken into account. However, the CSPs are very ductile even after a separation has occurred, as shown in static push-out tests, and there are no signs of concrete uplift in the monitored structure at moderate load levels. Before the potential uplift has been investigated further, it is recommended to utilize only the elastic capacity of a composite beam with post-installed CSPs and to design the shear connection for full composite action.

(8) Future beam tests will show if there is a need of anchoring devices in order to utilize the full potential of the CSPs, see (7).

(9) –

(10) –

(11) –

(12) The design recommendations for the CSP shear connectors are based on the tests and the conceptual model presented in (Hällmark et al. 2012c). If the suggested design recommendations are followed, this clause can be treated as fulfilled.

(13) –

B.2   Installation issues

The installation procedure includes generally five steps: (1) drilling through the steel top flanges, (2) drilling into the concrete, (3) tolerances measurements, (4) jacking of the CSP into the hole, and (5) sealing of the hole and restoring of the corrosion protection. These steps are illustrated in Figure B.2.
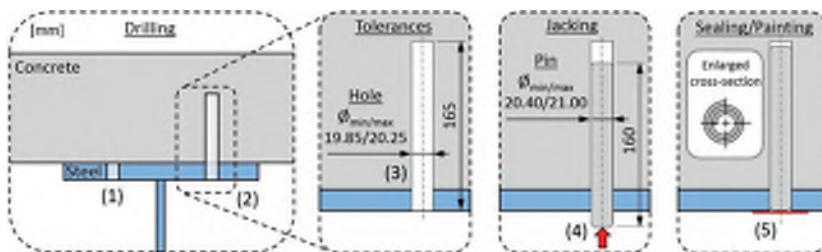
Figure B.2 Schematic illustration of the installation procedure

Prior to the installation, some important decisions must be made about how to deal with the risk of collisions with reinforcement bars in the bottom of the concrete deck slab and the risk of exceeding the hole tolerances etc.

B.2.1 CSP positions

The position of the post-installed CSPs are adapted to the conditions in the existing bridge. Typical factors that need to be considered are:

- location of the transversal reinforcement
- location of the longitudinal reinforcement
- location of the CSPs due to design requirements in EN 1993-1-8 & EN 1994-2

Recommendations of how to deal with these factors are summarised below.

Location of the transversal reinforcement

To perform the post-installation of the CSPs, it is necessary to drill into the existing reinforced concrete deck slab. The holes need to pass the horizontal bottom layers of reinforcement, both the transversal and the longitudinal, but will in the general case be ended before they reach the reinforcement bars in the top layers. If no actions are taken to locate the reinforcement bars, the drilling will most likely cut some of the transversal reinforcement bars apart. These bars are mainly needed to distribute the shear forces to the concrete deck slab, since the main transversal moments are negative above the steel girder, implying that the bottom part of the deck slab is in compression in the transversal direction. However, since there are positive transversal moments between the girders, it must be assured that sufficient anchorage lengths are provided if the reinforcement bars are utilized in the design.

Two different approaches, of how to deal with the risk of collisions between the CSP-holes and the transversal reinforcement bars, are presented in the flow chart in Figure B.3.

For both approached, the input parameter is the distance between the transversal reinforcement bars, which governs the longitudinal distance between the CSP. The distance between the bars can be obtained either from the existing drawings or from sample measurement on selected sections along the bridge. The sample measurement can be performed from below the bridge deck with a cover meter or some other equipment that can indicate the positions of the reinforcement bars.

In the design of the strengthening work, the bridge designer can either state that the location of the transversal reinforcement bars needs to be established by measurements or specify the number of nearby reinforcement bars that are allowed to be cut apart, without affecting the structural capacity. The latter implies that the bridge designer establish a requirement that is transferred into the drilling control program, which is the governing document for the drilling operator. The drilling operation can continue as long as the requirement is fulfilled. If not, the drilling process needs to be stopped and the bridge designer needs to be contacted for further investigations.
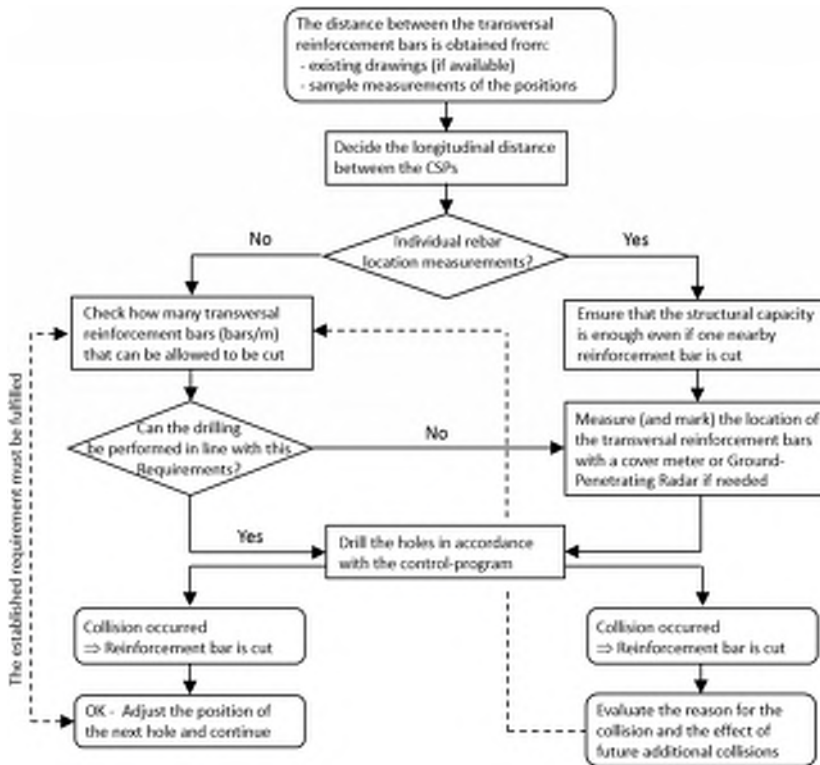
Figure B.3 *Flow chart for the CSP-positions in relation to the transversal reinforcement*

If measurements of the positions of the reinforcement bars are presumed, the measurements should be performed as close to the steel upper flange as possible, i.e. as close as possible to the drilling position. The measurements can be performed with a cover meter, Ground-Penetrating Radar (GPR) or other suitable equipment. If there is a collision between a hole and a reinforcement bar, despite the measurements, the reason for the collision should be evaluated and the bridge designer contacted for further investigations.

The design of the strengthening must always be done in a way that ensures that the structural capacity and the effect of the strengthening, is not affected by a loss of a single reinforcement bar. If this is not the case, another strengthening method should be considered as a supplement, or replacement, to strengthening by post-installed shear connectors.

Location of the longitudinal reinforcement

The positions of the longitudinal reinforcement bars above the steel girder are hard to establish by measurements, due to the steel girder top flange. The theoretical position taken from drawings of the existing bridge can be used as a first assumption when the positions of the post-installed CSPs are decided. However, the bridge designer must either establish at least a second alternative position of the connectors in the transversal direction, or ensure that the structural capacity will not be affected by the loss of the affected reinforcement bars. Repeated collisions with the reinforcement bars should be avoided if possible, since this result in an additional wear of the concrete diamond core drill, which is used in this stage of the drilling operation.

Location – design requirements

The European design code for composite steel-concrete bridges EN 1994-2 (2005) specifies the general design requirements for the location of the shear connectors in section 6.6. These requirements must be complemented by the requirements for positioning of holes for bolts and rivets, given by EN 1993-1-8 (2005). This is necessary since the CSP connection is quite similar to riveted- or bearing type bolt-connections, in the aspect of potential failures in the connecting steel plate.

Figure B.4 and Table B.1 summarise some of the important parameters that need to be taken into account when deciding the location of the CSPs. The denotations are based on EN 1993-1-8 (2005), which implies that some denotations deviates from those in EN 1994-2 (2005).
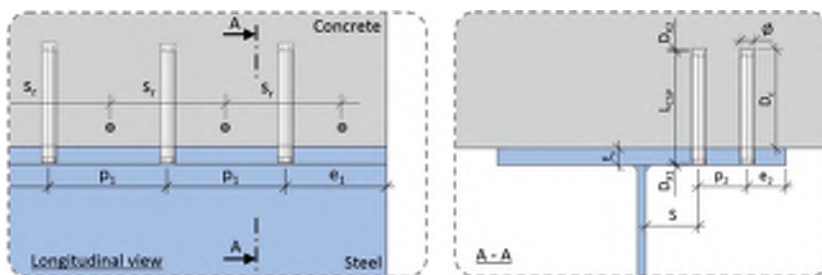
Figure B.4 *Definition of important parameters for CSP shear connections*

Table B.1 *Design requirements for some of the important CSP location parameters*

Parameters		EN 1993-1-8 (2005) – Table 3.3		EN 1994-2 (2005) – 6.6	
		Min	Max	Min	Max
p_1	Longitudinal spacing	2.2d	–	5d	see 6.6.5.5
p_2	Transversal spacing	2.4d	–	2.5d	–
e_1	End distance	1.2d	–	see 6.6.5.5	see 6.6.5.5
e_2	Edge distance	1.2d	–	35 mm	see 6.6.5.5

The longitudinal distance between the shear connectors (p_1) and the transversal distance (p_2) are governed by the requirements in EN 1994-2 (2005). In the absence of a large database of test results on CSPs, the requirements for headed stud connectors in section 6.6.5.7 (4) is suggested to be used also for CSPs. The same goes for the end distance (e_1) and the edge distance (e_2). For the latter (e_2), a fixed value (35 mm) that is based on the requirement for a welded connector is given. The requirement implies that the distance between the edge of the connector and the edge of the steel plate should not be less than 25 mm, which gives $e_2 = 35$ mm for a CSP with $\varnothing = 20$ mm. It can be discussed whether this requirement is relevant, or not, for a pin connection, but in the absence of additional information it is kept as a recommendation also for CSPs.

From Table B.1 it can be noted that the requirements in EN 1993-1-8 (2005) will not be governing the design, if the requirements in EN 1994-2 (2005) are followed.

In addition to the design requirements, the locations of the connectors are also governed by project specific execution requirements. These requirements are often related to the space needed for the drilling equipment. One such an example is the free distance between the web plate and the nearest holes, S. This parameter must be checked against the dimensions of the accessible drilling equipment. The requirement of anchoring the drilling equipment, upside down, might also affect the positioning of the holes. Different types of anchoring devices (magnetic, vacuum plate, mechanic etc.) have different requirements related to the surface they are connected to. If needed, a project specific drilling rig can be used, even though the use of such a rig is related to some development and manufacturing costs.

From an installation point of view, it is often preferable to locate all post-installed connectors on one side of the steel web-plate, if possible. This unsymmetrical shear transfer will cause a bending moment acting on the steel girder in the week direction. However, this moment will be counteracted by transversal force couples in the CSPs, over a long distance, which often are negligible.

B.2.2 Precision drilling

Based on the drilling experiences from real strengthening projects and the manufacturing of test specimens, it is recommended to use hole tolerances of 19.85 – 20.25 mm combined with a requirement of a relative hole diameter difference of maximum 0.1 mm, between the hole in the steel- and the concrete-part. These tolerances might be demanding for the drilling operator, but have been proven feasible.

The wearing down of the bits can be a significant cost factor since the required tolerances are very tight. It is recommended to start the drilling with a cutting drill bit, and stop just before the steel-concrete interface is reached. For the remaining part of the drilling, it is recommended to use a diamond core drill.

The drilling procedure should be followed by a control of the hole diameter, in both the steel- and the concrete-part, to ensure that the holes are within the tolerances. If the tolerances are exceeded, the hole should be abandoned and a new nearby hole should be drilled in an alternative position provided by the designer of the strengthening.

B.2.3 Jacking

Based on the experiences from real strengthening projects and the manufacturing of test specimens, it is recommended to start the installation of the CSPs without any use of lubricant. However, if the magnitude of the installation force becomes too big, for the jack or for the supporting bottom flange, tests have shown that lubricants can be used without jeopardizing the load capacity of the connectors. Suitable lubricants can be chosen on a case-to-case basis, depending of the requirements for the following sealing and painting works.

Experiences shows that the magnitude of the jacking force can vary a lot. The author recommends that the supports positions of the jacks are checked for a force of at least 250 kN, even though the installation force will probably be closer to 100 kN.

B.2.4 Corrosion protection

Based on the experiences so far, it is recommended to close the holes to prevent air and moisture ingress and to apply a suitable corrosion protection at top of the sealing.

A suitable corrosion protection system has to be chosen on a case-to-case basis, since the existing corrosion protection system will be an object specific condition. However, the compatibility between the corrosion protection system, the sealing material and any lubricants must be ensured, to avoid future adhesion problems.

B.2.5 Example of recommended installation requirements and methods

Based on the knowledge available, the following example is provided to illustrate how the recommended installation requirements can be used in the drawings, control programs, working instructions etc.

Conditions: Composite action is created in a non-composite steel concrete bridge by the installation of CSP 20x160 HWK, ISO 8748 (2007).

> $\varnothing_{CSP}$ 20 mm (20.40-21.00 prior to installation)
>
> L_{CSP} 160 mm
>
> H = Heavy Duty,   W = Alloy steel,   K = Plain, Oiled

Installation requirements

The bridge designer provides drawings and control programs in which the following information need to be presented:

- Planned position of the CSPs
- Alternative position of the CSPs, i.e. Plan B in case of collisions with reinforcement bars, exceeded tolerances etc.
- Drilling specification in terms of diameter, depth and corresponding tolerances
- Control frequency (the recommendation is to check every hole)

Some of the important dimensions are presented in Figure B.5 together with the corresponding recommendations.
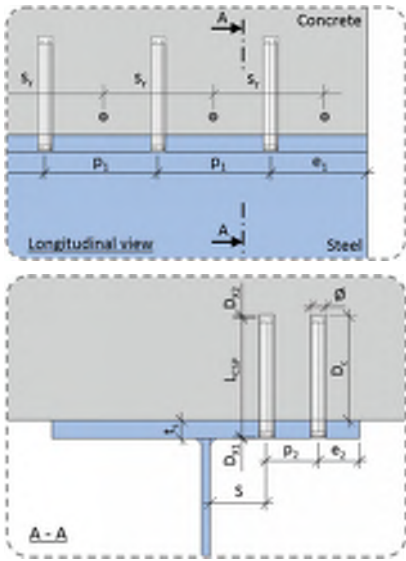
Recommendations:

p_1 should equal the theoretical distance between the transversal rebars (s_r)

$\varnothing_{hole}$ tolerances 19.85-20.25 mm

D_{X1} 1-2 mm to enable a levelled surface after the sealing of the hole

D_{X2} 5 mm to ensure that the CSP can be pushed to the specified depth

Information that needs to be provided:

Specify the sealing material and the execution, for instance:

"2-compoent epoxy mortar (that can be coated), shear strength > 20 MPa in hardened condition"

"The epoxy mortar is levelled with the bottom of the steel top flange and covered with a suitable corrosion protection system for the specific bridge."

"Suitable corrosion protection system:

---object specific conditions---"

Figure B.5 *Recommendations for some of the important installation parameters*

Installation methods

The suitable installation method can vary a lot between different bridges. However, it is often preferable if the post-installed CSPs are located only on one side of the steel web-plates. This enables an installation procedure where access to the steel top-flange is needed from just one side of the web plate. Two examples of such installation procedures, alternative (a) and (b), are illustrated in Figure B.6. If there is a need to install CSPs from both sides of the web plates, alternative (c) in Figure B.6 can be considered. If it is possible to get access to the ground below the bridge, it can also be considered to perform the installation works from the ground, in a boom lift or on temporary working platforms.
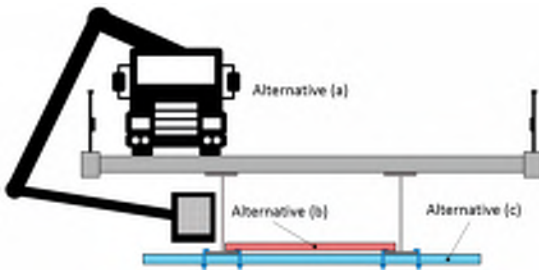
Figure B.6 *Examples of possible installation methods*

It is recommended to spend some time on the choice of the installation method, and an optimization of it, since the strengthening technique with CSPs is labour intensive and the majority of the costs are related to the hours spent on the installation on site.

PAPER I

Prefabricated Bridge Construction across Europe and America

Robert Hällmark, Harry White and Peter Collin

Prefabricated Bridge Construction across Europe and America

Robert Hällmark[1]; Harry White[2]; and Peter Collin[3]

Abstract: Determining the most efficient and economical way to build a new or replacement bridge is not as straightforward a process as it once was. The total cost of a bridge project is not limited to the amount spent on concrete, steel, and labor. Construction activities disrupt the typical flow of traffic around the project and results in additional costs to the public in the form of longer wait times, additional mileage traveled to get around the work zone, or business lost attributable to customers avoiding the construction. The risk of injury to workers because of traffic interactions or construction activities increase with each hour spent at the construction site. Finding a way to shorten the time spent on the jobsite is beneficial to the contractor, the owner, and the traveling public. Prefabricating certain bridge elements reduces the time spent at the construction site and reduces the effects on the road users and the surrounding community. For example, steel beams with composite concrete decks reduce the construction time over cast-in-place concrete superstructures. In some instances, entire structures have been fabricated off-site under strict environmental and quality controls and then shipped to the site and erected in a matter of days instead of months. The total cost of using prefabricated bridge elements (PBE) depends greatly on the scale of the prefabrication. The more that prefabrication is used, the lower the costs. Even under limited use, however, prefabrication is usually comparable to traditional construction techniques. However, when durability and user costs are taken into account, the overall cost may be significantly less than traditional piece-by-piece construction. To improve the competitiveness of prefabricated composite bridges, a European research and development project, ELEM RFSR-CT-2008-00039, was started in 2008. The overall objective of the project is to make prefabricated bridges more competitive through development of new cost-effective, time-efficient, and sustainable bridge structures. The project has started with a knowledge extension, in the form of the workshop on "Composite Bridges with Prefabricated Deck Elements." This workshop was held in Stockholm, Sweden, in March 2009 to share the knowledge and experience gained by agencies around the globe. During the workshop, experiences from Europe and the United States were presented in an effort to promote the use of accelerated bridge construction (ABC) and prefabricated bridge elements. **DOI:** 10.1061/(ASCE)SC.1943-5576.0000116. © 2012 American Society of Civil Engineers.

CE Database subject headings: Prefabrication; Bridges; Construction; Europe; United States.

Author keywords: Prefabricated bridge elements; PBE; Accelerated bridge construction; ABC; ELEM.

Introduction

Congestion is a growing problem in urban areas across the globe. The mobility needs of an increasing population demand that new roads and bridges be built even while existing infrastructure is maintained, widened, or reconstructed. Therefore, the total cost of a bridge or roadway project is not limited to the amount spent on concrete, steel, and labor: user costs must be considered.

Transportation construction, especially reconstruction of an existing roadway, disrupts the typical flow of traffic around the project area and results in additional user costs to the public in the form of longer wait times, additional mileage traveled to get around the work zone, inefficient movement of goods and services, and business lost attributable to customers staying away from the construction.

In recent years, transportation agencies around the globe have begun to use accelerated construction techniques (ACT) that incorporate prefabricated bridge elements (PBE). Prefabricating certain bridge elements reduces the time spent at the construction site and reduces the effects on the road users and the surrounding community.

For example, steel beams with composite concrete decks reduce the construction time over cast-in-place concrete structures. Additional time savings can be achieved by prefabricating the riding deck and the substructure. In some instances, entire structures have been fabricated off-site under strict environmental and quality controls. The fabricated components are then shipped to the site and erected in a matter of days instead of months.

Unfortunately, road user costs are often neglected when comparing design alternatives. The total expense of using a prefabricated bridge is usually comparable to traditional construction techniques. However, the overall cost may be significantly less than traditional construction when durability and user costs are taken into account (Culmo 2009). Even where there are advantages to using prefabrication, typical construction techniques are still often used out of familiarity and habit.

In some countries, prefabrication seems to be gaining momentum (Culmo 2009; Seidl 2009), but it is far from a common procedure everywhere. The workshop on Composite Bridges with Prefabricated Deck Elements was held in Stockholm, Sweden, in March 2009 to share the knowledge and experiences from Europe

[1]M.Sc. Civil Engineering, LTU/Ramböll Sverige AB, Luleå, Sweden. E-mail: Robert.Hallmark@ramboll.se

[2]New York State Dept. of Transportation, Albany, NY (corresponding author). E-mail: hwhite@dot.state.ny.us

[3]Professor, LTU/Ramböll Sverige AB, Luleå, Sweden. E-mail: Peter.Collin@ramboll.se

82 / PRACTICE PERIODICAL ON STRUCTURAL DESIGN AND CONSTRUCTION © ASCE / AUGUST 2012

Pract. Period. Struct. Des. Constr., 2012, 17(3): 82-92

and the United States concerning prefabricated bridge elements (PBE).

Costs of Bridges Using Prefabricated Bridge Elements

When looking at costs, it is important to consider not only the initial costs of a structure, which consist of the monetary cost of the materials and labor required to design and construct the structure, but also the societal costs associated with the construction noise and traffic disruption A U.S. study (Ralls 2008) states that, for agencies that use prefabrication infrequently, the initial cost of a structure built using PBE is slightly higher than for traditional piecemeal construction procedures. However, it is the overall, or life-cycle, costs of PBE structures that must be compared with traditional construction to determine which provides the best value.

A cost-benefit analysis (Degerman 2002) of a single-span railway crossing bridge in Norrfors, Sweden, that used PBE showed a dramatic positive effect on cost and schedule. The cost to prefabricate the bridge was presumed by the designers to be higher than the cost to cast the concrete deck on-site. However, a bidding contractor indicated that the prefabricated deck was actually less expensive, as the additional costs attributable to prefabrication is overcome by the savings achieved by eliminating formwork and other activities required when building a bridge over an operating railway.

Time spent on-site often causes disturbance of the local traffic patterns. Prefabrication can be used to shorten this time considerably, which indicates that the delay-related road user costs would be reduced. A study of a Swedish road bridge (Nilsson 2001), called the Rokan Bridge, compared the cost of constructing a prefabricated composite bridge, a conventional composite bridge with a temporary detour bridge, and a conventional composite bridge with the traffic directed to the nearest bypass roads. The conclusion from the study was that the most economical alternative, from a societal perspective, was to construct a prefabricated bridge and eliminate the need for the long-term detours.

Agencies that use prefabrication more consistently find that project bid prices are in line with, or sometimes lower than, traditional construction as contractors become more familiar with the methods. Once the prefabricated elements, connection details, construction procedures, and other details are standardized and become more familiar, prefabricated bridges should consistently result in lower initial construction costs and produce higher-quality final products.

To capitalize and on this theory, the Massachusetts Dept. of Transportation (MassDOT) has begun to bundle multiple accelerated bridge construction (ABC) projects along a travel corridor into a single contract (Commonwealth of Massachusetts 2010). This way, the designs on similar projects can be produced more efficiently and the construction methods become repetitive. Bundled design projects, as opposed to having separate contracts for each project, save procurement time and take advantage of the contractor's progress along the learning curve of ABC projects. MassDOT has already solicited bids on 13 bundled contracts that will address repairs to several hundred substructures and bridge decks, primarily located on interstate highways and major arterials across the commonwealth.

United States—Accelerated Bridge Construction

Accelerated bridge construction can be defined as "building the bridge first before setting up the traffic control cones, and then move it quickly into place, like in hours or a weekend." (Mistry 2008). Different prefabrication concepts have been used in the United States. The prefabrication level varies from prefabricated components in the superstructure to totally prefabricated bridges. A variety of design solutions have been proposed and tested during the years. The Federal Highways Administration (FHWA) publication titled *Connection Details for Prefabricated Bridge Elements and Systems* outlines the state of practice in the United States for ABC (FHWA 2009). The publication breaks down the details into three levels. Level 1 is for details that have become standard practice in at least one agency. Level 2 details have been used once and found to be practical to construct. Level 3 details are conceptual or experimental and have not been placed in field service. The Federal Highway Administration has also prepared two documents to assist decision makers on implementing ABC technologies in bridge projects.

The Utah Dept. of Transportation (UDOT) is just one example of a U.S. agency that believes accelerated bridge construction is the future, and it intends to include this concept in all future bridge projects. So far, UDOT has constructed bridges with precast deck panels, precast abutments, and precast approach slabs, and it has moved entire superstructures into place using self-propelled modular transports (SPMT) (UDOT 2004).

Prefabricated Bridge Girders and Decks

Prefabricated steel or prestressed concrete girders are the overwhelming choice in the United States and cast-in-place concrete girders are very rare. Prefabricated bridge decks are less commonly used, but are typically made of prestressed concrete panels, although there has been limited use of orthotropic decks, prefabricated aluminum decks, and fiber reinforced polymer (FRP) panels.

The prefabricated deck elements are almost always designed to provide composite action between the deck element and the girders. The composite action between steel girders and precast deck elements is primarily achieved by welded shear studs.
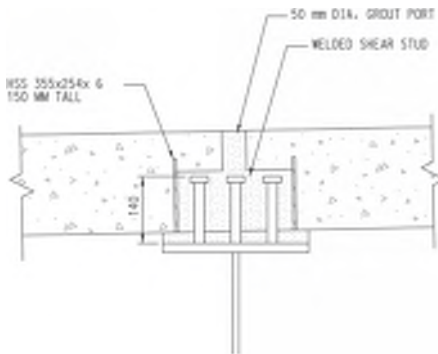
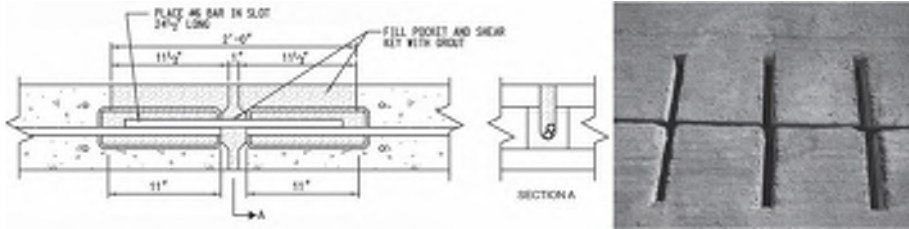

Fig. 1. Composite connection (FHWA 2009)

Fig. 2. Transverse connection at Live Oak Creek Bridge, Texas (FHWA 2009)

Composite action between prestressed concrete girders and deck elements can also be achieved by using headed studs cast into girder, as well as extended reinforcement. The prefabricated deck elements can either be made with full thickness pockets or with blind pockets with grouting ports, as shown in Fig. 1. There has been a tremendous amount of research in the area of prefabricated decks and their associated connections.

The design of the transverse joint between precast panels varies significantly between U.S. transportation agencies. Many states do not use waterproofing membranes and prefer to apply posttensioning force to the panels to ensure a crack free deck. Non-post-tensioned transverse joints are also used. For example, the bridge over Live Oak Creek in Texas uses blind pocket details with dowel bar connections at the joints and no posttensioning, as shown in Fig. 2. This solution works best on single spans where the deck is always in compression, but it has also been used in multi-span bridges where the areas over the piers are in tension.

Recently, the New York State Dept. of Transportation has developed a detail that uses full width precast Portland cement concrete panels that are connected using ultra-high-performance concrete (UHPC), as shown in Fig. 3. UHPC has compressive strengths exceeding 30 ksi (200 MPa) and postcracking tensile strengths of 1.5 ksi (10 MPa) while simultaneously being nearly impenetrable to chloride ions (FHWA 2010). Given these exceptional properties, composite action can be obtained using only 3-in. (75-mm)-tall shear studs. This eliminates possible interference between the more traditional 6-in.-tall shear studs and the transverse reinforcement. Also, the high postcracking tensile capacity indicates that the costs and time involved in posttensioning are not necessary to assure water tightness, even in areas of negative, or hogging, moment.

Prefabricated Superstructures

In 2004, a U.S. transportation team conducted an international scan to gather worldwide information about prefabricated bridge elements and systems (FHWA 2005). One of the top implementation recommendations was to introduce the concept of completely assembling bridge components off-site and then moving them into final position using different movement systems.

Self-propelled modular transports (SPMT), and similar types of vehicles, enable the superstructure to be prefabricated in pieces that weigh up to several thousand tons and are transported to the construction site for a rapid installation. The build-and-slide-into-place concept of building bridges has started to gain ground in the United States, and it has been used successfully by several agencies. For example, the Graves Avenue Bridge in Florida was

Fig. 3. Connection detail of precast panel and steel girder using UHPC (Reprinted with permission from NYSDOT)

Fig. 4. SPMT transportation of 4500 South Bridge, Utah (Reprinted with permission from Mammoet USA South, Inc.)

Fig. 5. Grouted reinforcing splice-sleeve connector (Reprinted with permission from Splice Sleeve North America, Inc.)

replaced in 2006 using SPMTs to remove the old bridge and install the new bridge. The new spans were built alongside the existing bridge to avoid traffic disturbance. The 59-ft (18-m)-wide superstructure had a span of 144 ft (44 m) and a weight of 1,430 tons (1,300 metric tons). A similar procedure was used in Utah when in October 2007 the single-span superstructure of the 4500 South Bridge, which weighed 1,650 tons (1,500 metric tons) and had a longitudinal inclination of 10%, was replaced in only 53 h, as can be seen in Fig. 4.

Complete Bridge Prefabrication

Prefabricated substructures are not common in the United States, although the concept has been used and is gaining in popularity. One method of prefabrication is to precast segments of the piers, abutments, walls, etc. at an off-site fabrication facility. Splice-sleeve connectors, as shown in Fig. 5, are cast into the segment during fabrication. The segments are then transported to the construction site, where they are rapidly assembled. The segments are

Fig. 6. Prefabricated substructures (FHWA 2009)
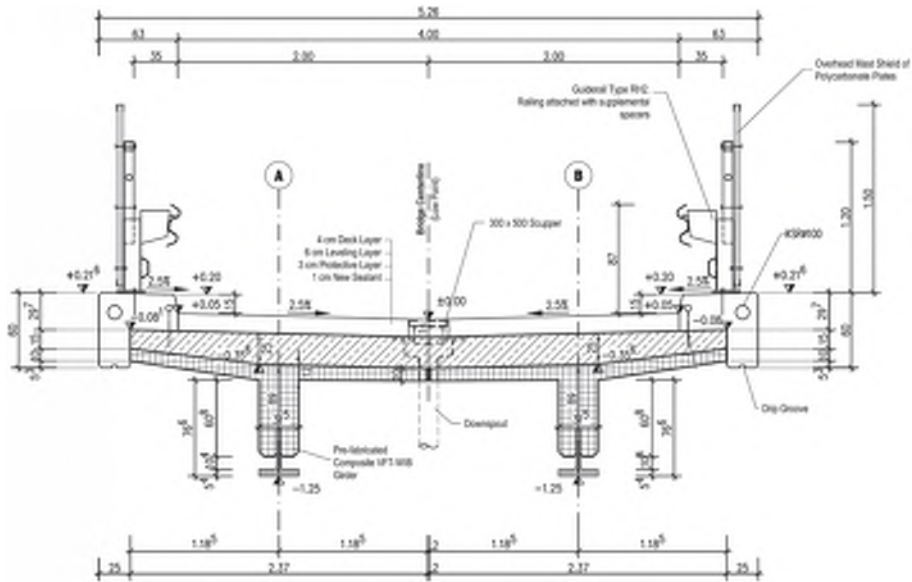
Fig. 7. VFT-bridge cross section (Reprinted with permission from Seidl and Braun 2009)

rigidly connected together by grouting the overlapping reinforcing bars within the splice-sleeve connector. There are many potential uses for prefabricated substructures with these connections, as can be seen in Fig. 6. Combined with prefabricated superstructures, it is possible to achieve complete bridge prefabrication.

Germany—Prefabricated Deck

In Germany, as well as many other countries, cast-in-place concrete decks are almost obligatory, and prefabricated decks are rare exceptions. However, prefabricated composite girders have begun to gain ground. A new construction method, called VFT (Verbund-fertigtträger, a pre-fabricated composite girder), has been developed to achieve a high level of prefabrication and, therefore, shorten the on-site construction time. The VFT construction method indicates that composite steel girders are prefabricated with precast partial depth slabs, as shown in Figs. 7 and 8. This method has been developed in Germany and tested on railway overpass bridges in Austria. (Seidl 2009; Seidl and Braun 2009)

Prefabricated full-depth slabs have also been tested in Germany. The Bahretal viaduct is an example of such a bridge. It is a six-span bridge with a length of 1,155 ft. (352 m). The composite superstructure is made of a steel box girder with transversal cantilever cross beams every fourth meter; see Fig. 9. Precast deck slabs, which are almost square shaped, are placed in the cantilever portion of the superstructure. Fresh concrete is cast between the precast elements

Fig. 8. Prefabricated VFT-girder (Reprinted with permission from Seidl and Braun 2009)

in the longitudinal direction of the bridge. The concrete deck on top of the upper flange of the box girder is also cast in place.

France—Prefabricated Decks

In France, bridges with prefabricated deck slab elements have been used for quite a long time. Two kind of transverse joints that have been used are match-cast joints and reinforced joints. Several bridges have been built using one of these two joints.

The first composite bridges with dry joints were erected in 1988 in Manosque on Escota Highway A51. These bridges were the first two built with the technique of prestress assembling of elements with carefully fitted keys in the joint faces that are simply glued to one another. The longest bridge was a four-span twin girder bridge with a length of 160 m and a maximum span of slightly more than 50 m. A detailed inspection carried out in 1995 showed no sign of cross-cracking of the slab element. Later inspections gave the same results, with the joints seeming to perform well (Berthellemy 2001, 2009).

A more recently used technique of dry joints is a system utlizing high-strength concrete. Because the deck is precast, high-strength concrete can be used without getting problems with large shrinkage. The durability of the slab will be better in many aspects, for example, better anticorrosion protection and better fatigue durability, because the prestressed concrete will remain in compression. The building process, as illustrated in Fig. 10, typically proceeds as follows (Berthellemy 2001, 2009):

1. Steel girders and match-cast deck elements are prefabricated off-site.
2. Elements are placed onto the girder, which has no shear studs at this stage.
3. The precast concrete elements are prestressed together, without connection to the steel.
4. Shear studs are welded to the steel beam through holes in the concrete.
5. The holes are filled with fresh concrete, which results in composite action between the deck and the girder.

United Kingdom (U.K.)—Precast Bridge Deck Systems

There are several examples of bridges with prefabricated deck elements in the U.K. Partial-depth precast deck elements have been used in several bridges all over the U.K. These elements act as a formwork to the cast-in-place concrete. There are, however, disadvantages to the use of these elements. For example, a large amount

Fig. 9. Bahretal viaduct with prefabricated full-depth slab elements (Reprinted with permission from Seidl 2009)
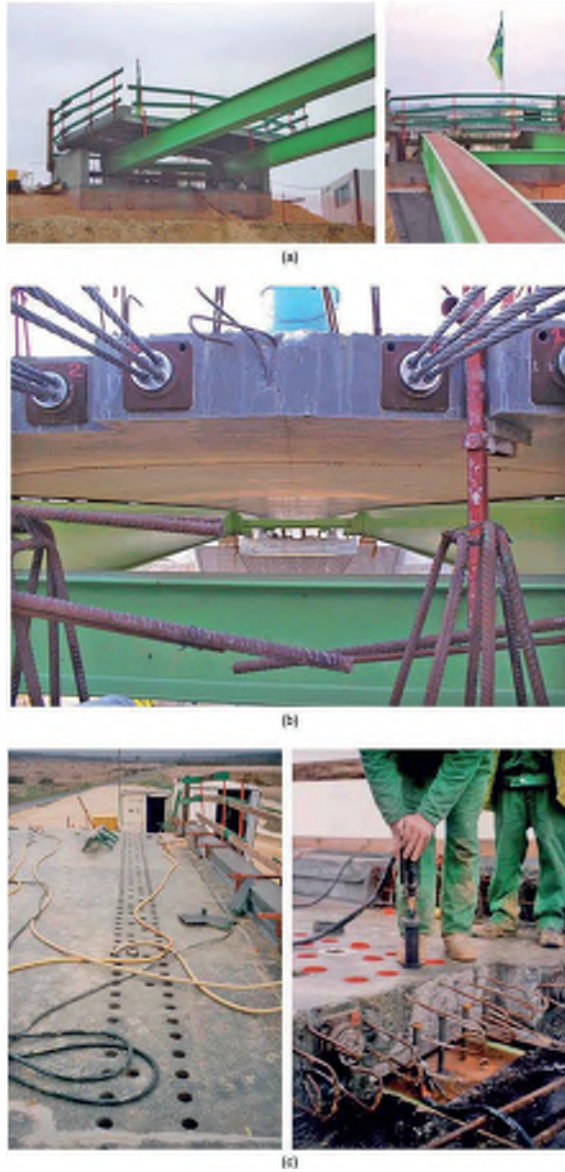
Fig. 10. The VINCI assembling process (Reprinted with permission from Berthellemy 2009): (a) elements are lifted and placed on girders without studs; (b) elements are prestressed; (c) studs are welded through holes in the deck
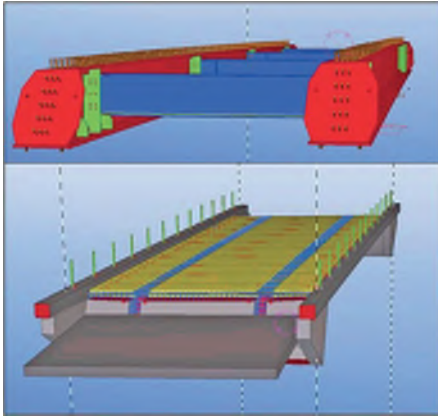
Fig. 11. 3D model of Laisentianjoki bridge (Reprinted with permission from Harju 2009)

Finland—Case Study: Laisentianjoki Bridge

In 2006, the Steel Bridges Development Group of Finnish Constructional Steelwork Association (TRY) started the development work for a new type of cantilever composite steel-concrete bridge. The targets for the study were to develop a composite bridge according to following criteria:

- Shortest possible installation time;
- Easy to build—Even in difficult conditions; and
- Extensively utilize 3-D design tools.

The outcome of the development project was the Laisentianjoki bridge, which was built in 2007. The bridge is 24.6 ft (7.5 m) wide with spans that are 6.5 ft + 59.0 ft + 6.5 ft (2.0 m + 18.0 m + 2.0 m). The superstructure consists of two main steel girders, 72 ft (22 m) each, and four cross beams. Both steel and concrete drawings were modeled in 3D, as shown in Fig. 11. The installation of the main girders and cross beams took approximately 6 h. Cross beam joints were bolted connections, so there was no need to treat the surface of the joints on-site. The bridge deck, wing walls, and end beam were constructed of prefabricated concrete elements. The panel joints and edge beams were cast in place so that the concrete and steel elements form a monolithic structure. The placement of the prefabricated elements was completed in approximately four days. The installation of the steel reinforcement, casting of the fresh concrete, and construction of the edge beams, as shown in Figs. 12 and 13, took eight additional working days (Harju 2009).

Sweden—Deck Elements with Dry Joints

Although Sweden has been building bridges using prefabricated deck elements for decades (Collin and Johansson 1999), the techniques are still rarely used. Different types of precast deck joints have been tried from reinforced cast-in-place wet joints to the latest solution with completely dry joints. The wet joints are similar to the techniques used in France, Scotland, the United States, etc. Wet joints require that some of the reinforcement be placed on-site

of reinforcement is required to achieve a moment capacity large enough to withstand the crane lift operations. Another disadvantage, compared with full-depth elements, is the need of in situ cast concrete, which reduces the speed of construction. Full-depth precast concrete decks would provide faster construction, but there has been some reluctance to use them in the U.K. (Gordon and May 2007).

In Scotland, much research has been conducted in the field of in situ cast joints between the precast deck elements, and different joints have been laboratory tested (Gordon and May 2006).

Fig. 12. Realized erection times for Laisentianjoki bridge (Reprinted with permission from Harju 2009)

Fig. 13. Construction sequence for the Laisentiajoki bridge (Reprinted with permission from Harju 2009): (a) large diameter steel piles being driven into the soil; (b) concrete filled piles with bearings in place; (c) steel girders being lifted into place; (d) completed steel structure; (e) prefabricated concrete end beams and wing walls being placed into final position and cast to the steel girders; (f) erection of prefabricated concrete deck elements; (g) prefabricated deck placed and awaiting concrete closure pour; (h) composite action is achieved by in situ cast concrete in the open channels

and that fresh concrete will be exposed as a part of the surface above the joints. Both of these items have associated time and durability concerns. Field placing reinforcement is yet another time-consuming procedure that must with done on-site. Any exposed field placed concrete provides an easier path for water and chlorides to permeate the concrete deck and begin attacking the reinforcing bars. Even if a waterproofing membrane is used, any field placed concrete must have time to mature before the waterproofing membrane can be installed. These are but a few of the items that increase construction time until the bridge can become operational and shorten the life of the final structure. To avoid these problems, a concept with dry joints has been developed in Sweden.

In a dry joint, match-cast overlapping concrete keys are used to transfer both lateral and vertical forces through the transverse joints and, thus, prevent vertical displacement between the deck elements at the joints. These keys are designed as a series of overlapping male-female connections along the joints, as given in Fig. 14.

The overlapping concrete keys require a longitudinal displacement of the elements during assembly. The tolerances for the deck slabs can be demanding because the distance between the transverse reinforcement bars in the slab and the shear studs on the steel girder is rather short. The required displacement is at least the depth of the overlapping concrete keys plus the tolerances, as indicated in Fig. 15. This technique has been used successfully on single-span bridges and is

Fig. 13. (*Continued*).

now developed to be used on multispan bridges. One key factor in multispan bridges will be the ability of the waterproofing system to withstand the negative moments and joint openings above an intermediate support.

European Research Project—ELEM

Studies conducted in the United States and Europe show the advantages of prefabrication in the field of bridge construction. To improve the competitiveness of prefabricated composite bridges, a European research and development project, ELEM RFSR-CT-2008-00039, was started in 2008. Four countries are represented in the research group: Sweden, Germany, Finland, and Poland. The success of the project relies on the cooperation between universities, engineering consultants, and steel producers. The overall objective of the project is to make prefabricated bridges more competitive through development of new cost-effective,

time-efficient, and sustainable bridge structures. Both wet and dry joints between the slabs are investigated, with particular attention given to the opening of dry joints above internal supports. To avoid leakage, suitable waterproofing and paving systems must be developed and thoroughly tested in the laboratory. The project also aims to determine how shear forces transfer through the concrete keys to each slab, and examine the actual design of the concrete keys. The project started with a knowledge extension, in form of an international workshop held in Stockholm, Sweden, in March 2009 and literature studies. The project has also included improvement of the details in element bridges, testing of the solutions in laboratories, and field monitoring on a one span bridge with dry joints. All presentations from the Workshop on Composite Bridges with Prefabricated Deck Elements are published in a Technical Report available at http://pure.ltu.se/portal/files/3112371/ELEM_Seminar_4_Mars_2009.pdf.

Fig. 14. Deck elements with dry joints (Reprinted with permission from Hällmark et al. 2009; first published in *Structural Engineering International SEI*, Vol. 19, Nr. 1, 2009, pp. 69–78, IABSE, Zurich, Switzerland, www.iabse.org)
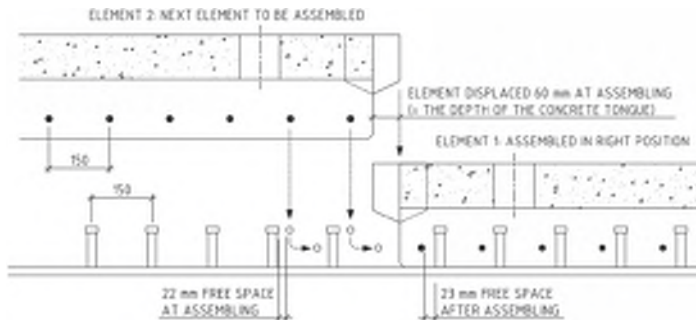

Fig. 15. Tolerances at assembling (Reprinted with permission Hällmark et al. 2009; first published in *Structural Engineering International SEI*, Vol. 19, Nr. 1, 2009, pp. 69–78, IABSE, Zurich, Switzerland, www.iabse.org)

Discussion and Conclusion

High-traffic pressure on an aging infrastructure network gives rise to demands from the traveling public for construction techniques that have as little effect on traffic as possible. Conventionally, bridges are built with cast-in-place concrete decks on girders that are cast-in-place concrete, precast concrete, or prefabricated steel. Accelerated construction techniques that use prefabricated elements lower road user costs by reducing traffic disturbance, lessening time spent on construction sites, and making the working environment safer. Prefabrication, especially of concrete decks, is a spreading methodology worldwide, but examples of prefabricated piers, abutments, walls and combined steel girders and partial concrete decks can be found.

Composite action between the girders and prefabricated deck elements is desirable and typically achieved by casting concrete into preformed pockets that surround shear studs attached to the girder flanges. The transverse joints between the elements must be carefully designed, depending on the demand for water tightness and ability to transfer loads between elements. Posttensioning offers good performance, but is not required to achieve satisfactory results. Blind pocket details with dowel bar connections promise composite action without exposing cast-in-place concrete to the elements.

The most thrilling and challenging technique is the idea of using completely dry joints. Overlapping male-female concrete keys are used to transfer both lateral and vertical forces through the joints and prevent vertical displacements between the deck elements. This solution has been used on single-span bridges but is now being further developed to be used on multispan bridges as well.

References

Berthellemy, J. (2001). "Composite construction—Innovative solutions for road bridges." *Proc., 3rd Int. Meeting on Composite Bridges*, Luleå Univ. of Technology, Luleå, Sweden.

PRACTICE PERIODICAL ON STRUCTURAL DESIGN AND CONSTRUCTION © ASCE / AUGUST 2012 / **91**

Pract. Period. Struct. Des. Constr., 2012, 17(3): 82-92

Berthellemy, J. (2009). "French experiences from prefabricated deck elements." *Proc., Workshop on Composite Bridges with Prefabricated Deck Elements*, Luleå Univ. of Technology, Luleå, Sweden.

Collin, P., and Johansson, B. (1999). "Wettbewerbsfaehige Bruecken in Verbundbauweise." *Stahlbau*, 68(11), 908–918 (in Swedish).

Commonwealth of Massachusetts. (2010). "Laboratory for Innovation." ⟨http://www.eot.state.ma.us/acceleratedbridges/pr_lab.htm⟩ (Jun. 21, 2011).

Culmo, M. P. (2009). "Prefabricated composite bridges in the United States including total bridge prefabrication." *Proc., Workshop on Composite Bridges with Prefabricated Deck Elements*, Luleå Univ. of Technology, Luleå, Sweden.

Degerman, H. (2002). "Samhällsekonomisk analys av hastighetsnedsättning vid bro söder om Norrfors." *Internal Rep.*, Banverket, Norra Regionen, Sweden (in Swedish).

Federal Highway Administration (FHWA). (2005). "Prefabricated bridge elements and systems in Japan and Europe." *FHWA-PL-05-003*, Office of Engineering, Bridge Division, Washington, DC.

Federal Highway Administration (FHWA). (2009). "Connection details for prefabricated bridge elements and systems." *FHWA-IF-09-010*, Office of Engineering, Bridge Division, Washington, DC.

Federal Highway Administration (FHWA). (2010). "Field cast UHPC connections for modular bridge deck elements." *FHWA-HRT-11-022*, Office of Engineering Bridge Division, Washington, DC.

Gordon, S., and May, I. (2006). "Development of in situ joints for pre-cast bridge deck units." *Proc. ICE—Bridge Eng.*, 159(1), 17–30.

Gordon, S., and May, I. (2007). "Precast deck systems for steel-concrete composite bridges." *Proc. ICE—Bridge Eng.*, 160(1), 25–35.

Hällmark, R., Collin, P., and Stoltz, A. (2009). "Innovative prefabricated composite bridges." *Struct. Eng. Int.*, 19(1), 69–78.

Harju, T. (2009). "CASE—Laisentianjoki Bridge." *Proc., Workshop on Composite Bridges with Prefabricated Deck Elements*, Luleå Univ. of Technology, Luleå, Sweden.

Mammoet USA. (2009). ⟨http://www.mammoet.com⟩ (Aug. 4, 2011).

Mistry, V. (2008). "Need for prefabricated bridge elements and systems for accelerated bridge construction." *WASHTO-X Webinar* (Jun. 17, 2008).

Nilsson, M. (2001). "Samverkansbroar ur ett samhällsekonomiskt perspektiv." Master's thesis, Luleå Univ. of Technology, Luleå, Sweden (in Swedish).

Ralls, M. L. (2008). "Benefits and costs of prefabricated bridges." *Accelerated Bridge Construction Study*, Utah Dept. of Transportation, Salt Lake City, UT.

Seidl, G. (2009). "Composite Element Bridges." *Proc., Workshop on Composite Bridges with Prefabricated Deck Elements*, Luleå Univ. of Technology, Luleå, Sweden.

Seidl, G., and Braun, A. (2009). "VFT-WIB-Brücke bei vigaun—Verbundsbrücke mit externer bewehrung." *Stahlbau*, 78(2), 86–93 (in German).

Splice Sleeve North America. (2009). ⟨http://www.splicesleeve.com⟩ (Aug. 4, 2011).

Utah Dept. of Transportation (UDOT). (2004). "Utah Dept. of Transportation," ⟨www.udot.utah.gov⟩ (Mar. 27, 2009).

92 / PRACTICE PERIODICAL ON STRUCTURAL DESIGN AND CONSTRUCTION © ASCE / AUGUST 2012

Pract. Period. Struct. Des. Constr., 2012, 17(3): 82-92

PAPER II

Innovative Prefabricated Composite Bridges

Robert Hällmark, Peter Collin and Anders Stoltz

Innovative Prefabricated Composite Bridges

Robert Hällmark, MSc, Ramböll, Luleå, Sweden; **Peter Collin,** Prof., Luleå University of Technology and Ramböll, Luleå, Sweden and; **Anders Stoltz,** Lic. of Technology, Skanska, Kalix, Sweden. Contact: Robert.Hallmark@ramboll.se

Summary

The competitiveness of composite bridges depends on different circumstances such as site conditions, local costs of material and staff, and the experience of the contractor. Two major advantages of composite bridges compared to concrete bridges are the ability of the steel girders to carry the weight of the formwork and the fresh concrete, and the shorter construction time which not only saves money for the contractor but even more for the road users. A further step is to prefabricate not only the steel girders, but also the concrete deck. In this paper, a new concept for composite bridges is described, with dry joints between the prefabricated concrete elements. The principal of the technique is presented, as well as some laboratory test simulating the load situation at an internal support in a multi-span bridge. Also, some experiences from an already built single span composite bridge with dry joints are presented.

Keywords: composite bridges; prefabricated decks; deck elements; dry joints.

Introduction

Composite bridges have become more popular in many countries.[1,2] The cost effectiveness of composite bridges is governed by different factors such as site condition, local cost of material and staff, and the experience of the contractor. In comparison to concrete bridges, one major advantage is that steel girders can carry the weight of the formwork and the fresh concrete, which means that the need for temporary structures is reduced, as indicated in *Fig. 1*.

In comparison with concrete bridges, in most cases less time is spent on the construction site if a composite structure is chosen. A shorter construction time saves money not only for the contractor but often even more for the road user. Unfortunately, the road-user costs tend to be neglected when alternative bridge designs are evaluated and compared.

The concrete deck is usually cast on-site, which means that the work with the formwork, reinforcement as well as the casting most often takes places outdoors. This work can be problem-atic and expensive during wintertime in countries with a cold climate.

A further step to improve the competitiveness of composite bridges is to prefabricate not only the steel girders, but also the concrete deck. The main advantages of precast concrete deck slabs, compared to conventional bridges with concrete decks cast onsite, are:

– A less number of man-hours outdoors at the construction site.
– A shorter construction time onsite, giving lower road-user costs.
– The deck elements are cast indoors, which is believed to result in high quality.
– An improved working environment for the workers while erecting formwork, placing re-bars and casting concrete.

It is also clear that some problems need to be solved in connection with prefabricated deck slabs in order to make the concept cost efficient. This will be discussed in the current paper, in addition to presenting some new solutions.

Deck Elements with Dry Joints

Concrete deck elements acting compositely with steel girders have been used in many countries around the world, e.g. Germany, USA, Russia, France and Sweden.[2–4] When dealing with prefabricated deck elements, two main questions should be answered.

(a) How should the horizontal shear forces be transmitted between steel and concrete?
(b) How should the vertical shear forces be transmitted between the deck elements?

Different technical solutions have been used to transfer the vertical shear forces from one deck slab to another. Post-stressed cables have been used to press the elements together. This system was, for example, used on a three-span bridge in Sweden,[2] but it turned out to be rather expensive. Many countries have used different kinds of reinforced site-cast joints in order to transfer the forces between the elements. Site-cast joints mean, however, that some re-bars must be placed onsite, and that fresh concrete will be exposed on the surface at each joint. These two processes are activities which increase the time spent at the construction site until the bridge can become operational, and should be avoided if possible. In order to avoid these problems a system with dry joints has been developed in Sweden.

A research and development project was carried out at Luleå University of Technology during 1998–2001. Within the framework of this project, a new concept for dry joints between roadway slab elements was developed. In order to transfer both lateral and vertical forces through the transverse joints, and to prevent vertical displacements between the deck elements at the joints, overlapping concrete keys were used. These keys were designed as a series of overlapping male-female connections along the joints, see *Fig. 2*.

The connections between the deck slab and the steel girders are achieved at the channels above the girders. These channels are filled with concrete when all elements are in their final positions, and the prestressing force has been applied. Transverse reinforcement bars from the bridge deck elements pass through the channel between the shear studs, which provide the interaction between the girders and the concrete after the channels have been cast, as shown in *Fig. 3*.

Fig. 1: One concrete bridge and one composite bridge during construction
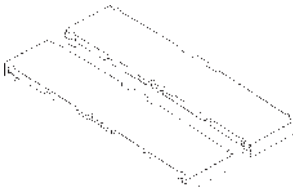
Fig. 2: Prefabricated deck slab units with dry joints

(a) The in-situ cast channel

(b) The channel in one slab element used in laboratory testing

Fig. 3: Site-cast channel in slab element right above the girders

The theoretical distances between the transversal reinforcement bars and the shear studs are rather short, and the tolerances can be demanding since the overlapping concrete keys require a longitudinal displacement of the elements at the assembling. The displacement has to be at least the depth of the overlapping concrete keys plus the tolerances (see section on Concrete Deck Elements and *Fig. 19*). Limited tolerances put higher demands on the steel workshop and the manufacturer of the concrete deck elements. In a bridge project involving prefabricated elements, it is a key factor that the demanded tolerances are fulfilled, since the possibilities of carrying out any last minute changes at the construction site are limited.

In the summer of 2000, an old bridge across Rokån outside Piteå in Sweden (Bridge 1883) was replaced using the concept of prefabricated deck slab elements with dry joints. Since many heavily loaded timber trucks use this bridge, the alternative would have been an expensive bypass road. Instead, a bridge with prefabricated retaining walls, girders, deck slab elements and foundation plinths, was chosen. Furthermore, the new bridge was temporarily erected next to the old bridge, which carried the traffic as usual. Then the old bridge was removed and the new bridge was launched sideways and placed on top of the prefabricated supports. After only 30 hours, the road was reopened and the new bridge was commissioned into use. *Table 1* shows the timetable for the project, and *Fig. 4* illustrates the work.

Laboratory Testing of Dry Joints

A laboratory testing of a prefabricated composite bridge was carried out and is described in detail in Ref. [5]. The aim of the test was to study the behaviour of a composite bridge with dry joints in the concrete element deck that open when negative bending moment is present. All the tests are made on elements with dry joints, and no epoxy is used.

The test setup was designed to imitate the load situation in an internal support of a multi-span bridge. The test specimen consisted of two steel girders and four deck slab elements (200 ×

Day	Time	Activity
Day 1	19:00	The old road was closed.
	22:00	The old bridge was removed using two mobile cranes. The dismantling work continued until 6 p.m. the next day.
	00:00	Old back walls and side wings were removed. The ground behind the abutments was excavated. New gravel fill was added up to the correct level.
Day 2	09:00	The prefab plinths were placed on the new gravel bed.
	10:00	The lifting contractor temporarily placed the new bridge on launching girders, which took 4 hours. Then the bridge was launched sideways, which took only 10 minutes.
	18:00	Installation of bearings and filling behind the retaining walls.
Day 3	01:00	The new bridge was opened to traffic.

Table 1: Timetable for the bridge replacement across Rokån

(a) Two more deck elements to go

(b) Sideways launch

(c) Bridge deck element in final position
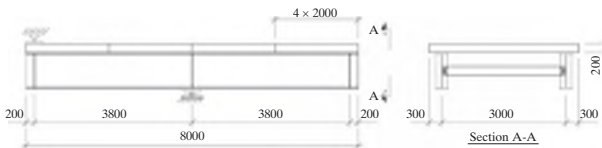
Fig. 4: Bridge BD1883 over Rokån

Fig. 5: Laboratory test specimen (Units: mm)

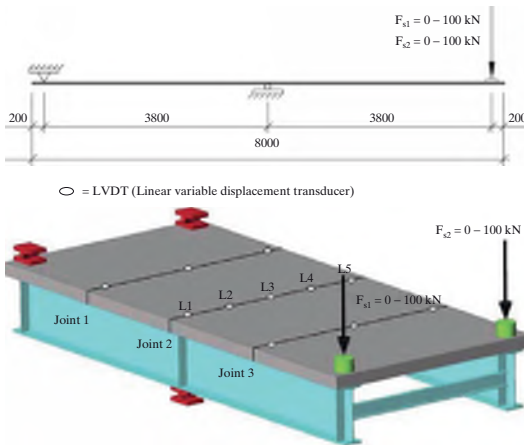
○ = LVDT (Linear variable displacement transducer)

Fig. 6: Static load test setup (Units: mm)

2000 × 3600 mm), with dry joints. The deck slab elements had been match cast, and were mounted on the girders in the same order as they had been cast.

Hydraulic jacks were used to move the elements towards each other. A compressive longitudinal lateral force of 400 kN was applied at the time when

all the elements were in the right position and the channels were grouted with concrete. The force was then kept constant for 2 weeks, during the hardening of the concrete.

The steel girders used were HEA 900 S460, and the concrete was classified as C55/65. The laboratory tests of the compression strength gave $f_{cc} = 73$–75 MPa. Shear connectors, $\varnothing 22 \times 100$ mm, introduced the composite action between the deck slabs and the steel girders. The scale of the test specimen was approximately 2 : 3 of a real bridge section. An illustration of the test specimen is shown in *Fig. 5*.

Four types of tests were performed on the specimen. In these tests, vertical and lateral displacements were monitored on the concrete surface at the joint above the internal support, as well as tensions in the steel girders and the deck slabs. The tests were as follows:

(1) Static load test: Static loads, increased in stages of 20 kN up to 100 kN, were applied at the unsupported end of the steel girders, see *Fig. 6*.
(2) Fatigue test of concrete keys: Fatigue loads of 5 to 140 kN were applied on opposite sides of the internal support, Joint 2 in *Fig. 6*. This test was performed in order to simulate the fatigue of the concrete keys, when a vehicle wheel crosses the joint at the same time as a load is acting in midspan giving a negative moment at the joint.
(3) Fatigue test of shear studs: Fatigue loads were applied at the unsupported ends of the steel girders in order to investigate how the shear studs are affected by fatigue loads. The test setup was the same as in (1), but the applied load was cyclic, see *Fig. 6*.
(4) Static load test of concrete keys until failure: Finally, a test was performed to find the failure load of the overlapping concrete keys.

Static Load Test—Joint Displacements

During the static load test, the element gaps as well as the vertical deflections at each joint were measured. The vertical deflections were also measured under the hydraulic jacks and at the supports, in order to make sure that the specimen was behaving symmetrically in the test setup.
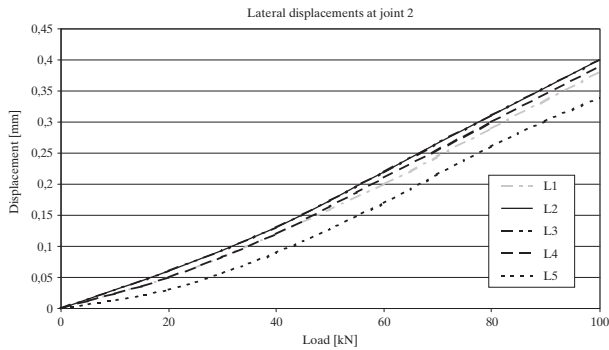
Lateral displacements at joint 2
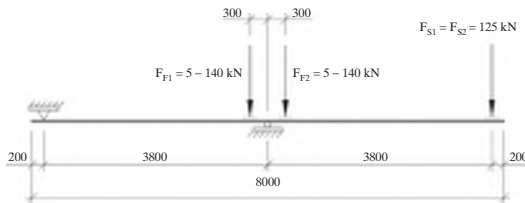
Fig. 7: Static load test setup

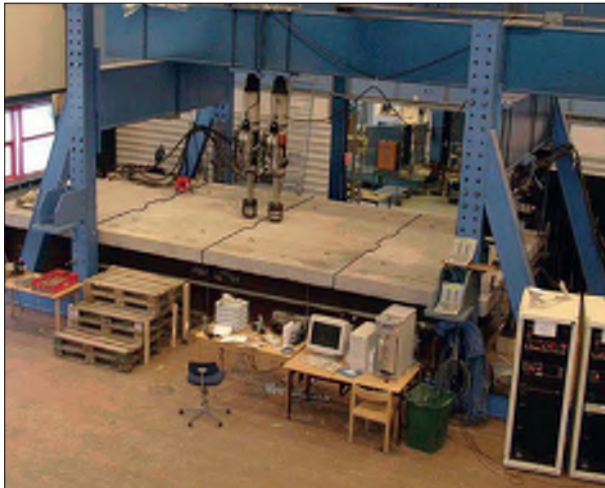*Fig. 8: Test setup for fatigue resistance test of concrete keys (Units: mm)*

Fig. 9: Photography of the test setup (the dry joints have been highlighted)

Static loads, F_{S1} and F_{S2}, were applied at the unsupported ends of the steel girders, as shown in *Fig. 6*. Only one of the loads was acting at the time, giving an unsymmetrical load situation. The load was increased in stages of 20 kN, from 20 to 100 kN.

The test results showed that the test specimen behaved more or less perfectly symmetrically and as predicted. A combination of this and the rest of the test results from the static load test, led to the conclusion that possible deviations in the arrangement of sup-

ports and loading rig did not affect the results.

The lateral displacement at Joints 1 and 3 varied rather identically during the whole test. The largest difference in lateral displacement between the two joints was 0,04 mm, which is about 20% of the total displacement. The lateral displacements measured at Joint 2 were, as expected, about twice as large as the displacement at Joints 1 and 3 at the same time. *Figure 7* shows the relationship between the lateral displacements, at Joint 2, and the static load. Only four of the five lines are visible in *Fig. 7*, since the sensors L2 and L3 gave the same values.

Fatigue Test of Overlapping Concrete Keys

The fatigue resistance test of the concrete keys was conducted in order to simulate a situation when a vehicle wheel crosses a joint at an internal support, at the same time that a load is acting in mid-span giving a negative bending moment over the support. A fatigue load of 5 to 140 kN was applied in 1 million cycles with a frequency of 1,5 Hz. Two hydraulic jacks, with a phase difference of 180°, were placed at opposite sides of the joint above the internal support. The fatigue loads were transferred to the specimen by steel plates with a size of $200 \times 200 \times 50$ mm. The size is less than that recommended according to EC 1-3 (400×400). The reason for using smaller plates was to concentrate the load to the overlapping concrete keys. During the whole test, a static load (2×125 kN) was applied at the unsupported ends of the steel girders, in order to open the joint between the elements, as shown in *Figs. 8* and *9*.

The test of the overlapping concrete keys indicated good results when subjected to fatigue load. The lateral opening of the joint at the internal support remains almost constant during the test of 1 million load cycles. The joint over the internal support had an opening of 1,06 mm due to the fact that the specimen was subjected to a global negative moment. The increase of the lateral opening of the joint, at the internal support, due to the fatigue load was 0,073 mm. The initial opening was determined by using feeler gauges before the test started. The average initial opening of the joint at the internal support was 0,15 mm. The total opening in the lateral direction caused by the loads was 1,13 mm. For the other
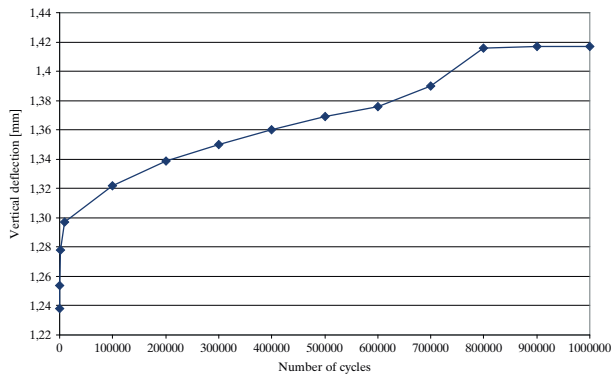
Fig. 10: The relative vertical deflection at the joint over the internal support
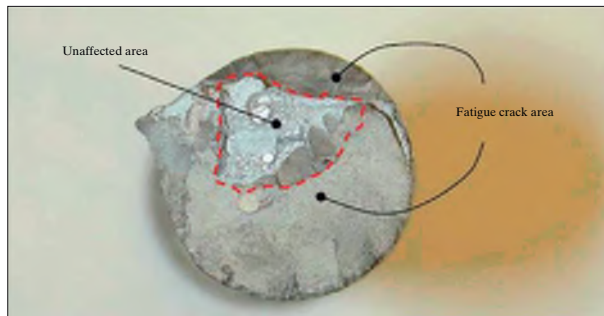

Fig. 11: Shear stud which has suffered from fatigue

two joints the lateral deflection was constant throughout the test.

The relative vertical deflection between the two concrete slabs on each side of the joint at the internal support caused by the pulsating loads was initially 1,24 mm. At the end of the test, after one million load cycles, this value was 1,42 mm (see *Fig. 10*). The vertical movement increased by 0,18 mm during the fatigue test. This vertical movement is a potential problem for the waterproofing and the surfacing, especially since joints over internal supports will experience tensile- and shear forces at the same time.

There were no indications that the concrete keys had suffered from fatigue decay during the test. No visible cracks of the concrete keys or dramatic change of behaviour was found during the test.

Fatigue Test of Shear Studs

In the setup for the fatigue test of the shear connectors, the cyclic loads were moved from mid-support to the cantilevering end of the test specimen. The test setup was the same as in the static load test (1), but the applied load was cyclical. The two jacks were synchronised and applied a load of 245 kN in one million load cycles. The load resulted, according to a FE-analysis, in a shear force of 44 kN on the shear connectors in the region closest to mid-support. At this stress range, the estimated number of cycles until fatigue failure are 262 000, according to Ref. [6].

For this part of the test, the lateral opening of the joints as well as the vertical deflection of the cantilevering end of the specimen were almost constant during the test. If many shear studs had suffered from fatigue, an increase of the lateral joint was expected as well as the vertical deflection. The relative vertical movement between the concrete slabs was measured at the internal support from 100 000 to 1 million load cycles. Due to technical limitations it was not possible to apply

the LVDT-gauge until after 100 000 load cycles, and it was only possible to measure the slip between one of the concrete slabs and the steel girders. The relative vertical movement increased with 0,05 mm, during the 900 000 registered load cycles. This was the only displacement parameter that indicated that some of the studs might suffer from fatigue. As a complement to the displacement measurements, two other techniques were used to detect the crack propagation of individual shear studs: acoustic emission (AE) technology and strain measurements. These measurements were not a main purpose of the test. Therefore, the results are only described briefly.

The AE measuring devices were applied at the upper flange in each end of one of the girders. The measuring devices were two microphones which were fixed by magnets. Two devices were used on each end of the girder. They were applied in the transversal direction in the middle between the edge of the flange and the web. The equipment that was used is described in detail in Ref. [7] and the test setup is described in Ref. [5].

The data from the AE-measurement indicated, after about 400 000 cycles, that there was a specific zone on the girder which gave acoustic emission during the cycles. Such a tendency is typical for a propagating crack. Cracks which are just opening and closing without propagating, do not give any acoustic emissions of the kind that has been registered. The measurement shows that the fatigue cracks are growing faster and faster when the number of cycles are increasing. The AE-signal is about 30 times higher after 1 015 000 cycles, than after 400 000 cycles.

The presumed propagating crack was traced by the AE-measurement to a position 200 mm from the internal support (Joint 2), at the cantilevering part. The margin of error was estimated at ±100 mm. When all the tests were completed, concrete was removed at the zone where fatigue failures of the studs were expected. In this zone, it was visually confirmed that two studs had large fatigue cracks. The remaining areas of these studs were about 25%, as shown in *Fig. 11*. These two studs were located 250 mm from the internal support, which is inside the margin of error from the AE-measurement. Thus, this test shows that it is possible to detect cracks in a composite structure by using acoustic emission technology.
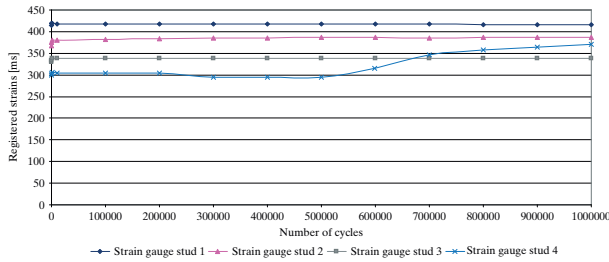
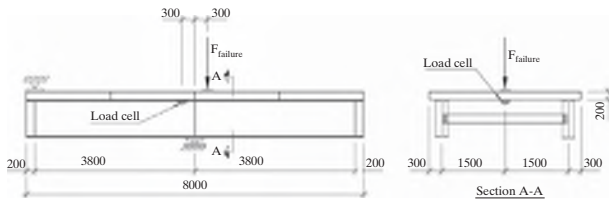Fig. 12: Strains registered by the four strain gauges at the upper flange, representing four studs

Fig. 13: Static load test setup (Units: mm)

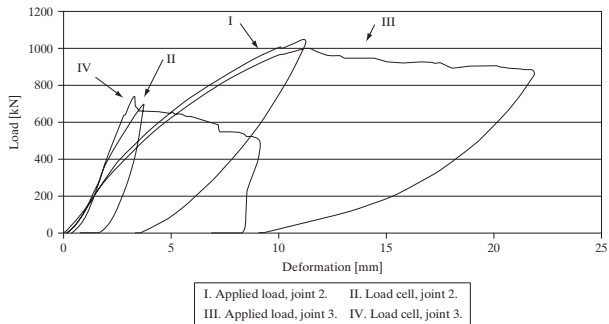| I. Applied load, joint 2. | II. Load cell, joint 2. |
| III. Applied load, joint 3. | IV. Load cell, joint 3. |

Fig. 14: Load deformation diagram at Joints 2 and 3

No AE-measurements were performed on the other girder. The strains in the upper flange, due to the bending of the shear studs, were however also measured by strain gauges. These were mounted underneath the upper flange, located below the studs and displaced 15 mm along the longitudinal axis. The result could be used to find out if some of the shear studs suffered from fatigue. The strain measurements indicated that two studs might have failed on this girder as well. One was at the same distance from the end of the girder as the stud that failed on the first girder. The surrounding concrete was removed and

the failure was visually confirmed. By studying the crack area, of the same kind as shown in *Fig. 11*, the remaining area of that stud was estimated to be 50%. The second stud which might have failed was not uncovered from the surrounding concrete, and the failure was not visually confirmed.

Figure 12 shows the strains registered by strain gauges at four studs in a row at the middle joint in the test setup, two studs on each side of the joint. Three of the studs show a constant behaviour throughout the fatigue test, while the fourth one shows a deviant behaviour.

The conclusion drawn from the measured strains, in *Fig. 12*, is that stud number four has suffered from fatigue, since the measured strain is increasing during the test. The surrounding concrete has probably been crushed and the resulting force acting on the bolt has been transferred upwards along the stud shank. The consequence of this is an excessive bending moment in the stud, and the observed rising strain is a result of the rising moment. The bending moment causes bending stresses, which result in a propagating fatigue crack. Similar strain behaviours were registered for another three studs, and the fatigue cracks were visually confirmed at three of the four studs which had suffered from fatigue according to the strain measurements.

Static Load Test of Overlapping Concrete Keys

After the fatigue test, an additional test was performed to check the resistance to the static load of the concrete keys. The joint at the internal supports that have been subjected to fatigue load, was tested, as well as an additional joint that had not been subjected to fatigue load as a reference. The test setup is shown in *Fig. 13*. It resembles the test setup used in section Concrete Deck Elements. Instead of using two jacks at each side of the joint, only one jack was used. The other jack is substituted to a load cell, which registers the force that is transferred directly through the concrete key.

The results confirm that Joint 2 at the internal support had not suffered from fatigue. The maximum static load capacity was about the same for the two tested joints. The maximum load applied was 1046 kN at Joint 2, and 1001 kN at Joint 3. These loads can be compared to the highest design vehicle wheel load in the Swedish Bridge Code [14], which is 163 kN.

Figure 14 shows a load deformation diagram, illustrating deformations caused by the forces applied at the concrete keys. The registered forces that have been transferred directly through the keys are plotted in the same diagram. At Joint 2, about 66% of the force is transferred through the keys, and about 73% in Joint 3.

Summary of Laboratory Tests

– The overlapping concrete keys can withstand the static load as well as the fatigue load, according to EC 1-3.
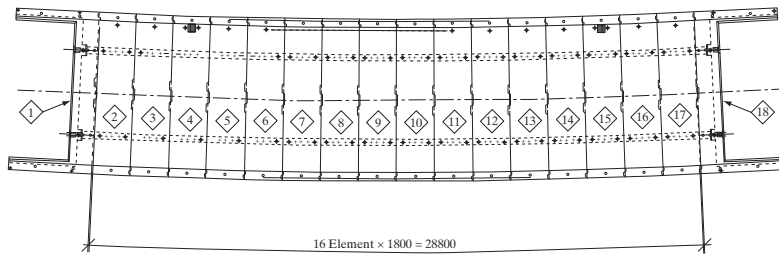
Fig. 15: General arrangement of the prefabricated bridge deck in road bridge AC1684 (Units: mm)
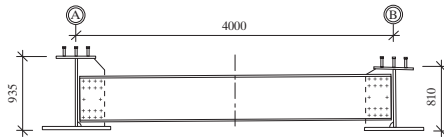

Fig. 16: Cross-section of the steel structure, c/c cross-girders 7,0 m (Units: mm)

– For a continuous girder bridge, the joint tends to open over intermediate supports. The total horizontal opening during the fatigue test was 1,1 mm. The relative vertical movement of the adjacent concrete slabs, caused by a passing wheel over an intermediate support, was stated to be 1,4 mm during the key fatigue test. This movement of the joint is a problem for the waterproofing and surfacing, thus it has to be investigated.

– Even if the slab elements under tension, near the intermediate support, are not included in the design calculations, it is strongly recommended that they should be properly connected to the steel girders. The connection should be as strong as possible without exceeding the tensile strength of the concrete. The force on the shear studs will vary with the traffic load and may cause fatigue failure. The laboratory test with 1 million load cycles caused at least three studs, but probably four, to fail from fatigue. The calculated force on the studs of 44 kN is high compared to the expected resistance to fatigue according to [12] and [13] for 1 million cycles. At the estimated number of stress-range cycles until failure, according to Eurocode 262 000 cycles, no signs of fatigue was observed. At 5 to 600 000 cycles, some studs seem to suffer from fatigue.

– Although not the main purpose of the test, acoustic emission was

adopted, and it was possible to detect the propagation of cracks in the headed shear connectors. The first indication of a propagating crack was registered after 400 000 cycles.

Experience from Bridge AC 1684

In 2002, the Swedish road bridge AC 1684 was built over a railway in Norrfors, replacing an old narrow bridge in bad condition. It was designed as a single span composite bridge with a span width of 28 m. The bridge deck was designed to be prefabricated, in 16 concrete deck elements and two prefabricated abutments (see *Fig. 15*), and assembled with dry joints. The construction costs were presumed to be a bit higher than for a conventional concrete bridge, but since the disturbance of the railway traffic could be minimized it was worth trying the new concept. One of the demands which the bridge designer had to deal with was the requirement of a bridge which could be assembled in less than 24 h. The time limit was governing by how long time the electricity on the railroad must be switched off. During this period, girders would be lifted in place, deck slab elements assembled, and bridge rails, as well as safety roof and safety net mounted. The elements were also prestressed with a force of 600 kN, in order to ensure that there would not be any gap between the elements.

This bridge project has been evaluated in Ref.[8] in order to gather experiences and the opinions about this type of prefabricated element bridges. It also [8] states that the most important experience is that all the participants must be aware of the aim of the project and their responsibilities. It is necessary that all partners realise the importance of the required precision.

Steel Girders

The bridge has a rather complex geometry, as shown in *Figs. 15* and *16*, and the lack of vertical and lateral surfaces requires an extra amount of information for the steel workshop. The extra information is needed in order to avoid small mistakes which may not be discovered before the units reach the construction site. If there is a mismatch between the studs and the transversal reinforcement in the grouting channel, the time benefits of a prefabricated bridge might be wasted.

During the assembling of the bridge, some tasks appeared to be a bit unpredictable and some proposals for improvement were raised. First, the two girders were not in the right positions. Measurement showed that they had a longitudinal displacement in relation to each other. A decision was taken to adjust the girders positions after they had been lifted in place. However, the measurements after the lift showed that the girders had gone back to the right position. In order to avoid these uncertainties, laterally adjustable cross stays could be mounted on the upper flanges. Displacements could then be adjusted by these. They will also give an extra lateral stiffness to the steel girders during the assembling of the deck elements. Another observation was the lack of reference points on the steel structure. This caused some problems when the first element was lifted in place, since it was not obvious where
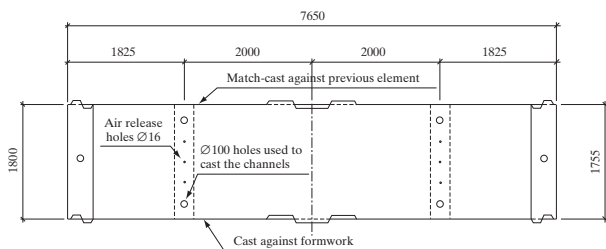
Fig. 17: Plan of a prefabricated bridge deck element (Units: mm)

Fig. 18: Bridge deck element is lifted in place

the right position was. This problem can be solved if the steel workshop adds some marks on the outside of the upper flange. These marks must be deep enough to be visible after the painting work is done.

Concrete Deck Elements

Each element had a dimension of 1800 × 7650 × 280 mm (see *Fig. 17*), giving an element weight of about 10 t. Experiences from previous projects have shown that the lifting devices should not be anchored in the grouting holes for the concrete channel. This conclusion was based on the observation of longitudinal cracks near the channels, caused by the bending moment due to the element's weight. Therefore, four spherical head lifting anchors were

used to lift the elements at AC 1684. These anchors were cast in recesses in the concrete surface, outside the channels. The channels were filled with concrete when the elements were fixed at the right position. The new positions of the lifting anchors gave a significant decrease of the bending moment in the channels, and cracks were avoided. *Figure 18* shows an element during the lifting.

The concrete keys transfer the shear forces from one element to another and are designed to transfer high axle loads. The keys in this bridge might be slightly larger than necessary, compared to the results from full-scale laboratory testing.[9] In order to get larger tolerances, the concrete keys could be designed slightly smaller. Such a change would require further studies of the concrete cover and the shear reinforcement in the key areas. *Figure 19* shows the principle of the element assembling, and the limited tolerances associated with this application.

Tolerances

One of the experiences gained from this bridge is that the tolerances are limited and very demanding. If possible, larger tolerances should be used
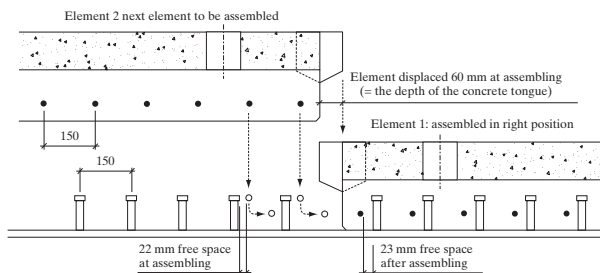
in order to minimize the risk of problems during the bridge assembling. As shown in *Fig. 19*, the theoretical tolerances between the channel reinforcement and the studs are about 22 to 23 mm. The positions of the studs and the reinforcement, as well as the width of the element, are very important. If the same error is repeated on each element it will soon lead to a fault larger than the tolerances at the assembling. This must be avoided if this method is to be competitive. The advantages of the method are the shorter construction time and the possibility of minimizing traffic disruption when replacing an old bridge. These advantages are lost if the prefabricated elements and the steel girders do not fulfil their tolerances[8], which are summarized in the following key factors in each phase of the bridge construction process, in order to ensure that all components are within their limits of tolerance:

Design phase:

– Detailed manufacture drawings, in which important distances are given with appropriate tolerances.
– Detailed and well-considered assembling instructions on the construction drawings and in the assembling plan.
– Plans for additional inspections and checking of own work during all phases of the bridge construction.

Manufacturing phase:

– Checking of own work, in order to fulfil the required tolerances.
– Be in agreement with the additional controls and the purpose of these.

Assembling phase:

– Be in agreement with the assembling instructions and the purpose of these.
– Preparation before the assembling.
– Coordination of the different participants during the assembling phase.

Extra Control Program

In order to achieve the demanded tolerances, extra control programs were developed for each phase of the bridge construction. In this section, the extra control program will be briefly described to illustrate how precisely the work has to be executed. The following items are checked by the manufacturer of the prefabricated concrete deck elements.
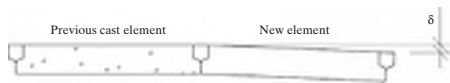

Fig. 19: Illustration of the narrow tolerances at assembling (Units: mm)

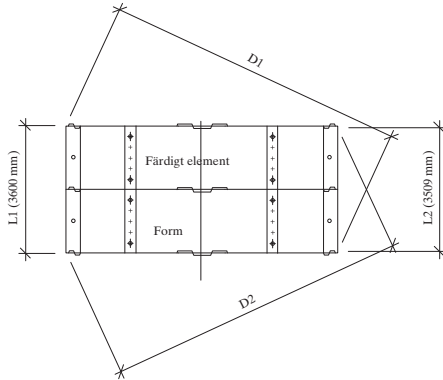*Fig. 20: Levelling tolerances for element formwork*

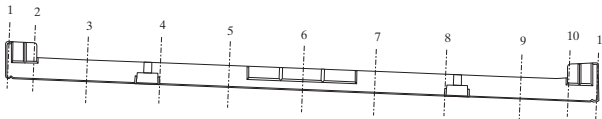*Fig. 21: Geometry checks of deck slab and formwork*

Fig. 22: Positions where the joint opening is checked

Checking the levelling of the formwork

The previous cast element is used as formwork on one side of the next element. The formwork for the new element was levelled with a precision of ±2 mm. The desired value of δ, shown in *Fig. 20*, was 2 mm (due to the vertical radius). It was checked before and after the concrete was cast, to ensure that there were no undesired deformations.

Checking of the geometry

It is very important that the elements in prefabricated bridges have the right geometry. This becomes even more important in Bridge AC1684, since it has both a horizontal and a vertical radius. Before the elements are cast, the formwork is measured together with the previous element, as shown in *Fig. 21*. The tolerances for L1, L2, D1 and D2 are ±3 mm.

Checking the concrete cover and effective cross-section

The desired concrete cover over the whole structure is 35 mm, and the tolerance is set at ±5 mm. The concrete cover and the effective cross-section is checked by measuring the position of the reinforcement before the element is cast. Tolerances for the effective cross-section vary, depending on which part of the structure is checked.

Initial opening of the joint

After formwork removal, the initial opening of the joints is checked by the manufacturer of the elements. It is checked at 11 positions along the joint (see *Fig. 22*), on both top and bottom surfaces of the element. The average opening is not allowed to exceed 1,0 mm at this stage.

The joint opening is also checked by the contractor when the bridge deck has been assembled and prestressed by a force of 600 kN. The joint opening after prestressing should be 0 mm on the upper or lower side of the joint. This is checked by using a feeler gauge. The joint is considered as 0 mm if a feeler gauge of 0,3 mm cannot be pushed through the joint, at the same time as the joint does not exceed 1,0 mm at the opposite side (upper/lower side). Locally, a 1,5-mm joint opening

is allowed over a maximum distance of 1 m. The average opening of the joint is not allowed to exceed 0,4 mm, when all the measured values on the upper and lower side of a joint are taken into consideration.

Economy

The construction costs of the prefabricated bridge were presumed to be higher than the cost for a bridge with a concrete deck cast onsite. However, according to information received from the contractor, the cost of the prefabricated deck was the same as that of a deck cast onsite. Another contractor states that the prefabricated deck was less expensive according to their cost estimations. The extra costs due to the prefabrication is compensated by the saving achieved in formwork and other costs that appear when a bridge is built over an operating railway.[10]

Analyses made by the Swedish National Railway Administration (SNRA), estimate the costs to society if the bridge had been constructed in a conventional way.[10] The highest speed allowed on the railroad would then have to be decreased from 100 to 70 km/h over a two-km-long distance, during the construction time of the bridge. The cost for changes in signal equipment and signs was estimated at 16 500 , and the cost due to the loss of capacity was estimated at 22 000 .

The fee to the bridge designer is one of the costs that will be a bit higher for a prefabricated bridge, partly due to the lack of experience from similar construction projects. This cost is however low compared to other costs, and can probably be lowered when the bridge designers get some experience from this type of bridge.

For bridge BD1883, a study made in Ref. [11] compares the cost of constructing (A1) a prefabricated composite bridge (the system under study), (A2) a conventional composite bridge with a temporary bridge, and (A3) a conventional composite bridge with the traffic directed to the nearest bypass roads. The construction costs and the road-user costs for the three alternatives are shown in *Fig. 23*. The construction costs are inclusive of profit to the contractor, and some indirect taxes.

The most economical alternative in the social aspect, according to the study in Ref. [11] was to build a prefabricated composite bridge (A1). The construc-
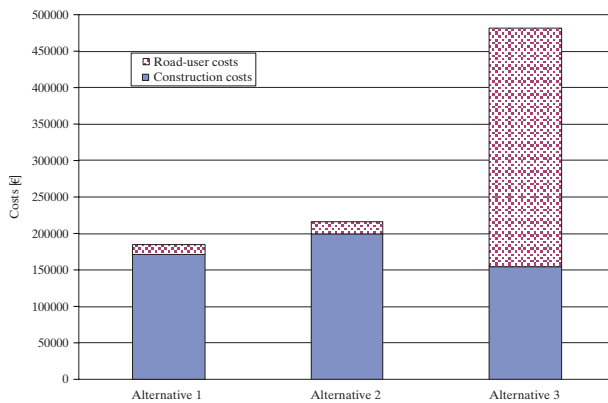
Fig. 23: Construction costs and road-user costs for concerned construction type 1 to 3

tion cost of a conventional bridge (A3) is lower, but the need for a temporary bypass road, or the indirect costs of directing the traffic to nearby roads are making the prefabricated composite bridge the most economical solution for society. The main reason why alternative 3 gets very high road-user cost is the fact that the nearest bypass roads resulted in a quite long pass for the road-users in this particular case.

Conclusions

Composite bridges are a well-established alternative to concrete bridges. The new concept for composite bridges with prefabricated decks described in this paper offers several advantages compared to concrete bridges and conventional composite bridges. Some of the advantages are the shorter erection time, better working environment, a dry bridge deck surface and a possibly higher quality.

Laboratory tests carried out on precast slab elements showed excellent abilities to withstand both static and fatigue loading. Pilot projects in northern Sweden erected in 2000 and 2002 showed that this design concept works well onsite.

Experiences from bridges constructed according to this concept show that it is possible to fulfil the demanded tolerances, even if the tolerances are limited. It is necessary that all partners involved are aware of the aim of the project and their responsibilities. Every step must be checked carefully since there is no time or possibilities for last minute changes at the construction site.

In a newly started European R&D project (ELEM), the concept of prefabricated deck elements will be studied by researchers and designers from Sweden, Finland, Germany and Poland. The estimated cost of the project is 1,5 million €. The project aims at building a multi-span bridge with dry joints, and monitoring the movements of these. This also includes experimental studies of whether the waterproofing can withstand these movements. Furthermore, the possibilities to allow larger longitudinal tolerances at the assembling stage, by placing the shear connectors in concentrated groups will be investigated.

References

[1] Collin P. Some trends in Swedish Bridge Construction. In *International Conference on welded Structures*, Budapest, 2-3 September 1996, 1996, 163–172.

[2] Collin P, Johansson B. Wettbewerbsfähige Brücken in Verbundbauweise. *Stahlbau* 1999; **68** Heft 11: 908–918.

[3] Biswas M. Precast bridge deck design systems. *PCI J. V.41, No.2,* . 1986: pp. 40–94.

[4] ARBED. *Innovative Composite Design of Motorway Overbridges*. Europrofil ARBED: Luxembourg.

[5] Stoltz A. Effektivare samverkansbroar. Licentiate Thesis 2001:141, Luleå University of Technology, Sweden, 2001, (in Swedish).

[6] EN 1993-1-9. *Eurocode 3 – Design of Steel Structures – Part 1-9: Fatigue*. CEN, European Committee for Standardization: Brussels, 2005.

[7] Boström S. Crack location in steel structures using acoustic emission techniques. Doctoral Thesis. Department of Civil Engineering, Division of Steel Structures, Luleå University of Technology, Sweden, ISSN: 1999, 1402–1544.

[8] Fahleson C. *Projektering, tillverkning och montage av elementbyggd samverkansbro*, Internal report Rambøll Sverige AB (former Scandiaconsult), Luleå, Sweden, 2003, (in Swedish).

[9] Lundmark R, Mikaelsson F. Elementbyggda samverkansbroar. Master's Thesis 1997:038, Luleå University of Technology, Luleå, Sweden, 1997, (in Swedish).

[10] Degerman H. Samhällsekonomisk analys av hastighetsnedsättning vid bro söder om Norrfors, Internal report Banverket, Norra regionen, 2002, Sweden, (in Swedish).

[11] Nilsson M. Samverkansbroar ur ett samhällsekonomiskt perspektiv – En jämförelse mellan platsgjutna och förtillverkade samverkansbroar. Master Thesis, Luleå University of Technology, Sweden, 2001, (in Swedish).

[12] EN 1991-2. *Eurocode 1 – Actions on Structure – Part 2: Traffic Loads on Bridges*. CEN, European Committee for Standardization: Brussels, 2003.

[13] EN 1994-2. *Eurocode 4 – Design of Composite Steel and Concrete Structures – Part 2: General Rules and Rules for Bridges*. CEN, European Committee for Standardization: Brussels, 2005.

[14] Bro 2004. *Swedish Regulations for Bridges*. Swedish National Road Administration: Borlänge, 2004, (in Swedish).

PAPER III

Concrete shear keys in prefabricated bridges with dry deck joints

Robert Hällmark, Peter Collin and Martin Nilsson

Concrete shear keys in prefabricated bridges with dry deck joints

Robert Hällmark
M.Sc./Bridge Designer
LTU/Ramböll
Kyrkogatan 2, Box 850
SE – 971 26 Luleå
robert.hallmark@ramboll.se

Martin Nilsson
Ph.D.
Luleå University of Technology
SE – 971 87 Luleå
martin.c.nilsson@ltu.se

Peter Collin
Professor/Bridge Manager
LTU/Ramböll
Kyrkogatan 2, Box 850
SE – 971 26 Luleå
peter.collin@ramboll.se

ABSTRACT

A prefabricated concrete deck with dry joints between deck elements has been developed to make prefabricated bridges even more competitive. This type of bridge deck has been used on single span bridges in Sweden, and is now under development for multi span bridges. This paper describes how the deck system works. Results from laboratory tests of shear keys between deck elements are also presented together with an analysis comparing the predicted capacity with the measured failure load.

Key words: Bridge, prefabrication, element, dry joints, shear keys, laboratory tests.

1. INTRODUCTION

There is always a need to widen, build or rebuild bridges. To reduce the construction time and to minimize the impact on the traffic situation, prefabricated bridges can be used. Prefabricated steel girders are rather common but prefabricated concrete deck elements are still a rare exception. In order to make prefabricated bridges even more competitive, a deck of prefabricated concrete elements with dry joints between the elements has previously been developed. This system has been used on a few single span bridges in Sweden and is now under development for multi span bridges. The aim of the R&D project is to enable the use of dry joints between elements in multi span bridges without pre-tensioning. Particular attention has been paid to the ease of manufacturing, [1][2][3].

To transfer both lateral and vertical forces through the transverse joints, and to prevent vertical displacements between the deck elements at the joints, overlapping concrete keys are used. These keys are designed as a series of overlapping male-female connections along the joints, see Figure 1 and 2. In order to ensure a good accuracy of fit in the dry joint, the elements are match cast.
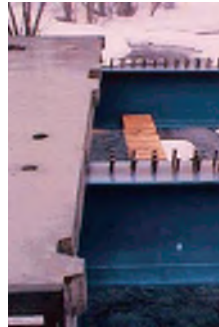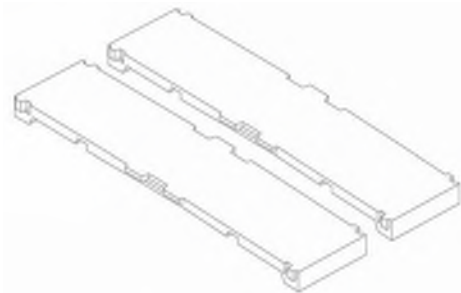

Figure 1 – 3D-sketch of two elements, illustrating the joint.   Figure 2 – Element during assembly

The theoretical distance between the transversal reinforcement bars in the concrete deck elements and the shear studs on the steel girders is limited, and the tolerances can be demanding since the overlapping concrete keys require a longitudinal displacement of the elements at the assembling. The displacement has to be at least the horizontal depth of the overlapping concrete keys plus the tolerances in the longitudinal direction of the bridge, see Figure 3. [2]
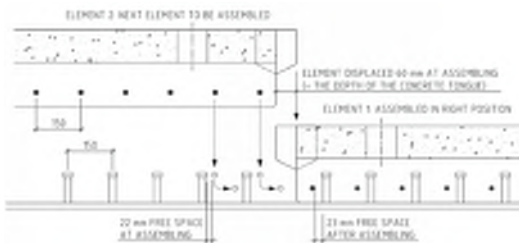

Figure 3 – Illustration of the limited tolerances. [2]

If possible, it would be preferable to use shear keys with smaller depth. However, the shear keys must be able to transfer the forces given in the design codes [4]. By using a FE-model of the bridge it can be shown that a maximum of about 40% of the traffic load acting on a single element is transferred through one of the joints. The rest of the load is transferred directly to the steel girders, or through the dry joint at the opposite side of the element. Therefore, the shear keys must be able to resist a load that is at least 40% of the design load given in the codes.

In order to find out how the shear keys transfer forces, and to be able to predict their strength and verifying the FE-model, laboratory tests have been performed.

2. Laboratory tests

Twelve static tests with three different layouts of the shear keys have been tested. The test set-up and the specimens are briefly described in the following sections.

2.1 Test set-up

The tests were focusing on pure shear capacity of the concrete keys. This means that no positive or negative effects were simulated, such as prestressing from the steel girders, or any misfit between the elements. A schematic and simplified sketch of the test set up is shown in Figure 4.
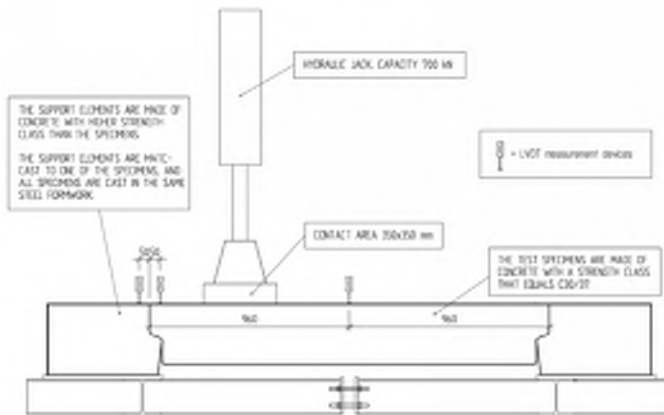

Figure 4 – Schematic and simplified sketch of the test set up.

The test specimens were placed in a test rig that consists of two concrete supports on top of a steel frame. The concrete support elements was match cast to one of the test specimens. All test specimens were made in the same steel formwork, and fitted well to the match cast supports. The supports were made in concrete with higher strength class (C40/50) than the specimens (C30/37). They were also heavily reinforced to avoid any failure in the support elements, and to make it possible to reuse them. The steel frame was used to keep the supports in the right positions and to make the demounting easier. The frame was constructed of HEA180 profiles. Figures 5 and 6 below show more detailed drawings of the support elements and the steel frame.

Before each the test was started, the bolt connections in the steel frame was tightened so that the frame could take care of the horizontal tensional forces that occurs due to the inclined contact surface in the shear keys. The bolts were tightened gently, aiming to get a remaining horizontal gap of ~0.5 mm at each shear key. The bolt connections were not used to clamp the specimen and the support elements together, giving a horizontal compressive force in the concrete.
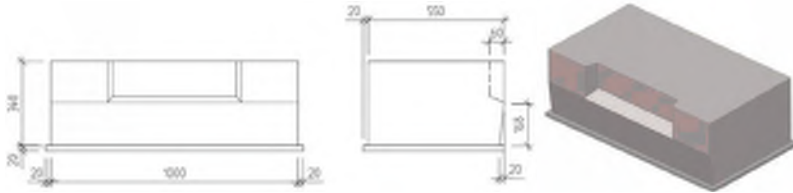
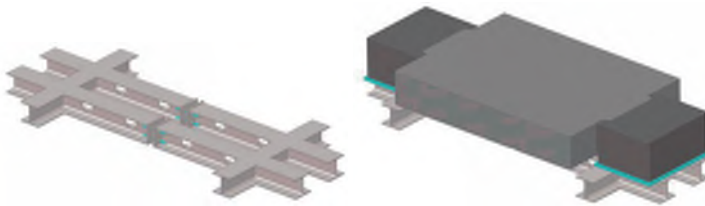*Figure 5 – Geometry drawings of support elements.*

Figure 6 – Illustration of test rig.

Each specimen had two shear keys that were tested under static load. The first shear key was tested until failure. After that, the hydraulic jack was moved to the opposite side of the specimen, and the second key was tested. When the second shear key was tested an extra vertical support was used, to make sure that the specimen was levelled horizontally and that the support area was uncracked, see Figure 7.
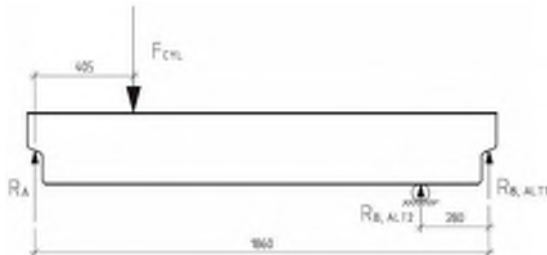

Figure 7 – Load situation with the extra support.

During the tests, data were recorded on 12 channels. Two channels were used to record the time elapsed and the load from the cylinder. The remaining ten channels were used to record deformations. Six measurement points were placed on top of the specimen. Three were placed on top of the support element and the last one was placed towards the floor measuring the reference deformation. The test set-up and the measurement devices are shown in Figure 8.

Figure 8 – Picture of test set-up.

2.2   Test specimens

The general geometry of the test specimens were 1.8×1.3 m, with a concrete shear key depth of 60 mm and a length of 540 mm, see Figure 9. The concrete strength in the specimens was aimed to be equal to strength class C30/37. For each specimen, six concrete cube tests were performed: 3 compressive and 3 tensile. The material test results are presented in Chapter 3.
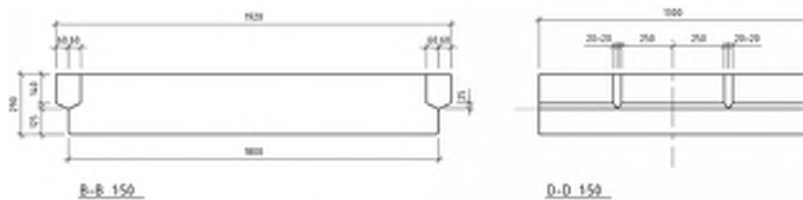

Figure 9 – General geometry of test specimens.

The first specimens (2 elements) were reinforced with exactly the same amount of reinforcement as used in deck elements in previously constructed single span bridges. In these specimens the shear keys were the same in both ends, shear key type 1. The second type of specimens (4 elements) had reduced shear key reinforcement in one of the shear keys, shear key type 2, compared to the first specimens. The other shear key, shear key type 3, was completely without reinforcement. With this design, four test results are gained for each type of shear key. Figures 10 and 11 show the reinforcement drawings of the specimens.
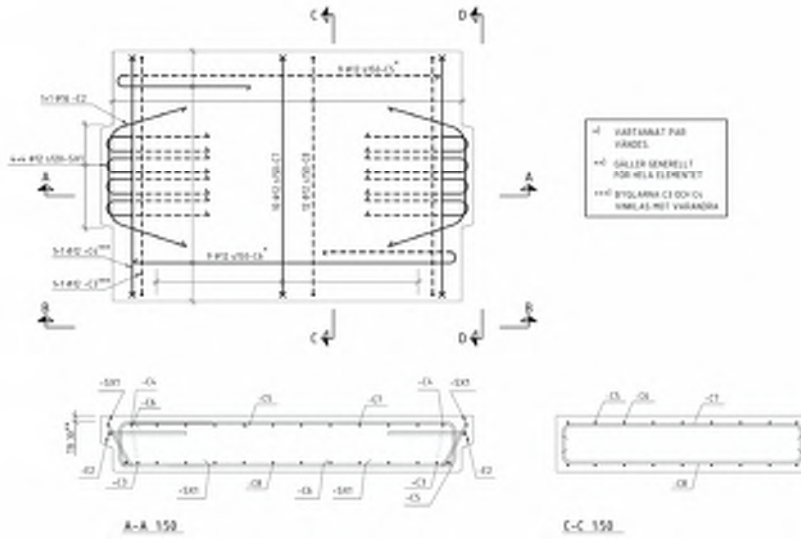
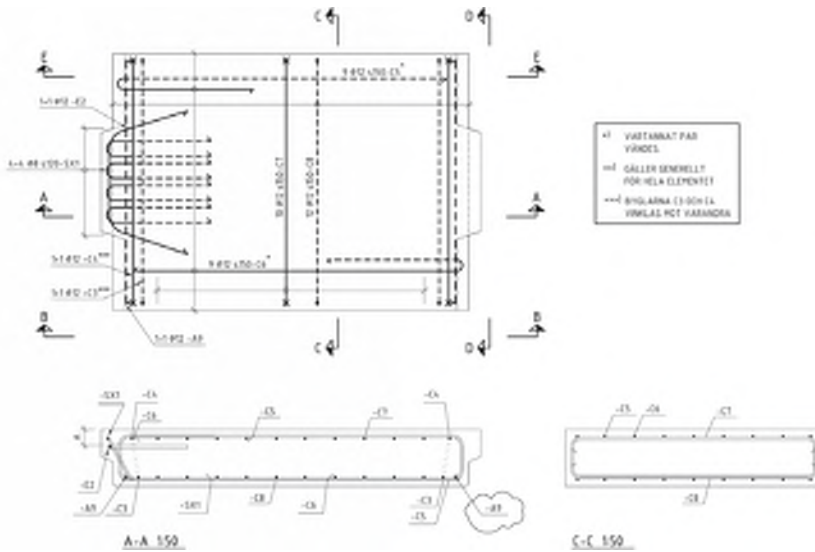*Figure 10 – Reinforcement drawing for specimens of type 1.*

Figure 11 – Reinforcement drawing for specimens of type 2.

3.   Results

3.1   Material tests

For each specimen, six cubes were cast out of the same concrete mix. Three of the cubes were used to determine the compressive strength and the other three were used to determine the tensile strength. The test cubes had the dimensions of 150×150×150 mm. The mean values for each specimen are presented in Table 1 below.

Table 1 – Concrete parameters.

Cast date	Test date	Age [days]	δ [kg/m³]	P_c [kN]	f_c [MPa]	P_{ct} [kN]	f_{ct} [MPa]	Specimen type
2010-03-15	2010-06-16	93	2334	1045	46.1	118	2.6	1
2010-03-16	2010-06-11	87	2345	1132	49.7	123	2.8	1
2010-03-18	2010-06-02	76	2372	1082	47.6	103	2.3	2
2010-04-07	2010-06-08	62	2330	967	42.6	94	2.1	2
2010-04-08	2010-06-11	64	2358	1009	44.5	115	2.6	2
2010-04-12	2010-05-31	49	2371	970	42.9	99	2.3	2

P_c = failure load, compressive test f_c = compressive strength
P_{ct} = failure load, splitting test f_{ct} = splitting tensile strength

3.2   Shear key tests

All tests were deformation controlled, with a stroke of 0.02 mm/s. Two different kinds of failures were observed when the reinforced shear keys were tested. Firstly, five of eight reinforced shear keys failed by cracks that activated the reinforcement, giving a ductile behaviour – failure type 1. The shear keys remained as one piece, but with some concrete crushing in the lower parts. Three specimen failed by cracks that were developed outside the reinforcement, resulting in a failure that separated the shear key from the rest of the specimen – failure type 2. This type of failure occurred under lower loads than the previously described failure.

Shear key type 1 – Ø12 reinforced (4 tests)
Two of four shear keys of type 1 resulted in failure type 1. The load-deformation curves from these two tests are shown in Figure 12 with solid lines, together with some photos of the failed shear keys, Figure 13.
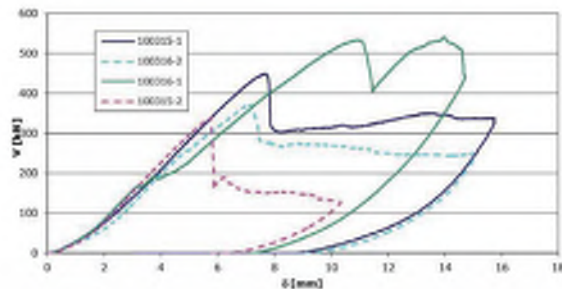

Figure 12 – Load-deformation curve for shear key type 1, failure type 1 (solid) and 2 (dashed).
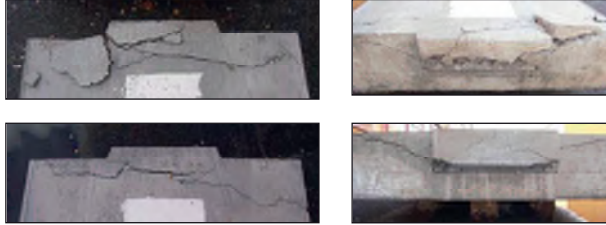
Figure 13 – Photos of shear key type 1 with a failure activating the reinforcement.

The last two specimens failed by cracks that developed outside the reinforcement, resulting in a failure that separated the shear key from the rest of the specimen. The load-displacement curves from these two tests are shown with dashed lines in Figure 12, together with some photos of the failed shear keys, see Figure 14.
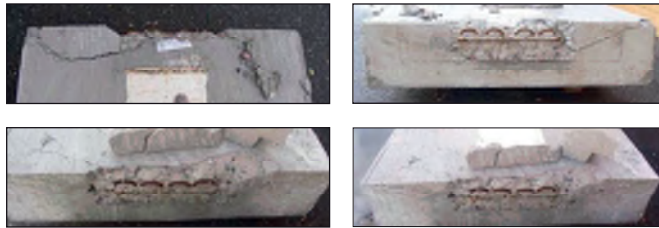

Figure 14 – Photos of shear key type 1 after failure in the concrete covering layer.

Shear key type 2 – Ø8 reinforced (4 tests)
The load-displacement curves from the tests are shown below together with some photos of the failed shear keys, see Figures 15 and 16.

Figure 15 – Load-displacement curve for shear key type 2.

Figure 16 – Photos of shear key type 2 after failure.

In one aspect, the results from these tests reminds of the tests of shear key type 1 – Ø12 reinforced, since three shear keys remains rather unaffected after cracking, and one shear key fail outside the reinforcement. The latter shows a very plastic behaviour before it finally fails in the concrete cover layer.

Shear key type 3 – unreinforced (4 tests)
The load-displacement curves from the tests are shown below together with some photos of the failed shear keys, see Figures 17 and 18.
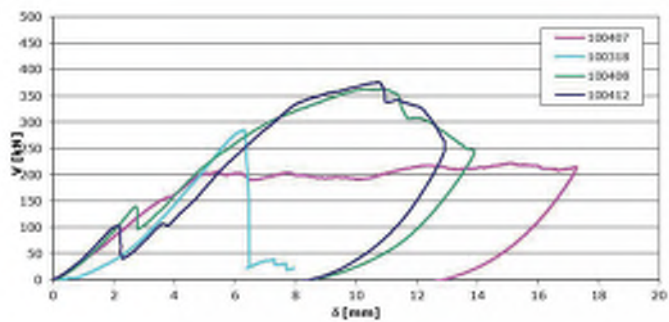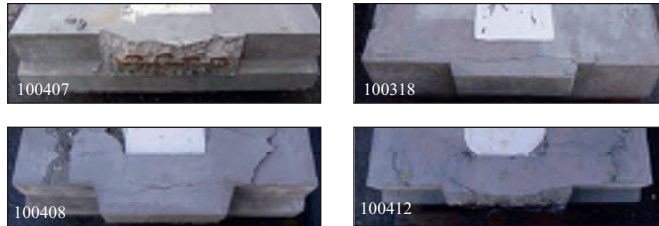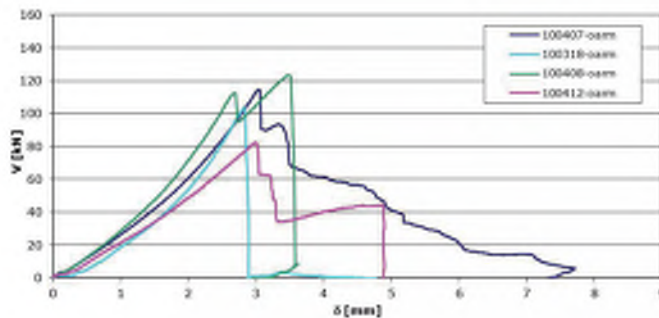

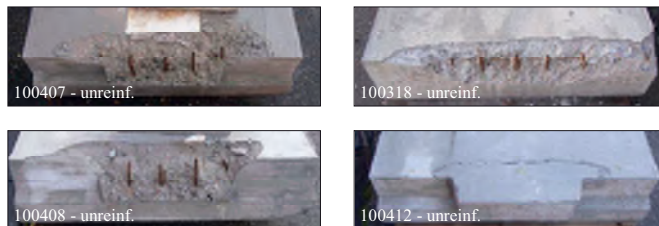*Figure 17 – Load-displacement curve for shear keys of type 3*

Figure 18 – Photos of shear-keys after failure.

4. Analysis

The strength of the shear keys has been estimated by using four different design models:
1. classical beam linear elastic analysis – shear key type 3 with failure type 2
2. Eurocode 2 – shear key type 1 and 2 with failure type 2 [6]
3. Eurocode 2 – shear key 1 and 2 with failure type 1 [6]
4. force equilibrium model

The material parameters from the test of concrete cubes are used to calculate the shear capacity for each shear key. The results from the design models are presented in Table 2.

1. Shear resistance for shear key type 3 with failure type 2

The shear resistance for failure type 2 in shear key type 3 without reinforcement can be estimated as, according to classic beam analysis and assuming that the shear strength is half the tensile strength [7],

$$V_{Rd,c} = \frac{2}{3} b_w h f_{shear} \approx \frac{1}{3} b_w h f_{ct} \tag{1}$$

where

b_w = 540 mm; the smallest width of the cross-section within the effective height

h = 165 mm; height of shear key

f_{ct} = is the splitting tensile strength of the concrete, see Table 1

2. Shear resistance for shear key type 1 and 2 with failure type 2 [5],

The shear resistance for failure type 2 can also be estimated by using formulas from [5],

$$V_c = b_w d f_v \tag{2}$$
$$f_v = 0.3 \cdot \xi \cdot (1 + 50\rho) f_{ct} \tag{3}$$
$$\rho = A_{s0} / (b_w \cdot d) \leq 0{,}02 \tag{4}$$

$\xi = 1.4$ when d ≤ 0.2 m

d = 140 mm

b_w = 540 mm

b_w the smallest width of the cross-section within the effective height

d   effective height

f_v shear strength of the concrete

f_{ct} tensile strength of the concrete

A_{s0} the smallest amount of bending reinforcement in the tensile part of the studied cross-section. This is set to 0, since there is no bending reinforcement in the shear key, only shear reinforcement.

3. Shear resistance for shear key 1 and 2 with failure type 1 [6],
This approach has been used on at least two bridges in Sweden, a bridge over Rokån and a bridge in Norrfors.

According to Eurocode 2 [6] the shear resistance for a section with inclined shear reinforcement is

$$V_{Rd,s} = \frac{A_{sw}}{s} z f_{ywd} \left(\cot\theta + \cot\alpha \right) \sin\alpha \qquad (5)$$

When shear reinforcement is used locally, with inclined rebars in one line (the –SX rebars), then the equation above can be simplified to

$$V_{Rd,s} = A_{sw} f_{ywd} \sin\alpha \qquad (6)$$

where

A_{sw} = is the area of the shear reinforcement

f_{yw} = 500 MPa, is the yield strength of the shear reinforcement

θ = is the angle of the shear crack (~45° observed in the test)

α = 60° is the inclination of the shear reinforcement

4. Force equilibrium model.
This model has been suggested, by Dr. Bo Westerberg (KTH, Stockholm), in order to describe the load carrying capacity in more detail. It is a force equilibrium model that involves both the reinforcement and compressive struts in the concrete, see Figure 19.
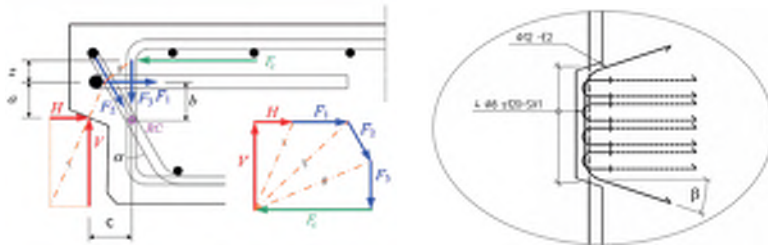
Figure 19 – Illustration of force equilibrium model and the notations.

The horizontal force H is believed to have great influence on the load carrying capacity. Without a compressive horizontal force, there is a risk for shear failure of the concrete cover at the edge of the shear key. The load carrying capacity is hard to predict in such a scenario, but it cannot be more than the shear strength of the concrete.

In the laboratory tests, the size of the force H is dependent on the shape of the supports, the rigidity of the test-rig etc. In a real bridge, this force will vary along the bridge and will depend on the global load situation as well as the local load situation.

Equilibrium equations:

$$\Sigma F \uparrow: \quad V - F_2 \cos\alpha - F_3 = 0 \tag{7}$$

$$\Sigma F \rightarrow: \quad H - F_c + F_2 \sin\alpha + F_1 = 0 \tag{8}$$

$$\Sigma M_{RC}: \quad V \cdot c + F_1 b + H(b-a) - F_c(b+z) = 0 \tag{9}$$

The load carrying capacity of the shear key can be estimated by using the maximum capacity of each rebar.

$$F_1 \le f_y A_{s1} \cos\beta \tag{10}$$

$$F_2 \le f_y A_{s2} \tag{11}$$

$$F_3 \le f_y A_{s3} \tag{12}$$

giving

Ø$_1$ = 12 mm

$$F_{1,max} = 500 \cdot 2 \frac{\pi \cdot 16^2}{4} \cdot \cos 18.5° = 191\,\text{kN}$$

$$F_{2,max} = 500 \cdot 8 \frac{\pi \cdot 12^2}{4} = 452\,\text{kN}$$

$$F_{3,max} = 500 \cdot 3 \frac{\pi \cdot 12^2}{4} = 170\,\text{kN}$$

Ø$_2$ = 8 mm

$$F_{1,max} = 500 \cdot 2 \frac{\pi \cdot 12^2}{4} \cdot \cos 18,5° = 107\,\text{kN}$$

$$F_{2,max} = 500 \cdot 8 \frac{\pi \cdot 8^2}{4} = 201\,\text{kN}$$

$$F_{3,max} = 500 \cdot 3 \frac{\pi \cdot 12^2}{4} = 170\,\text{kN}$$

As a first assumption the horizontal force, H, is set equal to zero. Then we assume that we are utilizing the shear reinforcement up to 100%. This gives the following result by Equation (7).

Ø$_1$ = 12 mm

$$V_{max} = 452 \cos 30° + 170 = 561\,\text{kN}$$

Ø$_2$ = 8 mm

$$V_{max} = 201 \cos 30° + 170 = 344\,\text{kN}$$

The moment equilibrium Equation (9) gives:

Ø$_1$ = 12 mm

$$F_c = \frac{561 \cdot 66 + 191 \cdot 65}{65 + 20} = 582\,\text{kN}$$

Ø$_2$ = 8 mm

$$F_c = \frac{344 \cdot 66 + 107 \cdot 65}{65 + 20} = 349\,\text{kN}$$

Assuming that the compressive strut in the concrete is developed over a height of 30 mm and the width of 540 mm, the compressive stress in the concrete can be calculated as:

Ø$_1$ = 12 mm

$\sigma_{Fc} = F_c/(w \cdot h)$

$\sigma_{Fc} = 582/(540 \cdot 30) = 35.9$ MPa

Ø$_2$ = 8 mm

$\sigma_{Fc} = F_c/(w \cdot h)$

$\sigma_{Fc} = 353/(540 \cdot 30) = 21.8$ MPa

These compressive stresses are below the compressive strengths that have been measured, and failures caused by concrete crushing could not be observed in the tests. The assumed distribution of forces in the rebars would be a possible solution according to this load model, resulting in yielding in the shear reinforcement. Anyhow, this is only one possible solution for this model, based on theoretical positions of the rebars. This load model should be calibrated to the test results, as should the influence of the horizontal force H. For example, frictional forces between the concrete surfaces will influence the result.

5. Test results vs. calculation models

Table 2 – Test results compared to results from calculation models.

Cast date 2010-	Test results V_{max} [kN]			Model 1 V_{max} [kN]				Model 2 V_{max} [kN]				Model 3 V_{max} [kN]				Model 4 V_{max} [kN]			
	Ø12	Ø8	-	Ø12	Ø8	-	η*	Ø12	Ø8	-	η*	Ø12	Ø8	-	η*	Ø12	Ø8	-	η*
03-15	449	-	-	80	-	-	5.61	84	-	-	5.36	392	-	-	1.15	561	-	-	0.80
03-15	337	-	-	80	-	-	4.21	84	-	-	4.03	392	-	-	0.86	561	-	-	0.60
03-16	532	-	-	83	-	-	6.41	88	-	-	6.07	392	-	-	1.36	561	-	-	0.95
03-16	370	-	-	86	-	-	4.30	88	-	-	4.22	392	-	-	0.94	561	-	-	0.66
03-18	-	285	-	-	68	-	4.19	-	73	-	3.88	-	174	-	1.64	-	344	-	0.83
03-18	-	-	104	-	-	68	1.53	-	-	73	1.42	-	-	0	-	-	-	0	-
04-07	-	222	-	-	63	-	3.52	-	67	-	3.30	-	174	-	1.28	-	344	-	0.65
04-07	-	-	114	-	-	63	1.81	-	-	67	1.70	-	-	0	-	-	-	0	-
04-08	-	363	-	-	77	-	4.71	-	82	-	4.42	-	174	-	2.09	-	344	-	1.06
04-08	-	-	123	-	-	77	1.60	-	-	82	1.50	-	-	0	-	-	-	0	-
04-12	-	376	-	-	68	-	5.53	-	71	-	5.30	-	174	-	2.16	-	344	-	1.09
04-12	-	-	82	-	-	68	1.21	-	-	71	1.16	-	-	0	-	-	-	0	-

* η = test result divided by the predicted value for the given calculation model.

According to the result presented in Table 2, calculation model 1 and 2 can be useful to estimate the strength for a shear key without reinforcement. The design values are on the safe side with a safety factor from 1.16 – 1.81. Model 3 gives results that are on safe side except for the failures in the concrete cover for test specimen type 1. With the assumptions made, design model 4 is the same as model 3, except the fact that model 4 makes the vertical reinforcement bars in the slab active. The result is often on the unsafe side, which could indicate that the vertical rebars does not influence the load carrying capacity as much as assumed in the calculations. This model needs to be studied more detailed, calibrated to the test results and maybe modified.

One thing that can be noted is that the shear keys that fail in the concrete covering layer still transfer forces that are far higher than the capacity of the concrete itself. Therefore, the reinforcement must have been activated, and should be included in the design formula in one way or another.

6. Conclusions

The results from the tests have a considerable scatter. Still some interesting points can be noted. Firstly, the tests show that unreinforced concrete can not transfer the design shear forces, caused by the vehicle models in Eurocode, from one element to another. This was an expected result, in line with the result from the calculations. However, in the reality we believe that the shear keys can transfer a higher load since the surrounding elements will deflect together with the loaded element, which probably gives longitudinal compressive forces which would counteract the tensile stresses that occurs due to the shear forces.

Secondly, the load carrying capacity of the previously used shear keys seems to be larger than necessary, especially if we can avoid a failure that is developed by a crack growing through the concrete covering. The shear keys with less amount of reinforcement (Ø8mm) are still strong enough to carry the load. However, we suggest some changes in the shear key reinforcement since we see some potential improvement. Two new reinforcement layouts are presented in Figure 18. In both cases the concrete cover layer has been reduced. In the left case, additional reinforcement have been added (-E8), and in the right case the SX-rebars have been replaced by EX-rebars. The geometry of the EX- and SX- rebars can be seen in Figure 10 and 20. By using stainless steel in some of the rebars in the shear keys, it would be possible to decrease the thickness of the concrete covering layer, and hopefully avoid a failure in the covering layer.
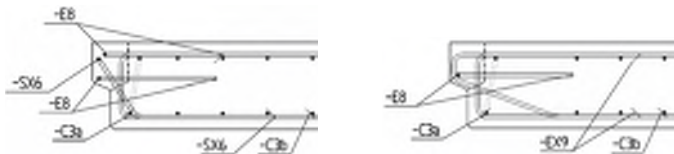
Figure 20 – Illustration of two suggested reinforcement layouts.

REFERENCES

1. Hällmark, R., Collin, P & Nilsson M., "Prefabricated composite bridges," Proceedings, IABSE Symposium, Bangkok, Thailand, Sept. 2009, Vol. 96, pp. 282-283.
2. Hällmark, R., Collin, P & Stoltz A., "Innovative Prefabricated Composite Bridges," Structural Engineering International, 2009, Vol. 19, no:1, pp. 69-78.
3. Collin et al., "International workshop on prefabricated composite bridges", March 4th 2009, Stockholm, ISBN: 1402-1536.
4. EN 1991-2, Eurocode 1 – Actions on structures - Part 2: Traffic Loads on Bridges. CEN, European Committee for Standardization: Brussels, 2005.
5. BBK04, Swedish Concrete Regulations, Boverket, Karlskrona, 2004.
6. EN 1992-1-1, Eurocode 2 – Design of concrete structures, Part 1: General rules and rules for buildings. CEN, European Committee for Standardization: Brussels, 2004.
7. Betonghandboken – Konstruktion, Ch. 3.7:2, AB Svensk Byggtjänst, Stockholm.

PAPER IV

The Behaviour of a Prefabricated Composite Bridge with Dry Deck Joints

Robert Hällmark, Peter Collin and Mikael Möller

The Behaviour of a Prefabricated Composite Bridge with Dry Deck Joints

Robert Hällmark, Civil Eng., **Peter Collin,** Professor, Luleå University of Technology, Ramøll, Sweden; **Mikael Möller,** Professor, Luleå University of Technology, Helsingborg, Sweden. Contact: robert.hallmark@ramboll.se

Abstract

This paper describes the monitoring of a one-span composite bridge in northern Sweden. The bridge was built in 2000, with prefabricated deck elements connected to steel girders, and the back walls as well as the piers were also prefabricated. The monitoring was required to clarify the doubts regarding whether a bridge with dry deck joints can be expected to perform as a conventional composite bridge, with *in situ* cast deck and sections with sagging moments. To get a better understanding of the long-term structural behaviour, the bridge was monitored both during 2001 and 2011, instrumented with equipment measuring the deflections and strains in the steel cross section. The bridge was loaded with a truck in midspan having a total weight of 25 t. When the truck was centred between the girders, the results showed a symmetric behaviour, with respect to deflections and stresses. For the case with the truck stationed right above one of the steel girders, anti-symmetric behaviour was observed and studied by means of finite element calculations, taking into account the stiffness of the composite section as well as the end screens and the earth pressure below them.

Keywords: composite bridge; prefabrication; deck elements; dry joints; monitoring.

Introduction

Composite bridges have the benefit that the steel section can carry the formwork and the wet concrete without the need for temporary supports. This makes this type of bridge highly suitable for water crossings and for bridges spanning existing roads, railways, and so on. Currently, much of the bridges are built in urban areas where congestion is a growing problem. The total construction cost of a bridge in such an area should be based not only on the cost of material and labour but also on the cost of the traffic disturbance. If this is done, solutions with high degree of prefabrication and short assembly times will be achieved. One way of increasing the degree of prefabrication is to use not only prefabricated steel girders but also prefabricated concrete deck elements.[1]

Since the late 1990s, a solution featuring concrete deck elements with dry joints has been developed in Sweden.

The joints are totally dry and transfer shear forces by overlapping shear keys (see *Fig. 1*). Longitudinal compressive forces are transferred by the contact pressure in the concrete surfaces at the transverse joints. In case of tensional forces, the steel section is designed to take the whole load, because there is no reinforcement going through the joints. This type of structure is described in more detail in Ref. [2].

A bridge deck of composite type is well suited for single-span bridges with mostly compressive forces in the concrete deck. Nevertheless, laboratory tests indicated that it would not be a problem to use this type of deck on multispan bridges as well, with regard to ultimate strength of the shear keys and shear key fatigue resistance.[2,3] In such a case, the requirement on the water insulation as well as the pavement should be specified according to the estimated joint openings.

During the development process, questions were raised whether this type of structure behaves as a fully composite section. To get better understanding of the composite action in a real structure, a single-span bridge with dry joints has been monitored. This study includes field monitoring done in years 2001 and 2011, as well as a finite element

(FE) analysis of the bridge. The results are also compared to the design calculations of the bridge, which were based on the beam theory.

This paper focuses on the stiffness behaviour of the superstructure, especially the interacting concrete area. In the design stage, this area was estimated according to Ref. [4]. *Figure 2* illustrates how the stress is modelled as concentrated into blocks, instead of the real distribution caused by the shear lag phenomenon. Equation 1 shows how the effective flange width is calculated in midspan sections. The equivalent span length, L_e, is set to $0{,}7L$, where L is span length and L_e is the equivalent span width.

$$b_{eff} = b_0 + \sum b_{ei} \quad \text{if} \quad b_{ei,max} \le L_e/8$$
$$\text{else } b_{ei} = L_e/8 \qquad (1)$$

There are, however, reasons to believe that a bridge with dry deck joints will behave differently, at least at moderate load levels, than a conventional composite bridge with an *in situ* cast concrete deck. The gaps in the joints are kept as small as possible by using match casting and limited tolerances that are regulated by a control programme. Nevertheless, there will always be gaps in the joints that have to be closed before the prefabricated deck elements can transfer compressive forces as effectively as an *in situ* cast deck slab. Thus, the formulas for the effective flange width might not be correct in serviceability limit state (SLS) for a bridge of this kind.

Rokån Bridge

In the year 2000, a single-span composite bridge having a prefabricated deck with dry joints was built in northern Sweden. The bridge was constructed to replace an old bridge over the stream Rokån. The project was very successful and the bridge could be replaced with minimum traffic disturbance. The road was closed for just 30 h before it was reopened for traffic over the new bridge.[2]
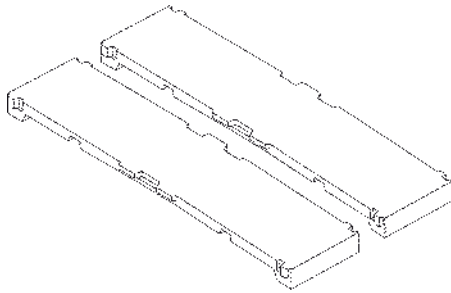
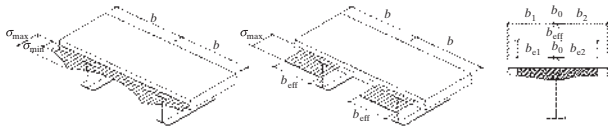*Fig. 1: Schematic drawing of two concrete deck elements with dry joints*

Fig. 2: Stress distribution caused by shear lag, and definition of effective flange width, b_{eff}
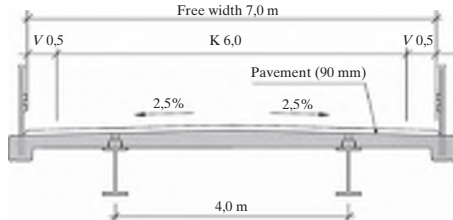

Fig. 3: Cross section drawing of Rokån Bridge

The superstructure is made of two I-girders and has a span length of 16,2 m (see *Fig. 3*). The bridge has prefabricated back walls connected to the ends of the steel girders. This gives extra rotational stiffness at the girder ends, which is generally neglected in bridge design.

Steel Girders

The bridge consists of two steel I-girders with the dimensions as shown in *Fig. 4*. As the bridge length is rather short, each steel girder is made as a single piece without any transversal joint. The web and the upper flange are made of S355J2G3 steel and the bottom flange is made of S460M. The real material properties have not been investigated. All material parameters have been taken from Ref. [5].

Concrete Deck

The concrete deck consists of eight deck elements, each with a length of 1,8 m, made of concrete of strength
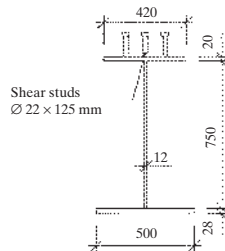

Fig. 4: Steel section (unit mm)

class C30/37. The dimensions of the deck slab are presented in *Fig. 5*. The deck elements were all precast in a concrete workshop and transported to

the bridge site on trucks, and each element had a weight of 9,0 t. In addition to the deck elements, the back walls and the wing walls were also precast as one unit. The reinforcement was mainly of grade B500B (f_y = 500 MPa), with the exception of the transversal reinforcement at the top surface, which was of grade K600S (f_y = 600 MPa).

Monitoring

In the spring of 2001, field tests were performed with a loaded truck, and global deflections as well as strains in the steel flanges were measured. Again in the spring of 2011, the bridge was monitored in order to study if and how the behaviour had changed after 10 years.

Test Setup

The same test setup was used in years 2001 and 2011. The deflections were measured with LVDT gauges at three positions on each girder, in the middle of the bridge (δ_3 and δ_4) and at the supports (δ_1, δ_2, δ_5 and δ_6; see *Fig. 6*). The steel strains were measured at the bottom of the top flange and at the top of the bottom flange, in three sections. With the origin at midspan, the studied sections were located at x = 0,200 m, 0,900 m and 7,175 m (see *Fig. 6*); 7,175 m from the centre line corresponds to 0,925 m from the abutment.

The strain gauges were glued to the flanges at the same positions as during the monitoring in the year 2001. The first section was located 0,200 m away from midspan and the second 0,900 m from midspan. The latter position was chosen because it coincides with a deck joint, and the first position was chosen because it is near the middle of an element. As there are web stiffeners at midspan, the strain gauges were moved 0,200 m in order to avoid measuring a disturbed longitudinal stress state. The third section that was monitored is located 0,925 m from a support section. This section was monitored in order to get an estimation of the degree of restraint at the end of the steel girder.

Vehicle Loads

The loading of the bridge was performed in a similar way in both tests. The following two sections specify the
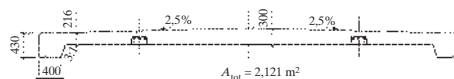

Fig. 5: Concrete deck slab dimensions (unit mm)

loads and the load positions in detail. In both cases, the axle loads were scaled before the test started. During the measurements, the vehicle always moved from left to right (shown in *Fig. 6*).

Test 2001

The bridge was loaded with a truck with three axels (see *Fig. 8*). During each test, the vehicle stopped in three positions. In each position, one of the axles was at midspan. The vehicle position in the transversal directions was also varied. The vehicle was positioned right above both girders and also along the centreline of the bridge.[6]

Test 2011

The bridge was loaded with a truck with three axels (see *Fig. 7*). During each test, the vehicle stopped in two positions. First with the front axle at the midspan and second with the bogie

centred at the midspan. The vehicle position in the transversal directions was also varied. The vehicle was positioned right above both girders and also along the bridge centreline.

Results

In the sections below, the results from the latest test are presented in detail, together with more summarized results from the earlier test.

Deflections

The presented deflections are all midspan deflections that have been compensated for the vertical deformations at the supports according to the equations below.

$$\delta_{G1} = \delta_3 - 0{,}5 \cdot (\delta_1 + \delta_5) \qquad (2)$$
$$\delta_{G2} = \delta_4 - 0{,}5 \cdot (\delta_2 + \delta_6) \qquad (3)$$

Test 2011—Load Centred above Steel Girders. In the case with the truck

load centred above girder 1 (Test 1), the measured deflections were 3,3 mm when the front load was in midspan and 4,1 mm when the bogie was in midspan (see *Fig. 9*). In the same figure, Test 2 is also plotted, showing the situation when the same load is centred above girder 2. The deflections are in line with the results from Test 1, ±0,1 mm.

Test 2011–Load Centred along the Centreline between the Girders. The results from Test 3 with the centred truck load are presented in *Fig. 10*. The bridge shows a very symmetric behaviour with the same deflection in both girders. The deflections were 2,0 mm when the front axis was in midspan and 2,6 mm when the bogie was in midspan.

Tests 2001 and 2011—Summarization of the Deflections. The deflections measured in 2001 are summarized in *Table 1*. The deflections measured in 2011 are also presented in the same table as a comparison.

Steel Stresses

The measured steel strains have been transformed into stresses by assuming $E_{steel} = 210$ GPa.

2011—Load Centred above Steel Girders. The steel stresses in a section 0,200 m
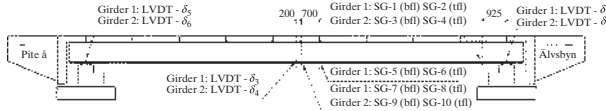
Fig. 6: Positions of the measuring devices on Rokån Bridge (unit mm)

Load position:

LP 1: Centred along one of the girders, axel 1 at midspan.
LP 2: Centred along one of the girders, bogie centre at midspan.
LP 3: Centred between the girders, axel 1 at midspan.
LP 4: Centred between the girders, bogie centre at midspan.

$F_{axel1} = 85{,}4$ kN $F_{axel2} = 82{,}3$ kN $F_{axel3} = 82{,}3$ kN
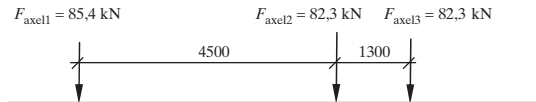
Fig. 7: Truck load and positions that were used in the test performed in 2011 (mm)

Load position:

LP 1: Centred along one of the girders, axel 1 at midspan.
LP 2: Centred along one of the girders, axel 2 at midspan.
LP 3: Centred along one of the girders, axel 3 at midspan.
LP 4: Centred between the girders, axel 1 at midspan.
LP 5: Centred between the girders, axel 2 at midspan.
LP 6: Centred between the girders, axel 2 at midspan.

$F_{axel1} = 75{,}5$ kN $F_{axel2} = 93{,}7$ kN $F_{axel3} = 80{,}9$ kN
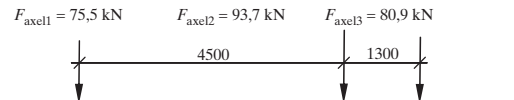
Fig 8: Truck load and positions that were used in the test performed in 2001 (mm)
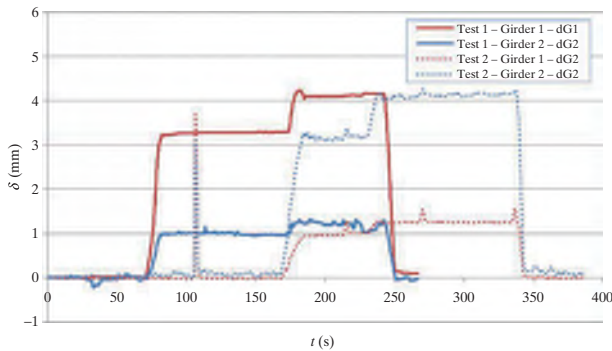
Fig. 9: Measured deflections with the truck centred above girder 1 and girder 2, respectively
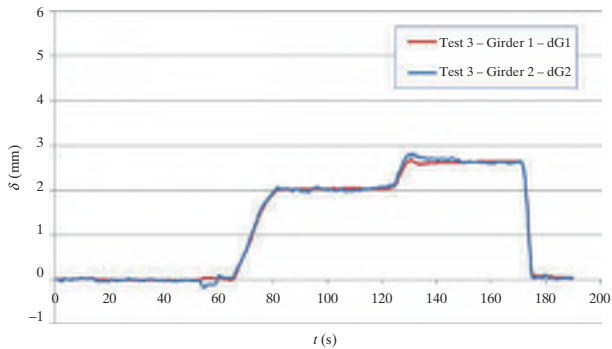
Fig. 10: Measured deflections with the truck centred between the girders

Year	Test 1			Test 2			Test 3		
2001	LP1	LP2	LP3	LP1	LP2	LP3	LP4	LP5	LP6
δ_{G1} (mm)	3,4	—	4,4	1,3	1,8	1,7	2,3	3,2	3,1
δ_{G2} (mm)	1,3	—	1,7	3,3	4,5	4,3	2,3	3,2	3
Year	Test 1		Test 2		Test 3				
2011	LP1	LP2	LP1	LP2	LP3	LP4			
δ_{G1} (mm)	3,3	4,1	1	1,3	2	2,6			
δ_{G2} (mm)	1,0	1,3	3,2	4,1	2	2,6			

Table 1: Measured deflections at midspan; LP = load position

away from the midspan are presented graphically in *Fig. 11*. The largest difference between the measured stresses in Tests 1 and 2 was less than 1 MPa.

2011—Load Centred along the Centreline between the Girders. The results from Test 3 with the centred truck load are presented in *Fig. 12*. The presented stresses were measured in a section 0,200 m from midspan.

Tests 2001 and 2011—Summarization of the Stresses. The stresses measured

in 2001 and 2011 are summarized in *Table 2*. Unfortunately, the only stresses that have been saved from the test in 2001 are the ones in the bottom flange at section $x = 0,200$ m, which is given in Ref. [6].

Analysis

The results from the measurements have been compared to different design models. First, a simplified beam model

by which this bridge was originally designed. Second, a more detailed FE analysis including the back walls and the restraint from the soil. All material parameters have been taken from Refs [5,9].

Design Models

Beam Model

In the simplified beam model, the bridge is regarded as simply supported and the girders are separated in the analysis. Because of the symmetry, half of the deck slab is assumed to contribute to the stiffness of each composite girder. The loads are then distributed between the girders depending on the location of the load resultants, in the transverse direction. This gives a load factor of 0,5 when the truck is standing right between the girders and a factor of 1,0 (respectively 0,0) when the truck is standing right above one of the girders.

The cross-sectional parameters have been calculated according to Refs [4,5,8], taking into consideration shear lag and local buckling. There is no reduction of the steel cross section, but the width of the interacting concrete is reduced from 3,355 to 2,873 m in the field section. In *Fig. 13*, the interacting part of the concrete is hatched. This figure also presents some of the important cross-sectional parameters.

FE-model

The bridge superstructure has been modelled with shell elements. The steel–concrete connection was modelled as fully composite, assuming no shear connection deformations.

The bridge has been modelled in three different ways, first without back walls, second with back walls and third with crushed rocks as backfill behind the back walls. In the last model, the crushed rocks are modelled with an elastic modulus of 50 MPa. The soil is modelled by volumetric elements with a depth of 1,0 m. One side of these elements is attached to the back walls and the other side is locked from longitudinal displacements. The three FE models are FEM-1, FEM-2 and FEM-3, and all are illustrated in *Fig. 14*.

In a simple design calculation (the beam model), the positive contribution from the edge beams is neglected. The FE analysis is, however, done in order to describe the reality as effectively as possible, and the edge beams are therefore included.
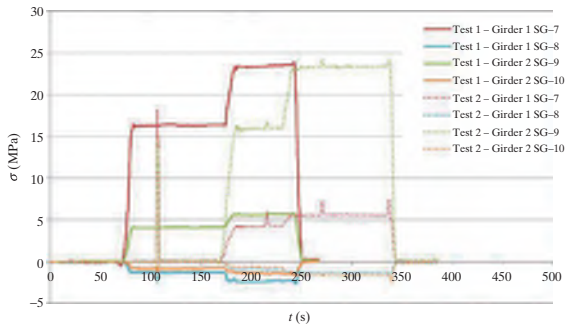
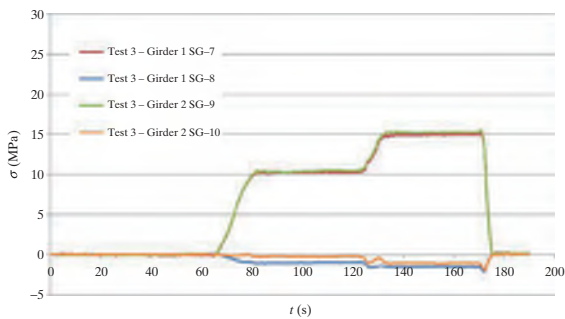*Fig 11: Measured stresses in Tests 1 and 2; 0,200 m from midspan*

Fig. 12: Measured stresses in Test 3; 0,200 m from midspan

Year		Test 1			Test 2			Test 3		
2001	x (m)	LP1	LP2	LP3	LP1	LP2	LP3	LP4	LP5	LP6
σ_{SG-7} (MPa)	0,2	18,2	–	26,6	5,0	7,6	7,4	11,6	17,5	17,0
σ_{SG-9} (MPa)	0,2	4,9	–	6,8	17,2	26,3	25,6	11,6	17,5	16,7
Year		Test 1		Test 2		Test 3				
2011	x (m)	LP1	LP2	LP1	LP2	LP3	LP4			
σ_{SG-7} (MPa)	0,2	16,3	23,4	4,3	5,6	10,3	14,8			
σ_{SG-8} (MPa)	0,2	−1,3	−2,4	−0,9	−1,3	−1,0	−1,5			
σ_{SG-9} (MPa)	0,2	4,1	5,6	16,0	23,3	10,5	15,2			
σ_{SG-10} (MPa)	0,2	−0,8	−1,4	−0,6	−1,5	−0,3	−1,0			
Year		Test 1		Test 2		Test 3				
2011	x (m)	LP1	LP2	LP1	LP2	LP3	LP4			
σ_{SG-5} (MPa)	0,9	14,7	23,1	3,9	5,5	9,0	14,2			
σ_{SG-6} (MPa)	0,9	−1,9	−1,5	−0,7	−1,2	−1,0	−0,9			
Year		Test 1		Test 2		Test 3				
2011	x (m)	LP1	LP2	LP1	LP2	LP3	LP4			
σ_{SG-1} (MPa)	7,175	−7,4	−7,2	−1,2	−0,9	−3,9	−3,6			
σ_{SG-2} (MPa)	7,175	0,8	0,8	0,0	−0,2	0,4	0,1			
σ_{SG-3} (MPa)	7,175	−1,4	−1,0	−7,0	−6,9	−4,3	−3,9			
σ_{SG-4} (MPa)	7,175	0,1	−0,1	0,5	0,7	0,4	0,1			

Table 2: Measured stresses

Deflections

If the measured deflections are compared to the theoretical deflections of a simply supported I-girder, the measured deflections are significantly smaller than the calculated deflections (see *Table 3*). This is quite expected, because the torsional/warping stiffness of the superstructure will distribute a part of the moment to the other girder. The back walls will also give an extra rotational stiffness at the end of the steel girders. These two factors are often neglected in the design of a bridge of this type.

The FE models confirm that the back walls will contribute to the distribution of the deflections, if the bridge is loaded unsymmetrically. However, the effect from the back walls appears to be quite small. If the load is centred above one of the girders, the deflection in the most loaded girder will decrease by approximately 4% when the back walls are included in the analyses (FEM-1 vs. FEM-2). Torsional and warping stiffness of the superstructure itself appears to be the major reason for the distribution of the load, and the effect from the cross-beams is negligible.

The results presented in *Table 3* show that the beam model is very conservative, so are the FE models that do not include the soil stiffness. FEM-3, which is the only model that includes the soil stiffness, is the model that corresponds best to the reality. The results from 2001 indicate a somewhat stiffer behaviour than the measurements. The results from 2011 are very close to the deformations predicted by FEM-4. Thus, the deflection due to the traffic load is somewhat lower in 2011 than in 2001.

The soil model is quite simple, and the soil properties are a possible source of error. As no field measurement of the soil properties was done, tabled values have been used.

Stresses

The measured stresses have been compared to the calculated stresses according to the beam model as well as the FE analysis. Some of the measured stresses at the two midspan sections are presented in *Table 4*.

As expected, FEM-3 is the model that describes the reality best. The measured stresses are very close to the predicted stresses according to FEM-3, if the support section (*x* = 7,175) is
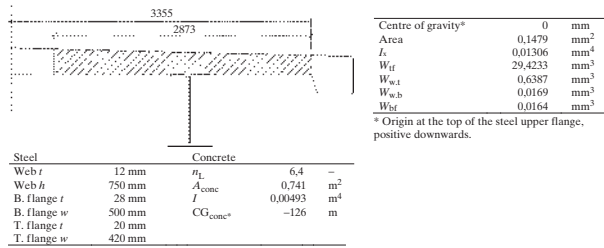
Centre of gravity*	0	mm
Area	0,1479	mm²
I_x	0,01306	mm⁴
W_{tf}	29,4233	mm³
$W_{w.t}$	0,6387	mm³
$W_{w.b}$	0,0169	mm³
W_{bf}	0,0164	mm³

* Origin at the top of the steel upper flange, positive downwards.

Steel			Concrete		
Web t	12	mm	n_L	6,4	–
Web h	750	mm	A_{conc}	0,741	m²
B. flange t	28	mm	I	0,00493	m⁴
B. flange w	500	mm	CG_{conc*}	−126	m
T. flange t	20	mm			
T. flange w	420	mm			

Fig. 13: Cross-sectional parameters for the beam model, assuming short-term loading
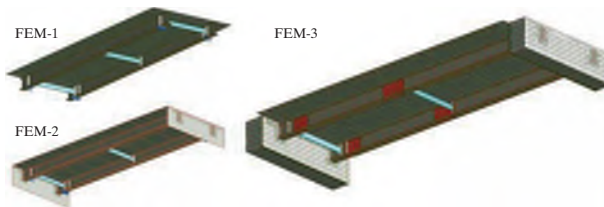

Fig. 14: Illustration of the three FE models

excluded. The stress distribution in this section is totally different compared with the measured distribution. However, the supports are modelled with no friction at all in the bearings; hence all four bearings are free to move in the longitudinal direction. If the supports in one end of the bridge are modelled as fixed or with frictional supports, the stress distribution in FEM-3 will

correspond rather well to the observed distribution, as well as to the absolute stress values.

Table 4 presents stress values at the midspan of an element and at a joint. When the two sections are compared, no significant differences in the position of the neutral bending axis can be observed. This indicates that the

interacting concrete area does not vary over an element in compression.

An interesting observation concerning the stresses is that the measured position of the neutral bending axis is situated slightly lower, compared to the position in the design models. In all design models, the neutral bending axis is positioned near the top of the upper flange. In reality, it appears to be positioned approximately 60 to 100 mm down from the top of the upper flange in the most loaded girder and approximately 140 to 180 mm in the other girder. If the load is centred between the girders, the neutral axis tends to be in the former interval.

The measured steel stresses can be used to estimate the interacting concrete area. The difference between the tensional and the compressive forces in the steel corresponds to the force taken by the concrete.

$$\sum F \rightarrow: \quad F_{steel.comp.} + F_{steel.tens.} + F_{conc.} = 0 \quad (4)$$

Assuming a linear stress distribution over the cross section, the force in the concrete can be calculated as follows:

$$F_{conc.} = -\left(\sigma_{bfl.m} \cdot t_{bfl} \cdot w_{bfl} + \frac{\sigma_{w.b}}{2} \right.$$
$$\cdot t_w (h_w - e_{neutral} + t_{tfl}) + \sigma_{tfl.m} \cdot t_{tfl} \cdot w_{tfl}$$
$$\left. + \frac{\sigma_{w.t}}{2} \cdot t_w (e_{neutral} - t_{tfl}) \right) \quad (5)$$

$F_{steel.comp.}$ = compressive normal force in the steel, $F_{steel.tens.}$ = tensile normal

Test 2001						Test 2011					
Load pos. 1	**Test**	**BM**	**FEM-1**	**FEM-2**	**FEM-3**	*Load pos. 1*	**Test**	**BM**	**FEM-1**	**FEM-2**	**FEM-3**
δ_3 (mm)	3,3	5,4	4,2	4,0	3,4	δ_3 (mm)	3,3	5,4	4,2	4,0	3,3
δ_4 (mm)	1,3	0,0	1,6	1,8	1,0	δ_4 (mm)	1,0	0,0	1,6	1,8	1,0
Load pos. 2	**Test**	**BM**	**FEM-1**	**FEM-2**	**FEM-3**	*Load pos. 2*	**Test**	**BM**	**FEM-1**	**FEM-2**	**FEM-3**
δ_3 (mm)	4,5	7,1	5,4	5,3	4,5	δ_3 (mm)	4,1	6,6	5,1	4,9	4,2
δ_4 (mm)	1,8	0,0	2,2	2,4	1,3	δ_4 (mm)	1,2	0,0	2,0	2,2	1,2
Load pos. 3	**Test**	**BM**	**FEM-1**	**FEM-2**	**FEM-3**	*Load pos. 3*	**Test**	**BM**	**FEM-1**	**FEM-2**	**FEM-3**
δ_3 (mm)	4,3	6,5	5,0	4,9	4,2	δ_3 (mm)	2,0	2,7	2,9	2,9	2,1
δ_4 (mm)	1,7	0,0	2,1	2,3	1,2	δ_4 (mm)	2,0	2,7	2,9	2,9	2,1
Load pos. 4	**Test**	**BM**	**FEM-1**	**FEM-2**	**FEM-3**	*Load pos. 4*	**Test**	**BM**	**FEM-1**	**FEM-2**	**FEM-3**
δ_3 (mm)	2,3	2,7	2,9	2,9	2,1	δ_3 (mm)	2,7	3,3	3,5	3,5	2,7
δ_4 (mm)	2,3	2,7	2,9	2,9	2,1	$\delta 4$ (mm)	2,7	3,3	3,5	3,5	2,7
Load pos. 5	**Test**	**BM**	**FEM-1**	**FEM-2**	**FEM-3**						
δ_3 (mm)	3,2	3,5	3,8	3,8	2,8						
δ_4 (mm)	3,2	3,5	3,8	3,8	2,8						
Load pos. 6	**Test**	**BM**	**FEM-1**	**FEM-2**	**FEM-3**						
δ_3 (mm)	3,0	3,3	3,5	3,5	2,6						
δ_4 (mm)	3,0	3,3	3,5	3,5	2,6						

Table 3: Test results compared to results from calculation models

x = 0,200 m LP 2		Measured	BM	FEM-1	FEM-2	FEM-3
Girder 1 — SG 8	σ_{tfl}	−2,4	1,2	0,3	0,3	2,4
Girder 1 — SG 7	σ_{bfl}	23,4	43,5	31,2	30,3	24,3
Girder 2 — SG 10	σ_{tfl}	−1,4	0,0	1,0	1,1	0,5
Girder 2 — SG 9	σ_{bfl}	5,6	0,0	12,2	13,1	6,6
x = 0,2 m LP 4		**Measured**	**BM**	**FEM-1**	**FEM-2**	**FEM-3**
Girder 1 — SG 8	σ_{tfl}	−1,5	0,6	0,7	0,4	1,6
Girder 1 — SG 7	σ_{bfl}	14,8	21,7	21,3	21,3	15,5
Girder 2 — SG 10	σ_{tfl}	−1,1	0,6	0,7	0,7	1,6
Girder 2 — SG 9	σ_{bfl}	15,2	0,6	21,3	21,3	15,5
x = 0,9 m LP 2		**Measured**	**BM**	**FEM-1**	**FEM-2**	**FEM-3**
Girder 1 — SG 6	σ_{tfl}	−1,5	1,1	0,1	0,1	2,6
Girder 1 — SG 5	σ_{bfl}	23,0	42,0	29,6	28,7	23,5
x = 0,9 m LP 4		**Measured**	**BM**	**FEM-1**	**FEM-2**	**FEM-3**
Girder 1 — SG 6	σ_{tfl}	−0,9	0,6	0,6	0,3	1,5
Girder 1 — SG 5	σ_{bfl}	14,2	21,0	20,7	20,8	14,9

Table 4: Test results from year 2011 vs. design models for section x = 0,200 and 0,900 m (MPa)

x = 0,2 m		Test 1		Test 2		Test 3		
		LP1	LP2	LP1	LP2	LP3	LP4	
Girder 1	$A_{int.conc}$	0,379	0,342	0,225	0,209	0,35	0,343	(m²)
	n_{ratio}	0,51	0,46	0,30	0,28	0,47	0,46	(-)
Girder 2	$A_{int.conc}$	0,237	0,197	0,472	0,409	0,497	0,406	(m²)
	n_{ratio}	0,32	0,27	0,64	0,55	0,67	0,55	(-)
x = 0,9 m								
Girder 1	$A_{int.conc}$	0,305	0,408	0,251	0,219	0,329	0,411	(m²)
	n_{ratio}	0,41	0,55	0,34	0,29	0,44	0,55	(-)

Table 5: Interacting concrete area and the n_{ratio}

force in the steel, $F_{conc.}$ = compressive normal force in the concrete, $\sigma_{bfl,m}$ = mean stress at the steel bottom flange, $\sigma_{tfl,m}$ = mean stress at the steel top flange, $\sigma_{w,t}$ = stress at the top of the web, $\sigma_{w,b}$ = stress at the bottom of the web, $e_{neutral}$ = position of neutral bending axis (along the z-axis with the origin at the upper side of the steel top flange, positive downwards),

e_{conc} = centre of gravity for concrete deck slab (along the z-axis with the origin at the upper side of the steel top flange, positive downwards),

t_{bfl} = steel bottom flange thickness
w_{bfl} = steel bottom flange width
t_{tfl} = steel top flange thickness
w_{tfl} = steel top flange width
t_{w} = steel web thickness
h_{w} = steel web height
n_0 = short term modular ratio E_{steel}/E_{conc}.

If the measured steel strains are extrapolated to the centre of gravity for the concrete deck, then the interacting concrete area, $A_{int.conc}$, can be calculated as below:

$$A_{int.conc} = \frac{F_{conc.}}{\dfrac{\sigma_{tfl}}{n_0} \cdot \left(\dfrac{e_{neutral} - e_{conc}}{e_{neutral}} \right)} \quad (6)$$

In *Table 5*, the interacting concrete area is presented together with n_{ratio}, the ratio between the measured interacting concrete area and the interacting concrete area according to Ref. [4], assuming that the prefabricated concrete deck behaves as a concrete deck cast on-site. In the section near the support, $x = 7,175$ m, no values are presented. As this section is close to one of the supports, the stress distribution in this section is not linear, and extrapolation of the measured strains is not possible.

The results from the measurement in 2001 are incomplete, and only the steel stresses at the bottom of the webs have been documented. Therefore, it is not possible to estimate the interacting concrete area in an appropriate manner, because it is impossible to find out how much of the load that is carried by the steel section or by the composite section respectively. However, the measured stresses at the bottom of the webs have been compared to FE analyses and also to the new measurements from 2011, and they correspond well.

Discussion and Conclusions

The composite type of bridge studied in this paper is often designed assuming a simple beam model. The tests show that such a model is very conservative when deflections and steel stresses are calculated. The FE models show that the torsional/warping stiffness of the superstructure will distribute the force between the steel girders, even if the load is acting right above one of the girders. The back walls appear to have a similar load distribution effect, but not that significant. It is also obvious that the soil behind the retaining wall will affect the bridge considerably, and the FE model that includes the soil (FEM-3) is the model that describes the reality best.

The tests show that the interacting concrete area is much smaller than the effective flange width for a concrete deck in a composite bridge, according to Ref. [4]. This conclusion is supported by tests on other bridges of same type.[7] The major reason for the interacting concrete area being much smaller is believed to be explained by the dry joints. These joints will always develop a small gap that has to be closed before the concrete can transfer the compressive forces over the joints. If there are small gaps in the joints, when the *in situ* cast channels are injected, these gaps will become permanent. This means that the *in situ* cast concrete alone will transfer the compressive forces over the joint, until the load is big enough to close the joints.

The significant difference regarding the position of the neutral bending axis between the most loaded girder and the other girder indicates that there are gaps in the joints that close when the load increases. For an increasing load, the neutral bending axis moves upwards towards the theoretical position for an *in situ* cast deck slab. In the ultimate limit state (ULS), a bridge deck of this

Fig. 15: Heavy transport vehicle crossing the bridge at the time of measurement

kind can be treated as an *in situ* cast deck. In the SLS and the fatigue limit state (FLS), the bridge designer should be careful not to underestimate the extra load effects on the steel due to the partial composite action.

In the SLS and FLS, the effective width of the concrete can be reduced in order to compensate for the gap effects. For the bridge presented in this paper, a reduction factor of ~0,5 appears to be a good estimation in case of moderate loading. In the ULS, it is still reasonable to use the effective flange width according to Ref. [4] for single-span bridge, because the joints will close when the load is increased. This phenomenon has been seen in large-scale laboratory tests, and also by FE models simulating gaps in deck joints.

During the tests in 2011 a heavy transport vehicle, ~200 t, crossed the bridge along the centreline (see *Fig. 15*). This vehicle gave steel stresses that were more than three times higher than the stresses for the test vehicle in the

same position, and around two times higher than the highest stress for the test vehicle (~50 MPa at the bottom of the web). Also for this higher load, the stress distribution at the steel sections was almost the same, with a neutral bending axis in the web ~100 mm below the top flange.

With regard to the long-term effect, it can be noted that the passive girder had a relatively larger deflection, compared with the active girder, in 2001 than in 2011. This might indicate that there were initial gaps in the joint, back in 2001, which have been closed or at least partly closed owing to abrasion of irregularities at the concrete surfaces in the dry joints. As no measurements of the absolute vertical position of the steel girders have been done in 2001 and 2012, this indication is hard to verify.

In all the models, the potential stiffness contribution from the pavement and the rails has been neglected. Their contribution is believed to be rather

low and the measurements do not indicate that the total stiffness is significantly underestimated. Another possible source of error in the FE modelling is the soil model, because it is based on tabled values and not on a field test.

References

[1] Hällmark P, White H, Collin P. Prefabricated bridge construction across Europe and America. ASCE—Pract. Period. Struct. Des. Const. 2009; **17**(3): 82–92.

[2] Hällmark R, Collin P, Stoltz A. Innovative prefabricated composite bridges. *Struct. Eng. Int.* 2009; **19**(1): 69–78.

[3] Hällmark R, Collin P, Nilsson M. Concrete shear keys in prefabricated bridges with dry deck joints. *Nordic Conc. Res.* 2011; **44**(2): 109–122.

[4] EN 1994-2. *Eurocode 4—Design of Composite Steel and Concrete Structures—Part 2: General Rules and Rules for Bridges*, CEN, European Committee for Standardization, Brussels; 2005.

[5] EN 1993-1-1. *Eurocode 3—Design of Steel Structures—Part 1–1: General Rules and Rules for Buildings*, CEN, European Committee for Standardization, Brussels; 2005.

[6] Collin P, Möller M, *Utvärdering av belastningsprov—Bro över Rokån"*, Technical Report 01:01, Luleå University of Technology, Division of Steel Structures, 2001 (in Swedish).

[7] Collin, P, Johansson B, Pétursson H, *Samverkansbroar med elementbyggda farbanor"*. Technical Report. Swedish Institute of Steel Construction, Publication 165; 1998. ISBN: 9171270221 (in Swedish).

[8] EN 1993-1-5. (2006), *Eurocode 3—Design of Steel Structures—Part 1–5: Plated Structural Elements*, CEN, European Committee for Standardization, Brussels.

[9] EN 1992-1-1. (2005), *Eurocode 2—Design of Concrete Structures—Part 1-1: General Rules and Rules for Buildings*, CEN, European Committee for Standardization, Brussels.

PAPER V

Large-scale tests on a composite bridge with prefabricated concrete deck and dry deck joints

Robert Hällmark, Peter Collin and Martin Nilsson

Large-scale tests on a composite bridge with prefabricated concrete deck and dry deck joints

Robert Hällmark
Peter Collin
Martin Nilsson

This paper describes the large-scale tests on a composite bridge with prefabricated deck elements and dry joints between the elements. The work is part of the European R&D project ELEM (RFCS-CT-2008-00039). This type of bridge has been used for three single-span bridges in Sweden and has contributed to minimizing construction time as well as disturbance to traffic. The behaviour at midspan and the behaviour over an internal support of a continuous bridge were studied in the tests, and the results analysed by FEM and discussed. Conclusions regarding the design of this type of bridge are drawn, with respect to the global analysis as well as cross-section capacity.

1 Introduction

Steel-concrete composite bridges can be made even more competitive by increasing the degree of prefabrication. Using precast concrete deck elements is one way of doing this. Bridges with prefabricated deck elements have been built worldwide for many decades, but are still rare exceptions, and different countries have developed their own ways of implementing the prefabrication techniques. Refs. [1], [2], [3], [4] present some global experiences gained from the use of prefabricated concrete deck elements.

This paper is limited to a prefabricated concrete deck system that has been developed in Sweden, starting in the late 1990s. This deck system has transverse joints that are totally dry, and no prestressing tendons are used. Shear forces are transferred from one element to another by overlapping concrete tongues (shear keys). These are designed as a series of male-female connections, see Fig. 1. This type of bridge deck is described in more detail in [5], [6]. The behaviour and strength of this kind of connection have been tested, and are discussed in [7].

In order to study the behaviour of a composite bridge with this type of deck, large-scale laboratory tests were performed in the summer of 2011. The tests focused on the behaviour with respect to shear lag, composite action, joint openings and the static capacity of the shear keys. However, this paper is limited to the study of the shear lag and composite action.

2 Laboratory tests

The specimen and the test setup were planned in a way that made it possible to perform tests simulating both a load situation in the span of a continuous bridge and a load situation at an internal support. The test specimen was designed with a real deck element (as used in a single-span bridge over the River Rokån in Sweden) as a model.

Since several different tests were performed on one specimen, all load situations had to be kept below the failure load, thus resulting in non-destructive testing. Only the last test was destructive, when a shear key was loaded to failure.

As a complement to these non-destructive tests, destructive tests were carried out on similar specimens by RWTH Aachen University in Germany. In the last section of this paper, the results from the Swedish and German tests are compared and discussed.

2.1 Test specimen

The test specimen consisted of two steel I beams, grade S355J2 + N (EN 10025-2:2004), and four prefabricated concrete deck elements on top of that. Composite action was achieved by shear studs, Ø22 × 185 mm. Fig. 2 shows the specimen.

Each concrete element measured $1.8 \times 3.5 \times 0.29$ m. The depth (0.290 m) and the length (1.8 m) of the elements tested match those of the prefabricated elements previously used in real single-span bridges. Full depth was used in order to get real dimensions for the shear keys and to avoid discussions about how scale factors affect the results. The length of the deck el-
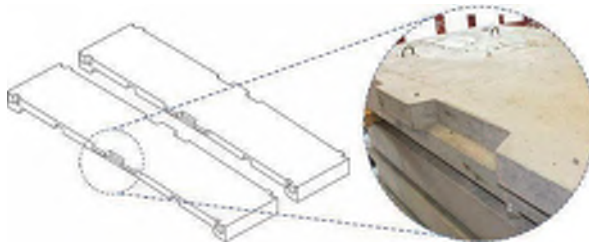

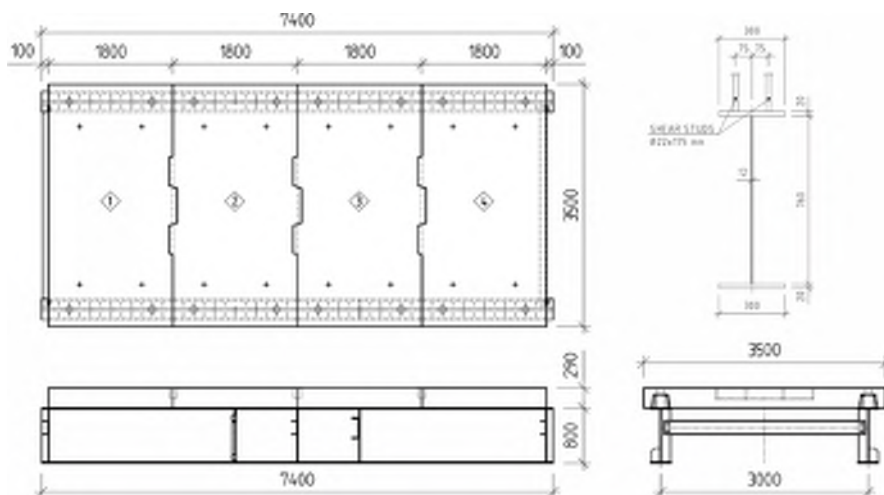*Fig. 1. Shear keys in a dry deck joint in a large-scale test specimen*

Fig. 2. Plan on and section through the test specimen [mm]

ements is generally governed by the distance between the parapet posts, which means 1.8–2.0 m in Sweden. By using the same position of the post on each element, this results in benefits for both production and design. The width of the concrete deck elements in the test bridge is 3.5 m and the distance between the steel beams is 3.0 m. Generally, the distance between the beams is somewhere between 4 and 7 m in Sweden, depending on the total width of the bridge.

This means that the specimen has been scaled down in the transverse direction, and that only the internal part of the deck slab is considered. Due to the size limitations of the test rig, the cantilevering parts of the deck slab have been omitted.

The concrete strength class ordered was C35/45. Three test cubes (100 × 100 × 100 mm) were cast for each element. The compressive strength of these cubes was tested at the same time as the large-scale tests were run-

ning. Self-compacting concrete (SCC) was used to cast the channels on top of the steel beams in order to achieve composite action. Six test cubes were cast. Three of them were tested after 12 days, when the large-scale tests started, the remaining cubes were tested after 28 days. Table 1 shows the SCC properties and the tested characteristics of the fresh SCC concrete. Table 2 shows the properties of the hardened concrete.

$$f_{c,cyl} = f_{c,cube}(0.84 - 0.0012 \cdot f_{c,cube}) \quad (1)$$

$$f_{ct} = 0.9 \cdot 0.9 \cdot f_{ct,sp} \quad (2)$$

$$E = 22 \cdot (f_{cm,cyl}/10)^{0.3} \quad (3)$$

All elements were produced by a concrete workshop specialized in prefabricated elements. In order to assure

Table 1. SCC specification for in situ channels, and measured properties

C35/45 SCC	Specification	Measured properties
VCT	< 0.4 –	
Air	> 4.0 %	
t_{500}	3–4 sec	5.5 sec
slump flow	720 ± 30 mm	620 mm

Table 2. Properties of hardened concrete

	Cast date	Test date	Age [days]	δ [kg/m³]	P_c [kN]	$f_{c,cyl}$* [MPa]	P_{ct} [kN]	f_{ct}** [MPa]	E*** [GPa]
Element 1	2011-03-31	2011-06-13	74	2295	592	45.9	–	–	34.7
Element 2	2011-04-05	2011-06-13	69	2282	622	47.6	–	–	35.1
Element 3	2011-04-05	2011-06-13	69	2319	629	47.9	–	–	35.2
Element 4	2011-04-06	2011-06-13	68	2331	620	47.3	–	–	35.1
SCC-channel	2011-05-20	2011-06-17	28	2353	1224	42.0	–	–	33.8
SCC-channel	2011-05-20	2011-06-01	12	2359	1175	40.5	134	3.0	33.5

* = Calculated value according to Equation 1, Betonghandboken 11.11:10 [8]
** = Calculated value according to Equation 2, EN 1992-1-1 (3.3) [9]
*** = Calculated value according to Equation 3 (f_{cm} in MPa), EN 1992-1-1 Table 3.1 [9]

the accuracy of fi t in this kind of joint, match-casting of the joints was necessary. The precision of the match-cast joints was measured with a feeler gauge before the channels were cast, and composite action achieved. The mean value of the gap was < 0.4 mm.

2.2 Test setup

Throughout this paper, the x axis is defi ned with its origin in the joint between elements 2 and 3, and is defi ned as positive in the direction of increasing element numbers.

Test setup 1
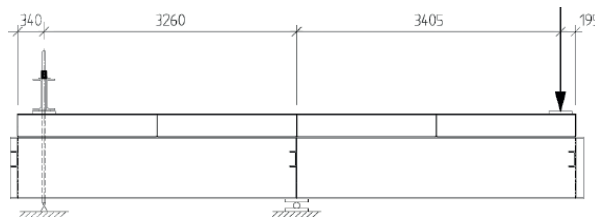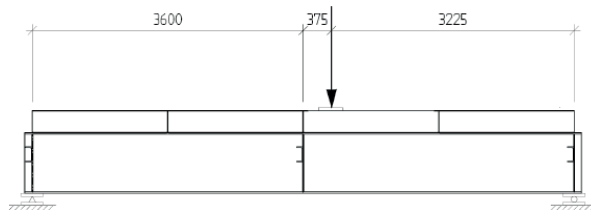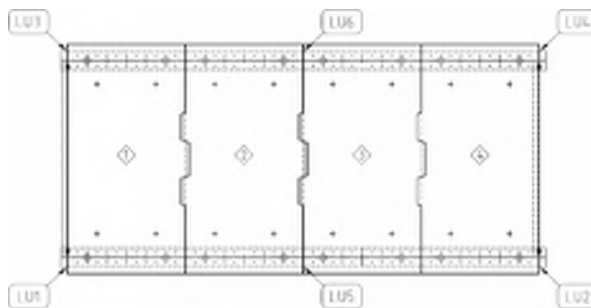Fig. 3 shows a sketch of the load situation in the first test setup, with an internal support at x = 0.000 m. Two things are of special interest under this load situation. Firstly, will the bridge beams behave as composite sections and stresses? Secondly, how much of the force will enter the very short concrete slabs and how will it be distributed due to shear lag?

Test setup 2
Fig. 4 shows a sketch of the second test setup. This setup was used to study whether or not a bridge of this kind behaves as an ordinary composite bridge in the spans. Whether the behaviour changes after a couple of large load cycles was also checked. This was done in order to find out if

Fig. 5. Two point loads applied straight above the steel beams

the irregularities in the dry joints are smoothed by local concrete crushing, resulting in a better fit after a couple of large load cycles. The shear-lag effect was also studied in order to find out if a bridge of this type behaves as a conventional composite bridge regarding shear lag in the span sections.

The load was applied in two different ways. First as a point load, 350 × 350 mm, acting on the centre-line of the bridge, then as two point loads acting straight above the steel beams. The latter was achieved by using a spreader beam as shown in Fig. 5.

The hydraulic jack used in all tests had a maximum capacity of 700 kN. During the static tests it was deformation-controlled with a stroke rate of 0.02–0.03 mm/s during the loading sequence, and 0.05 mm/s during unloading. In the case of cyclic loading, the jack was load-controlled with a frequency of 0.0333 Hz.

2.3 Measuring devices

During the tests, six channels were used to measure the deflections and nine channels were used for steel strain measurements. In total there were 51 channels measuring concrete strains, reinforcement strains, joint openings, etc.

Deflections

Deflections were measured in the middle and at the end of the beams. Six LVDTs (linear variable differential transformers) were used, denoted LU1 to LU6. The LVDTs were mounted vertically and measured the deflection on top of the low stiffeners. Fig. 6 shows a plan of the deflection measurement points.

Fig. 3. Test setup 1

Fig. 4. Test setup 2

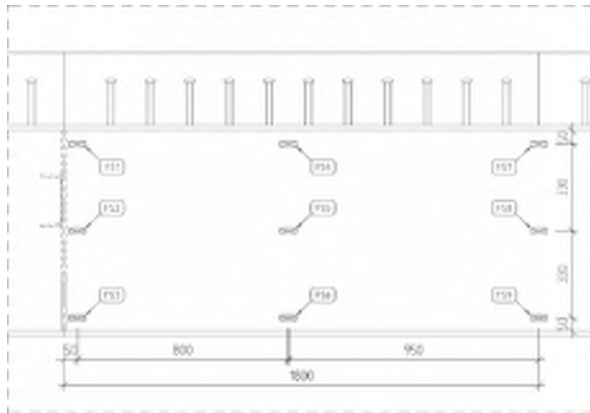
Fig. 6. Deflection measurement points

Fig. 7. Installation scheme for steel strain gauges

ation as well as the rotation due to the settlement at the negative support, see Eqs. (4)–(7).

$$LU2_{bend} = LU2 - LU5 + (LU1-LU5) \quad (4)$$

$$LU4_{bend} = LU4 - LU6 + (LU3-LU6) \quad (5)$$

$$LU5_{bend} = LU5 - (LU1 + LU2)/2 \quad (6)$$

$$LU6_{bend} = LU6 - (LU3 + LU4)/2 \quad (7)$$

The vertical deformations from tests 1–8, $LU2_{bend}$ and $LU4_{bend}$, are all plotted on the same load–deformation diagram, see Fig. 8. The vertical deformations from tests 9–13, $LU5_{bend}$ and $LU6_{bend}$, are shown in the same figure.

Steel strains

In order to study to what extent the concrete interacts with the steel, nine strain gauges were attached to one of the steel beams. By measuring the steel strains in the top and bottom of the web, the position of the neutral bending axis can be calculated and the area of interacting concrete estimated. In order to get a third reference point, an extra strain gauge was attached to the middle of the web. The strain gauges were all located over the length of Element 3. Fig. 7 shows the positions of the strain gauges.

2.4 Test schedule

The test schedule is presented in Table 3.

3 Results

The results from the deflections measurements and the steel strain measurements are presented in the following sections.

3.1 Deflections

The deflections given here are the deflections caused by pure bending, which means that the support settlements have been taken into consideration in the case of a simply supported beam, test setup 2 (tests 9–13). In test setup 1 (tests 1–8) the support settlements have been taken into consider-

Table 3. Test schedule

| Test no:	Type of load situation	Force	Number of cycles
Test 1	Set-up 1 – one point load	100 kN	–
Test 2	Set-up 1 – one point load	280 kN	–
Test 3	Set-up 1 – two point loads	310 kN	–
Test 4	Set-up 1 – two point loads	430 kN	–
Test 5	Set-up 1 – two point loads	5–250 kN	50 cycles
Test 6	Set-up 1 – one point load	250 kN	–
Test 7	Set-up 1 – two point loads	400 kN	–
Test 8	Set-up 1 – two point loads	5–250 kN	50 cycles
Test 9	Set-up 2 – two point loads	500 kN	–
Test 10	Set-up 2 – two point loads	5–450 kN	100 cycles
Test 11	Set-up 2 – one point loads	300 kN	–
Test 12	Set-up 2 – one point loads	450 kN	–
Test 13	Set-up 2 – one point loads	5–400 kN	100 cycles
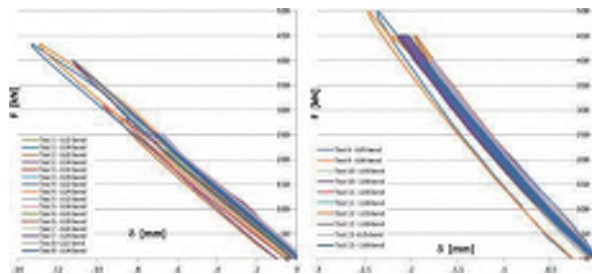
Fig. 8. F-δ diagram for tests 1–8, $LU2_{bend}$ and $LU4_{bend}$, and tests 9–13, $LU5_{bend}$ and $LU6_{bend}$

3.2 Steel strains

The steel strains were measured at three points in three sections. All strains have been transformed into stresses according to Hooke's law, assuming $E_{steel} = 210$ GPa.

$$\sigma = E \cdot \varepsilon \qquad (8)$$

The first section is located 0.050 m from the internal support, i.e. 0.050 m from the joint between elements 2 and 3. The second section is located 0.850 m from the internal support, i.e. 0.050 m from the middle of element 3. The third section is located 1.800 m from the internal support, i.e. at the joint between elements 3 and 4. Fig. 7 shows the locations of the steel strain gauges (FS1–9). The results from the measurements are summarized in Fig. 9 and Fig. 10.

4 Analysis

In Sweden, the general way of performing global analyses on composite bridges so far is by using beam models. The analyses in this section were performed with a focus on how the behaviour of this type of bridge section can be best described with ordinary beam models. Different design assumptions have been made, resulting in four different beam models. These models have also been compared with the test results. FE analyses were carried out, too, in order to see if more advanced modelling agrees better with the test results.

In all the models, the steel parts are modelled with E = 210 GPa and the concrete elements with E = 35.0 GPa, which corresponds to the material parameters of the tests.

4.1 Design models

Beam models

The beam models were developed in line with [9] and the general way of designing composite bridges in Sweden. One of the questions raised is to what extent the concrete interacts with the steel. The test results have been compared with four different beam models, with varying widths of interacting concrete, see Fig. 11.

BM-1

In the first model the beam is modelled as the steel cross-section only. This provides a reference value for how the bridges would behave if there was no interaction at all between steel and concrete.

BM-2

The second model assumes that the concrete interacts with the steel over the full width of the deck, and that there are no joints in the deck. This provides a reference value for how the bridges would behave if the part studied is a conventional composite cross-section subjected to a negative bending moment, and with no shear lag – generally, a span section.

BM-3

The third model includes the shear lag in the concrete deck. The distance L_e between the points of contraflexure for the bending moment is the length of the test bridge for positive moments, and the distance between the outmost shear studs within one element in the case of negative bend-
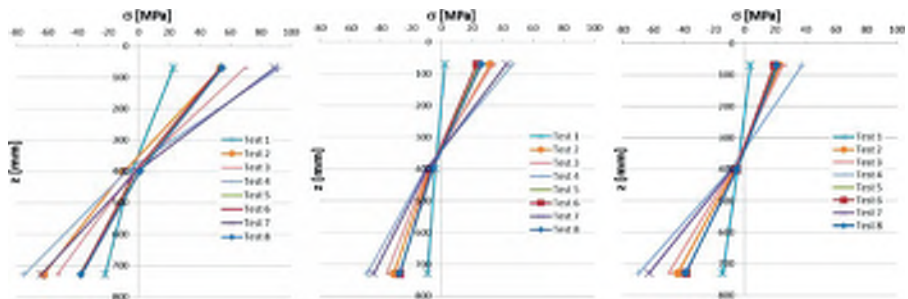

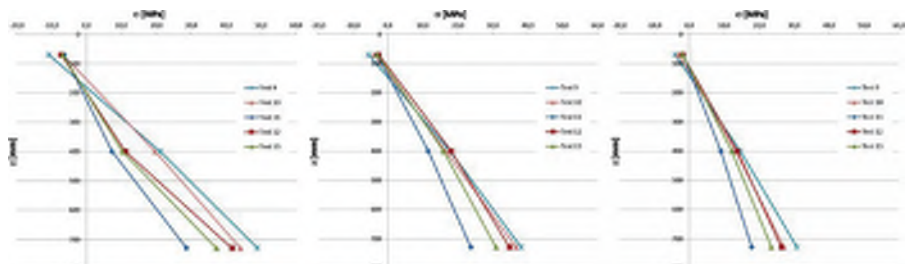Fig. 9. Longitudinal steel stresses in test setup 1, measured at section x = 0.050/0.850/1.800 m

Fig. 10. Longitudinal steel stresses in test setup 2, measured at section x = 0.050/0.850/1.800 m

Fig. 11. The four beam models
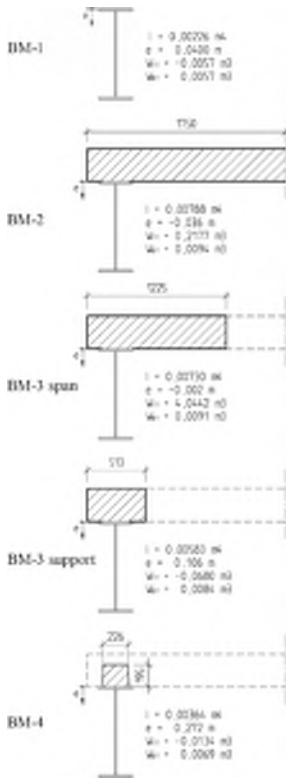

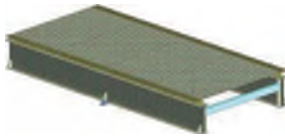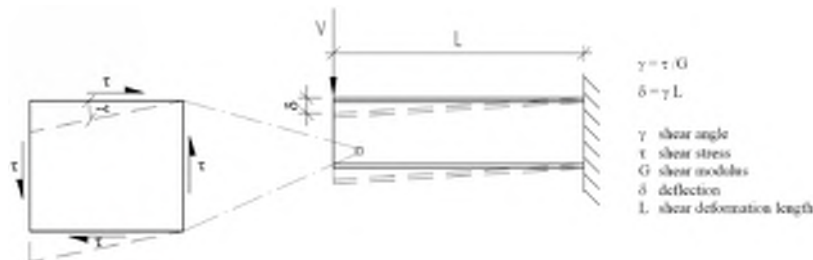*Fig. 12. The FE model*

ing moments. The latter results in a large reduction in the width of the interacting concrete.

BM-4
Only the in situ concrete is taken into account in this model.

FE models
All finite element calculations were carried out using Autodesk Robot, and all materials are modelled as linear elastic. The steel and concrete are modelled with shell elements. Rigid elements are used to model the eccentricity between the concrete deck slab and the top flange. The general model is illustrated in Fig. 12. FEM-1 is mainly interesting for test setup 1, FEM-2 and FEM-3 for test setup 2.

FEM-1
In this model the concrete deck elements are modelled with no connections at all in the dry joints. The elements are allowed to deform independently and freely. This model is mainly used to study the global behaviour at an internal support, and to calculate the steel stress distribution.

FEM-2
This model is similar to FEM-1, but the deck slab is modelled as one continuous slab without any joints, and is most interesting for test setup 2. This is a model that should be equal to the case with an in situ deck slab in compression.

FEM-3
FEM-3 is similar to FEM-2, but the joints are modelled as non-linear with initial gaps of 0.4 mm, which close under the deflection. The initial gap width was chosen based on feeler gauge measurements. However, the in

situ channels are modelled with no gap.

4.2 Deflections

The deflections are studied in order to discover to what extent the prefabricated concrete deck influences the stiffness and in order to obtain a better understanding of how a bridge of this type should be modelled in a global analysis.

The measured deflections are compared with the calculated deflections according to the four beam models, and to the deflections achieved with the FE models. The calculated deflections for the beam models are the results of the deflections caused by bending and support rotations, but also due to shear deformations in the web. For test setups 1 and 2, this extra deformation is calculated according to Eq. (9) and Fig. 13.

$$\delta_{Shear} = L \cdot \frac{V}{A_w \cdot G} \qquad (9)$$

The measured deflections were not truly elastic. In general, the results indicate a linear behaviour during the loading and unloading sequence, but part of the deformation remains. Tests 2 and 6 are used to illustrate the differences in deflection during the first large load cycle in comparison to the deflections when a similar load is repeated, see Fig. 14.

Since the calculation models assume a concrete stiffness that corresponds to short-term loading and a linear elastic behaviour, the elastic deformations are presented separately in Table 4 and Table 6.

Test setup 1
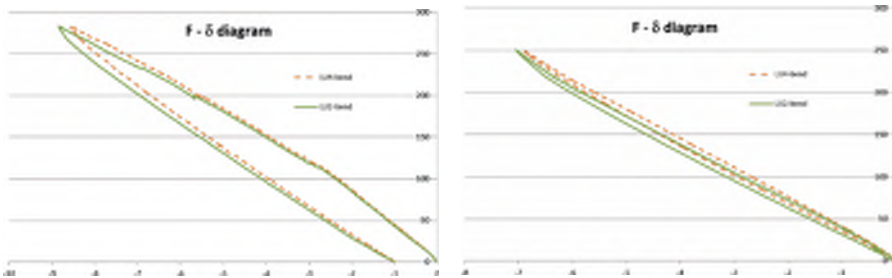The extra deflection caused by shear is included in the deflections presented

Fig. 13. Shear deformation notation

Fig. 14. Load–deformation diagram for test 2 (left) and test 6 (right), LU2$_{bend}$ and LU4$_{bend}$

Table 4. Test setup 1, vertical deflections at x = 3.600 m, measured vs. calculated [mm]

	Load	LU2		LU4		BM-1	BM-2	BM-3	BM-4	FEM-1	FEM-2	FEM-3
	F [kN]	δ	δ$_{el}$	δ	δ$_{el}$	δ	δ	δ	δ	δ	δ	δ
Test 1	100	–2.7	–2.3	–2.5	–2.3	–3.1	–1.1	–1.7	–2.0	–2.6	–	–
Test 2	280	–8.8	–7.8	–8.6	–7.6	–8.8	–3.0	–4.7	–5.7	–7.3	–	–
Test 3	310	–9.7	–9.2	–9.1	–8.8	–9.7	–3.3	–5.2	–6.3	–8.1	–	–
Test 4	430	–13.3	–12.8	–12.9	–12.4	–13.5	–4.6	–7.2	–8.8	–11.2	–	–
Test 5	5–250	–7.0	–7.0	–7.1	–7.1	–7.9	–2.7	–4.2	–5.1	–6.5	–	–
Test 6	250	–7.1	–7.0	–6.9	–6.9	–7.9	–2.7	–4.2	–5.1	–6.5	–	–
Test 7	400	–11.1	–10.9	–11.3	–11.1	–12.6	–4.3	–6.7	–8.2	–10.4	–	–
Test 8	5–250	–7.3	–7.3	–7.1	–7.1	–7.9	–2.7	–4.2	–5.1	–6.5	–	–

for the beam models. The first test is excluded throughout the analysis due to the large permanent deformations.

The first beam model, BM-1, gives the level of the maximum deflection that can occur, since it is based on the assumption of no composite action. The deflections predicted by BM-1 are all in the range of 7–15 % larger than the measured deflections.

The other beam models are all far too stiff; BM-2 and BM-3 predict deflections that are 40–65 % smaller than the measured values. Even BM-4 is too stiff, even though only the concrete channel is taken into account. In an ordinary composite bridge this would be an indication that the concrete had cracked, and should be replaced by the stiffness of the reinforced section. However, the measured concrete stresses were in this case very small, and there were no visual signs of cracking. In the comparison of the effective width (later in this paper), the interacting widths have been calculated for both concrete and reinforcement.

FEM-1 indicates a behaviour somewhat stiffer than the test results. The measured deflections are 3–10 %

larger than those predicted by the model.

The measured deflections are all very small since the specimen is very stiff. The longitudinal strains in the prestressed rebars that act as a negative support are almost of the same magnitude, resulting in rotation of the whole specimen about the internal support. The measured deflections have therefore been split into deflections caused by pure bending and deflections caused by rotation. This mathematical operation, which is based on the assumption of linear behaviour along the girder, adds a further source of error to the measured deflections.

Besides the comparison between the measured values and the different

design models, the measured deflections have been used to calculate the corresponding moment of inertia and the theoretical interacting concrete width b$_{eff,conc}$ assuming that the deck slab interacts evenly over its thickness, see Eqs. (10), (11), Fig. 15 and Table 5. The corresponding value has also been calculated for a cracked section, b$_{eff,reinf}$. However, the concrete stresses are low and no signs of cracking have been observed.

$$\delta_{bend} = \delta_{measured} - \delta_{shear} \qquad (10)$$

$$I = -\frac{Fa^2L_2}{4E\delta_{bend}} \cdot \left(1 - \frac{a}{3L_2}\right) - \frac{FaL_2L_1}{6E\delta_{bend}}$$
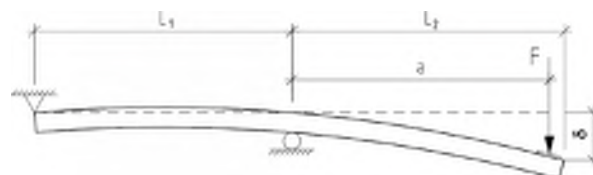$$\qquad (11)$$

Fig. 15. Schematic deformation figure and notation for test setup 1

Table 5. Calculated moment of inertia and effective concrete width for test setup 1

	Test set-up	F [kN]	L₁ [m]	L₂ [m]	L [m]	a [m]	δ_bend [mm]	I_calc [m⁴]	b_eff,conc [mm]	b_eff,reinf [mm]
Test 1	1	100	3.260	3.600	–	3.405	−2.1	0.003204	74	–
Test 2	1	280	3.260	3.600	–	3.405	−7.1	0.002605	24	830
Test 3	1	310	3.260	3.600	–	3.405	−8.3	0.002466	14	480
Test 4	1	430	3.260	3.600	–	3.405	−11.6	0.002435	12	404
Test 5	1	250	3.260	3.600	–	3.405	−6.5	0.002528	19	634
Test 6	1	250	3.260	3.600	–	3.405	−6.4	0.002570	22	740
Test 7	1	400	3.260	3.600	–	3.405	−10.0	0.002622	26	875
Test 8	1	250	3.260	3.600	–	3.405	−6.6	0.002491	16	542

Test setup 2

Among the beam models studied, the measured deflections are best described by BM-3. This produces deflections that are ~15 % smaller than the measured values. However, the measured deflections are very small, which means that the influence of small gaps in the joints can be quite high. This effect is believed to decrease as the load and the deformations increase. FEM-3 is used to study how the gaps influence the deflections.

FEM-2, which represents an in situ slab with full interaction between steel and concrete, produces deflections that are ~20 % smaller than the measured values. This indicates that the joints reduce the overall stiffness, resulting in larger deformations. The joints are modelled with small gaps in FEM-3. This means that the specimen must deflect before the deck elements transfer longitudinal forces across the joints. When the joints are modelled with a gap width of 0.4 mm, the deflections at midspan will be 10–13 % smaller than the measured values.

It is obvious that the joints influence the global stiffness. However, in the tests the percentage influence of the joints is believed to be disproportionately large because the permissible stresses in a real bridge are much higher. The stress levels in the bottom flanges in test setup 2 are always < 60 MPa. A gap will decrease the stiffness up to the point when it is closed, and from that point on the stress will be distributed over the composite section, even near the joints. Due to the rather low load, the joint gaps will have quite a high influence on the stiffness.

The corresponding moment of inertia and the interacting concrete width b_eff,conc have been calculated for the measured deflections, Eq. (12) and Fig. 16.

$$I = -\frac{F(L-a)\cdot L^2}{96E\delta}\cdot\left(3 - \frac{4(L-a)^2}{L^2}\right)$$

for

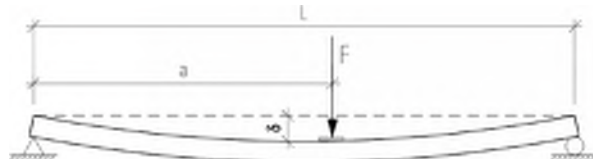$$a \geq -\frac{L}{2} \tag{12}$$

Fig. 16. Schematic deformation figure and notation for test setup 2

Table 6. Test setup 2, vertical deformations at x = 0.000 m, measured vs. calculated [mm]

	Load F [kN]	LU5 δ	LU5 δ_el	LU6 δ	LU6 δ_el	BM-1 δ	BM-2 δ	BM-3 δ	BM-4 δ	FEM-1 δ	FEM-2 δ	FEM-3 δ
Test 9	500	−2.4	−2.1	−2.5	−2.2	−4.7	−1.8	−1.9	−3.1	–	−1.6	−1.9
Test 10	5–450	−2.1	−2.0	−2.1	−2.1	−4.2	−1.6	−1.7	−2.8	–	−1.4	−1.8
Test 11	300	−1.4	−1.3	−1.4	−1.4	−2.8	−1.1	−1.1	−1.9	–	−0.9	−1.2
Test 12	450	−2.0	−1.9	−2.1	−2.1	−4.2	−1.6	−1.7	−2.8	–	−1.4	−1.7
Test 13	5–400	−1.8	−1.6	−1.9	−1.8	−3.7	−1.4	−1.5	−2.5	–	−1.2	−1.5

Table 7. Calculated moment of inertia and effective concrete width for test setup 2

	Test set-up	F [kN]	L₁ [m]	L₂ [m]	L [m]	a [m]	δ_bend [mm]	I_calc [m⁴]	b_eff,conc [mm]
Test 9	2	500	–	–	7.200	3.975	−1.5	0.005919	541
Test 10	2	450	–	–	7.200	3.975	−1.5	0.005552	437
Test 11	2	300	–	–	7.200	3.975	−1.0	0.005427	407
Test 12	2	450	–	–	7.200	3.975	−1.4	0.005730	485
Test 13	2	400	–	–	7.200	3.975	−1.2	0.005881	529

The effective concrete width is about two times larger than the width of the concrete channel. This is actually almost the area that is derived if it is assumed that L_e is the distance between the outmost shear studs within an element, $L_e = 1.5$ m.

4.3 Steel stresses

When the measured steel stresses are compared with the design models, there is good agreement in some sections and poor agreement in others.

Test setup 1

One thing that can be seen is that the measured steel stress distribution is non-linear in the sections near the open joints. The linear stress distribution seems to be disturbed near the tops of the steel beams. However, this is not unexpected, since a part of the stresses in the steel will enter and leave the concrete elements within a distance of 1.5 m. At the joints the steel section has to carry the whole load, and the forces that were carried by the concrete a few decimetres away will not be distributed over the whole section. Instead, the stresses will be concentrated around the upper flange because they will start to enter the concrete again after just 300 mm, which

is the longitudinal distance between the neighbouring studs in two elements. This effect can be seen in Fig. 9 and Fig. 10, which show the measured stresses, and is also obvious in the results of the FE analyses. Fig. 17 presents the stress distribution according to the FE analyses within the web plate for test 4. The support, at x = 0.000 m, exhibits a disturbed stress state in the bottom of the web, too. Section x = 1.800 m should exhibit a more representative stress distribution for the general case near an open joint.

Fig. 17 also shows that the neutral bending axis is only shifted slightly upwards in the middle of the element, indicating that the concrete's contribution to the stiffness is very limited. This is in line with the result of the tests. The stresses in the web plate are plotted in Fig. 18 from z = 0.070 to 0.730 m, for test 4, which means between the measured points, for all design models together with the measured values. The beam models fail to describe the stress distributions within the web because they are all linear. However, BM-4 gives a rather good estimation of the stress distribution over the composite section.

The stresses predicted by FEM-1 are quite close to the measured stresses. The only section where the

FE model fails to describe the stress state is near the support. The FE model indicates higher stresses near the bottom of the web due to the singularity point at the support. In reality, load distribution steel plates (70 × 300 × 300 mm) are used at the supports. These plates will probably interact with the bottom flange and decrease the longitudinal stresses locally, which could explain the lower stresses in the bottom of the web.

The FE results have also been used to estimate the effective width of the interacting concrete area in the middle between two joints. This was done by assuming a linear strain distribution from the neutral bending axis up to the centre of the concrete deck slab. This is a simplification because it has been noted that the stress distribution is not perfectly linear. At a joint the interacting concrete area is zero, and the FE model indicates that the effective width increases from the outmost row of studs to a maximum in the middle of an element.

If the steel stresses from the FE model are extrapolated up to the centre of gravity for the concrete deck, then the interacting concrete area Aint.conc can be calculated according to Eq. (13). The normal force in the deck slab is taken from the FE analyses.

$$A_{int.conc.} = \frac{F_{conc}}{\dfrac{\sigma_{tfl}}{n_0} \cdot \left(\dfrac{e_{neutral} - e_{conc}}{e_{neutral}} \right)} \quad (13)$$

where
F_{conc} normal force in concrete
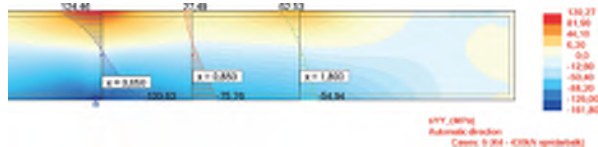σ_{tfl} stress at upper side of steel top flange

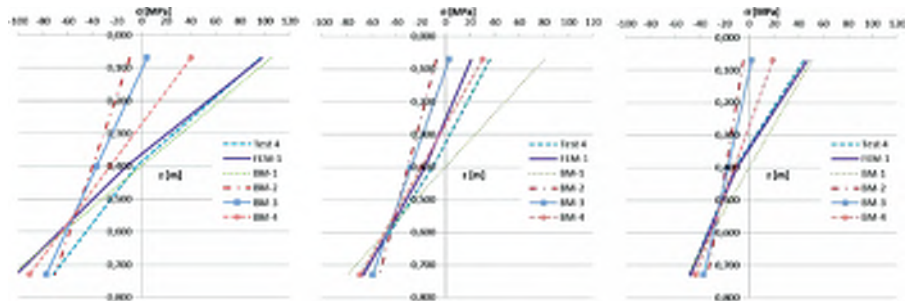Fig. 17. Longitudinal stresses in web plates, test 4, FEM-1

Fig. 18. Longitudinal stresses in the web plate in test 4, x = 0.050/0.850/1.800 m

$e_{neutral}$ position of neutral bending axis*

e_{conc} centre of gravity of concrete deck slab*

n_0 short-term modular ratio Esteel/Econc

(* along the z-axis with the origin at the upper side of the steel top flange, positive downwards)

FEM-1, test 4

$$A_{int.conc.} = \frac{475 \cdot 10^3}{\frac{27.5 \cdot 10^6}{6.0} \cdot \left(\frac{0.270 + 0.145}{0.270} \right)}$$

= 0.0674 m² and h_{conc} = 0.290 m ⇒ $b_{eff,conc}$ = 0.232 m

The calculated effective concrete width is almost the same as the mean width of the concrete channels, 0.225 m. However, this calculation is based on the assumption that the longitudinal concrete stress is distributed over the full depth of the concrete deck. The FE model and the measurements indicate that the forces that enter the concrete are not distributed evenly over the section. The effective width should be even less in order to take the uneven vertical distribution into account. And the mean value of the effective width over the length of an element will be ~100 mm, assuming a linear longitudinal distribution from the joints to the middle of an element.

Test setup 2

In this case, too, it is obvious that the interacting concrete area is heavily influenced by the joint gaps, see Fig. 20. FEM-3 is the model that comes closest to the measured values. It describes the measured stress state rather well at the first two sections, x = 0.050 and x =
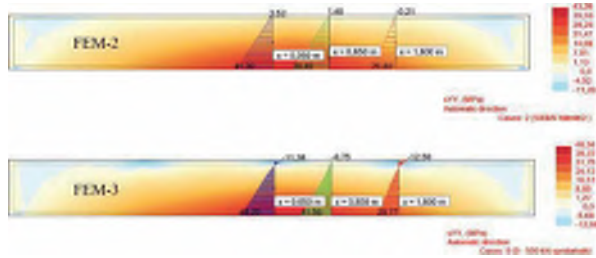

Fig. 20. Longitudinal stresses in web plates, test 9, FEM-2 and FEM-3

0.850 m, but underestimates the influence of the concrete at section x = 1.800 m, see Fig. 19. It would be possible to adjust the gaps individually in the model, trying to get closer to the measured stress distribution. However, if the model is calibrated for a better description of the stress state, it will become somewhat stiffer and then describe the deflections less accurately. Finding the exact FE model is beyond the scope of this study since the aim here is to find a reasonable design model for this type of bridge, and a non-linear FE model that simulates closing gaps is not the model this study is looking for.

It should be noted that FEM-2 and BM-3 produce similar results, which indicates that the shear-lag model in [9] works very well for an in situ superstructure of this type. If the effective concrete width is calculated from the FE model, see Eq. (13), it results in $b_{eff,conc}$ = 1.25 m. This can be compared with BM-3, which gives $b_{eff,conc}$ = 1.23 m.

In comparison to test setup 1, the measured stress state is almost linear, especially at a section near the middle of an element, x = 0.850 m. A beam model can therefore be adjusted to fit the measured stress state quite well. The adapted interacting concrete widths are presented in Table 8 for the section x = 0.850 m. Fig. 21 shows the correspondence between the meas-

Table 8. Effective concrete width for the beam model, adapted from the stress measurements

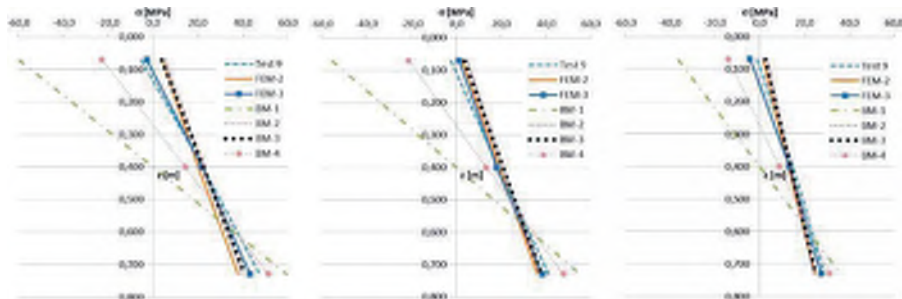|	F [kN]	x = 0.050 m $b_{eff,conc}$ [mm]	x = 0.850 m $b_{eff,conc}$ [mm]	x = 1.800 m $b_{eff,conc}$ [mm]
Test 9	500	400	500	450
Test 10	450	380	450	450
Test 11	300	300	450	450
Test 12	450	320	480	450
Test 13	400	320	470	450

Fig. 19. Longitudinal stresses in web plate in test 9, x = 0.050/0.850/1.800 m
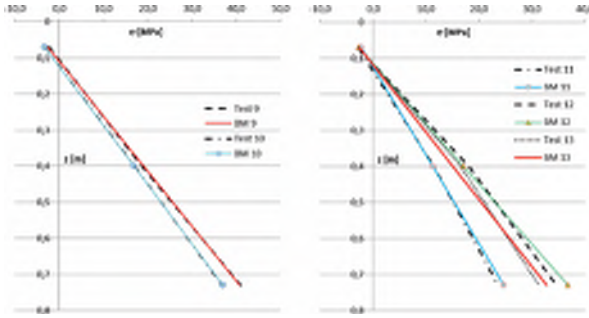
Fig. 21. *Measured steel stresses for tests 9–13 vs. adapted beam model, x = 0.850 m*

ured stresses and the adjusted beam model. In the cases with two point loads acting directly above the steel girders, tests 9 and 10, the correspondence is really good. In the case with a point load between the elements, tests 11–13, the stress distributions within the web are non-linear. In these cases the beam model still describes the stress state pretty well.

5 Discussion and conclusions

The deflections measured in both test setups indicate a lower stiffness than expected. In areas with negative bending moment, the effect of the interacting concrete seems to be negligible. In the case of positive bending moments, the interacting concrete area is limited to a width that is about two times larger than the width of the concrete channel.

Based on the former observation, in the global analysis of a multi-span bridge of this type it would be reasonable to model the support areas with the stiffness of the steel section only. This was also the model suggested before the tests were performed. The latter observation was more unexpected since it indicates that the effective width of the compressed concrete is a lot smaller compared with that of an in situ concrete deck. Single-span bridges of this kind have been designed with the assumption that the deck behaves as in situ concrete. The results from these tests together with results from field monitoring of a single-span bridge indicate that this assumption should be revised, at least in SLS and FLS since the dry joints have a significant influence on the stiffness

and the local stress distribution for moderate loads.

At the load levels used in the tests, the width of the interacting concrete is best described by assuming that L_e is equal to the maximum longitudinal spacing of the shear studs within a single element (1.5 m). This observation is also supported by the test results from RWTH Aachen University [11]. The model suggested for the global analysis is most suitable for SLS and FLS. It is reasonable to believe that the influence of the joint gaps will decrease as the load increases. This has been validated by performing calculations with increasing loads in FEM-3, and also by tests performed at RWTH Aachen University. These tests indicate that the composite section of a bridge of this type has an ultimate limit capacity in line with the capacity for a composite section, according to [10], with an in situ deck slab. The tests in Aachen show that this is valid even for joint gaps as large as 5 mm. This should be compared with 0.4 mm gaps, which was the permissible mean tolerance in the first three bridges constructed in Sweden with this type of deck. The results from these tests will be published in the final report of the RFCS project ELEM, which will be available in late 2012. [11]

The FE models as well as the measured data indicate that the vertical stress distribution is non-linear, especially near an open joint. Stress concentrations can be expected in the top of the steel beam. This should be kept in mind when designing this type of bridge, especially for fatigue loading. However, if the methods suggested

below are followed, the design should be on safe side.

The recommendations below are based on the test data available from just two different tests, carried out by LTU and RWTH, and further tests might give grounds for a revision of the recommendations.

When the resistance of a cross-section is checked, it is suggested to design the steel section to carry the whole load if the top fibre of the steel girder is in tension. For an in situ section, the resistance of the steel section plus the longitudinal reinforcement is normally used. This is generally the case in areas with hogging moments. However, prestressing forces can be used to keep the deck in compression in areas of hogging moments as well. If the top fibre of the steel girder is in compression, composite action can be assumed. However, it is suggested that different effective concrete widths be used for SLS and ULS. In ULS it is reasonable to use the effective concrete width according to [10], which is used on continuous deck slabs, since the influence of the joint gaps will diminish as the load increases. The plastic capacity in these sections will not be affected by small initial joint gaps (< 0.5 mm). In SLS and FLS the effective concrete width should be reduced in comparison to [10]. It is suggested that the distance L_e between the points of contraflexure for the bending moment be reduced to the distance between the outmost shear studs within one element.

Two possible reasons as to why the interacting concrete area in compression is limited to an area about twice as wide as the concrete channel have been discussed. In the first reason it is assumed that there are joint gaps that make the forces in the concrete enter and leave the element within a length equal to the maximum distance between the shear studs within the element. This assumption produces results close to the measured values. The other explanation is that the in situ channel and the concrete paste that leaks out and fills the joint gaps near the channel might make the initial gap more or less permanent outside this area. This part of the concrete will carry the total load until it is compressed up to the size of the gap, then the other concrete part will start to contribute to the load-

carrying capacity. Neither of these two explanations can be disproved by the test results.

References

[1] *Hällmark, P., White, H., Collin, P.*: Prefabricated Bridge Construction across Europe and America, ASCE – Practice Periodical on Structural Design and Construction, 2009, vol. 17, No. 3.

[2] *Ralls, M. L.* et al.: Prefabricated Bridge Elements and Systems in Japan and Europe, FHWA pub. No. FHWA-PL-05-003, pp. 64, Office of Engineering, Bridge Division, Washington DC, USA, 2005.

[3] *Gordon, S., May, I.*: Precast deck systems for steel-concrete composite bridges, Proceedings of the ICE – Bridge Engineering, 2007, vol. 160(1), pp. 25–35.

[4] *Collin, P., Johansson, B., Pétursson, H.*: Samverkansbroar med elementbyggda farbanor. Technical report, Swedish Institute of Steel Construction, pub. 165, 1998, ISBN 91 7127 022 1 (in Swedish).

[5] *Hällmark, R., Collin, P., Stoltz, A.*: Innovative Prefabricated Composite Bridges. Structural Engineering International, 2009, vol. 19, No. 1, pp. 69–78.

[6] *Stoltz, A.*: Effektivare samverkansbroar – Prefabricerade farbanor med torra fogar, licentiate thesis 2001:41, Luleå, Sweden, p. 188 (in Swedish).

[7] *Hällmark, P., Nilsson, M., Collin, P.*: Concrete shear keys in prefabricated bridges with dry deck joints, Nordic Concrete Research, 2011, vol. 22, No. 2, pp. 109–122.

[8] Betonghandboken – Konstruktion/ The Concrete Handbook, Svensk Byggtjänst, Stockholm, 1964.

[9] EN 1992-1-1. Eurocode 2 – Design of concrete structures – Part 1-1: General rules and rules for buildings, CEN, European Committee for Standardization, Brussels, 2005.

[10] EN 1994-2. (2005), Eurocode 4 – Design of composite steel and concrete structures – Part 2: General rules and rules for bridges, CEN, European Committee for Standardization, Brussels, 2005.

[11] *Möller F., Hällmark, R., Seidl, G.* et al.: Final Report – ELEM – Composite Bridges with Prefabricated Decks, RFSR-CT-2008-00039, technical report No. 6, 2011.

Authors:
Robert Hällmark MSc, Ramböll, Luleå, Sweden
Peter Collin, Professor, LTU/Ramböll, Luleå, Sweden
Peter.Collin@ramboll.se
Martin Nilsson PhD, LTU, Luleå, Sweden

PAPER VI

Strengthening Bridges with Postinstalled Coiled Spring Pin Shear Connectors: State-of-the-Art Review

Robert Hällmark, Paul Jackson, Peter Collin and Harry White

Strengthening Bridges with Postinstalled Coiled Spring Pin Shear Connectors: State-of-the-Art Review

Robert Hällmark[1]; Paul Jackson, Ph.D.[2]; Peter Collin[3]; and Harry White, P.E.[4]

Abstract: Many existing bridge structures experience much more significant loads and load cycles than were anticipated when the bridges were originally designed. An effective way to increase the load capacity and fatigue resistance of bridge structures with steel girders and a noncomposite concrete deck is to retrofit the structure with shear connectors to create a composite girder–deck structure. This article presents a state-of-the-art study of postinstalled shear connectors in general and coiled spring connectors in particular. The strengthening method is described, together with experiences from real bridge strengthening projects and a study of load capacity and structural behavior.

Author keywords: Shear connector; Composite action; Coiled spring pin; Bridge strengthening; Rehabilitation; Bridge.

Introduction

Many existing road bridges, all over the world, were not designed for the high service loads and the increased number of load cycles to which they are exposed to today. Complete replacement of all of these structures is impractical. To meet the ever-increasing demand, there will be a continuous need for strengthening bridges that are in good condition but may have slightly inadequate load capacity.

Today, steel girder bridges with concrete decks are normally designed as composite structures, with few exceptions. Some countries, like Sweden (STA 2016), make composite construction a requirement for structures of this type. However, even as late as the 1980s, steel girder bridges in Sweden were often constructed with a noncomposite concrete deck slab. One way of increasing the traffic load capacity for existing bridges of this type is to create composite action by connecting the concrete slab to the steel girders. This permits the steel girders to work with the concrete deck to carry traffic loads more efficiently than in the original noncomposite condition. Because the permanent loads are already in place, the effect will only influence the live loads and subsequent dead loads.

In the National Transport Administration's bridge management system in Sweden, Finland, and Norway, there are more than 2,000 noncomposite steel girder bridges in these three countries alone. This implies that there are many existing bridges with a potential for additional traffic load capacity if composite action can be created.

[1]Luleå Univ. of Technology, 971 87 Luleå, Sweden; Swedish Transport Administration, SE-781 89 Borlänge, Sweden.

[2]Ramboll, Ringwood Rd., Woodlands, Netley Marsh, Southampton SO40 7HT, UK.

[3]Professor, Luleå Univ. of Technology/Ramboll, 972 33 Luleå, Sweden.

[4]Engineering Research Specialist II, New York Dept. of Transportation, 50 Wolf Rd., Albany, NY 12232 (corresponding author). Email: hwhite@ dot.state.ny.us

Composite action can be achieved by many different types of shear connectors. Welded headed shear studs (WHSs) are by far the most common shear connector for newly constructed structures because the top flange is exposed, and the installation of the welded studs is quick and efficient. For existing structures, however, installing WHSs would require the removal of large sections of the concrete deck. Other types of connectors, especially connectors that can be installed from beneath the bridge without affecting the road surface, are more practical.

One type of such a connector is referred to as a coiled spring pin (CSP). The CSP has been found to provide excellent composite behavior using simple installation techniques that can be wholly accomplished from below the deck, without requiring the removal of any part of the concrete deck, and while subjected to live loads.

Postinstalled Shear Connectors

Postinstalled shear connectors are an excellent way to increase the load capacity of a bridge system with steel girders and a noncomposite concrete deck while also minimizing costs and impacts to the traveling public. To ensure composite action, various types of shear connectors have been used for postinstallation in existing steel–concrete structures. Although several types of postinstalled anchors are discussed herein, this list is by no means exhaustive. The examples shown are just to give the reader a basis for comparison between some of the most basic types.

The most common shear connectors for new steel–concrete composite bridges are undoubtedly WHSs, as shown in Fig. 1(a). Extensive research has been conducted on this type of shear connec- tor, and their design is covered by international material as well as design standards (CEN 2004, 2005; ISO 2008).

Strengthening of existing bridges by the installation of welded shear studs is possible but not practical. The strengthening work requires the removal of any overlay and waterproofing, water jetting to remove the existing concrete, installation of new welded shear studs, casting and curing of new replacement concrete, rewaterproofing, and resurfacing. During this time, the bridge area affected by the construction cannot be used. Note also that the concrete removal, especially for the fascia beams, must be performed in short intermittent stages because the transverse reinforcement may be inadequate to resist the bending moment from the weight of the slab
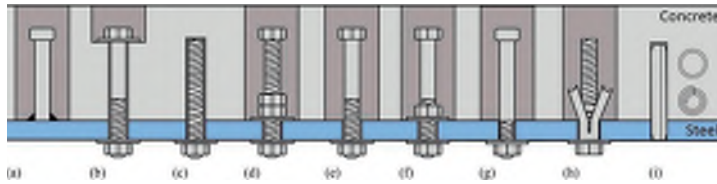
Fig. 1. Examples of different types of postinstalled shear connectors: (a) welded headed shear stud; (b) high-tension friction grip bolt; (c) adhesive anchor; (d) double-nut bolt; (e) bolt without embedded nut; (f) single-nut bolt; (g) threaded shear stud; (h) blind wedge or sleeve anchor bolts; and (i) interference-fit pins (slotted spring pin and coiled spring pin).

Fig. 2. Postinstallation of welded shear studs.

over longer stages. An example of the intermittent staging, taken from a project in Norway (Halden 2015) is shown in Fig. 2.

For structures with steel girders fabricated in the first half of the 20th century, welded shear connectors are not even possible because steel of that vintage is typically not suitable for welding. In these cases, other types of shear connectors must be used. There have been many studies of postinstalled shear connectors, many with a focus on partial composite action. Examples of such studies are presented in the following sections, which cover several types of shear connectors and include static and fatigue tests, finite- element analysis (FEA) computer modeling, full-scale beam tests, and strengthening projects on in-service bridges.

Friction grip bolts, as shown in Fig. 1(b), have been studied through laboratory tests and numerical analysis (Kwon 2008; Kwon et al. 2009; Chen et al. 2014; Liu et al. 2016). Similar tests and analyses have been done on adhesive anchors and the double-nut bolts, as shown in Figs. 1(c and d) (Kwon 2008; Kwon et al. 2009; Patel 2013; Ghiami Azad 2016; Kreitman 2016). The behavior of this type of connector has also been tested by field monitoring of two strengthened bridges (Kwon et al. 2009; Peiris and Harik 2016). The behavior of bolts with and without a single embedded nut, as shown in Figs. 1(f and e), has been compared to the behavior of WHSs of the same dimension (Dedic and Klaiber 1984). More recently, additional push-out tests combined with advanced numeri- cal modeling have been performed on bolts with single embedded nuts (Pavlovic et al. 2013).

Studies of demountable connectors, which are traditional shear studs machined and threaded in the lower part to enable them to be connected like bolts to the flange, as shown in Fig. 1(g), showed lower initial stiffness compared with welded studs of the same dimensions but similar behavior as welded studs for large-scale beam tests (Moynihan and Allwood 2014; Lam et al. 2013).

The use of blind wedge bolts, similar to what is shown in Fig. 1(h), has been studied to determine if they could be used as postinstalled composite connectors. The behavior of different blind bolts was evaluated by beam bending tests, push-out tests, and nonlinear finite-element analysis (Pathirana et al. 2015, 2016). The results indicated that the studied blind bolts could be used to create composite action, had higher shear capacity, and showed more ductile behavior than WHSs. The study did not include any fatigue testing.

Two examples of interference-fit shear connectors are slotted tension pins and coiled spring pins. The cross sections of these two types of pins are given in Fig. 1(i). The coiled spring pin is of most interest for bridge applications because the compressive stresses within the pin are more uniformly distributed compared with the slotted pin. Interference-fit, also referred to as press-fit or friction-fit, shear connector pins offer the possibility of converting a non-composite deck into a composite without interrupting the traffic on the bridge. This is possible because the pins are secured to the steel and concrete using only the force created by the compressed pin itself. It should be noted that chemical anchors, expansion bolts, and other types of postinstalled shear connectors also offer the possibility to complete the installation from below the bridge deck, but these types usually involve at least one work stage where the bridge is closed to live loads.

Coiled Spring Pins

A CSP is a type of tension pin or roll pin, as shown in Fig. 3. The static and fatigue behavior of coiled springs used to connect one steel part to another steel part is well known. The use of coiled spring pins as shear connectors in steel–concrete composite structures, where they will connect parts with completely different

Fig. 3. CSP and its cross section.

material properties, is not well documented. As such, CSPs have been used as fasteners in many industries for decades but are not a common shear connector in civil engineering structures (Pritchard 1992; Buckby et al. 1997).

Before installation, the unloaded CSP has a diameter slightly larger than the hole it will be installed in. At installation, the spring pin is compressed as it is forced into the smaller hole to achieve an interference fit. This is also sometimes referred to a press fit. After the installation, a radial spring force keeps the coiled spring pin connected to the steel and the concrete.

CSPs are a standard component, available in an outer-diameter range of less than 1 mm (0.039 in.) up to 20 mm (0.787 in.). The connectors available on the market are made from steel plates that are spirally wound 2.25 times around the central axis of the pin. The exact dimensions are governed by the international standard (ISO 2007). Only a few bridges around the world have been identified as using CSPs for strengthening purposes. All the bridge applications so far have used heavy-duty types of pins with an outer diameter of 20 mm (0.787 in.) and a steel plate thickness of 2.2 mm (0.087 in.).

Bridge Strengthening Projects

The typical reasons that a bridge would undergo a conversion from noncomposite to composite are to increase the live-load capacity of the beams/girders or to increase the fatigue resistance of the existing shear studs. A less typical reason, as will be outlined by the Swedish example, is an exception in which the shear connectors were installed to make the bridge silent. In addition to the projects presented in this article, the use of CSPs has been considered in additional bridge rehabilitation projects in the United Kingdom but has not been realized.

Docklands Light Railway

The first bridge application found in the literature is the upgrade of the Docklands Light Railway (DLR) in London in 1988. In the late 1980s, even before the new composite bridges were finished and opened to traffic, the projected traffic had increased eightfold. The increased load and number of load cycles significantly reduced the fatigue life of the shear studs, in some cases from 120 years down to 30 years. As a consequence, the existing shear connection had to be strengthened. To do this without disturbing the train traffic on the bridge, new shear connectors had to be installed from under the bridge deck.

Different solutions were considered and tested in a lab- oratory on push-out specimens. Both slotted tension pins and CSPs showed greater strength and fatigue capacity than the original welded shear studs of 19 mm (0.748 in.) in diameter, with the CSPs performing slightly better. As a result, CSPs were installed on the bridge (Pritchard 1992).

In 2008, the bridges were further strengthened with additional CSPs. This was done to increase the fatigue capacity due to increases in the number of trains and the number of cars per train. The design of the second strengthening was based on the outcome of the first DLR strengthening project and the knowledge achieved from the two projects that is presented in the two following sections. No new tests were performed.

Canadian Bridge

In the early 1990s, coiled spring connectors were considered for upgrading the fatigue life of a composite bridge on a light railway system in Canada. The tests previously performed for the DLR project were considered to be insufficient to validate the capacity of this type of connector in the Canadian multispan composite box-girder bridge. To gather more data on the load–slip behavior, under both static and cyclic loading, 15 tests were performed on push-out test specimens. The design of the strengthening of this bridge was based on these test results and the established design formulas. In 1995, the strengthening work was finished after 6 months of instal-lation, without any interruption of the traffic running on the bridge (Buckby et al. 1997).

Tinsley Viaduct

The Tinsley Viaduct in the United Kingdom is a steel–concrete box-girder road bridge that was strengthened with CSPs in 2001. Unlike the previous two projects, the Tinsley Viaduct was mainly strengthened for static load. Because the steel flange thickness [9.5– 17.5 mm (0.374–0.689 in.)] was far below the flange thicknesses tested for the DLR and the Canadian bridge [at least 25 mm (1 in.)], new laboratory tests were performed but have not been published.

Pitsund Bridge

The Pitsund Bridge is the only Swedish experience, so far, of CSPs used as postinstalled shear connectors. This seven-span continuous bridge was built in 1984, mainly as a noncomposite steel–concrete structure. The end spans of this bridge are above the riverbank, where a lot of residential houses are located. After a couple of years, nearby residents started to complain about loud (72- to 105-dB) banging sounds occurring in the early morning hours of the winter months. The bridge owner started several investigations, of which the final one suggested that the loud bangs were caused by sudden shear failures of unintentional composite action when the bridge was loaded by heavy trucks on winter mornings. The unintentional composite action was probably caused by an ice layer at the interference surface between the steel and the concrete, which developed during the cold winter nights when the traffic was low. To solve this problem, 1,200 coiled spring connectors were installed in 2006. Fig. 4 shows the bridge 10 years after the strengthening. Prior to the installation, other types of shear connectors were evaluated. Coiled spring pins were chosen because they could be installed from below, without affecting the waterproofing or riding surface. Since the installation of the pins, the bridge has been quiet (Olsson 2017).

Installation

The installation procedure for CSPs, illustrated in Fig. 5, generally includes the following steps: precision drilling, jacking, and corro-sion protection. There is some preliminary investigation work

required to identify the location of the transverse reinforcing bars in the bottom layer of the concrete slab to avoid drilling through them.

Precision Drilling

The holes must be drilled up vertically through the steel top flange and into the concrete deck. This can be done by using different drill bits for the steel and concrete or by using one diamond drill bit for the whole drilling operation. The wearing down of the bits can be a significant cost factor because the required tolerances are very tight. Fig. 5(c) presents the pin tolerances, prior to the installation, from the product data sheet provided by the manufacturer of the CSPs, 20 mm (0.787 in.) in diameter, that have been used in the laboratory tests and the projects. Previous research highlights that the tolerances of the holes must be tight to ensure proper field performance of the CSPs (Buckby et al. 1997). This can be challenging for the drill operators, but the required tolerances are achievable. For the DLR and the Canadian bridge presented previously, the hole diameters were allowed to vary between 19.85 and 20.25 mm (0.781–0.797 in.), which also was reported as the manufacturer's tolerances in these cases (Pritchard 1992; Buckby et al. 1997). For the Canadian bridge, this was achieved without exceeding the additional requirement of relative differences of 0.1 mm (0.004 in.) in diameter between the hole in the steel and the concrete. During the installation of approximately 2,500 pins, only 14 holes failed to meet these criteria. Holes that did not meet the tolerance requirements were abandoned, and new holes were drilled nearby (Buckby et al. 1997). Two of the authors of this paper, Hällmark and Collin, have used the same tolerances when fabricating push-out specimens with

Fig. 4. Pitsund Bridge after postinstallation of CSPs.

CSPs. The drilling was performed by an external drilling contractor, following the given specification of tolerances. After the drilling, all holes were measured. The results showed that the tolerances were met when drill bits with an outer diameter of 19.90 mm (0.783 in.) were used, whereas a few holes failed to fulfill the upper tolerance when 20.00-mm (0.787-in.) drill bits were used instead. The largest hole diameter measured was 20.31 mm (0.800 in.), and the test results showed no clear signs that this would have affected the ultimate load capacity.

Jacking

The pins are chamfered over a length of 4.5 mm (0.177 in.) on both ends to an end diameter less than 19.6 mm (0.772 in.), which is smaller than the recommended minimum hole size. This makes it possible to push the CSPs into the holes using a hydraulic jack to create an interference fit.

Lubricants have been used to lower the jacking force required for the installation of some of the pins (Pritchard 1992; Buckby et al. 1997). Laboratory tests indicate that the use of lubricants has a negligible effect on the ultimate load capacity, although the measured slip increases slightly (Buckby et al. 1997). These conclusions are supported by additional push-out tests with and without lubrication (Hällmark et al. 2017a).

The jacking force required to insert the CSPs in the drilled holes varied from 62 to 205 kN (14.0–46.1 kip) during the installation of the 2,500 CSPs in the Canadian bridge (Buckby et al. 1997). The authors of this article measured forces between 50 and 130 kN (11.3–29.25 kip) when jacking lubricated pins into push-out test specimens with varying hole diameters from 19.95 to 20.31 mm (0.785–0.800 in.).

Corrosion Protection

Once the installation is complete, it is important to seal the holes to prevent moisture from entering and corroding the CSPs. In the case of the Pitsund Bridge, penetrating corrosion protection was applied on the new steel surfaces after drilling. The coating system had a drying time of 24 h, which implies that it also had a lubricating effect because the installation of the pins was done directly after the drilling (Olsson 2017).

In one case, the coiled spring pins were recessed 2 mm (0.079 in.) into the steel flanges, and those recesses were filled by sealant before local repainting (Pritchard 1992). It should be noted that any reduction in the contact area between the steel flange and the coiled spring pin due to the pin chamfer or any recess must be considered
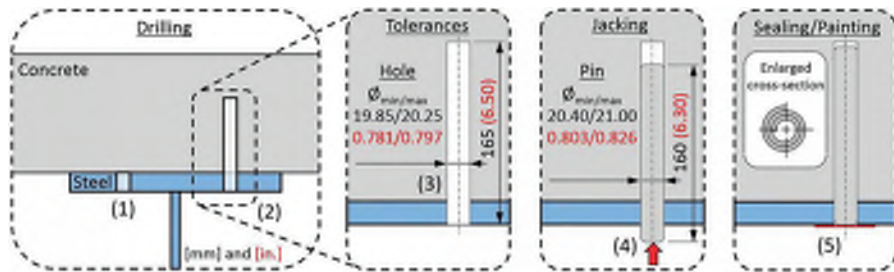

Fig. 5. Installation procedure.

in the design. This effect can be significant for thinner steel flanges where the chamfer and recess may make up a larger percentage of the available contact area. Similarly, the effect may be negligible for thicker plates.

Time and Costs. To gather information about the expenditure of time for the installation and the related costs, a case study of the Pitsund Bridge was done (Olsson 2017). This study was based on interviews with the bridge owner, the drilling contractor, and the engineer who designed the strengthening. The presented costs were gathered from invoices and exchange rates dated in 2006.

The moveable working platform, used by the drilling and jacking contractor, was long enough to permit the installation of approximately 30 CSPs before it needed to be moved. This was also the maximum number of holes drilled and pins able to be installed during a working day. At the beginning of the project, the average installation cost was approximately USD130 per pin, whereas it dropped to approximately USD 80 per pin at the end of the project. It should be noted that this was the first time the contractor worked with this type of strengthening and that there was a need to fabricate some support structures for the installation. The reduction in cost per pin during the project suggests that costs would be less from a contractor with experience performing this type of work (Olsson 2017).

Load Capacity. This section focuses on the load capacity of the CSP shear connector. However, the capacity of the reinforced concrete deck must also be checked according to applicable design codes. As presented earlier, some tests have been performed for projects where CSPs were used. All tests have been done with coiled spring pins with a 20-mm (0.787-in.) diameter and of the heavy-duty type.

It should be noted that the push-out tests reported on CSPs, so far, have all been done on nonconventional push-out test specimens (Pritchard 1992; Buckby et al. 1997; Hällmark et al. 2017a; Fahleson 2005). The authors of this article, and also Pritchard and Buckby, did not use the conventional push-out test because the limited space between the flanges in the standard test setup makes it hard to drill and drive the CSPs into the holes. Fig. 6 illustrates the specimens used by Hällmark in 10 static push-out tests. Similar specimens have been used by Buckby and Fahleson. In this type of specimen, the force is applied on a central concrete block attached to two steel plates by shear connectors. This design enables an easier installation of the postinstalled shear connectors because there are no obstacles for the drilling and jacking equipment.

Static Capacity. Fig. 7 summarizes the static push-out test results on CSPs published so far. The failure load per pin (P_U) is plotted over the mean value of the associate compressive cylinder strength ($f_{cm,cube}$) of the concrete. The tested steel plate thickness is also presented in the label of each test series.

Pritchard (1992) reported that the theoretical static strength (single shear) for CSPs was 170 kN (38.2 kip), which was higher than the 139 kN (31.2 kip) achieved by the welded studs of 19-mm (0.75-in.) diameter, although no detailed information on the test results was given. The tests were performed on pins connecting two steel plates of 35-mm (1.38-in.) thickness and a concrete block with a specified strength of 40 MPa (5.80 ksi). Buckby performed three similar tests but with varying steel plate thicknesses (Buckby et al. 1997). Based on these test results, Buckby recommends that a nominal static strength of 130 kN (29.2 kip) is used for pins installed in C30/37 concrete (f_c' approximately 4 ksi) and for steel flange thicknesses in the range of 25–35 mm (1.0–1.38 in.). This recommendation is illustrated as a dashed line in Fig. 7, and the test series that meets the associated criterion of the steel plate thickness is given with gray markers. Fahleson (2005) reports an ultimate load of 198 kN (44.5 kip) per pin. This value is based on a single test with a steel flange thickness of 30 mm (1.18 in.) and a concrete cube strength of 56 MPa (8.12 ksi). Tests performed for the Tinsley Viaduct project and the Chelsea River Bridge project, both in the United Kingdom, have also been studied and evaluated by one of the authors in 2007 and 2011, respectively. For the Tinsley Viaduct, six tests were performed with coiled spring pins through steel plates of 17.5-mm (0.69-in.) and 9.5-mm (0.37-in.) thicknesses. The three tests with the 17.5-mm (0.69-in.) steel plates gave a mean load capacity of 248 kN (55.8 kip) per pin, whereas the three tests with the 9.5-mm (0.37-in.) plates gave a mean load capacity of 140 kN (31.5 kip) per pin. The mean concrete compressive cube strengths were 51 MPa (7.40 ksi) and 54 MPa (7.83 ksi), respectively. For the Chelsea River Bridge project, two static load tests were performed with a steel plate thickness of 6 mm (0.24 in.), giving the load capacity of 84 kN (18.9 kip) and 89 kN (20.0 kip) per pin. The corresponding concrete cube strengths were 37.8 MPa (5.48 ksi) and 40.1 MPa (5.82 ksi), respectively. Recently, Hällmark et al. (2017a) performed five additional push-out tests on CSPs. The dimensions of the specimens are illustrated in Fig. 6. The concrete cube strength was 46 MPa (6.67 ksi), and the characteristic value of the ultimate capacity was established as 132 kN (29.7 kip), in line with the method described in Annex B of Eurocode 4 (CEN 2004). These
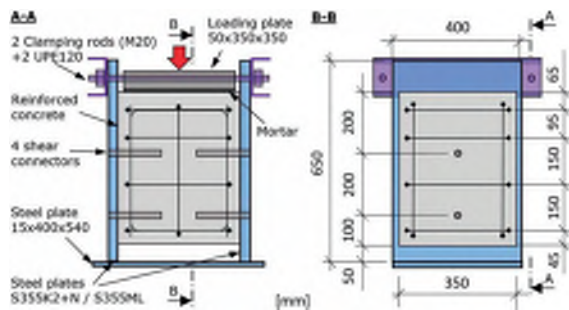

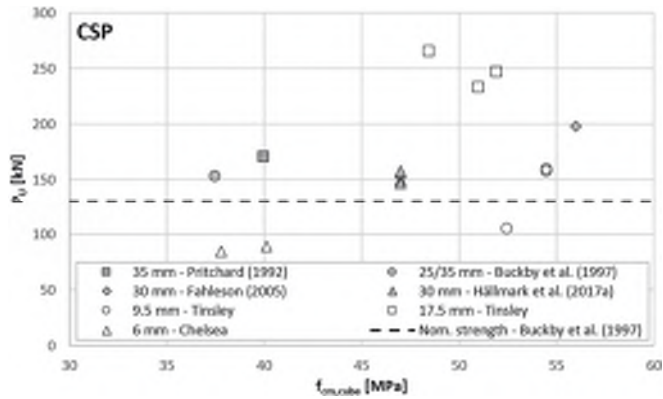Fig. 6. Push-out test specimen (dimensions are in mm).
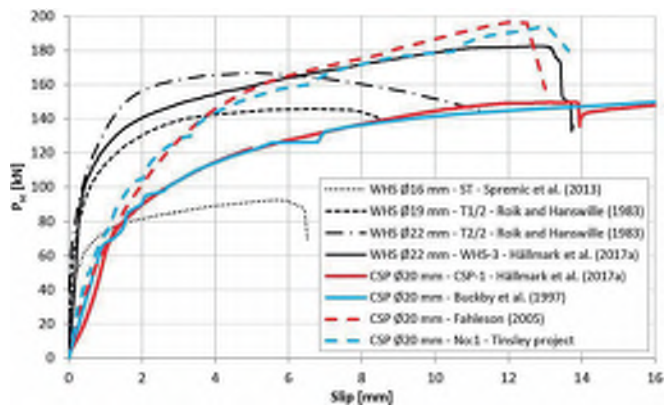
Fig. 7. Static test results.

Fig. 8. Load–slip curves for push-out tests on specimens with CSPs and WHSs, respectively (diameter in mm).

tests were complemented by five tests on specimens with WHSs to evaluate the potential impact of the nonstandard test setup.

For the majority of the tests presented previously, the main failure mechanisms were failure of the concrete surrounding the pins and extensive yielding of the CSPs. In some cases, the pins failed at plastic slip levels that by far exceed the requirements of ductility given in Eurocode 4 (CEN 2005). The specimens with steel plate thicknesses of 6 and 9.5 mm showed a slightly different failure mode, with extensive yielding at the contact surface between the pins and the steel plates before the final failure of the specimens.

Typical load–slip curves for the push-out tests with CSP are illustrated in Fig. 8. The curves are re-created from the data presented by Buckby et al. (1997), Hällmark et al. (2017a), and

Fahleson (2005) and from additional tests evaluated by the authors. To highlight the differences compared with the headed shear studs, typical load–slip curves for different stud dimensions are included in the diagram.

From Fig. 8, it can be noted that there was a significant difference in the initial stiffness of the CSPs compared with the WHSs. For the specimens tested with the nonconventional push-out test, it can also be noted that the force continued to increase at high levels of plastic slip, which was not the case for the specimens with WHSs tested with the standard push-out test (CEN 2004). This behavior can probably be explained by the existence of clamping forces, provided by the tension rods shown in Fig. 6, and the corresponding steel strips that were used in the tested specimens (Buckby et al.

1997; Fahleson 2005). All tests on CSPs that have been found in the literature, including those known by the authors but not yet published, have been done with some type of clamping.

Fatigue Capacity

Fatigue tests have been performed on CSPs (Pritchard 1992; Buckby et al. 1997; Fahleson 2005). Additional fatigue tests are known by the authors, but these results have not been published in public reports. A compilation of the fatigue tests known so far is given in Fig. 9, which contains fatigue test data from four different projects, with different views of when the fatigue failure occurred. In the case of the first strengthening of the DLR and also the Pitsund

Bridge, failure was defined as the physical fracture of a CSP. For the Tinsley Viaduct, it was decided to interpret a slip of 5 mm as a fatigue failure. Buckby et al. (1997) had a similar approach but used a slip of 2 mm (0.078 in.) as the fatigue criterion.

Normally, the fatigue resistance of shear elements is given in terms of the stress range. This is done because most shear studs are circular in cross section, and the calculation of their shear area is straightforward. In contrast, the manufacturers of CSPs generally list only the outside diameter in their literature, and the thickness can only be found in the product standard. The determination of the CSP area, given the rather complex clothoid spiral cross-sectional geometry, is complex and makes transforming the shear forces into
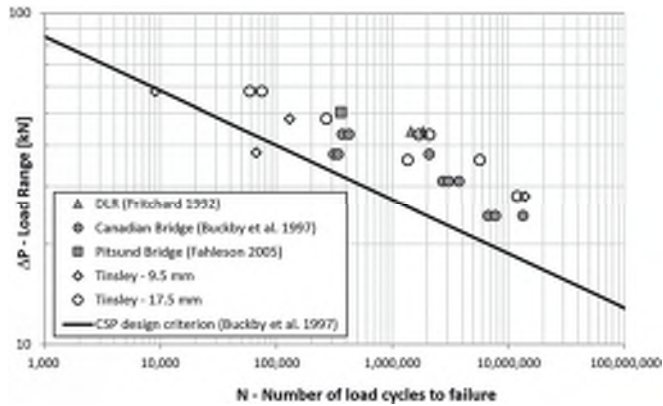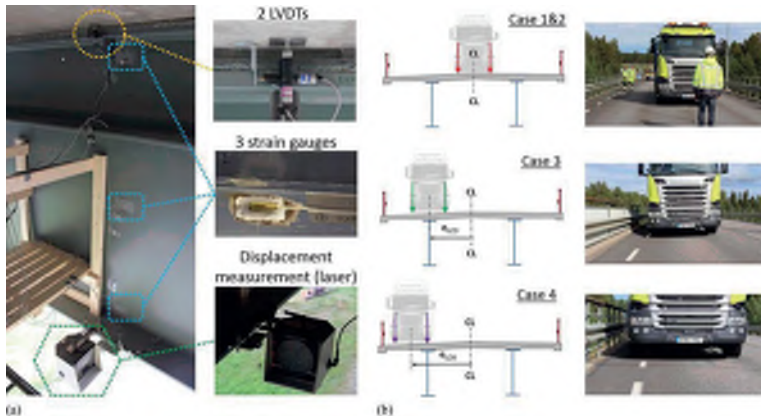

Fig. 9. Compilation of fatigue test results.

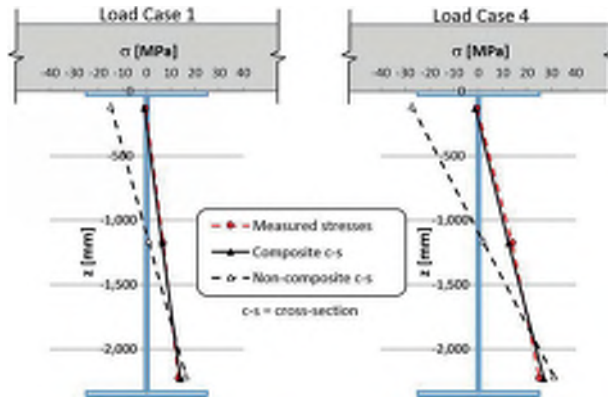Fig. 10. Monitored span in the Pitsund Bridge.

Fig. 11. Measured steel stresses versus theoretical stresses for composite and noncomposite cross sections.

shear stresses difficult. Therefore, in this article, the fatigue capacity for CSPs is considered in terms of the load range (ΔP) on a *P-N* curve instead of the stress range ($\Delta \tau$) on an *S-N* curve.

Buckby presents a formula [Eq. (1)] to estimate the fatigue life of the connectors, assuming a steel plate thickness between 25 and 35 mm (1.0–1.38 in.) and a concrete strength class corresponding to C30/37 (f_c' approximately 4 ksi) (Buckby et al. 1997).

$$\text{Log}_{10}N = 14.767 - 6.1\,\text{Log}_{10}\Delta P \qquad (1)$$

where ΔP = load range (kN) on one CSP; and N = number of cycles until failure.

Long-Term Behavior

Static and fatigue tests have been performed by different researchers, but no other type of long-term tests have been conducted in laboratory so far. The strengthened bridges, however, offer a possibility to study the long-term behavior of this type of shear connection. One possible long-term effect, not covered by the fatigue tests, might be loss of the clamping force between the concrete and the steel due to creep in the concrete.

To study the behavior of this type of shear connection in a real structure, the Pitsund Bridge was monitored by the authors in 2016 (Hällmark et al. 2017b). Because the monitoring was done 10 years after the installation of the shear connectors, it offered the possibility to see if there were any indications of different behavior compared with the laboratory tests. The bridge was monitored regarding the longitudinal strains in the steel girders at different vertical and longitudinal positions. The slip at the steel–concrete interface was also measured, together with the midspan deflection. The instrumentation of the midspan bridge section is shown in Fig. 10(a). The only vehicle allowed to be on the bridge during the monitoring was the test vehicle, which was a four-axle truck with a total weight of 31.4 tonnes (34.6 t). The truck was positioned in several predetermined locations on the bridge deck while the measurements were taken [Fig. 10(b)].

The results from the measurements indicated no signs of weaker long-term behavior of the shear connection. It should be noted that for many sections and load positions, this type of loading introduces

a significant normal force acting on the steel–concrete interface. This results in a positive frictional force, which does not exist in the push-out tests. The measured vertical strain distributions in the steel girders, as shown in Fig. 11, indicate a neutral axis that corresponds well to a theoretical composite section (CEN 2005) for a monitored midspan beam section with the vehicle positioned at midspan for Load Cases 1 and 4, as shown in Fig. 10. The steel strains have been transformed to stresses by Hooke's law, assuming an elastic modulus of 210 GPa (30,458 ksi). The measured slip under the traffic load was less than 0.04 mm (0.0016 in.), and the vertical separation was less than 0.03 mm (0.0011 in.). There were no signs of rapid increases in slip when the test vehicle crossed the bridge. A rapid increase could have been an indication that the friction capacity was exceeded and that the connectors were activated after a small initial slip.

Structural Behavior

Coiled spring pins can be used to either create or strengthen the shear connection between steel girders and a concrete deck. When a shear connection is being created, there will be only one type of shear connector at the shear interface, which makes the establishment of design assumptions a rather straightforward process. However, because there are no heads on the coiled spring connectors, uplift forces could be an issue.

When a structure is being strengthened for insufficient fatigue capacity in an existing shear connection, there will be at least two different kinds of shear connectors at the shear interface. This requires that the actual distribution of shear forces between the different shear connectors be established because the fatigue life will be highly dependent on the relative stiffness of the different connectors. Therefore, it is crucial to establish design criteria that cover the worst-case scenario for both the existing shear studs and the subsequently installed coiled spring pins. For the second strengthening of the DLR bridges, because of the wide range of stiffness observed in tests on the pins, a range of relative stiffness for the pins and studs was considered to cover the worst case for both the new pins and the existing welded studs. In this case, the design was always governed by the fatigue life of the original studs so that minimum pin stiffness governed the design.
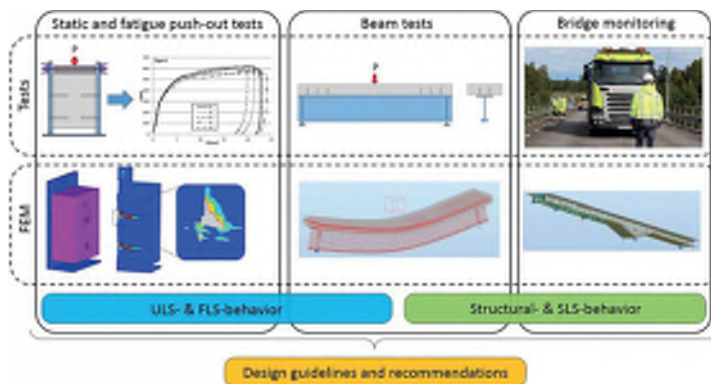
Fig. 12. Overview of the ongoing research on CSPs used as postinstalled shear connectors.

Conclusion

This article presents several types of shear connectors suitable for postinstallation to strengthen existing steel–concrete structures with no, or insufficient, shear connection. If the steel is weldable, and it is possible to partially or completely close the bridge without a significant impact on the traffic, welded shear studs might be a good choice. This is especially true if the waterproofing layer is going to be replaced anyway. If the steel is not weldable, or if fatigue is crucial in the shear connectors or in the upper flange, bolted shear connectors may be a better choice. To reduce the impact on traffic, shear connectors that are installed from below can be used, such as adhesive anchors or interference-fit connectors. These types of postinstalled shear connectors may not be the mainstream solution but are a good option in situations when reduced traffic impact is a high priority. The strengthening works done at the DLR, the Canadian bridge, and the Pitsund Bridge show that it is possible to perform the installation of CSPs while eliminating most, if not all, impacts on traffic.

The installation procedure for CSPs involves tight hole tolerances to ensure the interference fit. Nevertheless, experiences from real bridges and from the manufacturing of test specimens show that the required tolerances can be achieved during field operations.

The static load capacity of the CSPs is dependent on several parameters. To develop general guidelines for the design of this type of shear connector, more information needs to be gathered. If the type of the CSP is kept constant [20-mm (0.787-in.) diameter, heavy-duty type], the most important parameters are the thickness of the top flange steel plate, concrete strength, and hole tolerances.

A formula to estimate the fatigue life of CSPs has been presented. This formula is based on the test results from 12 fatigue push-out tests and applies to the studied type of CSP and a limited span of steel plate thicknesses and concrete strength.

Future Research

This article is a part of the outcome of the state-of-the-art review of CSPs used as shear connectors in steel–concrete bridges. Future research will be performed, with the aim of developing design guide- lines and recommendations for bridge retrofitting by the use of

CSPs. Fig. 12 gives a schematic overview of the upcoming research, which includes additional static and fatigue push-out tests, field monitoring of a strengthened bridge, and large-scale beam tests. All tests will be supplemented by finite-element analysis, which will be calibrated to the test results and used for parametric studies.

To get more test data on CSPs, 20 static push-out tests and 12 fatigue tests will be performed. The tests will be done with varying parameters, such as steel flange thickness, concrete strength, and hole tolerances. The influence of the possible clamping effect, in the non- conventional push-out tests, will be studied in future research. The push-out tests will be complemented by numerical modeling and three large-scale beam tests. The question of potential uplift, because the pins have no heads, will be investigated in the beam tests.

The criteria of what constitutes fatigue failure for a CSP must be established. Some researchers who have studied the strengthening of existing shear connections with insufficient fatigue capacity have set limits on the allowable amount of slip as the design criteria based on the reasoning that CSPs and welded headed shear studs have a similar stiffness at small slips. New tests performed by the authors of this article indicate that CSPs need an initial slip to compress the pin and activate the stiffening behavior. To find out to what extent it is reasonable to assume that the CSPs will contribute to the shear transfer under fatigue loading, further testing and finite-element modeling will be performed.

Acknowledgments

References

Buckby, R., M. Ogle, R. P. Johnson, and D. Harvey. 1997. "The performance of coiled spring pin connectors under static and fatigue loading." In *IABSE*

Proc., Int. IABSE Conf. on Composite Construction—Conventional and Innovative, 669–674. Zurich, Switzerland: International Association for Bridge and Structural Engineering.

Dedic, D. J., and F. W. Klaiber. 1984. "High-strength bolts as shear connectors in rehabilitation work." *Concr. Int.* 6 (7): 41–46.

CEN (European Committee for Standardization). 2004. *Design of composite steel and concrete structures, part 1.1*. Eurocode 4. Brussels, Belgium: CEN.

CEN (European Committee for Standardization). 2005. *Design of composite steel and concrete structures, part 2*. Eurocode 4. Brussels, Belgium: CEN.

Chen, Y. T., Zhao, Y., West, J. S., & Walbridge, S. (2014). Behaviour of steel–precast composite girders with through-bolt shear connectors under static loading. *Journal of Constructional Steel Research, 103*, 168-178.

Fahleson, C. 2005. *Provning av skjuvförbindare*. [In Swedish.] Rep. No. 05035. Luleå, Sweden: Luleå Univ. of Technology.

Ghiami Azad, A. R. 2016. "Fatigue behavior of post-installed shear connectors used to strengthen continuous non-composite steel bridge girders." Ph.D. thesis, Dept. of Civil, Architectural and Environmental Engineering, Univ. of Texas at Austin.

Halden, J. 2015. "Strengthening of steel bridges, examples from Norway." In *Proc., Int. Workshop on Strengthening of Steel/Composite Bridges*, 46–54. Luleå, Sweden: Luleå Univ. of Technology.

Hällmark, R., P. Collin, and M. Möller. 2017a. "Testing of coiled spring pins as shear connectors." In *Proc., IABSE Symp. Engineering the Future*, 1201–1208. Zurich, Switzerland: International Association for Bridge and Structural Engineering.

Hällmark, R., P. Collin, M. Petersson, and E. Andersson. 2017b. "Monitoring of a bridge strengthened with post-installed coiled spring pins." In *Proc., IABSE Symp. Engineering the Future*, 1193–1200. Zurich, Switzerland: International Association for Bridge and Structural Engineering.

ISO. 2007. *Spring-type straight pins—Coiled, heavy duty*. ISO 8748:2007. Geneva: ISO.

ISO. 2008. *Welding—Studs and ceramic ferrules for arc stud welding*. ISO 13918:2008. Geneva: ISO.

Kreitman, K. 2016. "Strengthening continuous steel girder bridges with post-installed shear connectors and inelastic moment redistribution." Ph.D. thesis, Dept. of Civil, Architectural and Environmental Engineering, Univ. of Texas at Austin.

Kwon, G., M. D. Engelhardt, and R. E. Klingner. 2009. "Strengthening bridges by developing composite action in existing non-composite bridge girders." Struct. Eng. Int. 19 (4): 432–437.

Kwon, G. U. 2008. "Strengthening existing steel bridge girders by the use of post-installed shear connectors." Ph.D. thesis, Dept. of Civil, Architectural and Environmental Engineering, Univ. of Texas at Austin.

Lam, D., X. Dai, and E. Saveri. 2013. "Behaviour of demountable shear connectors in steel-concrete composite beams." In *Proc., Int. Conf. on Composite Construction in Steel and Concrete VII*, 618–631. Reston, VA: ASCE.

Liu, X., Bradford, M. A., Chen, Q. J., & Ban, H. (2016). Finite element modelling of steel–concrete composite beams with high-strength friction-grip bolt shear connectors. *Finite Elements in Analysis and Design, 108*, 54-65.

Moynihan, M. C., and J. M. Allwood. 2014. "Viability and performance of demountable composite connectors." *J. Constr. Steel Res.* 99: 47–56.

Olsson, D. 2017. "Achieving composite action in existing bridges: With post-installed shear connectors." M.S. thesis, Dept. of Civil, Environmental, and Natural Resources Engineering, Luleå Univ. of Technology.

Patel, H. V. 2013. "Strengthening of non-composite steel girder bridges with post-installed shear connectors: fatigue behavior of the adhesive anchor." M.S. thesis, Dept. of Civil, Architectural and Environmental Engineering, Univ. of Texas at Austin.

Pathirana, S. W., B. Uy, O. Mirza, and X. Zhu. 2015. "Strengthening of existing composite steel-concrete beams utilising bolted shear connectors and welded studs." *J. Constr. Steel Res.* 114: 417–430.

Pathirana, S. W., B. Uy, O. Mirza, and X. Zhu. 2016. "Bolted and welded connectors for the rehabilitation of composite beams." *J. Constr. Steel Res.* 125: 61–73.

Pavlovic, M., Z. Markovic, M. Veljkovic, and D. Budevac. 2013. "Bolted shear connectors vs. headed studs behaviour in push-out tests." *J. Constr. Steel Res.* 88: 134–149.

Peiris, A., & Harik, I. (2014). Steel bridge girder strengthening using postinstalled shear connectors and UHM CFRP laminates. Journal of Performance of Constructed Facilities, 29(5).

Pritchard, B. 1992. *Bridge design for economy and durability: Concepts for new, strengthened and replacement bridges.* London: Thomas Telford.

Roik, K., and G. Hanswille. 1983. "Beitrag zur Bestimmung der Tragfähigkeit von Kopfbolzendübeln." [In German.] *Stahlbau* 52 (10): 301–308.

Spremic, M., Z. Markovic, M. Veljkovic, and D. Budjevac. 2013. Push-out experiments of headed shear studs in group arrangements. *Adv. Steel Constr.* 9 (2): 139 –160.

STA (Swedish Transport Administration). 2016. *Swedish bridge requirements*. [In Swedish.] TDOK 2016:0204. Borlänge, Sweden: Swedish Transport Administration.

PAPER VII

Post–Installed Shear Connectors: Monitoring a Bridge Strengthened with Coiled Spring Pins

Robert Hällmark and Peter Collin

Post-Installed Shear Connectors: Monitoring a Bridge Strengthened with Coiled Spring Pins

Robert Hällmark, ⬡ MSc., Department of Civil, Environmental and Natural Resources Engineering, Luleå University of Technology & Swedish Transport Administration, Luleå, Sweden; **Peter Collin,** Prof., Department of Civil, Environmental and Natural Resources Engineering, Luleå University of Technology & Ramböll, Luleå, Sweden. Contact: robert.hallmark@ltu.se

Abstract

Traffic density and vehicle weight have been increasing over time, which implies that many existing road bridges were not designed for the high service loads and increased number of load cycles that they are subjected to today. One way to increase the traffic load capacity of non-composite steel–concrete bridges is to post-install shear connectors. This paper presents a study of a steel–concrete bridge that has been strengthened with post-installed coiled spring pins, a type of connector which can be installed from below while the bridge is still in service. The strengthening method and design procedure are presented, along with the results from field monitoring performed to evaluate the behaviour of the strengthened structure. The results from the strengthened and non-strengthened sections show that the coiled spring pins counteract the slip and increases the degree of composite action. Finite-element models of the field tests were created in order to compare the results using different design assumptions and establish a suitable level of detail for modelling the shear connectors.

Keywords: shear connector; composite action; monitoring; strengthening; coiled spring pin.

Introduction

There are many existing steel–concrete non-composite bridges which were designed in the era before composite bridges and are still in service today. Since traffic loads and the number of load cycles tend to increase over time, some of these bridges will need to be strengthened or replaced in the near future. If the main reason for strengthening is due to the main steel girders having insufficient load capacity, the introduction of composite action could be considered as an appropriate strengthening method. Different types of shear connectors can be used for post-installation and the most suitable choice for a specific bridge is dependent upon several factors. If there is a need for a major rehabilitation of the concrete deck, there will be traffic disturbances regardless of which type of shear connector is installed. In such cases, welded studs might be the first alternative to use if the steel is weldable. When the bridge deck slab is in good condition however and the only reason for strengthening is insufficient global moment capacity, it is beneficial to be able to install the shear connectors

with no or only minor traffic disturbances. Examples of shear connectors suitable for post-installation are presented in Ref. [1]. Expansion bolts and adhesive anchors are two examples of shear connectors that can be installed from beneath the concrete deck.[2–6] Another interesting type of shear connector that can be installed from below the bridge deck, while the bridge still is in service, is the coiled spring pin (CSP). Such an installation is possible since the CSP is connected to the steel and the concrete only by means of the radial force created by the compressed pin itself. CSPs are made from steel plates that are spirally wound 2.25 times around the central axis of the pins (*Fig. 1a*). Before installation, the CSP has a diameter that is larger than the hole into which it will be installed. At installation, the CSP is compressed when it is jacked into the smaller hole to achieve an interference fit, a procedure that is described in more detail in Ref. [1]. CSPs are available on the market and have been used as fasteners in different industries for several decades—but they are not commonly used as shear connectors in steel–concrete composite structures.[7,8]

The research preformed on CSPs for civil-engineering applications is summarised in Ref. [1].

The static capacity and fatigue capacity of CSPs that are used as shear connectors between steel and concrete are studied in Refs. [7–10]. The CSPs show very ductile behaviour under static loading as well as a longer fatigue lifetime when compared to welded headed shear studs with the same cross-sectional area, mainly due to the absence of welds in the shear connection. The CSPs transfer shear forces from the steel to the concrete, in which inclined compression struts are developed around the lower part of the CSPs where the concrete is crushed. As the loads increase, the local concrete crushing will result in additional bending in the CSPs. The transfer mechanisms are expected to be similar to the ones described in Ref. [11] for welded headed shear studs, with the difference that the absence of heads implies that only frictional forces acting on the perimeter of the CSPs will counteract vertical movements of the upper end of the pin. This component is negligible in comparison to the tensional force developed in a loaded headed stud, implying that the favourable frictional contribution at the steel–concrete interface will also be negligible.

All tests reported so far are push-out tests used to establish the load-slip behaviour of the connection; however, push-out tests might be too conservative in comparison to beam tests.[12] Ref. [13] presents some examples of modified push-out tests, carried out in order to obtain better agreement with beam tests. Some of these modifications are taken into consideration in the new push-out tests performed on CSPs in Ref. [10]; there is however still uncertainty about how the CSPs behave on a structural scale. One significant difference between CSPs and headed shear
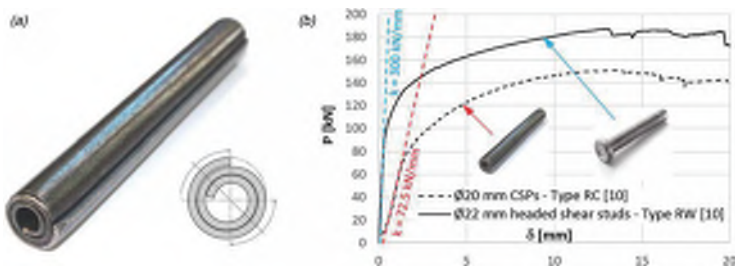
Fig. 1: (a) Coiled spring pin; (b) load-slip diagrams for CSPs and headed studs

studs is the initial stiffness of the connectors; comparisons of the push-out tests performed in Ref. [10] indicate that the initial stiffness of headed shear studs with a diameter of 22 mm is about four times that of the studied CSPs with a nominal diameter of 20 mm (*Fig. 1b*). For the CSPs there is also a tendency for an S-shape to occur at the beginning of the load-slip curve obtained from the push-out tests. This implies that it is not obvious that CSPs can fulfil the requirements given in Ref. [14] to provide the amount of stiffness sufficient to enable the steel and concrete parts to be treated as a single structural member. In order to investigate this, the Pitsund Bridge in Sweden has been monitored. As far as the authors know, this bridge is one of only a few bridges in the world that has been strengthened with CSPs; other such bridges that have been identified are located in Canada and the United Kingdom (UK).[1]

This paper describes the monitoring of the Pitsund Bridge and the evaluation of the test results, together with a comparison between different design assumptions regarding the shear connection. The results provide information about the structural behaviour in the serviceability limit state (SLS), while future large-scale beam tests are planned to investigate the behaviour in the ultimate limit state (ULS).

The Pitsund Bridge

The Pitsund Bridge is a seven-span bridge with a total length of 399 m and a free width of 9 m (*Fig. 2*). The superstructure is divided into three separate parts. The first four and last two spans consist of continuous steel girders with a concrete deck slab on top, whereas the fifth span is movable, designed as a bascule bridge with two leaves. This is an independent structure and outside the scope of this paper.

Background

As late as the 1980s, non-composite slabs were the common way to construct concrete decks on steel girder bridges in Sweden. The Pitsund Bridge was finished in 1984 and its original design featured spans both with and without composite action. *Figure 2* illustrates the different types of shear connections along the bridge. In the red part, there are no shear connectors, except right above the supports where steel strips welded to the steel upper flanges provide local connections (*Fig. 3*). In the blue part, the bridge was designed as a composite structure with welded headed studs. The black part was originally designed with no composite action, but was strengthened in 2006 by the post-installation of shear connectors.

Welded headed studs were the first type of shear connector to be evaluated in the strengthening project, but since the bridge deck was in good condition, focus was shifted towards shear connectors that enabled an installation procedure from below, meaning that the pavement and waterproofing could be kept intact. After evaluating several types of shear connector, two types were investigated in more detail: injection bolts and CSPs. The injection bolts are made of S355 steel with an outer diameter of 36 mm and an inner diameter of 16 mm. The studied CSPs are made of steel grade AISI 6150 with an outer diameter of 20 mm and a steel plate thickness of 2.2 mm. This type of CSP is labelled *heavy duty* and the pin dimensions are governed by an international standard.[15] All information presented in this paper applies to this type of CSP and the dimensions presented above.

Two static push-out tests were performed in 2005 to evaluate the installation procedure and get an indication of the load capacity of the two types of shear connector. The layout of the test specimens were the same as the tests reported in Ref. [8], while the details about the tests and the results are presented in Ref. [9] and briefly summarised below. The CSPs failed at a load of 198 kN/pin after a slip of
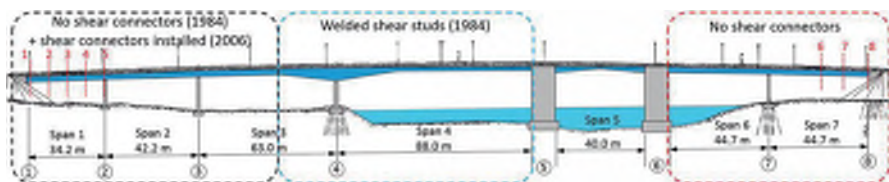

Fig. 2: Elevation drawing of the Pitsund Bridge illustrating the different types of shear connection
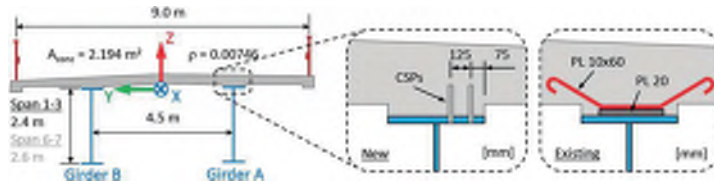
Fig. 3: Typical cross section of the superstructure and illustration of the shear connections

12 mm, while the much stronger injection bolts were loaded up to 364 kN/pin. In the latter case, the test was aborted at a slip larger than 35 mm due to limitations in the test set-up. In both cases, the concrete cube strength was within the interval of 56.1 to 56.8 MPa.

The information gained from manufacturing the test specimens indicated that it would be easier to install the CSPs, as this would avoid the need for different steel parts and for grouting. These experiences and the fact that the CSPs show a sufficient load capacity, even though significantly lower than the injection bolt, resulted in the choice of using CSPs to strengthen the bridge.

The shear connection was designed to withstand the shear forces caused by traffic and temperature in the ULS. Concrete shrinkage was neglected in the design of the shear connection, since the concrete was cast more than 20 years before the CSPs were installed. The design values of the traffic loads, in both ULS and fatigue limit state (FLS), are in line with the requirements for new bridges in the prevailing Swedish bridge code.[16] It should also be noted that the bridge designer only used the elastic capacity of the composite section in the design of the strengthening process.

Since only a single push-out test was performed within the frames of the strengthening project, the design of the CSPs was also checked against the recommendations given in Ref. [8], which specify a nominal static strength of 130 kN for pins installed in C30/37 concrete and for steel flange thicknesses in the range of 25 to 35 mm. Regarding the fatigue capacity, the recommendations in Ref. [8] were evaluated together with an additional fatigue test reported in Ref. [9]. The design requirement was that the bridge should resist 100 000 fatigue load cycles, in line with the requirements in Ref. [16] for road bridges with moderate traffic volumes. The fatigue design capacity (ΔF_R) was set to 50 kN/CSP for 100 000 cycles, based on the test reported in Ref. [9] that failed after 369 000 cycles at 50 kN/pin. A more conservative value of 40 kN/pin for 100 000 cycles is presented in Ref. [8].

The longitudinal distances between the shear connector rows were adapted to the distance between the transversal reinforcement in the bottom layer, while the number of connectors in each row was adapted to the design shear forces. This resulted in a row distance of 300 mm and 1200 post-installed CSPs, which equals a mean of 5.8 CSPs/m in each girder.

Bridge Data

The cross-sectional geometry of the monitored parts of the bridge and the definition of the coordinates system are illustrated in *Fig. 3*, in which some cross-sectional parameters are also presented. It should be noted that the edge beams are included in the concrete area A_{conc} and that the given reinforcement ratio ρ is representative of the support cross sections, where it can be assumed that the concrete is cracked. In *Table 1*, steel girder dimensions are presented for the monitored sections in Spans 1 and 7. The origin of the coordinates system used throughout this paper is located in the centreline of the bridge at Support 1, with increasing x-values towards Support 4. The vertical z-axis is positive upwards with its zero at the interface between the steel and the concrete. The two I-girders are referred to as Girders A and B, in line with the name convention presented in *Fig. 3*.

Monitoring

In 2016, the Pitsund Bridge was monitored in order to study the structural behaviour of a bridge strengthened with CSPs and determine to what extent composite action is achieved under service loading. The monitoring was focused on four topics: (a) the vertical distribution of the longitudinal strains in the steel main girders, (b) the horizontal slip at the steel–concrete interface, (c) the vertical separation (uplift) at the steel–concrete interface, and (d) the vertical displacement of the main girders (deflection).

Two spans with different shear connections were monitored: Span 1 with post-installed CSPs and Span 7 without shear connectors (*Fig. 2*). These spans have similar dimensions on the steel and concrete parts (*Fig. 3*, *Table 1*), which offers the possibility to compare the behaviour of a non-strengthened section with a strengthened section. The monitored sections are defined in *Table 2* and illustrated as red lines in *Fig. 2*. The

Steel girder	Span 1				Span 7			
	Mid-span		Support 2		Mid-span		Support 8	
	W/D*	T	W/D	T	W/D	T	W/D	T
Top flange	550	30	650	35	580	40	550	40
Web	2300	13	2300	18	2500	14	2500	15
Bottom flange	550	30	650	35	580	40	550	40

*T = steel plate thickness; W/D = steel plate width/depth; all units in mm.

Table 1: Steel girder dimensions in the monitored sections

Measured sections		x (m)	Monitored girders	Steel strain	Slip	Vertical separation	Deflection
Section 1	End support	0.9	A	–	x	x	–
Section 2	Quarter point	9.9	A	–	x	x	–
Section 3	Mid-span	17.8	A + B	x	x	x	x
Section 4	Quarter point	27.7	A	x	x	x	–
Section 5	Internal support	33.5	A	x	x	x	–
Section 6	Mid-span	70.4*	A + B	x	x	x	–
Section 7	Quarter point	78.4*	B	x	x	x	–
Section 8	End support	89.5*	B	–	x	x	–

*Defined in a local coordinate system for Spans 6 and 7, starting at Support 6 ($x = 0$).

Table 2: Monitored sections and instrumentation in each section

typical instrumentation consisted of three strain gauges, which measured the longitudinal strains in the steel web at different heights, and two Linear Variable Differential Transformers (LVDTs), which measured the relative vertical and horizontal displacement (slip) at the steel–concrete interface. The deflections were only measured in Section 3. *Figure 4* illustrates the instrumentation of the girders and *Table 2* summarises the instrumentation used in each section.

During the monitoring, a test vehicle was positioned in predetermined positions, during which time no other vehicles were allowed on the bridge. The four-axle test vehicle has a total weight of 31.4 t; the vehicle dimensions and axle loads are presented in *Fig. 5*. The front axle and rear bogie were weighted separately, but individual wheel loads could not be measured in the truck weighing station. This implies that the load distribution between the axles within the bogie and the distribution between the wheel loads within an axle had to be estimated. Different distributions

between the bogie-axles would have had a negligible impact on the results, since the measured spans are long in comparison to the distance between the axles. An uneven distribution of the load in the transversal direction could, however, have affected the results significantly. To assure that this was not the case, the test vehicle was driven along the centreline of the bridge in both directions during the monitoring—see Load Cases (LCs) 1 and 2 in *Fig. 5*. This made it possible to compare the deflections and strains measured in the two girders and evaluate if there were any indications of systematic differences due to varying wheel loads within an axle.

Finite-Element Modelling

The finite-element models presented in this paper were all implemented with a focus on the modelling of the shear connection, in order to study the correspondence between the design models and the measured behaviour. The material models are all linear-elastic, since the studied load-levels generate

stresses far below the yielding point of the steel and the concrete compression strength. Regarding the concrete parts under tension, cracking is expected over internal supports. However, since this is an existing structure with an unknown load history, there is no point in trying to capture the cracking of the concrete related to the test vehicle. Therefore, the models are based on the simplified design approach used in section 5.4.2.3 (3) of Ref. [14], which is a likely design model in a real-world situation. This implies that the concrete slab was treated as cracked at the internal supports over a distance that equals 15% of the adjacent span lengths, and that the cracked concrete was modelled with flexural stiffness corresponding to the contributions from the longitudinal reinforcement only.

The material parameters in the finite-element models are based on information from the bridge drawings and material standards, since no material samples have been taken from the bridge. The steel grade in the main structure corresponds to S355 by current standards and is modelled with a modulus of elasticity of 210 GPa and a Poisson's ratio of 0.3. The non-cracked concrete parts are modelled with a modulus of elasticity of 32 GPa and a Poisson's ratio of 0.2, while the corresponding parameters for the cracked parts are set to 1.57 GPa and 0.0. The former equals the modulus of elasticity for the reinforcement bars (210 GPa) multiplied by the reinforcement ratio (0.746%), which is defined as the longitudinal reinforcement area divided by the area of the concrete cross section.

The commercial finite-element software Autodesk Robot[17] was used for the 3D finite-element analysis. Only the superstructure was modelled, with nodal supports at the positions of the bearings. All supports are defined as being stiff in the vertical direction (z), while the horizontal behaviour is adapted to the different types of bearing. Only Support 4 is fixed in the longitudinal direction (x) for Girders A and B, while the transversal direction is fixed for all supports along Girder A and free for all supports along Girder B. The primary superstructure, the steel girders and the concrete deck are modelled with shell elements while the crossbeams are modelled with beam elements. The elements were chosen from the
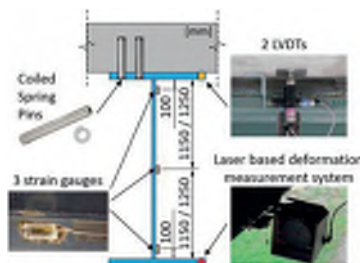

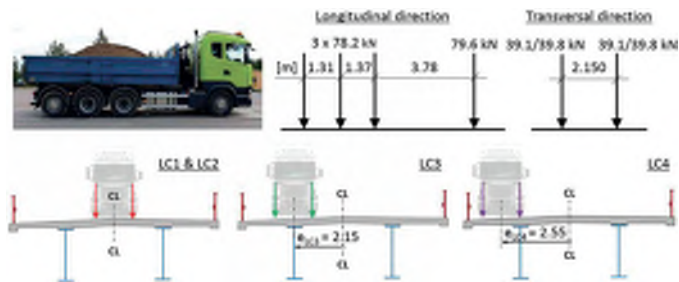*Fig. 4: Schematic illustration of the instrumentation*

Fig. 5: Test vehicle loads and load positions

perspective of a bridge designer, with the intent that the design model should be practical to use.

The connection between the steel and the concrete is modelled by stiff connection elements, located directly above the steel web plate, and the connections to the concrete shell elements are modelled as being rigid. The corresponding connections to the steel upper flanges are modelled as fixed for rotations and vertical movements, meaning that uplift is not simulated, while the horizontal stiffness of the connection are modelled with linear springs, which were given three different stiffnesses (k) in this study:

FEM 1: $k_{x,y} = \infty$ simulates a rigid shear connection between the steel and the concrete;
FEM 2: $k_{x,y} = 0$ simulates a non-composite cross section;
FEM 3: $k_{x,y} = 72.5$ kN/mm/CSP is the horizontal shear connector stiffness based on push-out test results.

Figure 6 shows a schematic illustration of the modelling of the connection elements. The longitudinal distance between the connection elements corresponds to the general distance between the CSPs, which in this case is 300 mm. The number of CSPs in each row

varies along the bridge, which implies that the horizontal spring stiffness of the connection elements varies as well. The spring stiffness of a single CSP is set to 72.5 kN/mm, based on the push-out test results presented in Refs. [8, 10]. The load-deformation curve from the push-out tests indicates a behaviour which can be approximated as linear up to a level of at least 60 kN/CSP (*Fig. 1b*). During monitoring, the shear force acting on a single CSP was far below this limit, which implies that there is no need to use non-linear springs to simulate the shear connection.

Test Results and Analysis

In the following sections, the test results are presented and compared against the results generated by the finite-element models. The measured steel strains are transformed into stresses by Hooke's law, assuming a linear elastic material. It can be noted that the strain measurements were only performed on one side of the web plates, which implies that the contributions from any out-of-plane bending of the web plates cannot be evaluated from these test results.

Steel Stresses

For the concentric load cases LC1 and LC2, the magnitudes and vertical

distribution of the longitudinal stresses are almost identical in Girders A and B. This is illustrated for LC1 in *Fig. 7a*, in which the measured stresses are indicated by points that are connected with straight lines. These results show that the vehicle was loaded symmetrically and that the bridge behaved symmetrically. The deflection measurements, taken simultaneously on both girders, confirm the symmetrical behaviour.

The interpolation between the two upper strain gauges in Sections 3A and 3B indicates that the neutral axes are positioned between 130 and 220 mm below the steel–concrete interface for LC1 and LC2. This can be compared to the theoretical position of the neutral axis in the composite section, which is positioned 215 mm below the steel–concrete interface. Two possible explanations for the difference are the concrete having a higher elastic modulus or stiffness contributions from non-structural details such as the pavement and steel railings. Since no concrete test samples have been taken from the bridge, the elastic modulus is an unknown parameter that has been modelled with the standard value for the relevant strength class. However, since the upper strain gauges were positioned close to the neutral axes, small contributions from different effects — or
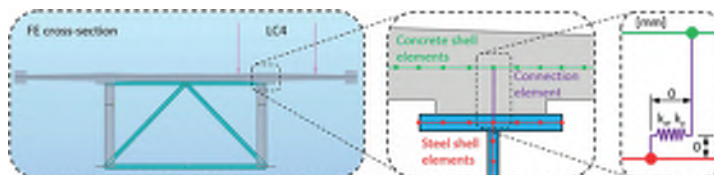

Fig. 6: Schematic illustration of the connection elements and the finite-element cross section
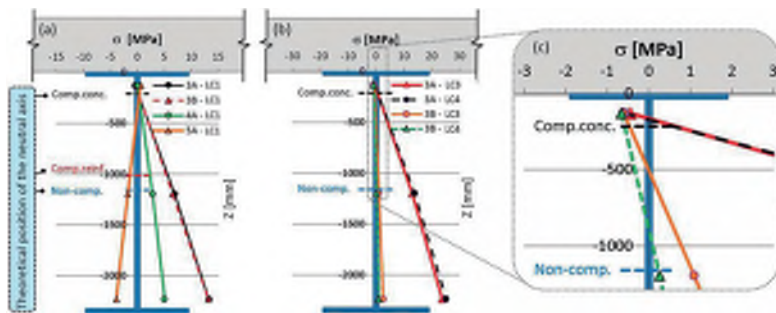
Fig. 7: Measured steel stresses in Span 1

sources of errors—could give disproportionate shifts of the neutral axis when it is established by interpolation between the two upper strain gauges.

The measured stresses in Sections 4A and 5A, representing a quarter point respectively an internal support (*Fig. 2*), are also plotted in *Fig. 7a*. It can be observed that the neutral axes are almost identical in the quarter point (Section 4A) and the mid-span (Sections 3A and 3B). At the internal support (Section 5A), the measured position of the neutral axis is far above the theoretical position of a cracked section with stiffness contribution from only the reinforcement bars, in line with the design assumptions of Ref. [14]. The test results indicate that the concrete deck slab itself contributes significantly to the cross-sectional stiffness. This could be explained either by tension stiffening between the cracks or the fact that the concrete section might be non-cracked. The impact of an increased stiffness contribution from the concrete under tension has been studied in a modified finite-element model in which the concrete elastic modulus and the longitudinal distribution of the cracked concrete at an internal support varied. These modifications are not related to the CSPs or the post-installation but are derived from the uncertainties of material parameters and global behaviour, and are therefore not within the scope of this paper. However, the modified finite-element model shows that it is possible to get a good agreement between a model and the test results in all sections.

Figure 7b shows the measured steel stresses in the mid-span (Section 3) for the eccentric load cases LC3 and

LC4. To highlight the differences between Girders A and B with respect to stress magnitudes and the position of the neutral axes, the simultaneously measured stresses are plotted in *Fig. 7b* and then enlarged in *Fig. 7c*. It can be seen that Girder B takes about 5 and 10% of the test vehicle load in LC3 and LC4, respectively, in terms of both deflections and stresses in the steel bottom flanges. It can also be observed that the measured neutral axis differs between Girders A and B when the bridge is loaded eccentrically. This observation, which is also relevant for Span 7 could be an indication that the shear connection is dependent on external vertical forces which create higher frictional forces in the contact surfaces between the steel and the concrete. For Span 1, this could also be an indication that an initial slip is needed before the CSPs start to transfer shear forces. However, the majority of this effect is not related to the shear connection—it can instead be explained by the structural behaviour of the cross section under eccentric loading. The eccentric loading of the superstructure results in torsional effects, including warping stresses in the cross section. Since the normal stresses related to the vertical bending moment are small in the girder furthest from the eccentric load, the influence of the torsional effects can be significant. These effects are captured by the finite-element models, which give vertical strain distributions that are similar to the measurements.

A comparison between the measured steel stresses and the finite-element stresses was carried out for Span 1. *Figure 8* illustrates the compared

steel stresses in Sections 3 to 5 for Girder A and LC1. It can be observed that the finite-element model with a rigid shear connection (FEM 1) gives a good prediction of the steel stresses in the areas where the concrete deck slab is under compression, whereas all models fail to predict the steel stresses when the concrete is under tension near an internal support (Section 5). This result is expected since the measurements show that the concrete under tension contributes to the flexural stiffness, whereas the initial finite-element models only consider the contribution of the reinforcement area.

For Span 7, it should be noted that the most loaded girder was Girder B, while it was Girder A in Span 1. Even though there are no shear connectors in Span 7, the results of the strain monitoring show that there is a high degree of composite action (*Fig. 9*). The measured positions of the neutral axis in Girder B are about 460 to 520 mm below the steel–concrete interface. The corresponding theoretical positions of a composite section and a non-composite section are 320 mm and 1140 mm, respectively. Similar observations are recorded in Refs. [6, 18], wherein strains were measured in non-composite structures under service loads. These observations can be explained by the existence of frictional forces or other interlocking phenomena at the steel–concrete interface. The positive effect however cannot be utilised by a bridge designer, in line with Ref. [14], since it is hard to estimate and could result in a sudden failure. This implies that there is a need to install shear connectors to attain a reliable shear connection, even if tests show that the frictional forces might provide sufficient capacity in the SLS.
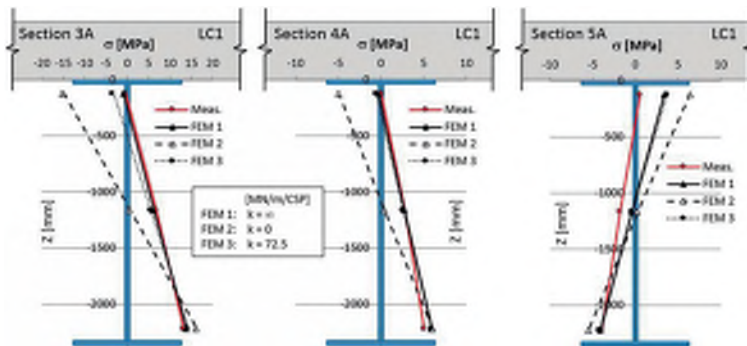
Fig. 8: Measured vs modelled steel stresses for LC1

The strain measurements for LC4 in Span 7 give an indication that the neutral axis drops as the load increases. However, this effect is not observed for LC3, which implies that no statement can be made regarding this effect. Nevertheless, it is reasonable to assume that the neutral axis will shift towards the theoretical position for a non-composite section as the load increases towards the ultimate capacity of the cross section.

Deflection and Displacement

In *Table 3*, the deflection measured in Section 3 is compared with the deflection predicted by the three finite-element models. Deflection measurements of less than 1.00 mm are excluded from the comparison, since the precision of the deflection

measurements is estimated to be ± 0.05 mm, which would lead to large percentage variations.

Based on the results presented in *Table 3*, a rigid connection seems to be the best estimate of the shear connection at the tested load levels. However, there are several unknown parameters that are capable of shifting the position of all the modelled deflection curves, which implies that no firm conclusion can be drawn based only on the measured deflection. Some of these parameters include the elastic modulus of the concrete, the stiffness contribution from the concrete under tension and the longitudinal distribution of the cracked concrete deck slab at the internal supports. However, if the measured deflections are considered together with the

strain then it can be concluded that the rigid connection gives the best estimate among the studied stiffnesses.

The measured slips in Span 1 are all within an interval of ±0.00 to 0.04 mm (*Fig. 10*), while slips of up to 0.26 mm were registered in Span 7. This comparison indicates that the coiled spring pins are reducing the slip significantly. The slips according to FEM 3, also plotted in *Fig. 10* but with a different scale on the vertical axis, show similar shapes to the curves of the measured slips, but with magnitudes that are 5 to 10 times greater.

The results from FEM 3 show that the stiffness of the shear connectors alone cannot explain the measured stiffness of the shear connection at the tested load levels. The higher stiffness can partly be explained by the contribution from frictional forces, since composite action is observed even in Span 7. Another aspect might be the fact that the behaviour of shear connectors in push-out tests is not directly comparable to the behaviour in a girder, even though push-out tests are the common method used to establish the load capacity of connectors. The frictional forces are not modelled, since the evaluation presented in this paper focuses on the CSPs and their impact on the structural behaviour.

According to Ref. [14], all types of shear connector must be able to prevent the separation of the concrete deck from the steel girders. However, the uplift forces are generally not considered in the design of the shear connection, since the welded headed studs may be assumed to provide sufficient resistance to uplift, in line with
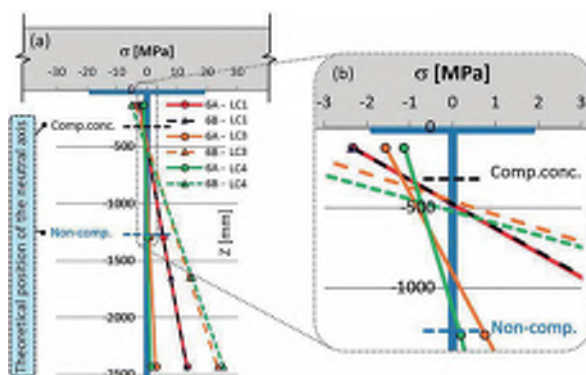

Fig. 9: Measured steel stresses for Section 6 of Span 7

Load case	Meas. − $\delta_{meas.}$ (mm)		FEM 1 − δ_{FEM} (mm)		$\delta_{FEM\ 1}/$ $\delta_{meas.}$		FEM 2 − δ_{FEM} (mm)		$\delta_{FEM\ 2}/$ $\delta_{meas.}$		FEM 3 − δ_{FEM} (mm)		$\delta_{FEM\ 3}/$ $\delta_{meas.}$	
	A*	B	A	B	A	B	A	B	A	B	A	B	A	B
LC1	−3.30	−3.40	−3.70	−3.70	1.13	1.10	−7.20	−7.17	2.19	2.12	−4.10	−4.10	1.24	1.21
LC2	−3.30	−3.30	−3.70	−3.70	1.13	1.13	−7.20	−7.16	2.18	2.18	−4.10	−4.10	1.24	1.24
LC3	−6.00	−0.70	−6.60	−0.80	1.11	–	−12.40	−1.99	2.08	–	−7.30	−0.90	1.23	–
LC4	−6.50	−0.30	−7.20	−0.30	1.11	–	−13.40	−1.05	2.07	–	−7.90	−0.30	1.22	–

*A = Girder A; B = Girder B.

Table 3: Measured vs. modelled deflection

Ref. [14]. This is not the case for the CSPs, where only frictional forces at the pin surface can counteract the uplift, together with the gravity forces from dead weight and traffic. The measurements show no clear indications of uplift of the concrete deck in the parts with CSPs with registered separations of less than 0.03 mm. This result is to be expected, since the forces acting on the shear connectors are rather low—partly due to the fact that for obvious reasons the tested load levels are a lot smaller than the ultimate load, and partly due to the observation that frictional forces seem to contribute significantly at the tested load levels.

In Span 7, small vertical displacements are registered in Sections 6 and 7, while the registered displacements in Section 8 are about ten times greater than the comparable measurements in Section 1. The uplift in Section 8 was not expected, but might be a consequence of the steel strips acting as a local shear connection between the steel and the concrete right above the support (*Fig. 3*). These strips were not designed for composite action, but will certainly experience high shear forces since they will counteract the slip. The possibility of severe concrete crushing around these strips or fracturing of the strips cannot be excluded, allowing for both vertical and horizontal movements. This effect is however somewhat out of scope of this study and is not investigated further.

The results of the monitoring indicate that the installation of CSPs does not cause concrete uplift at the studied load levels. However, the potential problem with uplift is one of the issues that needs to be investigated further and that might affect the final design of the shear connections.

Conclusions

The strengthening and monitoring of the Pitsund Bridge shows that it is possible to create composite action by installing CSPs on a non-composite steel–concrete bridge. The measured steel strains indicate that the strengthened superstructure behaves like a composite bridge at the tested load levels. The test results for both the strengthened and non-strengthened spans indicate that frictional forces or other interlocking phenomena are significantly contributing to the shear transfer at the studied load levels. Bridge designers cannot rely on the frictional connection for the ULS design, but the friction will probably contribute by significantly reducing the fatigue stresses in the shear connectors, thus extending the fatigue lifetime of the shear connections. The comparison between the initial finite-element models and the test results shows that a rigid model of the shear connection seems to be a good design assumption at the tested load levels (SLS).

The comparison of the slip measurements in the strengthened and non-strengthened spans confirms that the CSPs counteract the slip by transferring shear forces to the concrete deck. At the tested load levels, there are no clear signs of uplift in the strengthened span.

There are still some research questions left to answer regarding the structural behaviour of the shear connections created by post-installed CSPs, especially in the ULS. The potential uplift problem is one issue that needs to be investigated further via large-scale composite beam tests. These tests will also provide information about the structural behaviour of the connections in the ULS. Additional static and fatigue push-out tests can also be conducted in order to study how different parameters can affect the load capacity.
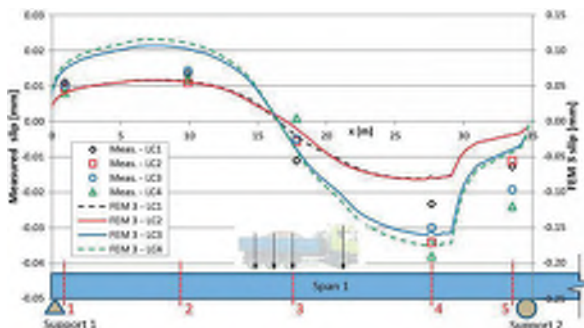
Fig. 10: Measured vs modelled slips for Span 1

ORCID

Robert Hällmark 🄳 http://orcid.org/0000-0003-1435-0071

References

[1] Hällmark R, Jackson P, Collin P. Post-installed shear connectors – coiled spring pins. *Proceedings from the 19th IABSE Congress*, Stockholm, September, 2016. pp. 1227–1234.

[2] Kwon G. *Strengthening existing steel bridge girders by the use of post-installed shear connectors. PhD Thesis*, University of Texas at Austin, USA, 2008.

[3] Kwon G, Engelhardt MD, Klinger RE. Strengthening bridges by developing composite action in existing non-composite bridge girders. *Struct. Eng. Int.* 2009; **19**(4): 432–437.

[4] Schaap B. *Methods to develop composite action in non-composite bridge floor systems. Master Thesis*, University of Texas at Austin, USA, 2004.

[5] Hungerford B. *Methods to develop composite action in non-composite bridge floor systems: Part II. Master Thesis*, University of Texas at Austin, USA, 2004.

[6] Peiris A, Harik I. Steel girder bridge with RC Deck Retrofit from non-composite to composite behaviour. *Proceedings from the 19th IABSE Congress*, Stockholm, September, 2016, pp. 1964–1971.

[7] Pritchard B. *Bridge Design for Economy and Durability – Concepts for New, Strengthened and Replacement Bridges.* London: Thomas Telford Service Ltd, 1992, 172.

[8] Buckby RJ, Ogle M, Johnson RP, Harvey D. The performance of coiled spring pin connectors under static and fatigue loading. *Proceedings from IABSE: Composite Construction – Conventional and Innovative*, Innsbruck, September, 1997. pp. 669–674.

[9] Fahleson C. *Testing of shear connectors – Project no: 05035.* Technical Report, Luleå University of Technology, Sweden, 2005 (in Swedish).

[10] Hällmark R, Collin P, Möller M. Testing of coiled spring pins as shear connectors. *Proceedings from the 39th IABSE Symposium*, Vancouver, September, 2017. pp. 1209–1216.

[11] Lungershausen H. *Zur Schubtragfähigkeit von Kopfbolzendübeln. Ph.D Thesis*, Ruhr-Universität Bochum, 1988.

[12] Hicks SJ, Smith AL. Stud shear connectors in composite beams that support slabs with profiled steel sheeting. *Struct. Eng.. Int.* 2014; **24** (2): 246–253.

[13] Nellinger S. *On the behaviour of shear stud connections in composite beams with deep decking. PhD Thesis*, University of Luxembourg, Luxembourg, 2015.

[14] EN 1994-2. *Eurocode 4 – Design of Composite Steel and Concrete Structures– Part 1-1: General Rules and Rules for Bridges.* Brussel, Belgium: CEN, 2005.

[15] ISO 8748. Spring-type straight pins – Coiled, heavy duty, ISO – the International Organization for Standardization, Geneva, Switzerland, 2007.

[16] Bro 2004. The Swedish Road Administrations Bridge Code, VV Publ 2004:56. Borlänge, Sweden, 2004.

[17] Autodesk Robot Structural Analysis Professional 2017, Autodesk Inc, San Rafael, USA, 2018.

[18] Andersson A. *Fatigue assessment of railway bridges: a case study of the steel bridges between Stockholm Central Station and Söder Mälarstrand.* Licentiate Thesis, KTH, Stockholm, Sweden, 2009 (in Swedish).

PAPER VIII

Post–installed Shear Connectors: Push–out Tests of Coiled Spring Pins vs. Headed Studs

Robert Hällmark, Peter Collin and Stephen J. Hicks

Post-installed Shear Connectors:
Push-out Tests of Coiled Spring Pins vs. Headed Studs

Robert Hällmark*[1], Peter Collin[1a,] and Stephen J. Hicks[2b]

[1]Department of Civil, Environmental and Natural Resources Engineering, Luleå University of Technology, 971 87 Luleå, Sweden
[2]Heavy Engineering Research Association, Gladding Place Manukau, Auckland 2241, New Zealand

Abstract. Steadily increasing traffic volumes and traffic loads lead to a continuously growing demand for bridge rehabilitation, strengthening and replacement projects. For existing steel girder bridges with non-composite concrete decks, the traffic load capacity can often be increased significantly if composite action can be created afterwards. Different kinds of shear connectors are more or less suitable for post-installation. Coiled spring pins are one type of interference fit connector that can be installed from below the bridge deck during traffic, in order to minimize the impact on road users. This paper describes an experimental study on the static capacity and stiffness of coiled spring pins used as shear connectors at steel-concrete interfaces. Six push-out test series are presented, with a total of 28 tests, together with an alternative type of test set-up. The results show that the failure of the coiled spring pins is very ductile and that the load capacity is predictable and sufficient for a cost-effective application. The tests also indicate a significantly lower stiffness of the connectors in comparison to welded headed studs of similar dimensions, which might be of great importance if an existing shear connection is strengthened.

Keywords: push-out test; coiled spring pin; headed shear studs; strengthening; shear connector; post installation; composite; steel; concrete

1. Introduction

Traffic density and vehicle weight have been increasing over time and the tendency seems to continue (Lumsden 2004). Finland is an example of a country that in recent years has increased the maximum truck weight from 60 tonnes up to 76 tonnes (Blanquart *et al.* 2016); Sweden is planning for a similar change. An analysis, presented by the Swedish Transport Administration, indicates that the latter would suggest that approximately 1000 bridges need to be strengthened in Sweden. This implies that there will be a continuous demand for strengthening or replacement of existing bridges in both Nordic countries and worldwide.

Steel girder bridges with concrete decks are normally designed as composite structures, in order to utilize the advantages of the different materials. This has, however, not been the case for such a long time. As late as the 1980s, steel girder bridges in Sweden were often designed with a non-composite concrete deck on top. According to the national bridge managing systems in Sweden, Finland and Norway, there are more than 2000 bridges of this type. One way of increasing the traffic load capacity or prolonging the fatigue life for existing bridges of this type is to create composite action by connecting the concrete slab to the steel girders by post-installed shear connectors. The composite steel-concrete cross-section will carry traffic loads more efficiently than in the original non-composite condition. Since the permanent loads are already in place, the effect will only influence the live loads and any subsequent applied dead loads. It should be highlighted that there are many structural details that need to be checked when a bridge

structure is strengthened, to assure that the load capacity can be increased by installing shear connectors, for instance the transverse and the longitudinal reinforcement of the deck slab, as well as the shear capacity of the web plates. However, the present paper is confined to the capacity of the shear connection itself.

There are many different types of shear connectors that can be used for post-installation, with some more suitable than others. Welded headed shear studs are by far the most common type of shear connector in new structures. For existing structures, other types of connectors might be more interesting, especially connectors that can be installed from beneath the bridge without affecting the road surface. Research has been made on numerous types of shear connectors, with some examples of connectors suitable for post-installation presented by Hällmark et al. (2016), the present authors. Internationally, probably the most comprehensive studies on post-installed shear connectors have been performed at the University of Texas at Austin by Hungerford (2004), Schaap (2004), Kayir (2006) and Kwon *et al.* (2009, 2010a, 2010b, 2011). More recent studies have been performed by Pathriana *et al.* (2015, 2016a, 2016b) and Henderson *et al.* (2017).

One type of type of connector suitable for post-installation is the Coiled Spring Pin (CSP) shown in Fig. 1a. The CSP is a type of interference fit connector, or tension pin, that is anchored to the connecting parts by the radial forces that are developed when the larger CSP is press fitted into the smaller hole. There is no need for welding, grouting, adhesives, etc. since the connectors rely on mechanical forces. This makes it possible to perform the installation in

*Corresponding author, Ph.D. Student
 E-mail: robert.hallmark@ltu.se
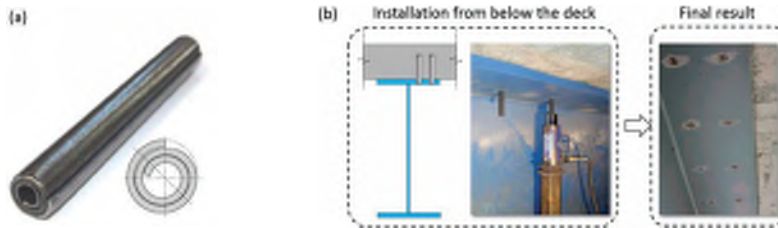
[a]Professor
[b]Ph.D.

Fig. 1 (a) Coiled spring pin, (b) Installation procedure and final result

existing bridge structures from below the bridge deck, as illustrated in Fig 1b, with little or no impact on the traffic running on the bridge (Pritchard 1992, Buckby *et al*. 1997). These advantages, combined with a lack of knowledge about the behaviour of CSPs in steel-concrete composite construction, resulted in the authors of this paper focussing on this type of shear connector.

The CSP is a standard component that is used as a fastener in different industries. The pins are manufactured from steel plates that are spirally wound 2.25 times around the central axis of the pin and available with outer diameters from less than 1 mm up to 20 mm. The dimensions are standardized according to international standards, of which ISO 8748 (2007) is the most relevant for shear connectors in bridges, since it covers the "Heavy Duty" type with the largest shear capacities. For civil engineering applications only a few studies have been reported to date, Pritchard (1992), Buckby *et al.* (1997), Fahleson (2005), and to the authors knowledge there are only a few bridges from around the world that have been strengthened with CSPs (Hällmark *et al.* 2016). The reported studies have all been confined to the strongest standard CSP with an outer diameter of 20 mm and a steel plate thickness of 2.2 mm. The static and fatigue capacity of the connectors are well known when they are used as shear connectors between two steel parts, but there are only a limited number of tests published for steel-concrete connections. The tests reported to date have all been project specific tests on non-standard specimens, performed in order to verify the use of CSPs in a specific structure. No validation tests on connectors with known shear capacity have been reported for the alternative test set-ups and the only design recommendations that have been published are those provided by Buckby *et al.* (1997). These recommendations are limited in respect to both concrete strength (equivalent to C30/37) and thickness of the upper steel flange (25-35 mm).

There is an information and knowledge gap on the structural behaviour and the load capacity for CSPs, used as shear-connectors in steel-concrete interfaces, and there is a need for additional testing and knowledge sharing. If it would be possible to develop more general design guidelines for the use of CSPs as shear connectors in steel-concrete interfaces, future project specific tests could be eliminated, thereby removing some of the barriers for this strengthening method. As a first step towards more general design guidelines, the authors of this paper have performed 28 additional static tests, to bridge the gap in knowledge of different parameters that impact the behaviour of CSPs, as well as verify the previous tests that have been performed on non-standardized

push-out specimens. This paper presents the experimental part of the research and will be complemented by a subsequent paper presenting the numerical analyses and the parametric studies that have been calibrated to the test results.

2. Push-out tests

The preferred method to establish the static capacity and the load-slip behaviour of a steel-concrete shear connection is push-out tests. It is also possible to perform composite beam tests. However, the latter is more expensive to perform in sufficient numbers and harder to evaluate, since the forces acting on the shear connectors must be calculated from the measured strain distribution, which results in a need for extensive measurements and a knowledge of the stress-strain behaviour of the materials used in the tests.

The European design rules for shear connections in steel-concrete composite bridges are given by EC4-1-1 (2004) and EC4-2 (2005). These codes address the general requirements for shear connectors and present rules for the design of Welded Headed Studs (WHS). For other types of shear connectors, the static load capacity and ductility must be established from testing (this is the case for the CSPs, since only a few tests have been reported in the literature so far (Pritchard 1992, Buckby *et al.* 1997, Fahleson 2005). A standard test method for push-out tests is presented in Annex B of EC4-1-1. Even though push-out tests are the common method to establish the static and fatigue capacity of shear connectors, the test method and the layout of the specimen have been discussed for several decades. Some examples of factors that have been investigated are the eccentricity between the load and the supports, the support conditions, the absence of compressive normal force at the steel-concrete interface corresponding to a real structure, the width and height of the slab and the number of shear connector rows (Döinghaus 2002, Ernst 2010).

The eccentricity might be the most discussed factor, since it is believed to have a negative impact through uplift and tension forces on the connectors, but also a positive contribution by an increased contact pressure in the top of steel-concrete interface. The impact of the eccentricity is also strongly dependent on the support conditions. If the supports are free to move in the normal direction to the face of the tests slabs (roller based), the shear connectors will experience tensile forces that are not comparable to the load situation in a beam. Tests reported by Hicks (2014) have shown that elimination of normal forces at the supports

reduce the measured shear resistance by approximately 30%. To avoid this reduction, Roik *et al*. (1989) recommended that the moment should be balanced through the provision of a tensile tie or rigid angle restraints at the base of the test slabs. The impact of the degree of horizontal restraint has also been investigated, through numerical analysis, by Guezouli and Lachal (2012), who also have performed studies on the frictional contribution to the load transfer through the push-out specimen (Guezouli *et al*. 2013).

2.1 Test methods

The standard push-out test specimen recommended by EC4-1-1 is not suitable for testing of post-installed shear connectors, see Fig. 2a. The layout of the standard specimen, with the limited space between the flanges in the steel section, makes it difficult to perform the drilling through the steel flange and into the concrete. In order to create the space needed for the drilling- and jacking-equipment, the steel section would have to be enlarged to disproportionate dimensions, or cut into two separate parts prior to the installation of the shear connectors. After the installation, the two halves would then have to be joined together into one unit. To avoid this labour-intensive process, alternative push-out tests specimens have been evaluated by the present authors for the testing of CSPs.

The focus of the design of an alternative test set-up and test specimen was to ensure that there was enough space to install the CSPs, without jeopardizing the validity of the test results. For CSP testing, different kinds of inverted push-out tests have been used by Pritchard (1992), Buckby *et al.* (1997) and Fahleson (2005). The test specimens are inverted by changing the position of the steel and the concrete parts, which simplifies the post installation of the shear connectors. The test specimen used by Buckby *et al.* (1997) is illustrated

in Fig. 2b. Later tests by Fahleson (2005) were performed on almost an identical test arrangement, while additional unpublished tests in UK follow the main principle of the inverted specimen. In the Tinsley Viaduct strengthening project (another unpublished test series from UK), the test specimens were designed more like the standard specimen, but manufactured in two halves that later were bolted and clamped together after the installation of the shear connectors, see Fig. 2c.

The horizontal test set-up for single shear connector testing shown in Fig. 2d, was developed at the University of Austin and used in a comprehensive study of different types of post-installed shear connectors (Schaap 2004, Hungerford 2004, Kayir 2006, Kwon 2010a). The test set-up was influenced by the ideas presented by Gattesco and Giuriani (1996) where one connector was tested at a time and to minimize the eccentricity between the applied load and the supports, together with avoiding rotations in the concrete block during the test. Other types of horizontal test set-ups have been used by different researchers, in particular Ernst (2009) and Lam (2007). The impact of normal compression forces at the steel-concrete interface has been studied by Hicks and Smith (2014) for composite beams with profiled steel sheet decking. Test results from beam tests have been compared to push-out test results on specimens with and without normal forces, corresponding to between 0 to 16% of the vertical force applied to the steel-concrete interface. A recommendation for a new improved test set-up for specimens with steel sheet decking was subsequently presented, where horizontal normal forces are applied to the standard push-out test specimen. This recommendation is supported by additional studies by Easterling *et al.* (1993), Bradford *et al.* (2006) and Nellinger *et al* .(2017). The latter also presents a review of alternative push-out test set-ups. Other alternative push-out test specimens are presented by
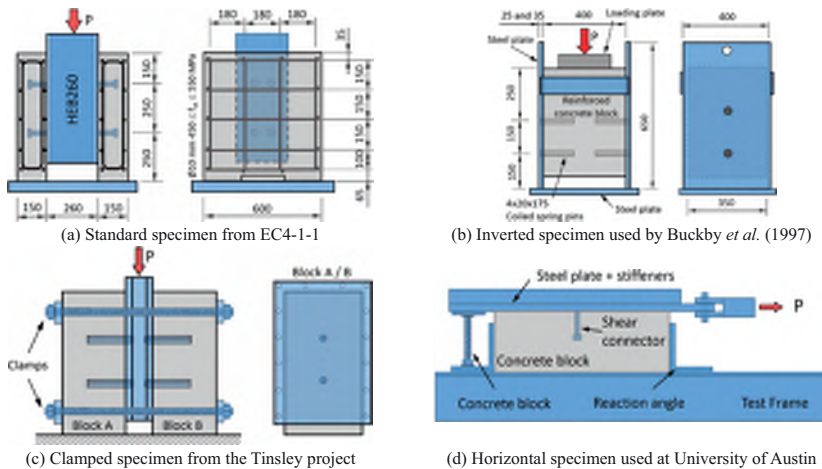

(a) Standard specimen from EC4-1-1

(b) Inverted specimen used by Buckby *et al.* (1997)

(c) Clamped specimen from the Tinsley project

(d) Horizontal specimen used at University of Austin

Fig. 2 Push-out test specimens [mm]

Döinghaus (2002), where the two most interesting specimens for the present authors are the single push-out test specimen (SPOT) and an inverted test specimen with two steel beams on the sides and a concrete block in the middle. Equivalent test results are reported from these two types of specimens.

The majority of the tests conducted on CSPs have so far been undertaken on the type of specimen illustrated in Fig. 2b (for both static and fatigue loading). However, the test results have not been verified by similar tests on WHSs with known shear resistance and load-slip behaviour. In order to verify the previous tests and to ensure that the results can be compared with those obtained from the standard push-out test, the tests presented in this paper have been performed with specimens that are almost identical to those used by Buckby *et al.* (1997) and Fahleson (2005), with some modification of the clamping. The alternative test methods presented in this section all involve some type of clamping, which is necessary to avoid too conservative results due to separation of the specimens during the tests. This separation is mainly driven by the geometry of the test set-up, and does not correspond to the behavior in a real structure with a continuous shear connection. Since the CSPs have no heads, the test results become even more sensitive to separation. The differences between the assumed behavior of CSPs and headed studs, in terms of force components, are schematically illustrated in Fig. 3.
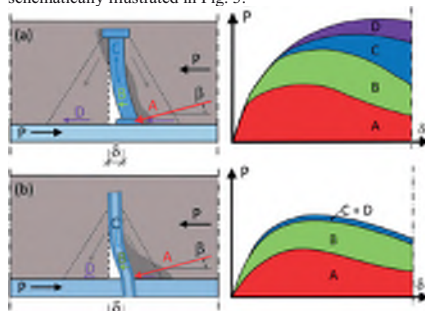

Fig. 3 (a) Load transfer model for headed studs, (b) suggested load transfer model for CSPs

The force components involved in the shear behaviour of welded studs, embedded in solid concrete slabs, are often described by the illustration in Fig. 3a, originally presented by Lungershausen (1988). Initially, the external shear force, P, is predominantly acting on the lowest part of the shear connector by a compression strut, A, that is inclined at an angle β. When the load increases, concrete crushing will occur near the weld collar, which implies that the additional shear force, B, is shifted higher up in the stud shank. The shift of the force results in increased shear deformations and bending of the stud. Since the ends are restrained from vertical movements by the head and the weld collar, a tension force, C, will be developed in the stud shank. The tension force is balanced by a compression force in the concrete, which gives an additional contribution to the frictional capacity at the steel-concrete surface, through the force

component D. The final failure is expected directly above the weld collar as a result of the combination of shear and tensile stresses (Roik *et al.* 1989, Nellinger *et al.* 2017).

If the failure of the CSPs is now considered, it seems reasonable to assume that the force components A and B will contribute in a similar way as for the shear studs. However, since the CSP has no head, there will be no restraint from vertical movement in the top of the connectors, except the assumed minor contribution from the vertical frictional forces acting on the pin. This should imply that the force components C and D only give negligible contributions to the total shear capacity of the shear connector. A schematic illustration of the suggested load-bearing behaviour is shown in Fig. 3b.

The design code EC4-2 (2005) for new composite bridges, requires that the shear connectors shall be capable of preventing separation of the concrete element from the steel element, if the separation is not prevented by other means. This requirement is considered to be met if the connector can resist a tensile force equivalent to 10% of the ultimate shear connector resistance. The existence of the head in the welded headed stud is the main reason why the tensional force component C is developed. Since the CSP has no head, the C component is expected to be far smaller than the EC4-2 requirement. On the other hand, without the head it is not obvious that the 10% criterion is of any relevance. From the authors' perspective, a separating force with this magnitude will not occur in beams with solid slabs, and especially not in the serviceability limit state. This standpoint is supported by field monitoring performed on a bridge strengthened with CSPs by Hällmark *et al.* (2017). In the ultimate limit state, smaller separations just before failure should not be a problem as long as the CSPs continue to exhibit ductile behaviour with no loss in shear capacity. The issue regarding any potential separation needs to be investigated further, but cannot easily be simulated by push-out tests. Thus, the push-out test specimens are designed to test the pure shear capacity of the connection, with clamping rods to avoid separation caused by the geometry of the specimen. However, two reference specimens are tested without clamping forces. The clamping forces are measured during the tests and are investigated further in this paper. The potential uplift will be investigated at a global structural level, by beam tests and FE-modelling, but this is outside the scope of the present paper.

2.2 Test specimen and test set-up

The specimen used in the tests is shown in Fig. 4. The geometry of the specimen is similar to those reported by Buckby *et al.* (1997) and Fahleson (2005), with exception of the welded steel clamping plates that have been replaced by clamping rods instead. The latter consists of threaded rods (M20) with tension load cells, measuring the clamping forces during the tests. Three different combinations of shear connectors have been tested: (a) four welded headed shear studs; (b) four coiled spring pins; and (c) two welded headed shear studs in the upper positions combined with two coiled spring pins in the lower positions. The latter was tested in order to study the behaviour of an existing shear connection
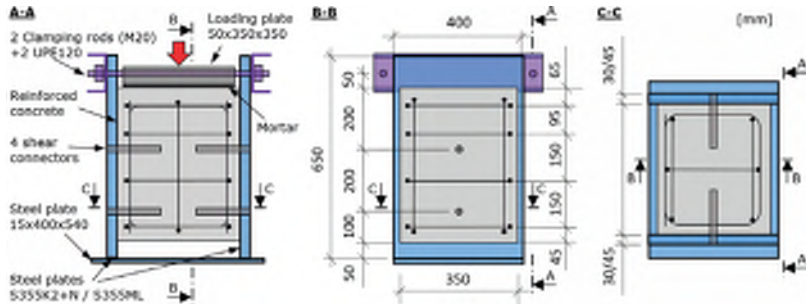
Fig. 4 Test specimen dimensions

strengthened with CSPs, which can be of interest if a bridge with existing welded shear studs is strengthened.

The steel parts of the test specimens were manufactured and assembled in a steel workshop, including the drawn arc stud welding for the specimens with WHSs. The steel parts were transported to a concrete workshop where the reinforcement cages were constructed before being cast in concrete. Prior to casting, form oil was applied to the steel plates to reduce the friction at the steel-concrete interface. Since the concrete block has two sides with shear connectors, there are no upper and lower side in comparison to a real concrete beam. This means that the specimen cannot be cast in a horizontal position, like in a real composite beam according to the EC4-1-1 recommendation. However, the intention of this recommendation is to reduce the risk that the concrete just below the connectors is poorly compacted, as presented by Maeda *et al.* (1983). This is not of importance when post-installed shear connectors are tested, since they are installed in holes drilled in the hardened concrete. The concrete blocks were therefore cast standing vertically. For each concrete batch (corresponding to 3-5 test specimens), eleven 150 × 150 × 150 mm cubes were cast and stored indoors together with the specimens. Test samples were also taken from the batch of reinforcement bars that was used for the specimens. At a concrete age of 7 days, holes were drilled for the installation of the CPSs. The general installation procedure is schematically illustrated in Fig. 5. In order to get interference-fit, the holes were drilled with an undersized diameter compared to the diameter of the CSP. Although the

manufacturer of the CPSs recommended a hole diameter of 20.00-20.21 mm, the hole tolerance was set at 19.85-20.25 mm in the tests, with an additional requirement of a relative difference between the steel and the concrete parts less than 0.10 mm.

The holes were made using a cutting drill through almost the entire thickness of the steel plate (Step 1). The remaining drilling was done with a diamond core drill (Step 2). After drilling, the diameter of the holes in the concrete and the steel parts were measured (Step 3). The installation of the CSPs was performed with a hydraulic jack (Step 4), registering the force needed to push the pin into the hole. The installation force varied between 30-100 kN, which can be compared with the installation forces of between 62-205 kN reported by Buckby *et al.* (1997). Whilst the pins were lubricated with grease in the majority of the test specimens, in a similar way as that reported by Buckby *et al.* (1997), no significant difference was observed between lubricated and non-lubricated specimens. In a real structure, the jacking would have been followed by sealing of the hole and painting to restore the corrosion protection (Step 5).

2.3 Test procedure

The testing procedure was in line with the recommendations in EC4-1-1 Annex B, with one exception in that the recommended cycling between 5% and 40% of the expected failure load was changed to an interval between 10-40% instead. This change was done, since the hydraulic
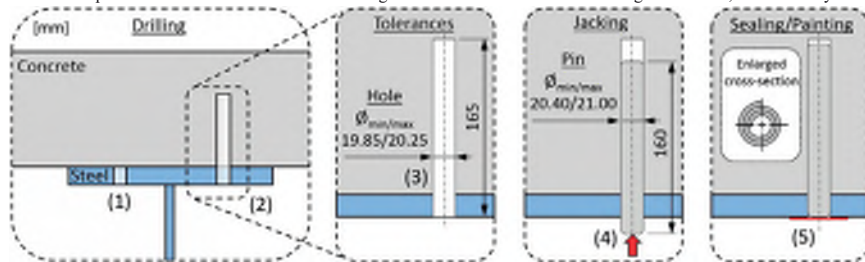

Fig. 5 Installation procedure for CSPs

actuator was not suited for cycling at such low load levels.

The general loading procedure, which is schematically illustrated in Fig.6a, started with a loading up to 240 kN, followed by 25 cycles between 80 kN and 240 kN. The specimen was then unloaded prior to being loaded to failure. The loading was displacement controlled and applied by a 2.0 MN hydraulic actuator, through a spherical bearing and a load distribution plate on top of the concrete. In the first series of tests, the displacement rate was as low as 0.005 mm/s. It was later increased up to 0.03 mm/s, which were used in the majority of the tests. This rate still ensured that failure did not occur in less than 15 minutes, in line with the procedure described in EC4-1-1. The influence of stress relaxation that might occur under permanent loading has not been taken into consideration in these test series, neither has any possible impact on the static capacity caused by previous fatigue loading been considered. The effect of the former should be negligible, since the connectors only contributes to the load cases applied after the installation.
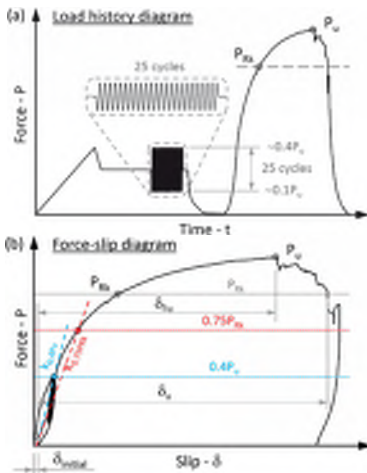

Fig. 6 Load-history diagram and corresponding load-slip diagram for the push-out tests

Throughout the test procedure, the applied force and the stroke were recorded directly from the hydraulic actuator. In addition to this, 14 external sensors were used to monitor displacements and forces, as shown in Fig. 7. The vertical displacement (the slip) at the steel-concrete interface was monitored by four linear variable differential transformers (LVDT-V) placed on each vertical side of the test specimen, in a position between the shear connectors, while corresponding horizontal displacements were recorded by four additional sensors (LVDT-H). For the specimens with CSPs, additional LVDTs (LVDT-CSP) were installed to measure the relative horizontal movement of the end of the pin in relation to the steel plate. In order to be able to evaluate the contribution from the clamping rods, two tensions loads cells (TLC) were also used. Before the final failure test

commenced, the nuts in the tension rods were tightened until the TLCs registered a clamping force of approximately 1 kN/rod. However, no clamping force was applied during the initial cycling.
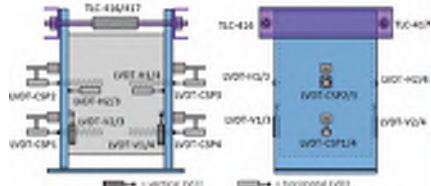

Fig. 7 Instrumentation of the test specimen

2.4 Test program

The static push-out test program contained six different test series with a total of 28 specimens. All the specimens had the same geometry, except for one test series (Type D) in which another steel plate thickness was tested.

The first two test series were reference tests performed in order to evaluate the test set-up and to obtain comparable results for headed shear studs (Type RW) and coiled spring pins (Type RC). One specimen in each reference series was tested without the clamping rods; these specimens are denoted RWX and RCX, respectively. In the following four test series, three different parameters were varied: the concrete strength; steel plate thickness; and the shear connector configuration. Table 1 summarises the test program and the varied parameters.

Table 1 Summary of the test program

Type	No.	Shear connectors	Concrete Str.class	Steel plates t [mm]	Grade
RW	5	4 CSP	C30/37	30	S355K2+N
RC	5	4 WHS	C30/37	30	S355K2+N
A	5	4 CSP	C20/25	30	S355K2+N
B	5	4 CSP	C40/50	30	S355K2+N
D	5	4 CSP	C30/37	45	S355ML
E	3	2 CSP/2 WHS	C30/37	30	S355K2+N

2.5 Material parameters and tolerances

The steel parts of the test specimens were manufactured from plates in grade S355K2+N and S355ML (see Fig. 4), where the latter was used only for the 45 mm thick plates in the Type D specimens. Tensile tests performed by the steel manufacturer show a yield strength of 408 MPa and a tensile strength of 511 MPa for the S355K2+N, whilst 418 MPa and 509 MPa was recorded for the S355ML. The headed studs were made in steel material quality S235J2+C470, type SD1 according to ISO 13918 (2008), and welded according to ISO 14555 (2014). The measured yield stress, tensile strength and maximum elongation was 470 MPa, 522 MPa and 25%, respectively. The exact dimensions of the studs were not measured prior to the testing, but the nominal diameter was 22 mm and the length before welding was 125 mm. The elastic modulus has not been reported from the tensile tests

performed by the steel manufacturer, and no additional tests were performed.

The tested CSPs were of a standard type available on the market and manufactured according ISO 8748 (2007). The designation of tested pins is Coiled Spring Pin ISO 8748 – 20 x 160 – HWK. The letters indicate that the pin is of type Heavy Duty (H) and made out of AISI 6150 Alloy Steel (W) with no surface treatment (K), while the digits represent the nominal outer diameter of 20 mm and the length of 160 mm (see Fig. 8a). The thickness of the steel plates used to manufacture this type of pins are 2.2 mm. From test samples from the steel plate before they were formed into coiled springs and heat-treated, the manufacturer reported a yield stress 550 MPa and a tensile strength 690 MPa. In order to establish the material data for the final product, four test coupons were taken from the pins (see Fig. 8b), and tensile tests were undertaken according to EN ISO 6892-1 (2016). The mean value of the tested yield stress and the tensile strength were 1516 MPa and 1606 MPa, respectively. Failure occurred at an elongation of about 5%, and no test result deviated more than 3% from the mean value.
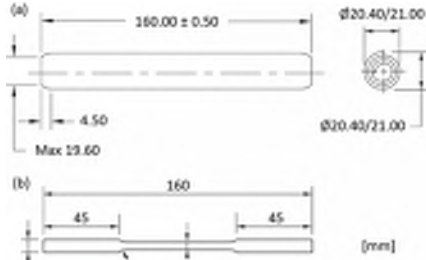

Fig. 8 Dimensions of the tested CSP and the test coupons

The reinforcement consisted of Ø10 mm standard deformed bars, K500C-T, in line with the reinforcement for the standard test specimen in EC4-1-1. The mean value of the tested yield stress and the tensile strength were 533 MPa and 649 MPa, respectively.

The concrete properties were determined by compressive cube strength tests, performed on standard cubes with sides of 150 mm. The specimens in each test series were cast from the same concrete batch and cured in air indoors without cover. For each concrete batch, three cube were tested after 28 days. Every push-out test was also followed by a cube compression test. The specimens within the same series, were generally tested at an age of 15 days or a few days more, which implies that the age effect between the specimen in the same series were not that big. The results from the concrete cube strength tests are summarized in Table 2, where $f_{cm,cube}$ is the mean strength of the cube tests performed at the same dates as the push-out test and $f_{cm28,cube}$ is the mean strength of the tests performed after 28 days. The mean values of the secant modulus of elasticity have been calculated according to equation (1) from EC2-1-1 (2005), where f_{cm} is the compressive cylinder strength given in MPa. The concrete cube strength has been transformed into the cylinder strength by multiplying with factor 0.8.

$$E_{cm} = 22 \cdot (f_{cm}/10)^{0.3} \tag{1}$$

3. Test results

The test results from the push-out tests are summarized in the following sections. It can be noted that the presented displacements are all mean values of the LVDTs that measured the same type of displacement in different parts of the specimen.

3.1 Load-slip behaviour

The test results regarding the load-slip behavior are summarized in Table 2 together with the test results from the concrete testing. The presented parameters are the failure load (P_u), the characteristic resistance of the shear connectors (P_{Rk}), the slip at the maximum load (δ_{Pu}) and the slip capacity (δ_u) measured at the characteristic load level. The secant stiffness is also presented at two load levels. The initial stiffness ($k_{0.4Pu}$) is represented by the stiffness up to 240 kN, measured after the 25 shake down cycles between 80-240 kN. The presented serviceability stiffness ($k_{0.75PRk}$) equals the stiffness measured at a load level corresponding to 75% of the characteristic load capacity, established by the simplified EC4-method presented below. Both types of secant stiffness are illustrated in Fig. 6b.

The characteristic resistances have been evaluated both according to the simplified method given in Annex B in EC4-1-1 and according to the more general statistical method in line with Annex D in EC0 (2002). In the former method, provided that the individual test result from three nominally identical specimens deviate less than 10% from the mean value ($P_{u,m)}$, the characteristic resistance is taken as the minimum failure load multiplied with 0.9, see equation (2). The EC4-1-1 simplified method is based on the EC0 'use of additional prior knowledge', which assumes that the coefficient of variation V_r is known from a significant number of previous tests. It may be deduced that this code assumes $V_r = 11\%$ (Johnson 2011).

$$P_{Rk,EC4} = 0.9 P_{u,min} \tag{2}$$

The second method is described by Equation (3), where k_n is the characteristic fractile factor and V_{Pu} is the coefficient of variation of the failure load. The value of V_{Pu} is calculated according to equation (4), while the value of k_n can be found in Table D1 in EC0. The latter is dependent on the number of tests (n) and if the coefficient of variation is known from previous tests. In this case, V_{Pu} are conservatively assumed to be unknown, which gives k_n equal to 3.37, 2.63 and 2.33 for number of tests n = 3, 4 and 5, respectively.

$$P_{Rk,EC0} = P_{u,m}(1 - k_n V_{Pu}) \tag{3}$$

$$V_{Pu} = \left(\left(\frac{1}{n-1} \sum \left(P_{u,i} - P_{u,m} \right)^2 \right)^{0.5} \right) / P_{u,m} \tag{4}$$

It should be noted that, while the test results from the two reference tests performed without the clamping rods (RCX

and RWX) are presented in Table 2, they are excluded from the evaluation of the characteristic values.

The load-slip diagrams for the test specimens are presented in Fig. 9. All specimens show a ductile behavior and exceed by far the ductility criterion of a characteristic slip (δ_{uk}) of at least 6 mm, in accordance with EC4-1-1. Some of the curves ends abruptly in a vertical line, this does not correspond to the real behavior but can be explained by the fact that the measuring LVDTs, with a maximum stroke of 25 mm, run out of stroke at these levels. If the stroke registered on the hydraulic jack was plotted instead, this phenomenon would not be observed. It can also be noted that the specimens with CSPs have an S-shape in the beginning of the load-slip curves, while the specimens with WHSs have a more linear behavior in this part of the curve.

Different failure mechanisms were observed for the different types of specimens. The Type RW specimens, with only WHSs, failed by shear failure through the weld of the studs. The failure was preceded by large deformations due to concrete crushing near the bottom part of the studs and yielding in the steel stud shank. Vertical and diagonal cracking of the concrete elements were also observed.Fig.10a shows the concrete block after the testing of specimen RW1, while Fig. 10b shows the corresponding steel plate. The distribution of the crushed concrete zone and the crack pattern can be observed in the previous picture and the small remaining parts of the failed welds in the latter picture. The specimens with only CSPs showed a very ductile failure, with registered slips exceeding 20 mm without any observed shear failure of the connectors. Fig. 10c shows the concrete part of specimen RC1 after the test. Also in this case, the large slips are caused by concrete crushing and yielding of the connectors. Two distinct plastic hinges were developed in the CSPs, one at the interface between the steel and the concrete and the other a few centimeters into the concrete. The largest difference in comparison to the studs, is that the CSPs in most cases remains in one piece even at very large slips, which can be seen in Fig. 10c. It should also be noted that the typical failure of the CSPs involves yielding
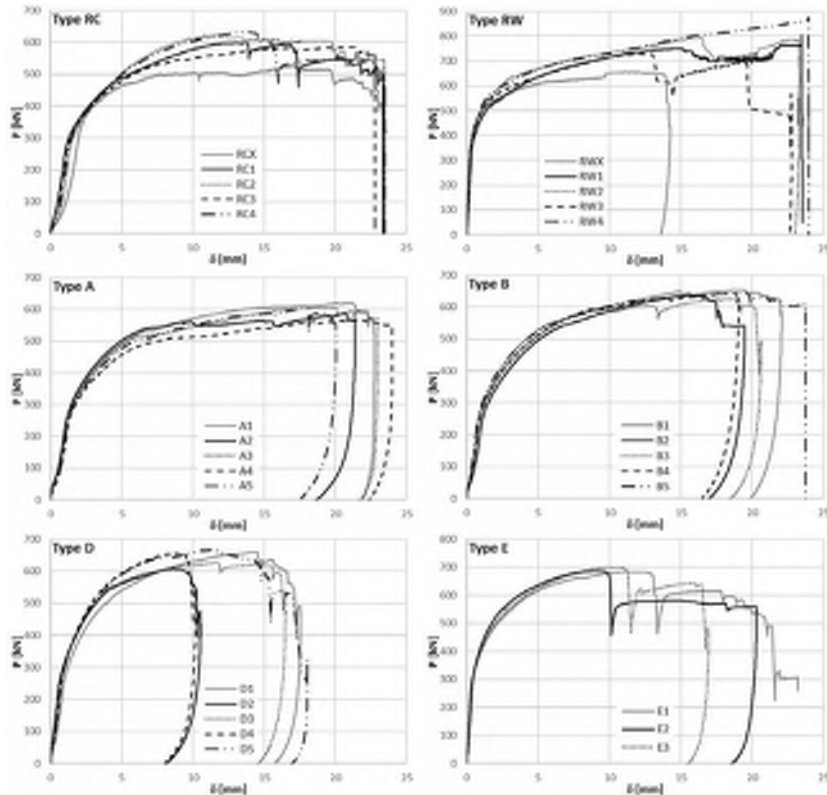

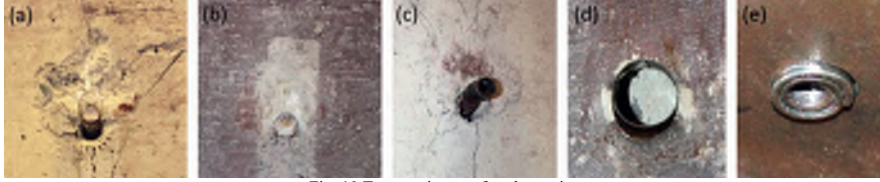Fig. 9 Load-slip diagrams for the tested specimens

Fig. 10 Test specimens after the testing

at the edge of the bearing steel plate, which is shown in Fig. 10d. In some cases, as for specimens of Type D, a shear failure occurred in the CSPs. Such a failure was followed by a reverse movement of the end of the failed CSP. This implies that the end of the failed pins were sticking out, as shown in Fig. 10e, indicating which pins that have failed.

3.2 Transverse separation and CSP end-displacement

The measured transverse separations indicate an almost linear behaviour in relation to the measured slip, with a magnitude of 10-20% of the vertical slip. This corresponds to a separation of 1.3-2.5 mm at the ultimate load level. For the majority of the specimens, the measurements indicate a remaining transverse separation after the initial 25 load cycles of between 10-40% of the ultimate load. When the specimen is loaded to failure, the separation growth rate is

initially small or even negative, representing a closing of the gap created by the initial cycles. The results from the specimens with WHSs (Type RW and E) deviate from the specimens with only CSPs, which is expected since they are a lot stiffer and have heads that counteract the transverse separation.

In order to gain a full perspective of the behaviour of the test specimen compared to the load situation in a beam, the transverse separation also needs to be evaluated together with the clamping force, which is done in the next Section.

The end displacements of the CSPs (δ_{CSP}) are plotted in Fig. 11a in relation to the vertical slip (δ). The displacement is positive when the CSPs are moving into the steel plate. The selected specimens from each series correspond to those that were closest to the mean values of the respective series. The plotted curves are the mean values for all CSPs within the specimens, which are terminated when the first pin fails or

Table 2 Load-slip test results

Series/ specimens			$f_{cm,cube}$ [MPa]	$f_{cm28,cube}$ [MPa]	E_{cm} [GPa]	P_u [kN]	$P_{u,m}$ [kN]	$P_u / P_{u,m}$ [-]	$P_{Rk,EC4}$ [kN/SC]	$P_{Rk,EC0}$	δ_{Pu} [mm]	δ_u [mm]	δ_{uk} [mm]	$k_{c0.4}$ [kN/mm]	$k_{0.75PRk}$
Type RC	RC1	C30/37	47.0 Min: 44.7 Max: 48.8	46.3 Min: 44.6 Max: 48.3	32.7	598	611	0.98	132	138	13.7	17.4	14.3	60.8	37.4
	RC2					625		1.02			12.0	20.8		46.5	35.6
	RC3					586		0.96			21.3	>22.0		55.8	35.4
	RC4					633		1.04			13.5	15.9		50.2	34.4
	RCX					530	-	-	-	-	11.6	-	-		
Type RW	RW1	C30/37	52.9 Min: 51.4 Max: 55.8	53.9 Min: 51.2 Max: 55.7	33.9	811	805	1.01	165	163	14.8	>22.0	12.1	372	94.4
	RW2					800		0.99			16.3	>22.0		458	124
	RW3					733		0.91			12.8	13.4		272	119
	RW4					876		1.09			>22.0	>22.0		265	144
	RWX					659	-	-	-	-	17.0	-			
Type A	A1	C20/25	30.3 Min: 27.8 Max: 32.7	33.4 Min: 32.2 Max: 34.4	28.7	619	597	1.04	128	138	21.1	> 22.0	17.9	57.6	36.6
	A2					586		0.98			20.7	> 21.0		55.1	38.9
	A3					606		1.01			18.8	> 22.0		57.5	35.2
	A4					571		0.96			21.3	> 22.0		47.8	30.8
	A5					605		1.01			17.9	19.9		50.8	33.4
Type B	B1	C40/50	47.0 Min: 44.0 Max: 48.4	50.8 Min: 49.7 Max: 51.7	32.7	654	640	1.02	141	154	19.0	> 22.0	16.0	74.0	36.0
	B2					636		0.99			15.5	17.8		56.8	31.8
	B3					625		0.98			18.8	20.3		74.0	39.8
	B4					643		1.00			18.8	18.9		69.5	36.3
	B5					642		1.00			18.8	22.0		81.7	40.6
Type D	D1	C30/37	50.2 Min: 48.8 Max: 51.8	52.0 Min: 48.9 Max: 53.8	33.4	659	643	1.03	137	146	14.2	14.6	9.2	67.5	44.2
	D2					607		0.94			8.7	10.4		105	54.1
	D3					626		0.97			11.6	16.2		80.6	54.7
	D4					656		1.02			9.1	10.2		84.4	56.4
	D5					666		1.04			11.2	15.4		90.0	54.3
Type E	E1	C30/37	46.3 Min: 45.2 Max: 46.8	43.1 Min: 42.5 Max: 43.7	32.6	682	689	0.99	153	165	11.9	13.1	8.7	271	72.0
	E2					686		1.00			8.9	9.7		192	86.4
	E3					698		1.01			10.0	11.4		176	76.6

when the slip reaches 20 mm. When the first pin fails, it starts to move in the opposite direction compared to the other connectors as described in section 3.1, implying that the mean value is no longer relevant. The CSP end-displacements show a linear behaviour in relation to the vertical slip, after an initial phase with small or no movements up to a slip of approximately 1 mm. For the specimens with four CSPs and 30 mm steel plate thickness (Type RC, A and B), the mean value of the CSP-movements varies between 0.3-1.0 mm after a slip of 10 mm. However, 13 of 15 tests are within the interval of 0.6-1.0 mm, and the two divergent tests are both of Type A. The specimens of Type D, with 45 mm steel plates, all show smaller CSP-movements with magnitudes of 0.1-0.25 mm after a slip of 10 mm. The corresponding values for the Type E specimens are 0.3-0.4 mm.
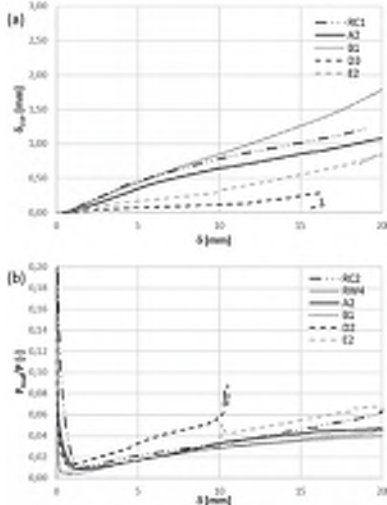

Fig. 11 (a) CSP end-displacement vs. the slip, (b) the clamping force plotted vs. the slip.

When the CSP-movements are compared to the measured hole diameters, no strong correlation can be found. The most interesting observation is that the steel plate thickness seems to be of high importance for the CSP end-displacement.

3.3 Clamping force

The relation between the total clamping force registered in the two rods (P_{Rod}) and the applied load (P) has been plotted over the slip in Fig. 11b. The initial shape of the curve is explained by the fact that the tests started with an initial clamping force of ~2 kN, which gives the infinity as the starting point for the relationship. It can be noted that the total clamping force prior to the failure are below 8% of the applied vertical load for all tests specimens. When the clamping force is plotted over the applied load it can be

observed that the initial clamping force decreased in the beginning of the test, this observation is discussed in the next chapter.

4. Analysis

The analysis is focused on two main aspects, the load capacity of the shear connection and the evaluation of the test set-up.

4.1 Load capacity and stiffness

The design rules for shear studs in EC4-2 are based on empirical examinations over the years (Hicks *et al.* 2014). The design requires a double verification of the shear connection resistance, where equation (5) gives the shear resistance in case of a failure in the shear studs, while equation (6) and (7) gives shear resistance in case of a failure in the concrete.

$$P_{Rd,s} = \frac{0.8 f_u \pi d^2 / 4}{\gamma_V} \tag{5}$$

$$P_{Rd,c} = \frac{0.29 \alpha d^2 \sqrt{f_{ck} E_{cm}}}{\gamma_V} \tag{6}$$

$$\alpha = \begin{cases} 0.2 \left(\dfrac{h_{sc}}{d} + 1 \right) & for \quad 3 \le h_{sc}/d \le 4 \\ 1 & for \quad h_{sc}/d > 4 \end{cases} \tag{7}$$

where γ_V is the partial factor, d is the diameter of the shank of the studs, f_u is the ultimate tensile strength of the stud material (limited to 500 MPa), f_{ck} is the characteristic cylinder compressive strength and h_{sc} is the overall nominal height of the stud.

As a first step in the evaluation, the test results have been compared against equation (5) and (6), by plotting the relationship between the shear capacity (P_R) and the concrete compressive strength (f_{ck}), see Fig. 12. The results are presented separately for the WHSs and the CSPs in Fig. 12a and Fig. 12b, respectively (with the exception of specimen Type E which is plotted in both diagrams since it contains both types of shear connectors). The dependency of the stud diameter in equation (5) has been rewritten as a dependency of the connectors shear area, A_{sc}, to enable a comparison towards the CSPs. The partial factors have also been excluded and mean measured values of the variables are used within the equations.

From Fig. 12, it can be noted that all test results are on the safe side compared to the lowest design capacity given by equations (5) and (6). Also the characteristic values, presented in Table 2, are all clearly on the safe side if the EC0 model is used, while the EC4 model gives characteristic values that are almost equal to the design criteria for the Type RC and D specimens and on the safe side for the others. As shown in Fig. 12b, there seems to be a correlation between the measured shear resistance and the concrete compressive strength, but not as strong as equation (6) indicates. Linear regressions based on the characteristic values evaluated by the EC0 and the EC4 models, shows that the shear capacity

of a single CSP increases by 0.8-0.9 kN/MPa. Regarding the shear resistance of the pin itself, the tested tensile strength have been used and the limitation of the ultimate tensile strength required by EC4 has not been taken into consideration ($f_u \leq 500$ MPa). If this is done the shear resistance, $P_{R,s}$, would be lowered to 152 kN for WHSs and 95 kN for CSPs. For CSPs, this would imply that the expected failure according to the design formulas would have been a shear failure of the pins at low loads levels.

A study of the impact of different steel flange thicknesses has been done by a comparison between the specimens of Type RC, B and D, which have steel flange thicknesses of 30 mm and 45 mm, respectively. The mean concrete compressive cube strength is comparable for the studied specimens, with a range of 47-50 MPa. Regarding the failure load, the test results indicate no significant difference between the two tested steel flange thicknesses. However, there is a difference in the ductility of the shear connection and in the stiffness. The Type B specimens with the lower steel plate thickness shows a more ductile behavior with a longer yielding plateau on the load-slip curve, while the Type D specimens with the thicker steel plates have a more distinct and earlier failure. The characteristic slip capacity (δ_{uk}) is 55% and 75%, respectively bigger (Type RC and B) for the 30 mm plates in comparison to the 45 mm plates.

The initial stiffness ($k_{0.4Pu}$) and the serviceability stiffness ($k_{0.75PRk}$) both indicate a dependency of the steel plate thickness. A comparison between the Type RC, A, B and D specimens, shows that the initial stiffness varies between the test series, with mean values of 53.3, 53.8, 71.2 and 85.4 kN/mm, respectively. The Type D specimens are the stiffest and deviate a bit from the others, even though the Type B specimens also are somewhat stiffer in comparison to the two other types. A similar comparison of the serviceability stiffness shows a stronger dependency of the steel plate thickness. The mean values of $k_{0.75PRk}$ for the tests with 30 mm steel plates are all within the interval 35.0-36.9 kN/mm, whereas the corresponding value for the Type D specimens is 52.7 kN/mm. In this comparison, it should be noted that the stiffness $k_{0.75PRk}$ are not corresponding to exactly the same load levels, since the characteristic capacity has been evaluated for each individual test series. In the study presented by Buckby *et al.* (1997), the initial stiffnesses ($k_{e0.44}$) after three shake down cycles, with a load range of 0.1-0.44 Pu, varied between 90-110 kN/mm and 65-120

kN/mm, for steel plate thicknesses of 25 mm and 35 mm, respectively. From these results it is hard to identify any impact of the steel flange thickness, on the stiffness. Nevertheless, it is expected that an increased rigidity in the connection between the CSP and the steel flange would increase the stiffness of the connection. This is also supported by additional project specific tests from the UK, on specimens with steel plate thicknesses from 6 – 17.5 mm. However, the absolute stiffness varies a lot between the different tests, which is believed to be dependent on the different types of test set-ups and the presence of different clamping forces and constraints, which is discussed in the next section.

A similar comparison of how the stiffnesses are related to the concrete strength, shows no clear signs of a dependency. The mean stiffnesses for the Type RC and A specimens are almost identical, even though the concrete cube strength is 47.0 MPa and 30.3 MPa, respectively. More tests providing a broader spectrum of concrete strengths would have been useful. The tests were planned to be representative for three concrete strength classes C25/30, C30/37 and C40/50. Unfortunately, for the two higher strength classes the delivered concrete appeared to have almost the same concrete strength, even though different concrete mixes were used. In the absence of additional tests, a parametric study will be performed on FE-models calibrated to the tests results presented in this paper, in order to broaden the study of the impact of the concrete strength as well as the steel plate thickness.

The Type E specimens were tested to establish the behavior of the CSPs used in combination with existing shear studs. The test results show that there is a big difference in the initial load-slip behavior of the CSPs compared to WHSs. This difference is less important in the ULS since both types of connectors show a very ductile behavior with large slips before the final failure. When the stiffer WHS starts to yield the CSPs will take the additional load until both types of connector yield. If the failure load (P_u) for the Type E specimen is estimated based on the mean failure loads for the Type RC and RW, with comparable concrete compressive strengths, the predicted failure load would be 708 kN compared to the measured mean value of 689 kN (-2.7%). If a similar comparison is done for the initial stiffness and the serviceability stiffness, the prediction would be 198 kN/mm and 78.0 kN/mm, respectively. This can be compared to the
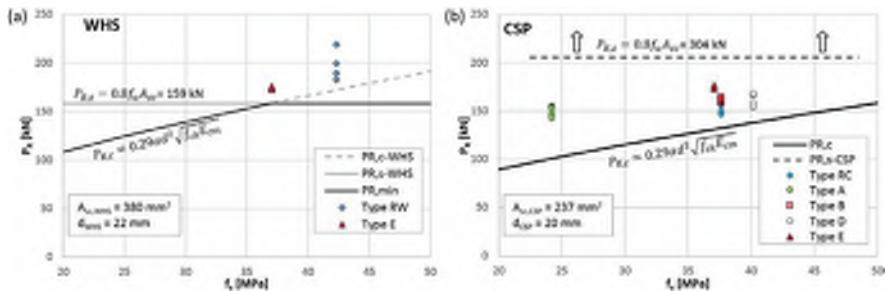

Fig. 12 Test results vs. the shear resistance criteria in EC4-2

measured mean stiffnesses of 213 kN/mm (+7.6%) and 78.3 kN/mm (+0.3%). It should be noted, that this comparison is based on the load-slip diagrams that commence after the 25 shake down cycles. The force applied during the shake down cycles will be unevenly distributed between the two types of connectors, due to the large difference in the stiffness. This implies that the CSPs will not follow the load-slip curves that corresponds to the 26th loading up to 240 kN, for a test with only CSPs. The response will instead be more similar to the first load cycle, since the impact of the shake-down cycles have limited effect on the weaker CSPs. Fig. 13 illustrates the mean load-slip curves for test specimens Type RC, RW and E, together with a combined curve RW/RC representing a test specimen with 2 WHSs and 2 CSPs. The initial S-shape of the CSP curve is not observed in the first load cycle, which explains the different shapes of the Type E curve and the RW/RC curve at slips up to ~1.2 mm. However, it is obvious that the Type E specimens exhibit a stiffer behaviour than the prediction based on the combined load-slip behavior of the Type RW and RC specimens. One explanation to the higher stiffness might be the impact of the reduced transversal separation through the headed shear studs. To illustrate the effect of a 35% stiffness increase of the CSPs, the RW/RC-stiff curve is plotted in Fig. 13 for comparison purposes.

Based on the test results presented above for the Type E specimen, a conservative estimation of the total shear connection stiffness, and a good estimation of the failure load, can be done through superposition of the load-slip curves for two CSP and two WHSs, tested separately. This information can be useful in order to estimate the shear connection stiffness in a global model and to establish the ultimate capacity of a shear connection with different types of connectors. In the SLS and Fatigue Limit State (FLS) stages the local force distribution between the shear connectors are of higher importance and need to be studied separately in the design stage. Secant modulii for the studied load levels can be used in the comparison, in order to simplify the design model and avoid non-linear spring elements.

The analysis of the shear connector stiffness is based only on the push-out tests presented above. However, a field monitoring performed, by Hällmark *et al.* (2017), on a bridge strengthened with CSPs indicate that the shear connection behaves as a totally rigid connection at the tested load levels,

which corresponds to approximately 80% of the FLS load. Future beam tests will be performed to study the stiffness on a structural level in the ULS.

4.2 Evaluation of the test set-up

In comparison to the standard push-out test, a clamping force is used in the test set-up presented in this paper. As highlighted by Hicks *et al.* (2014), the standard specimens are designed to transfer the forces in a similar way as a composite girder. However, the eccentricity between the load introduction point in the concrete and the centre of the support will result in a moment, see Fig. 14a. This moment, 0.5P·e, will be counteracted by frictional forces (F_f) at the base and compression forces (F_c) in the compression zones against the steel beam at the top, but also by tensional forces (F_t) developed in the shear studs.

If the external forces acting on the steel plates are plotted for the push-out test set-up presented in this paper (see Fig. 14b), some important differences can be noted. The steel plates are a lot thinner than the concrete slabs in the standard test (3.3-5 times), which implies that the eccentricity between the load introduction point and the support point is a lot smaller, which in turn leads to a smaller eccentricity moment and a smaller compression force in the top of the steel-concrete interface. The load transferred to the steel plate by each CSP will consist of both the vertical force component (F_V) and the support reaction caused by the moment (M_V).

The position of the force resultant ($F_{B,R}$) will be dependent on several different parameters, such as the steel plate thickness and the load level, assuming constant CSP properties. A thicker steel plate will provide a longer distance between the counteracting force couple in the holes, provided by the contact bearing pressure. A higher load level will result in an increased concrete crushing around the connectors, which shifts the load introduction point on the CSPs away from the steel concrete interface, which gives a higher moment. The material parameters of the steel and the concrete will, of course, also influence the behaviour.

Another difference is the absence of heads on the connectors, so that the tensional force component at the steel concrete interface is limited to the friction at the CSP-surface. The combination of a lower eccentricity moment and
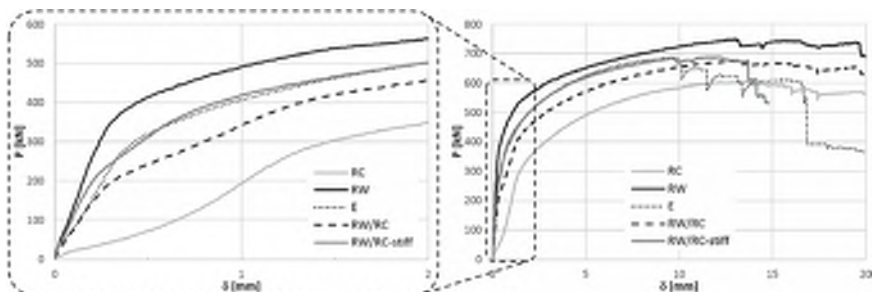

Fig. 13 Mean load-slip curves for the Type RC, RW and E specimens and predictions of the Type E curve
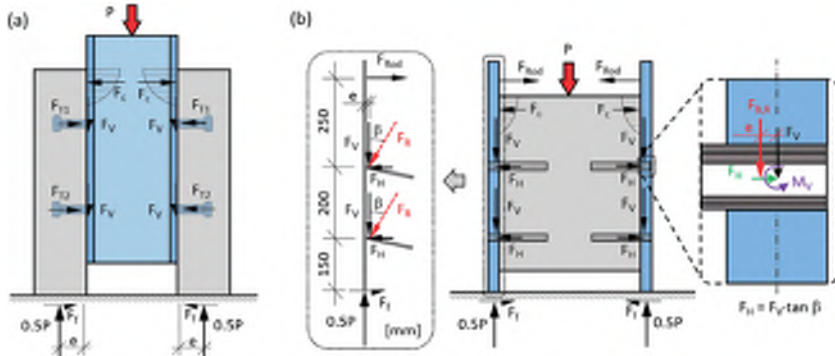
Fig. 14 (a) Forces acting on the concrete slabs, (b) Forces acting on the steel plates

the negligible tensile capacity of the connectors implies that a clamping force is required to balance the horizontal force components developed during the tests.

Initially, the connectors are perpendicular to the steel-concrete interface. When the load on the CSPs increases, the CSPs will deform and the slip at the steel-concrete interface will increases as well. If the direction, β, of the force F_R, in Fig. 14b, is assumed proportional to the slip, δ, and the inclined compressive strut, F_R, is divided in a vertical and a horizontal force component of F_V and F_H, respectively. Then the total clamping force in the two rods, F_{Rod}, could be expressed by a moment equilibrium around the support point assuming an equally load distribution between the four shear connectors, as follows:

$$F_{Rod} = \frac{(0.15 + 0.35)F_V \tan(\delta \cdot C_\beta) - 2F_V e}{0.6} + F_{Rod.ini} \quad (8)$$

where C_β is a fictive rotational stiffness factor, e is the eccentricity of the vertical bearing force resultant, $F_{B,R}$, acting on the steel plates and $F_{Rod.ini}$ the initial clamping force in the two rods when the tests starts.

As presented in section 3.2, due to the initial shake down cycles there is an existing gap between the steel and concrete when the final test starts. The horizontal force F_c is therefore neglected in (8). The C_β and the e parameters are unknown,

but can be estimated after the tests through curve fitting, in order to find out if the specimens behave in line with equation (8). Fig. 15a illustrates the relationship between the mean value of the measured clamping force, P_{Rod}, and the slip, δ, together with the prediction of the clamping force in line with the force model presented in equation (8). It should be highlighted, that the force model presented in this section has been studied only to provide an insight in how the forces are distributed within the test set-up. No attempt has been made to create a general model for the prediction of the forces prior to the test.

For the specimens with steel plate thickness 30 mm (Type RC, A and B) the adapted values on the parameters C_β and e are 1.0°/mm and 6.0 mm, respectively. Whilst the corresponding values for the Type D specimen, with steel plate thickness 45 mm, are 1.5°/mm and 3.0 mm. As shown in Fig. 15a, the calibrated force model manages to simulate the measured forces in the clamping rods quite well at moderate slip levels, while the model deviates from the measured values when the plastic slip increases. The e and C_β parameters seems to be strongly dependent on the steel plate thickness, while it is hard to identify any correlation to a varying concrete strength. It can be noted that the tests commenced with an initial clamping force of ~2-3 kN, which decreased during the initial loading, before it started to grow.
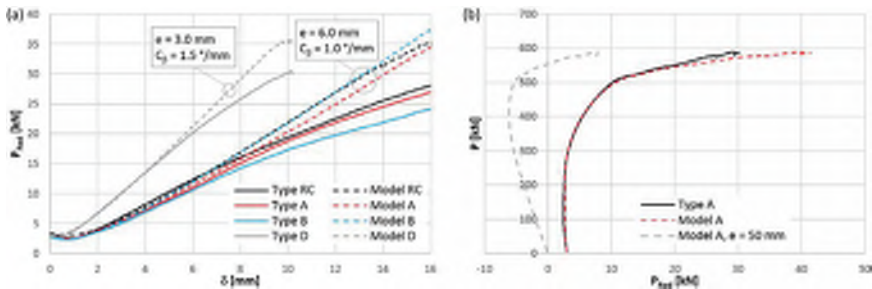

Fig. 15 (a) Clamping force vs. the slip, (b) Total load vs. the clamping force

The initial decrease is caused by the eccentricity moment, which is very small in comparison to a standard push-out test. This implies that the horizontal force component acting on the connectors will be dominating when the load level increases. Keeping the other parameters constant, if the eccentricity, e would be increased the eccentric moment would be more dominating and there should be no problems with separations at moderate load levels. In Fig. 15b, the relationship between the applied force, P, and the clamping force, P_{Rod}, has been plotted based on the mean values from the tested specimen Type A. A prediction of the clamping force, in line with equation (8), for a specimen with 50 mm eccentricity is also plotted in Fig. 15b, to illustrate the impact of an increased eccentricity. As shown in the figure, this would suggest that there would be no tensional forces in the rods before the load exceeds approximately more than 90% of the ultimate capacity. At lower load levels, a compressive force, F_c, would instead be developed in the upper part of the steel-concrete interface, as illustrated in Fig. 14b. An eccentricity of this magnitude or larger would be possible to achieve, if the steel plates were replaced by H- or T-sections instead, or by using the standard test set-up.

If there were no clamping forces, the steel plates would rotate around the support point and separate from the concrete already at low load level, which was observed in the two reference tests (RCX and RWX) that were tested without clamping rods. In a steel girder bridge, the steel girder would by far be the stiffest part and would not be affected substantially by any separating forces. However, the weaker concrete part would be subjected to a vertical uplift force due to inclination of the compressive strut. This potential uplift cannot easily be simulated in a push-out test, since there are several factors that would affect this such as the curvature of the loaded structure, the existence of a continuous shear connection, the concrete dead load etc. The potential uplift will instead be investigated through a future beam test series performed by the authors.

During the tests presented in this paper, gaps occurred at the steel-concrete interface from the top of the specimen down below the lowest shear connector, at load levels far below the ultimate load capacity. This implies that the critical parts of the concrete, above the shear connectors, should not benefit from any positive constraint in the ultimate state. This might not be the case for some of the other test set-ups previously used for testing CSPs. If the results presented in

this paper are compared to results from tests on similar specimens, but with higher constraints, different shapes on the load-slip curves are observed. The static test reported by Fahleson (2005), was performed on a similar specimen as in this report, but with four welded steel straps that connected the two steel plates at two levels on each side, whereas Buckby *et al.* (1997) used the same specimen but with only steel straps in the upper part of the specimens, see Fig. 2b. In Fig. 16a, the load-slip curves presented by these researchers are plotted together with the mean load-slip curves for the specimens presented in this paper with CSPs only. In addition to these tests, a load-slip curve from a project specific push-out test (Tinsley Viaduct) is also plotted. The latter test was performed on a specimen of the type shown in Fig. 2c.

As shown in Fig. 16a, the curves from the Tinsley tests and the test reported by Fahleson (2005) are deviating from the others, characterized by the steeper inclination in the plastic part of the curve. These two test set-ups are associated with a high degree of constraint, with two pairs of clamping rods respectively steel straps at levels near the positions of the connectors. Even though the clamping forces have not been reported from these tests, it is expected that the stiffer behaviour is a result of the higher constraint and the additional contribution from the friction at the steel-concrete interface caused by this constraint. Another interesting observation is that the load-slip curve reported by Buckby *et al.* (1997) are almost equal to the load-slip curves presented in this paper. This implies that the results reported by Buckby *et al.* (1997) and Fahleson (2005) deviate a lot, even though the tested specimens were almost identical, with the exception of an extra pair of clamping steel plates near the lower shear connectors in the tests by Fahleson (2005).

Whilst there are too few tests available to draw any general conclusions about different test set-ups, based on the available results, the test set-up presented in this paper and the test set-up used by Buckby *et al.* (1997), seems to give comparable results. The positive effect of the constraint caused by the clamping force should be negligible in the ultimate limit state, since a gap have been both measured and visually observed over almost the entire height of the steel-concrete interface, with the exception of the lowest centimetres where the specimens might have been in contact also in the ultimate state. The measured clamping forces are also small in comparison to the horizontal forces in push tests that are recommended by Hicks and Smith (2014), who
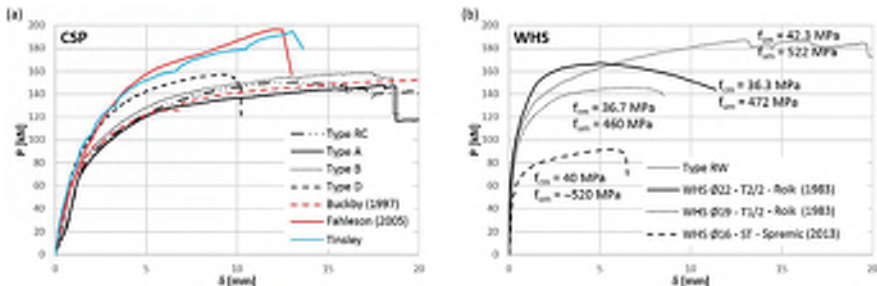

Fig. 16 Load-slip diagrams for different types of push-out tests: (a) CSPs, (b) WHSs

compared the performance of headed studs in full-scale beams and companion push-out test specimens with profiled steel sheeting. However, since there are no beam tests performed on CSPs, the behaviour and the shear connection stiffness at a structural level cannot be determined with certainty.

A comparison of the results from the reference tests performed on WHSs and load-slips curves reported by Roik and Hanswille (1983) and Spremic *et al.* (2013), for different shear stud dimensions, indicate that the alternative test set-up gives a more ductile failure than the standard test set-ups, see Fig. 16b. The ultimate capacity is also a bit higher, but this can be explained by the fact that the material parameters differs between the two curves for the Ø22 mm specimen. If the ultimate capacity values for the WHS tests are compared to test results on specimens with similar concrete strength and tensile strength of the studs, summarised by Hicks (2017), then the ultimate load capacity corresponds quite well to the test results from standard tests. The load-slip curves follow each other up to a load level of approximately 60% of the ultimate load, before they separate. The difference in the ductility between the test set-up is not crucial, since the ductility criteria of 6 mm in EC4-2 is fulfilled by far.

5. Conclusions and future research

Based on the experimental study presented in this paper, the following conclusions can be drawn:

A nominal static strength of 130 kN per coiled spring pin (CSP) was recommended by Buckby *et al.* (1997), for pins installed in C30/37 concrete and with 25-35 mm steel flanges. The tests presented in this paper, with cube strengths within the interval of 30-53 MPa, indicate that 130 kN/CSP can be used for a wider range of concrete strength classes since the tested characteristic resistances of the CSPs are higher for all tests evaluated in line with the EC0-model. However, the Type A specimens give a characteristic strength slightly below this value (128 kN/CSP) if the simplified method in EC4 is used. Yet, the results indicate that the impact of the concrete strength on the ultimate load capacity seems to be quite low. The same conclusion is valid for the tested steel plate thicknesses. The evaluation of the test results has so far been done according to the double verification criteria in EC4-2, checking the resistance in case of a failure in the shear studs respectively the concrete. For a deeper understanding of the CSP behavior, a third verification criteria, taking into account the bearing failure in the steel flanges due to the contact pressure caused by the CSPs, should be considered. This will be investigated by FE-models calibrated to the test results presented in this paper.

Even though the impact of the steel plate thickness on the ultimate capacity is quite low, this parameter seems to influence the stiffness of the shear connection quite a lot and also the ductility. Furthermore, the influence of the concrete strength on the stiffness seems to be very low at moderate load levels. It should also be highlighted that there is a big difference in the stiffness of coiled spring pins and welded shear studs. This is of high importance if an existing shear connection is strengthened with coiled spring pins, for the behavior at moderate load levels.

The evaluation of the test set-up shows that it is necessary to apply a clamping force on this type of push-out test, in order to avoid separations driven by the geometry of the specimen. The clamping used in the test series will not give any positive constraint effects in the ultimate state, since a gap is developed early in the test. However, the evaluation of previously used test set-ups indicate that higher degrees of constraint might give non-conservative test results due to positive effects from the constraint also in the ultimate state.

Future push-out tests are considered to be performed on standard specimens, with a steel section that are cut into two halves prior to the installation of the CSPs and then welded back into one unit after the installation of shear connectors. It should be noted that the HE260B section specified by EC4-1-1 in the standard test has to be replaced, since the steel flange thickness is a parameter that will affect the test results.

The experimental results presented in this paper will be evaluated further and compared to FE-modelling. The FE-models will be used to perform a parametric study to find out if it is possible to present more general design guidelines and to develop design formulae. This study of the static capacity of CSPs, has been complimented by a fatigue test series with 12 specimens, which will be reported separately. Finally, in order to extend the push-out test results to beam behaviour, beam tests are planned.

Acknowledgments

References

Blanquart, C., Clausen, U., and Jacob, B. (2016), *Towards Innovative Freight and Logistics*. John Wiley & Sons, Hoboken, NJ, USA.

Bradford, M. A., Filonov, A., Hogan, T. J., Ranzi, G., and Uy, B. (2006). "Strength and ductility of shear connection in composite T-beams", *Proceedings of the 8th International Conference on Steel, Space & Composite Structure*s, Kuala Lumpur, Malaysia, May.

Buckby, R., Ogle, M., Johnson, R. P., and Harvey, D. (1997), "The performance of coiled spring pin connectors under static and fatigue loading". *Proceedings of the International IABSE Conference: Composite construction - conventional and innovative,* Innsbruck, Austria, September.

Döinghaus, P. (2002), "Zum Zusammenwirken hochfester Baustoffe in Verbundträgern", Ph.D. Thesis, RWTH Aachen, Germany. (in German)

Easterling, W. S., Gibbings, D. R., and Murray, T. M. (1993), "Strength of shear studs in steel deck on composite beams and joists". *Engineering Journal*, **30**(2), 44-54.

EC0 (2002), EN 1990 Eurocode – Basis of structural design, European Committee for Standardisation; Brussels. Belgium.

EC2-1-1 (2005), EN 1992-1-1 Eurocode 2- Design of concrete structures – Part 1-1: General rules and rules for buildings,

European Committee for Standardisation; Brussels. Belgium.

EC4-1-1 (2004), EN 1991-1-1 Eurocode 4 - Design of composite steel and concrete structures – Part 1-1: General rules and rules for buildings, European Committee for Standardisation; Brussels. Belgium

EC4-2 (2005), EN 1994-2 Eurocode 4 - Design of composite steel and concrete structures – Part 2: General rules and rules for bridges, European Committee for Standardisation; Brussels. Belgium

Ernst, S., Bridge, R. Q., and Wheeler, A. (2009). "Push-out tests and a new approach for the design of secondary composite beam shear connections". *Journal of Constructional Steel Research*, **65**(1), 44-53.

Ernst, S., Bridge, R. Q., and Wheeler, A. (2010). "Correlation of beam tests with pushout tests in steel-concrete composite beams". *Journal of structural engineering*, **136(**2), 183-192.

Fahleson, C. (2005), "Laboratory report: Testing of shear connectors", Laboratory Report No: 05035, Luleå University of Technology, Luleå, Sweden.

Gattesco, N., and Giuriani, E. (1996), "Experimental study on stud shear connectors subjected to cyclic loading". *Journal of Constructional Steel Research*, **38**(1), 1-21.

Guezouli, S., & Lachal, A. (2012). "Numerical analysis of frictional contact effects in push-out tests". *Engineering Structures*, *40*, 39-50.

Guezouli, S., Lachal, A., and Nguyen, Q. H. (2013). "Numerical investigation of internal force transfer mechanism in push-out tests". *Engineering Structures*, *52*, 140-152.

Henderson, I. E. J., Zhu, X. Q., Uy, B., and Mirza, O. (2017). "Dynamic behaviour of steel-concrete composite beams retrofitted with various bolted shear connectors". *Engineering Structures*, *131*, 115-135.

Hällmark, R., Collin, P., Petersson, M., and Andersson, E. (2017), "Monitoring of a bridge strengthened with post-installed coiled spring pins", *Proceedings of the 39th IABSE Symposium – Engineering the Future*, Vancouver, Canada, September.

Hällmark, R., Jackson, P. and Collin, P. (2016), "Post-installed shear connectors–coiled spring pins". *Proceedings of the 19th IABSE Congress*, Stockholm, Sweden, September.

Hicks, S. J. (2017), "Design shear resistance of headed studs embedded in solid slabs and encasements", *Journal of Constructional Steel Research*, *139*, 339-352.

Hicks, S. J., and Smith, A. L. (2014), "Stud shear connectors in composite beams that support slabs with profiled steel sheeting", *Structural Engineering International*, *24*(2), 246-253.

Hungerford, B. E. (2004), "Methods to develop composite action in non-composite bridge floor systems: Part II*, M.Sc. Thesis, The University of Texas at Austin, USA.

ISO 13918 (2008), Studs and Ceramic ferrules for arc stud welding, ISO – the International Organization for Standardization; Geneva. Switzerland.

ISO 14555 (2014), Welding – Arc stud welding of metallic materials, ISO – the International Organization for Standardization; Geneva. Switzerland.

ISO 6892-1 (2016), Metallic materials – Tensile testing – Part 1: Method of test at room temperature, ISO – the International Organization for Standardization; Geneva. Switzerland.

ISO 8748 (2007), Spring-type straight pins – Coiled. heavy duty. ISO – the International Organization for Standardization; Geneva. Switzerland.

Johnson, R. P. (2011), *Designers Guide to Eurocode 4: Design of Composite Steel and Concrete Structures*, Thomas Telford, London, UK.

Kayir, H. (2006), "Methods to develop composite action in non-composite bridge floor systems: Fatigue behavior of post-installed shear connectors"*, M.Sc. Thesis, The University of Texas at Austin, USA

Kwon, G., Engelhardt, M. D., and Klingner, R. E. (2009), "Strengthening bridges by developing composite action in existing non-composite bridge girders", *Structural Engineering International*, **19**(4), 432-437.

Kwon, G., Engelhardt, M. D., & Klingner, R. E. (2010a). "Behavior of post-installed shear connectors under static and fatigue loading". *Journal of Constructional Steel Research*, **66**(4), 532-541.

Kwon, G., Engelhardt, M. D., & Klingner, R. E. (2010b). "Experimental behavior of bridge beams retrofitted with postinstalled shear connectors". *Journal of Bridge Engineering*, **16**(4), 536-545.

Kwon, G., Engelhardt, M. D., & Klingner, R. E. (2011). "Parametric studies and preliminary design recommendations on the use of postinstalled shear connectors for strengthening noncomposite steel bridges." *Journal of Bridge Engineering*, **17**(2), 310-317.

Lam, D. (2007), "Capacities of headed stud shear connectors in composite steel beams with precast hollowcore slabs", *Journal of Constructional Steel Research*, *63*, 1160-1174.

Lumsden, K. (2004), "Truck masses and dimensions - impact on transport efficiency", Research Report; Department of Logistics and Transportation, Chalmers University of Technology, Gothenburg, Sweden.

Lungershausen, H. (1988), "Zur Schubtragfähigkeit von Kopfbolzendübeln", Ph.D. Thesis, Ruhr Universität Bochum, Germany. (in German)

Maeda, Y. et al. (1983), "Effects of concrete placing direction on static and fatigue strength of stud shear connectors", Technology Report No. 1733, Osaka University, Japan.

Nellinger, S., Odenbreit, C., Obiala, R., and Lawson, M. (2017), "Influence of transverse loading onto push-out tests with deep steel decking", *Journal of Constructional Steel Research*, **128**, 335-353.

Pathirana, S. W., Uy, B., Mirza, O., & Zhu, X. (2015). "Strengthening of existing composite steel-concrete beams utilising bolted shear connectors and welded studs". *Journal of constructional steel research*, *114*, 417-430.

Pathirana, S. W., Uy, B., Mirza, O., & Zhu, X. (2016a). "Flexural behaviour of composite steel–concrete beams utilising blind bolt shear connectors". *Engineering Structures*, *114*, 181-194.

Pathirana, S. W., Uy, B., Mirza, O., & Zhu, X. (2016b). "Bolted and welded connectors for the rehabilitation of composite beams". *Journal of Constructional Steel Research*, *125*, 61-73.

Pritchard, B. (1992), *Bridge Design for Economy and Durability: Concepts for New, Strengthened and Replacement Bridges*. Thomas Telford, London, UK.

Roik, K., and Hanswille, G. (1983), "Beitrag zur Bestimmung der Tragfähigkeit von Kopfbolzendübeln", *Stahlbau*, **52**(10), 301-308.

Roik, K., Hanswille, G. Cunze, A. and Lanna, O. (1989), "Harmonisation of the European Construction Codes – Report on EUROCODE 4 Clause 6.3.2: Stud Connectors", Research Report No: EC4/8/88, Bochum, Germany.

Schaap, B. A. (2004), "Methods to develop composite action in non-composite bridge floor systems: Part I*, M.Sc. Thesis, The University of Texas at Austin, USA

Spremic, M., Markovic, Z., Veljkovic, M., and Budjevac, D. (2013), "Push-out experiments of headed shear studs in group arrangements", *Advanced Steel Construction*, **9**(2), 139-160.

PAPER IX

Post–installed Shear Connectors: Fatigue Push–out Tests of Coiled Spring Pins

Robert Hällmark, Peter Collin and Stephen J. Hicks

Post-installed Shear Connectors:
Fatigue Push-out Tests of Coiled Spring Pins

Robert Hällmark*[1], Peter Collin[1a,] and Stephen J. Hicks[2b]

[1]Department of Civil, Environmental and Natural Resources Engineering, Luleå University of Technology, 971 87 Luleå, Sweden
[2]Heavy Engineering Research Association, Gladding Place Manukau, Auckland 2241, New Zealand

Abstract. The number of heavy vehicles and their weight have been increasing over time, implying that many bridges are experiencing traffic loads with higher magnitude and frequency than they were originally designed for. In some cases, it will be necessary to either replace or strengthen the structures to keep the bridges in service. For existing non-composite steel girder bridges, post-installation of shear connectors can often be used to increase the traffic load capacity significantly. One type of shear connector that is suitable for post-installation, even though not commonly used, is the Coiled Spring Pin. These interference fit connectors can be installed from below the bridge deck during traffic, in order to minimize the impact on road users. This paper describes an experimental study on the fatigue strength of Coiled Spring Pins and a compilation of previously performed fatigue tests on this type of connector. The new test series, with nine specimens, are evaluated statistically and a fatigue strength design equation is proposed. The results show that there are large variations between different test series, while tests within the same series show good agreement. The reasons for this are discussed in the paper along with recommendations for future testing.

Keywords: push-out test; fatigue; coiled spring pin; shear studs; strengthening; shear connector; post installation; composite; steel; concrete

1. Introduction

Many existing bridges are experiencing higher traffic loads and an increased number of load cycles than they originally were designed for. To keep these bridges in service, bridge assessment is often the first and the most cost effective method. However, if the assessment indicates that the load capacity is too low, an effective and well adapted strengthening method is often advantageous compared to a bridge replacement, both in terms of costs and environmental impact. The appropriate strengthening methods varies between different types of bridge structures and also between structures of the same type, since object specific conditions need to be taken into account, implying that an investigation for the individual structure is often required.

Steel girder bridges with concrete decks are nowadays designed as composite structures, which has also been the case in the recent decades. However, there are many existing non-composite steel concrete bridges in the Nordic countries and some of them were constructed as late as the 1980s. According to the national Transport Administrations bridge managing systems in Sweden, Finland and Norway, there are more than 2000 existing bridges of this type. If an assessment indicates that the traffic load capacity is too low, in terms of global moment capacity, post-installation of mechanical shear connectors is one possible method to increase the load capacity for this type of bridge (Kwon 2008, Peiris & Harik 2014). Post-installed shear connectors create a shear transfer at the interface between the steel girders and the concrete deck slab, implying that the traffic loads and any subsequent applied dead loads will act on a composite cross-section, which gives a better use of the existing structural parts.

There are many types of shear connectors that can be used in steel-concrete composite bridges (Schaap 2004, Hungerford 2004, Hällmark et al. 2016). Undoubtedly, the most common type of shear connector in new structures is the welded headed stud, for which detailed design criteria are provided by national and international standards, such as EC4-2 (2005) and AASHTO (2017). In new structures, welded headed studs offer an effective installation procedure with the drawn arc stud welding performed in the steel workshop under controlled conditions and with good access to the upper flanges. In an existing structure, this type of installation procedure would require the removal of any pavement, waterproofing and the concrete above the steel upper flanges. Such an installation procedure would often be impractical, if the concrete deck slab is in good condition, since it would require the bridge to be partly or totally closed during the installation. However, there are other types of shear connectors that are more suitable for post-installation, especially connectors that can be installed from below the bridge deck with no or minimized impact on the traffic running on the bridge. A comprehensive study of different type of post-installed shear connectors has been performed at the University of Texas at Austin, by Hungerford (2004), Schaap (2004), Kayir (2006) and Kwon et al. (2009, 2010a, 2010b, 2012), while more recent studies have been performed by Pathriana et al. (2015, 2016a, 2016b) and Henderson et al. (2017). Hällmark et al. (2016) presents a compact review of some of the research performed on post-installed shear connectors such as high tension friction grip

---

*Corresponding author, Ph.D. Student
 E-mail: robert.hallmark@ltu.se

[a]Professor
[b]Ph.D.

bolts, adhesive anchors, mechanical anchors, embedded bolts, threaded shear studs, blind bolts and interference fit connectors.

The Coiled Spring Pin (CSP) is one example of an interference fit connector that is suitable for post installation. The CSP is a standardized product that is manufactured from steel plates that are spirally wound 2.25 times around the central axis of the pin, see Fig. 1.

Fig. 1 Coiled spring pin

The type of CSP that is best suited as shear connectors in bridges is the "Heavy Duty" type, with the highest shear capacity, which is covered by the international standard ISO 8748 (2007). Even though CSP is a standardized product that have been used as fasteners for different applications over many years, there are only a few civil engineering applications that have been found in the literature (Pritchard 1992, Buckby et al. 1997, Fahleson 2005, Olsson 2017). As a post-installed shear connector, the CSPs can be installed from below, like adhesive- and mechanical-anchors, and offer a single-component installation with no adhesives, grouting, welding or tightening. The typical installation procedure, illustrated in Fig. 2, includes the following steps: (1-2) precision-drilling through the steel and the concrete; (3) jacking; and (4) sealing (corrosion protection). The CSPs rely on the radial spring forces that are developed instantly when the pins are press fitted into the holes drilled through the connecting parts, which implies that the connectors can be installed even with traffic on the bridge (Pritchard 1992, Buckby et al. 1997, Olsson 2017).
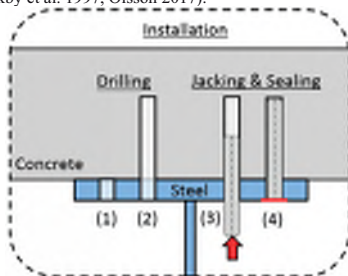

Fig. 2 Schematic illustration of the CSP installation

For types of shear connectors other than headed shear studs EC4-2 (2005) states that "the behaviour assumed in design should be based on tests and supported by a conceptual model". This implies that the design of the shear connection with CSPs has to be based on design models supported by test results. For the use of CSPs in bridge applications, the present authors have identified an information and knowledge gap about the static and fatigue capacity as well as the structural behaviour. So far, the only recommendations available in the literature are those published by Buckby et al. (1997), which are based on project specific tests for a bridge strengthening project in Canada. These recommendations are limited both in terms of concrete strength and in terms of thickness of the steel upper flanges.

If it would be possible to develop more general design criteria and guidelines for the use of CSPs as post-installed shear connectors, the need for future project specific tests could be reduced or eliminated, thereby removing the barriers for bridge designers to use this strengthening technique. In order to progress towards more general design guidelines for CSPs, the present authors have performed static and fatigue push-out tests as well as field monitoring of a bridge strengthened with CSPs. The static tests and the bridge monitoring have been reported in Hällmark et al. (2018a) and Hällmark et al. (2018b), while this paper presents a new fatigue push-out test series of nine specimens, together with an evaluation of all available fatigue tests on CSPs, so far.

2. Fatigue push-out tests

The fatigue strength of shear connectors is generally tested by fatigue tests on standard push-out test specimens. Beam tests can also be used, but this involves several uncertainties that must be investigated or measured to assure that the test result is based on correct assumptions. Roik & Hansville (1990) present some of the difficulties with the interpretation of beam tests results. For instance, the shear forces transferred by the studs must be estimated by strain measurements, which is a rather inexact method. The force acting on a connector will also be dependent on the varying slip along the steel-concrete interface and the modulus of elasticity for the steel and the concrete, where the latter can vary quite a lot. Beam tests are suitable for evaluation of the structural behaviour, such as deflection and redistribution of forces, while properly designed push-out tests are suitable for testing the static and the fatigue strength of the shear connectors, as well as the connector stiffness represented by the load-slip behaviour.

In order to establish the static strength and the ductility of shear connectors Annex B of the European design code for steel-concrete composite structures (EC4-1-1 2004) presents a standard test method and a standard specimen. EC4-1-1 (2004) also states that fatigue test specimens should be prepared in line with Annex B, but no test procedure is presented for the fatigue test. This has led some researchers to modify the test specimen by including a tie or angle at the base of the slabs to prevent the development of unrealistic uplift forces on the shear connectors (Hansville et al. 2007).

For the testing of post-installed shear connectors, especially connectors designed to be installed with access only from below the concrete deck, the standard specimen is
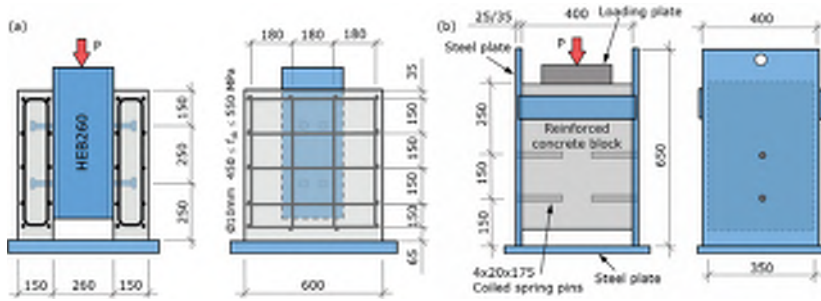
Fig. 3 Test(a) Standard push-out specimen from EC4-1-1, (b) Inverted push-out test specimen [mm]

not suitable since the geometry makes it difficult to perform an installation of the connectors after the manufacturing of the specimen. The limited space between the steel flanges in the HEB260 section, see Fig. 3, implies that the drilling operation cannot easily be performed without enlarging or splitting the steel section. There are several possibilities to modify the push-out test to make it more suitable for testing of post-installed shear connectors. Prior to a previously performed static test series on CSPs, Hällmark et al. (2018a) performed a survey on different types of alternative push-out tests that enable better access for post-installation of shear connectors. One of the most interesting alternatives was a horizontal test set-up that enables post-installation of the connectors from above. Such a test set-up has been used by Schaap (2004), Hungerford (2004), Kayir (2006) and Kwon (2010a). Ernst (2009) and Lam (2007) have also used horizontal specimens in their tests of headed studs, but with a different design that would require an installation from below the specimen, if it were used for testing of post-installed shear connectors. Other interesting alternatives were different types of inverted test set-ups presented and used by Buckby et al. (1997), Pritchard (1992), Fahleson (2005) and Döinghaus (2002) among others. The inverted tests are inverted by the means that the steel and the concrete parts have switched positions, implying that there is a concrete block in the middle surrounded by two steel plates or beams. This makes the drilling and installation of the post-installed connectors easier. The specimen tested by Buckby et al. (1997) is presented in Fig. 3 to illustrate the difference in comparison to the standard specimen from EC4-1-1 (2004). Based on the survey presented in Hällmark et al. (2018a), the authors decided to use an inverted specimen for the recently performed static test series and the fatigue tests presented in this paper. The layout of the specimen is presented in detail in the next section.

When using a non-standardised test specimen, it is of importance that the test set-up is verified and compared to standard tests. Therefore, five reference tests were performed on headed shear studs and the results were compared to test results from standard specimens with the same dimensions of the headed studs and with similar concrete strength. The evaluation indicated that the ultimate capacity and the initial load-slip behaviour is comparable to standard push-out tests

(Hällmark et al. 2018a). It should, however, be noted that the alternative test set-up shows a higher ductility at large plastic slips. The latter should have no influence on the fatigue tests.

Some important factors that are affecting the fatigue lifetime of headed studs are highlighted by Roik & Hansville (1990). From the authors' perspective, it is likely that the majority of the factors are the same for CSPs. The most important factor is the fatigue stress range, which is defined as the difference in shear stresses between the maximum and the minimum shear forces acting within the fatigue load cycle. The magnitude of the peak load within the fatigue load cycle is another parameter that will affect the fatigue lifetime. A high peak load will lead to earlier, and more widely spread, concrete crushing near the root of the shear connectors, which will result in additional bending stresses in the connectors that reduce the fatigue lifetime. The same effects will be obtained if the concrete strength is lowered, resulting in concrete crushing at lower load levels.

2.1 Test specimen

The test specimens used in the fatigue tests presented in this paper are shown in Fig. 4. The geometry of the specimens is similar to a previously performed static test series containing 28 specimens (Hällmark et al. 2018a). In the static test series (Hällmark et al. 2018a), threaded rods (M20) with tension load cells (TLC) were used for the clamping. In the fatigue tests, the same type of clamping method was introduced but with threaded rods (M20) without TLCs. In the static tests, the TLCs were used to verify the clamping force and the behaviour of the test set-up. The results showed that the relationship between the clamping force and the vertically applied load was increasing during the tests. However, the total clamping force never exceeded 8% of the applied load (even in the ultimate state), and varied between 1-2% at load levels corresponding to those used in the fatigue tests presented in this paper. A clamping force of this size would be in the same order of magnitude as the positive contribution from the weight of the concrete deck in a bridge structure and should not cause unconservative results. Prior to the static tests, the nuts on the clamping rods were tightened in order to achieve ~1 kN/rod. In the fatigue tests, the nuts were tightened with a similar torque, even

though there were no load cells confirming the resulting clamping force.

Two different shear connector locations were tested. In six out of nine tests, the four CSPs were located at two different heights within the specimens in line with the previously performed static tests, see Type F1 in Fig. 4a. The three remaining tests were performed on specimens in which the four shear connectors were all positioned at the same height, see Type F2 in Fig. 4b.

The manufacturing of the concrete parts of the specimens was not done in line with all the recommendations for the push-out tests given in EC4-1-1 (2004). As highlighted by Roik & Hanswille (1990), the concrete quality at the root of the shear connectors will be important for the fatigue test results. To avoid small air pockets or other deficiencies in the concrete around the connectors, the concrete parts of the test specimens should be cast horizontally, to simulate the real and more favorable situation in a normal composite beam (Akao et al. 1982). For the alternative type of specimen presented in this paper, the concrete block has two sides with shear connectors, which implies that there are no upper or lower sides. Consequently, the specimens could not be cast in a horizontal position with a distinct upper and lower side like in a real composite beam. The concrete blocks in the tested specimens were instead cast standing vertically, contrary to the recommendations presented above. This recommendation is however believed to be less important when push-out specimens for post-installed shear connectors are cast, since the connectors will be installed afterwards in holes drilled into the cured concrete.

Before casting, form oil was applied to the steel plates to reduce the friction at the steel-concrete interface. At a concrete age of 7 days or more, holes were drilled for the installation of the CPSs. The drilling was done with a cutting drill through the outer steel plates, followed by diamond core drilling into the concrete. The drills had undersized diameters, 19.90 mm, compared to the diameter of the CSPs, 20.40-21.00 mm. The hole tolerance was set to 19.85-20.25 mm, with an additional requirement of a relative difference between the steel and the concrete parts less than 0.10 mm. Before the CSPs were installed in the holes, the hole diameters were measured both in the steel and the concrete parts. The measurements showed that all holes were within the tolerances, with the majority of the holes in the upper half of the tolerance interval.

The installation of the CSPs was performed using a hydraulic jack, which registered the force needed to press fit the pin into the hole. All pins were lubricated with grease prior to the installation and the installation force varied between 46-144 kN.

2.2 Testing procedure

The fatigue testing was performed with a hydraulic jack with a capacity of 600 kN, which applied a unidirectional force-controlled load, varying between the predetermined load levels. All tests started with an initial frequency of 1 Hz, to ensure that the specimen was stable within the testing rig. After some thousands of cycles, the frequency was increased up to the desired frequency of 4 Hz.
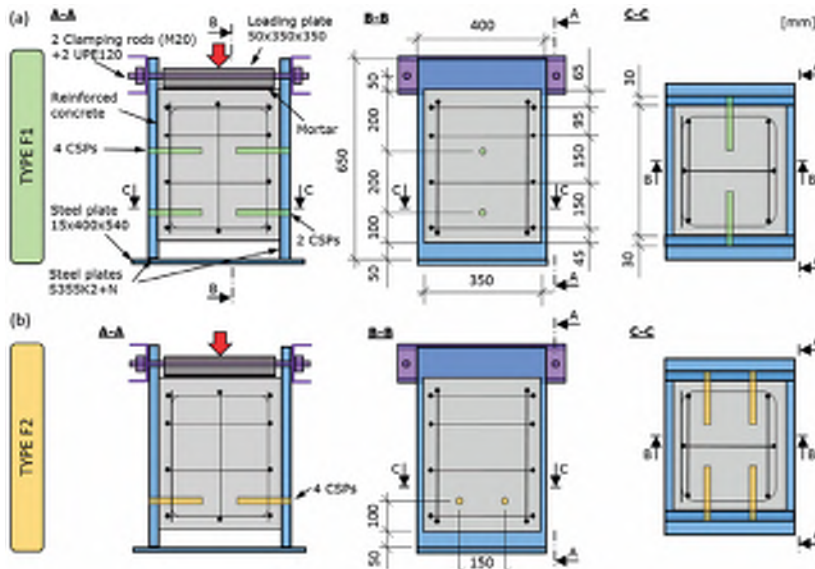

Fig. 4 Fatigue test specimens, (a) Type F1 and (b) Type F2

The testing procedure, schematically illustrated in Fig. 5, started with an initial loading (P_{ini}) up to 0-22.5 kN/CSP above the maximum load in the fatigue load cycle ($P_{max,f}$). This overload was used in order to break the bond between the steel and the concrete and to simulate the impact of loads higher than the fatigue loads. After the initial loading, the fatigue load cycling was started with the load range ΔP_f. The minimum load in the fatigue load cycle ($P_{min,f}$) was kept constant at 5 kN/CSP in all tests, while different $P_{max,f}$ where tested within the interval of 35-55 kN/CSP. This gives an R-ratio ($P_{min,f}/P_{max,f}$) between 0.09-0.14.
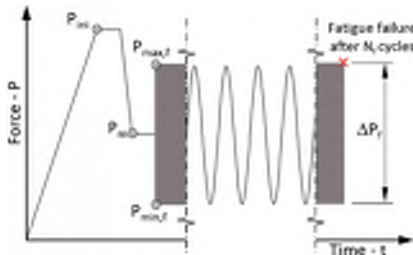

Fig. 5 Schematic illustration of the loading procedure

The applied force and the stroke were registered directly from the hydraulic jack, throughout the tests. In addition to this, eight Linear Variable Differential Transformers (LVDT) were used to measure the vertical slip at the steel-concrete interface and the corresponding horizontal separation. The four LVDTs measuring the vertical movements were placed on each vertical side of the test specimen in a position between the shear connectors. The corresponding horizontal displacements were registered by four additional sensors, mounted horizontally close to the position of the vertical LVDTs. These sensors were activated in the beginning of all tests to measure the slip in comparison to the measured stroke. When the behaviour of the specimens had been stabilized for some thousands of cycles, the LVDTs were locked in their inner extreme position, implying that the cyclic movements did not respond in any movement in the LVDTs. The LVDTs were released with varying intervals, in order to measure the slip and compare it against the registered the stroke. When the slip started to increase more rapidly, the LVDTs were activated in order to measure the final failure. This procedure was undertaken to avoid fatigue damage to the LVDTs.

2.3 Material parameters and tolerances

The fatigue test specimens were manufactured together with the static test specimens used in the tests presented in (Hällmark et al. 2018a). This implied that the steel parts with the same thickness came from the same steel batch, for both the static and the fatigue specimens. Also the tested coiled spring pins and the reinforcement bars were all from same batch. The material tests presented below are therefore valid both for the static and the fatigue specimens.

The steel parts of the fatigue test specimens were manufactured from plates in grade S355K2+N (see Fig. 4). Tensile tests performed by the steel manufacturer show a yield strength of 408 MPa and a tensile strength of 511 MPa. The elastic modulus has not been reported from the tensile tests performed by the steel manufacturer and no additional tests have been performed.

The tested CSPs were of standard type ISO 8748 – 20 x 160 – HWK. The letters indicate that the pin is of type Heavy Duty (H) and made out of AISI 6150 Alloy Steel (W) with no surface treatment (K), while the digits represent the nominal outer diameter of 20 mm and the length of 160 mm, see Fig. 6. The thickness of the steel plates used to manufacture this type of pin are 2.2 mm, in line with the product standard ISO 8748 (2007). Four test coupons were taken from the pins and tensile tests were performed in line with ISO 6892-1 (2016). The mean value of the tested yield stress and the tensile strength were 1516 MPa and 1606 MPa, respectively with no test result deviating more than 3% from the mean value. However, the test results deviate significantly from the yield stress and tensile strength of the pin base material before cold forming and heat treatment (550 MPa and 690 MPa, respectively), provided by the manufacturer of the CSPs.
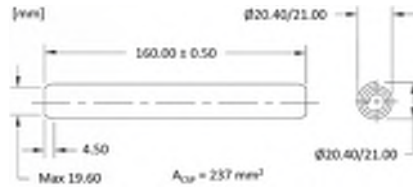

Fig. 6 Dimensions of the tested CSP

The reinforcement consisted of Ø10 mm standard deformed bars, K500C-T, which is in line with recommendations for the standard test specimen in EC4-1-1 (2004). The mean value of the tested yield stress and the tensile strength were 533 MPa and 649 MPa, respectively.

For each concrete batch, cube compression tests were performed after 28 days of curing, together with at the beginning and at the end of each fatigue test. All fatigue tests were performed on specimens with an age of more than 28 days, up to 12 month, which implies that the age effect between the specimens was not that big.

The results from the concrete cube strength tests are summarized in Table 1, where $f_{cm,cube}$ is the mean strength of the cube tests performed at the beginning and at the end of each fatigue test. The mean values of the elastic modulus, E_{cm}, have been calculated according to (1) from EC2-1-1 (2005), where f_{cm} is the compressive cylinder strength given in MPa. The concrete cube strength has been transformed into the cylinder strength by multiplying with factor 0.8.

$$E_{cm} = 22 \cdot (f_{cm}/10)^{0.3} \qquad (1)$$

Table 1 Fatigue and concrete test results

Specimen		Concrete	$f_{cm,cube}$ [MPa]	E_{cm} [GPa]	P_{ini} [kN]	$P_{max,f}$ [kN]	$P_{min,f}$ [kN]	ΔP_f [kN]	R [-]	$P_{max,f}/P_u$ [-]	N_f [10^6]
Type F1	F1:1	C30/37	48.5 Max: 49.6 Min: 46.3	33.0	50	50	5	45	0.10	0.38	0.086
	F1:2				62.5	55	5	50	0.09	0.42	0.066
	F1:3				62.5	40	5	35	0.13	0.31	0.367
	F1:4				62.5	40	5	35	0.13	0.31	0.267
	F1:5				50	40	5	35	0.13	0.31	0.306
	F1:6				50	40	5	35	0.13	0.31	0.447
Type F2	F2:1	C30/37	59.4 Max: 61.1 Min: 57.6	35.1	45	35	5	30	0.14	0.27	2.813
	F2:2				50	40	5	35	0.13	0.31	0.438
	F2:3				45	35	5	30	0.14	0.27	0.760

3. Test results

The fatigue tests were run until there was an observed fatigue failure, at N_f load cycles, in at least one of the connectors. The fatigue test results are summarized in Table 1, together with the concrete test results and detailed information about the applied load cycle.

After the testing was completed, the steel plates were separated from the concrete block in order to visually inspect the failure of the CSPs. In contrast to headed shear studs, there was not a single distinct crack surface that could be inspected after the tests. The failed CSPs have in many cases separated into small pieces, which made it hard to identify the initiation of the fatigue crack and the propagation direction. It should be noted that some cracks and damage might have been caused by the removal of the external steel plates after the tests were complete, or by the last load cycles before the displacement limits were reached and the tests automatically stopped. The typical fatigue failure of CSPs seems to occur at a section a few millimeters into the steel plate, even though some of the CSPs had a second failure a few centimeters into the concrete, after concrete crushing and large deformation. The latter is expected to be a secondary static failure mode, occurring after the fatigue failure, since the fatigue stresses are expected to be lower in this section. Figure 7 shows some representative examples of the observed shear failure. The corrosion, visible in some of the pictures, occurred during storage of the already tested specimens, before they were opened up and photographed, and has not affected the test results.

In seven out of nine fatigue tests, failure occurred on only one side of the specimen. On the other side, the CSPs seemed to be unaffected by the fatigue loading, whereas some minor concrete crushing could be observed above the pins and small local plastic deformations at the hole edges, see Fig. 8. In two of the nine tests, F1:1 and F1:5, failure was observed on both sides of the specimen. In these cases, fatigue cracks seem to have been developed on both sides of the specimen. The tests were terminated when the CSPs on one side failed, while the final fracture on the other side occurred during the removal of the steel plate from the concrete block.

In line with observations made on previously performed static push-out tests, the end of the CSPs starts to move out from the steel plate after failure has occurred. The movements have magnitudes of a few millimeters and can easily be observed without any inspection or measurement equipment.
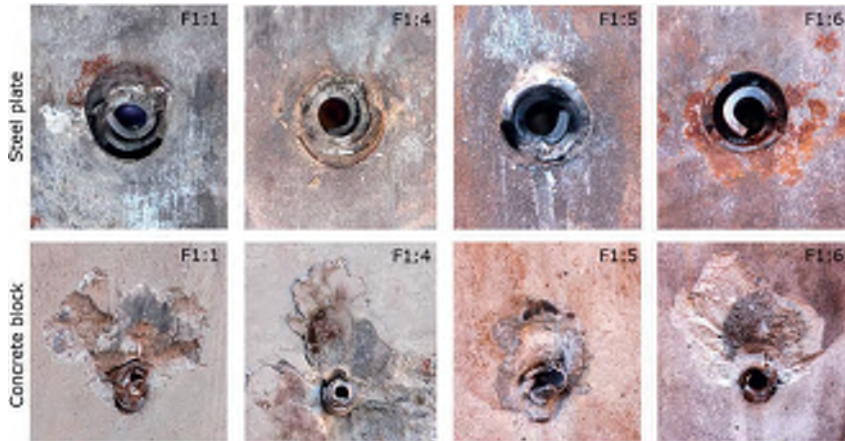
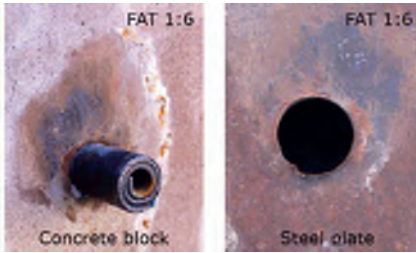

Fig. 7 Examples of CSP fatigue failures

Fig. 8 Examples of a CSP that did not fail in the tests

3.1 P-N relationship

Generally, the fatigue strength of shear connectors is given in terms of shear stress range. For welded headed studs, the calculation of the nominal shear area is a straightforward procedure only dependent on the diameter of the stud shank. In contrast, the manufacturers of CSPs only generally provide the outside diameter in their product documentation, while the thickness can be found in the product standard ISO 8748 (2007), but not the shear area. The determination of the CSP shear area is complex, due to the clotoidal cross-sectional geometry, and makes transforming the shear forces into shear stresses more difficult. From a bridge designer's perspective, the fatigue capacity of CSPs will be more directly applicable if it is considered in terms of load range (ΔP) on a P-N curve instead of stress range ($\Delta \tau$) on an S-N curve.

For the nine fatigue tests, the P-N relationship is plotted on a double logarithmic scale in Fig. 9. The test results have been separated according to the two types of test specimen. From this limited number of tests, no significant differences can be observed between the two types of test specimen. In the remainder of this paper, the Type F1 and F2 specimens will be presented and evaluated together as one test series.

3.2 δ-N relationship

To illustrate how the permanent slips, δ, were accumulated during the tests, the registered slips have been plotted against the number of load cycles in Fig. 10. The

plotted slip corresponds to the mean value of the measured slips registered by the four LDVT-sensors, when these were active. Between the intermittent slip measurements, the change of the continuously registered stroke has been used to fill out the gaps in the diagram and make the curve continuous.
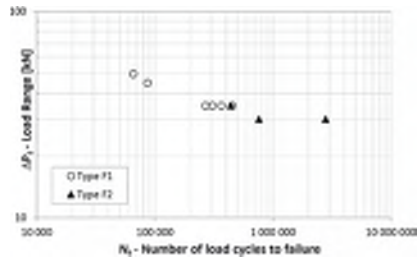

Fig. 9 Fatigue test results illustrated as a P-N relationship

4. Analysis

The presented test results from the present investigation have been evaluated statistically, by a linear regression analysis, with the aim to develop a suitable design criterion for fatigue design of CSPs. Previously performed fatigue tests on CSPs (Pritchard 1992, Buckby et al. 1997, Fahleson 2005, Hällmark et al. 2016) are also presented and taken into account in the evaluation. It should however be noted that test results from specimens with steel plate thickness less than 15 mm have been excluded from this evaluation.

In contradiction to the design of shear studs, the authors have chosen to present the fatigue strength in terms of forces (P) instead of shear stresses (τ). This implies that the analysis presented in this paper is only valid for Heavy-duty CSPs with a nominal diameter of 20 mm and produced in line with ISO 8748 (2007). However, this type of CSP has been used in all bridge strengthening projects and research studies presented so far (Pritchard 1992, Buckby et al. 1997, Fahleson 2005, Hällmark et al. 2016) and are the most likely one to be used in future civil engineering applications, since it is the strongest CSP among the standardized types and dimensions.
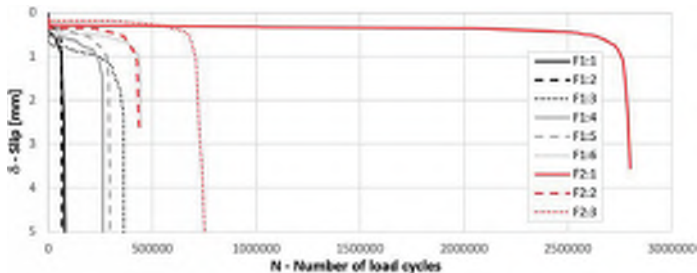

Fig. 10 Permanent slip accumulated during the tests

Table 2 Results from the linear regression analysis

Parameters:	Equations:	(a) New tests	(b) All tests
Number of tests (n)	N	9	31
Mean value of log P	$\overline{\log \Delta P} = \dfrac{\sum \log \Delta P_i}{n}$	1.56	1.57
Variance of log ΔP	$Var(\log \Delta P) = \dfrac{\sum\left(\log \Delta P_i - \overline{\log \Delta P}\right)^2}{n-1}$	0.00537	0.01037
Mean value of log N	$\overline{\log N} = \dfrac{\sum \log N_i}{n}$	5.54	5.95
Variance of log N	$Var(\log N) = \dfrac{\sum\left(\log N_i - \overline{\log N}\right)^2}{n-1}$	0.234	0.448
Covariance of log ΔP and log N	$Cov(\log \Delta P, \log N) = \dfrac{\sum\left(\log N_i - \overline{\log N}\right)\left(\log \Delta P_i - \overline{\log \Delta P}\right)}{n-1}$	-0.033	-0.052
Coefficient of determination (R^2)	$R^2 = \dfrac{Cov(\log \Delta P, \log N)^2}{Var(\log \Delta P)\cdot Var(\log N)}$	0.851	0.585
Slope (m)	$m = \dfrac{Cov(\log \Delta P, \log N)}{Var(\log \Delta P)}$	-6.086	-5.028
log N -Inters. (log a)	$\log a = \overline{\log N} - m\cdot \overline{\log \Delta P}$	15.02	13.84

4.1 Linear regression

The test results presented in Fig. 9 and the fatigue strength curves in EC3-1-9 (2005) are all presented using a double logarithmic scale. The evaluation of the test results is based on the assumption that there is a linear relationship in this double logarithmic scale, i.e. there is a linear relationship between the log P (or log S) and the log N as described in equation (2):

$$\log N_i = \log a + m \cdot \log \Delta P_i \qquad (2)$$

where m is the slope and log a is the intercept of the log N-axis. A linear regression analysis, based on the least square method, has been performed on two groups of test results: (a) the new test results presented in this paper; and (b) the new test results combined with previous tests performed by other researchers. Table 2 presents the detailed results from the linear regression analysis, while Fig. 11 illustrates the

analyzed fatigue strength test results and the two solid regression lines.

For the new test series (a), the coefficient of determination, R^2, indicates that there is a good agreement between the linear regression line and the test results, since 85% of the variance of log N can be explained by log P. Good agreement is also obtained if the two other larger test series are analysed separately, with R^2 equal to 89% for the Tinsley tests and 84% for the tests presented by Buckby et al. (1997). However, if all available fatigue test results are included in the analysis, group (b) presented above, the agreement is not so good with R^2 equal to 59%. There are several factors that can explain why the linear regression lines gives a better agreement on a single test series rather than all test series analysed as one sample, for instance different types of test specimens, varying material parameters and dimensions. There are, however, two other factors that the authors would like to highlight.
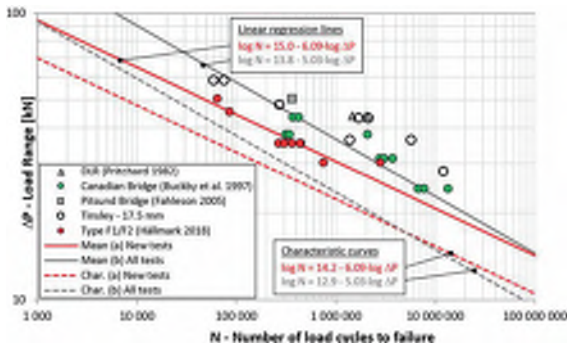

Fig. 11 Fatigue strength test results with their associated regression lines and characteristic curves

Table 3 Parameters used to establish the characteristic curves

Parameters:	Equations:	(a) New tests	(b) All tests
Number of tests	N	9	31
Student´s t-score	t(0.05) for n-2 degrees of freedom	1.895	1.699
Standard deviation for log N	$\sigma_{\log N} = \sqrt{\dfrac{n}{n-2}(1-R^2)\cdot Var(\log N)}$	0.212	0.446
Force at N_c [kN]	$P_c = 10^{(\log 2\cdot 10^6 - \log a)/m}$	27.1	31.6
Correction factor f for $\hat{\sigma}$ at N_c	$f = 1 + \dfrac{1}{n} + \dfrac{(\log \Delta P_c - \overline{\log \Delta P})^2}{Var\,(\log \Delta P)}$	4.029	1.507
Characteristic log $\Delta P_{c,k}$	$\log \Delta P_{c,k} = \log \Delta P_c + \dfrac{t(0.05)\cdot \sigma_{\log N}\cdot \sqrt{f}}{m}$	1.301	1.315
Characteristic $\Delta P_{c,k}$ [kN]	$\Delta P_{c,k} = 10^{\log \Delta P_{c,k}}$	20.0	20.6
Characteristic log a_k	$\log a_k = \log N_c - m\cdot \log \Delta P_{c,k}$	14.2	12.9
Characteristic $\Delta \tau_{c,k}$ [MPa]	$\Delta \tau_{c,k} = \Delta P_{c,k}/A_{CSP}$	84.4	87.1

Firstly, there are differences in the definition of the fatigue failure between the different researchers that have performed the fatigue tests presented in Fig.9. This is partly a consequence of the fact that different researchers have had different purposes with their tests. Some have evaluated the fatigue capacity of the CSPs with the purpose to strengthen an already existing shear connection (Pritchard 1992, Buckby et al. 1997), implying that the stiffness of the existing shear connectors needs to be taken into account. Buckby et al. (1997) handled this by using a restriction of the permanent slip of 2 mm, giving the strictest fatigue failure definition so far. Another approach was used by the authors of this paper, as well as Pritchard (1992) and Fahleson (2005), who considered the fatigue failure to occur when the first CSP failed under the fatigue load. A combination of these two approaches was used in the Tinsley strengthening project, where the fatigue failure was considered to occur when the first CSP failed, or when the permanent slip reached 5 mm. Figure 9 contains results from both types of failures for the Tinsley project. If the fatigue failure in the tests by Buckby et al. (1997) instead was considered to occur when the first pin failed or when the permanent slip reached 5 mm, these results would be shifted a bit to the right in Fig. 9. The authors do not have access to the fatigue load-slip curves from all previously performed tests, but the single load-slip curve presented in the paper by Buckby et al. (1997), indicates that the final failure occurred at 1.4 times the number of cycles when the permanent slip passed 2.0 mm. This could possibly imply that the test results by Buckby et al. (1997) would fit even better to the other test results if a similar fatigue definition had been used, with the exception of the recent tests by the authors that would deviate even more from the other test series.

Secondly, the testing procedure for the tests performed by the authors, presented in section 2.2, deviates from the other test series in that an initial static overload was used. The purpose of the overload, which was up to 50% higher than the maximum load in the fatigue cycle, was to break the bond between the steel and the concrete prior to the fatigue testing and to simulate the impact of loads greater than the fatigue loads, which are expected to occur in a real structure. However, this overload is expected to cause an additional concrete crushing near the root of the CSP, at the steel-concrete interface, leading to an increased slip in the fatigue tests in comparison to a test without the overload. Since the CSPs act as a dowel, an increased slip implies that the bending of the CSP will be increased, as well as the fatigue stress range, resulting in an earlier fatigue failure. The magnitude of the increased stress range cannot be evaluated from the test results, but will be investigate further in future FE-modelling of the tests.

A combination of different types of test specimens, different definitions of fatigue failure and the use of initial loading in the recent tests, implies that the test results are not directly comparable to each other. As a consequence of this, a statistical evaluation based on all available test results, group (b), should not be given too much attention.

4.2 Characteristic curve

The characteristic fatigue curves in EC3-1-9 (2005) represent 95% probability of survival, which correspond to the lower 5% fractile of the tested fatigue strength. The characteristic capacity can be written based on the linear form presented in equation (2), using the formulas in equation (3) and (4) presented by Schneider & Maddox (2003),

$$\log N_{c,k} = (\log a + m\log \Delta P) - t_{5\%}\hat{\sigma}\sqrt{f} \qquad (3)$$

$$f = 1 + \frac{1}{n} + \frac{(\log \Delta P_c - \overline{\log \Delta P})^2}{\sum_{i=1}^{n}(\log \Delta P_i - \overline{\log \Delta P})^2} \qquad (4)$$

where $\overline{\log \Delta P}$ is the mean value of the n values of log ΔP_i, $t_{5\%}$ is the t-score for a one sided 95% confidence interval in the Student´s t-distribution with n_f degrees of freedom and $\hat{\sigma}$ is the standard deviation of the regression line described in the previous section. The degrees of freedom, n_f, is in this case equal to n-2, since there are two coefficients in the regression line (m and log ΔP) that have to be estimated. In line with EC3-1-9 (2005), the characteristic fatigue strength is presented at two million cycles ($N_c = 2 \cdot 10^6$). Table 3 presents the values on the ingoing parameters in equation (3) for the two groups of test results. The characteristic curves for each group are plotted in Fig. 11 as dashed lines.

From Table 3, it can be noted that the correction factor (f) at two million cycles is quite high for the new test series (a). This is mainly due to the fact that the mean value of the tested load ranges deviates more from the predicted load range at two million cycles, in comparison to the other tests series. It is expected that additional tests at lower stress ranges would reduce this correction factor significantly.

In order to make a comparison against the detail category for automatically welded headed studs, the cross-sectional area of the CSPs (A_{CSP}) have been used to transfer the characteristic fatigue strength from force range ($\Delta P_{c,k}$) into stress range ($\Delta \tau_{c,k}$). The stress ranges, presented in Table 3 for group (a) and (b) are 84 MPa and 87 MPa, respectively. These values can be directly compared to the detail category, 90 MPa, of welded headed studs. Test series (a) and (b) indicate that CSPs have a slightly lower detail category than headed studs (90 MPa). However, a similar analysis performed on the tests presented by Buckby et al. (1997) indicates a detail category that is significantly higher than headed studs.

Based on the new test results, group (a), a recommended characteristic fatigue strength curve is presented in equation (5) and rewritten in (6) using the equation format adopted in EC3-1-1 (2005),

$$\log N = 14.2 - 6.09 \cdot \log \Delta P \quad (5)$$

$$\Delta \tau_R^{6.09} N_R = 84.4^{6.09} \cdot 2 \cdot 10^6 \text{ (from } \Delta \tau_R^m N_R = \Delta \tau_c^m N_c) \quad (6)$$

where $\Delta \tau_R$ is the fatigue shear strength (in MPa) of the Ø20 mm CSP, using the nominal area of 237 mm^2, $\Delta \tau_c$ is the reference value at $N_c = 2 \cdot 10^6$ cycles for CSPs (i.e. the detail category), m is the slope of the fatigue strength curve and N_R is the number of stress cycles.

On considering Fig.9, it might be argued whether the results from test F2:1 should be included in the analysis, due its deviation from the other tests; in particular, the identical test F2:3. However, its exclusion would result in only a minor change to the characteristic fatigue load capacity at 2 million cycles, $\Delta P_{c,k}$, with R^2 increasing to 95% and the slope of the curve changing to m = 5.0. As a consequence of this, the authors have chosen to include this test in the present analysis.

To illustrate the differences between the fatigue strength curve for CSPs compared with headed studs, equation (6) is plotted in Fig. 12 together with the EC4-2 (2005) fatigue design criterion for headed studs and the previously presented fatigue design criteria for CSPs by Buckby et al. (1997), see equation (7).

$$\log N = 14.767 - 6.1 \cdot \log \Delta P \quad (7)$$

5. Discussion and conclusions

The research presented in this paper shows that there are large variations in the test results between different fatigue test series performed on CSPs. However, tests within the same test series shows good agreement to the linear regression lines, with R^2 between 84-89%. The authors have identified several possible reasons for these large variations such as different types of test specimens and dimension, varying material parameters, different definitions of when fatigue failure is deemed to have occurred and the use of an initial overload or not.

The different types of specimens used in the fatigue tests so far have had different layouts and different degrees of clamping, provided by threaded rods or welded steel strips. For future tests, it would be beneficial if one standardized type of specimen could be used, to remove the uncertainties
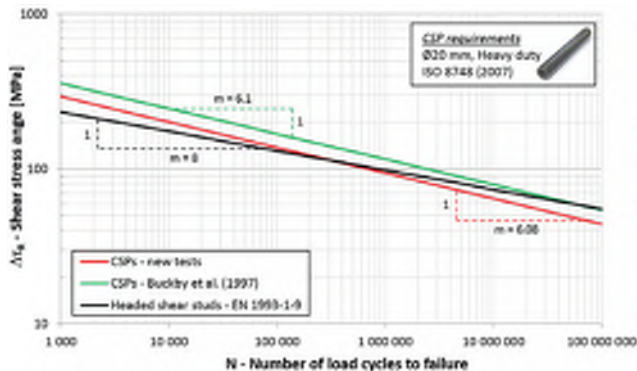

Fig. 12 Fatigue strength curves for CSPs and headed studs

about the different degrees of clamping and the varying eccentricities between the load position and the support points. The latter results in a bending moment that has to be transferred over the steel-concrete interface, either by the shear connectors or by the clamping devices. The authors suggests that the next test series is performed on specimens that are similar to the standard push-out specimen in EC4-1-1 (2005), but with welded H-sections in the middle, to be able to test relevant steel flange thicknesses. In order to enable the installation of CSPs the steel beam needs to be manufactured, or cut, in two halves and welded together after the installation of CSPs. Such a change would result in some additional work with the specimens, but is nothing exceptional since a similar manufacturing process has been used for push-out specimens with headed studs (Hanswille et al. 2007)

The different definitions of the fatigue failure, between the different test series, makes it difficult to use all available test results in the development of a fatigue design criterion. If the CSPs are installed in a structure in order to create composite action, not to strengthen an already existing connection, the authors suggest that the failure is defined as when the first CSP fails, or when the mean slip reaches 5 mm. For the tests presented in this paper, the latter criterion gives at most a few percentages shorter fatigue lifetime than the former criterion.

The recent tests by the present authors deviate most from the other test series, and this deviation cannot be explained by a different fatigue definition or different material parameters. The type of specimen is also similar, in some cases almost identical, to those used by Pritchard (1997), Buckby et al. (1997) and Fahleson (2005). There are some difference in how the vertical steel plates were connected to each other, to avoid separation at the steel-concrete interface. In the recent tests, threaded rods without pre-tensioning were used, while welded steel strips were used in previous tests. In a static push-out test, the stiffer steel strips might provide a higher degree of confinement for the central concrete block at large slips, when there are forces that want to separate the steel and the concrete part. However, this should not affect the fatigue test results substantially, since the slips are small and there are no signs of horizontal separation during the tests, in contrast to the visible separation in the static tests. Instead, the initial overload prior to the start of the fatigue tests could be the reason for the difference in the fatigue test results. Future FE-modelling and research might be able to give an estimation of the impact of the initial overload and to evaluate if the CSPs fatigue strength are more dependent on overloads than headed studs.

Based on the tests presented in this paper it is recommended that the characteristic fatigue strength curve presented in equation (5) is used for the fatigue design of the shear connection in a bridge strengthened with CSPs. This is a conservative design recommendation compared to the previous recommendation by Buckby et al. (1997). Future research, containing additional tests and FE-models of the tests presented in this paper, might provide additional information about the CSP fatigue strength, which makes it possible to develop the fatigue design criterion further.

References

AASHTO. (2017), AASHTO LRFD bridge design specifications, 8th edition, Washington D.C., USA.

Akao, S., Kurita, A. and Hiragi, H. (1982), "Concrete placing methods and fatigue of shear studs", International Assoc. for Bridge and Structural Engineering, IABSE Reports Volume 37, pp. 617-624.

Buckby, R., Ogle, M., Johnson, R. P., and Harvey, D. (1997), "The performance of coiled spring pin connectors under static and fatigue loading". *Proceedings of the International IABSE Conference: Composite construction - conventional and innovative,* Innsbruck, Austria, September.

Döinghaus, P. (2002), "Zum Zusammenwirken hochfester Baustoffe in Verbundträgern", Ph.D. Thesis, RWTH Aachen, Germany. (in German)

EC2-1-1 (2005), EN 1992-1-1 Eurocode 2- Design of concrete structures – Part 1-1: General rules and rules for buildings, European Committee for Standardisation; Brussels. Belgium.

EC3-1-9 (2005), EN 1993-1-9 Eurocode 3 - Design of steel structures – Part 1-9: Fatigue, European Committee for Standardisation; Brussels. Belgium.

EC4-1-1 (2004), EN 1991-1-1 Eurocode 4 - Design of composite steel and concrete structures – Part 1-1: General rules and rules for buildings, European Committee for Standardisation; Brussels. Belgium

EC4-2 (2005), EN 1994-2 Eurocode 4 - Design of composite steel and concrete structures – Part 2: General rules and rules for bridges, European Committee for Standardisation; Brussels. Belgium

Ernst, S., Bridge, R. Q., and Wheeler, A. (2009). "Push-out tests and a new approach for the design of secondary composite beam shear connections". *Journal of Constructional Steel Research*, **65**(1), 44-53.

Fahleson, C. (2005), "Laboratory report: Testing of shear connectors", Laboratory Report No: 05035, Luleå University of Technology, Luleå, Sweden.2

Hanswille, G., Porsch, M. and Ustundag, C. (2007). "Resistance of headed studs subjected to fatigue loading: Part I: Experimental study". *Journal of constructional steel research*, **63**(4), 475-484.

Henderson, I. E. J., Zhu, X. Q., Uy, B., and Mirza, O. (2017). "Dynamic behaviour of steel-concrete composite beams retrofitted with various bolted shear connectors". *Engineering Structures*, *131*, 115-135.

Hungerford, B. E. (2004), "Methods to develop composite action in non-composite bridge floor systems: Part II", M.Sc. Thesis, The University of Texas at Austin, USA.

Hällmark, R., Jackson, P. and Collin, P. (2016), "Post-installed shear connectors–coiled spring pins". *Proceedings of the 19th IABSE Congress*, Stockholm, Sweden, September.

Hällmark, R. Collin, P. & Hicks, S. J. (2018a). "Post installed shear connectors: Push-out tests of coiled spring pins vs. headed shear studs", submitted to Steel and Composite Structures (May 2018, paper ID SCS85549X)

Hällmark, R. & Collin (2018b). "Post-Installed Shear Connectors: Monitoring of a Bridge Strengthened with Coiled Spring Pins", accepted for publication in Structural Engineering International 4/2018.

ISO 6892-1 (2016), Metallic materials – Tensile testing – Part 1: Method of test at room temperature, ISO – the International Organization for Standardization; Geneva. Switzerland.

ISO 8748 (2007), Spring-type straight pins – Coiled. heavy duty. ISO – the International Organization for Standardization; Geneva. Switzerland.

Kayir, H. (2006), "Methods to develop composite action in non-composite bridge floor systems: Fatigue behavior of post-installed shear connectors"*, M.Sc. Thesis, The University of Texas at Austin, USA

Kwon, G., Engelhardt, M. D., and Klingner, R. E. (2009), "Strengthening bridges by developing composite action in existing non-composite bridge girders", *Structural Engineering International*, **19**(4), 432-437.

Kwon, G., Engelhardt, M. D., & Klingner, R. E. (2010a). "Behavior of post-installed shear connectors under static and fatigue loading". *Journal of Constructional Steel Research*, **66**(4), 532-541.

Kwon, G., Engelhardt, M. D., & Klingner, R. E. (2010b). "Experimental behavior of bridge beams retrofitted with postinstalled shear connectors". *Journal of Bridge Engineering*, **16**(4), 536-545.

Kwon, G., Engelhardt, M. D., & Klingner, R. E. (2012). "Parametric studies and preliminary design recommendations on the use of postinstalled shear connectors for strengthening noncomposite steel bridges." *Journal of Bridge Engineering*, **17**(2), 310-317.

Lam, D. (2007), "Capacities of headed stud shear connectors in composite steel beams with precast hollowcore slabs", *Journal of Constructional Steel Research*, **63**, 1160-1174.

Olsson, D. (2017), "Achieving Composite Action in Existing Bridges: With post-installed shear connectors", Master Thesis, Luleå University of Technology, Sweden.

Pathirana, S. W., Uy, B., Mirza, O., & Zhu, X. (2015). "Strengthening of existing composite steel-concrete beams utilising bolted shear connectors and welded studs". *Journal of constructional steel research*, *114*, 417-430.

Pathirana, S. W., Uy, B., Mirza, O., & Zhu, X. (2016a). "Flexural behaviour of composite steel–concrete beams utilising blind bolt shear connectors". *Engineering Structures*, *114*, 181-194.

Pathirana, S. W., Uy, B., Mirza, O., & Zhu, X. (2016b). "Bolted and welded connectors for the rehabilitation of composite beams". *Journal of Constructional Steel Research*, *125*, 61-73.

Peiris, A. and Harik, I. (2014), "Steel bridge girder strengthening using postinstalled shear connectors and UHM CFRP laminates", J*ournal of Performance of Constructed Facilities*, **29**(5).

Pritchard, B. (1992), *Bridge Design for Economy and Durability: Concepts for New, Strengthened and Replacement Bridges*. Thomas Telford, London, UK.

Roik, K. and Hanswille, G. (1990), "Harmonization of the European Construction Codes – Background Report on EUROCODE 4 – Limit state of fatigue for headed studs", Research Report No: EC4/11/90, Bochum, Germany.

Schaap, B. A. (2004), "Methods to develop composite action in non-composite bridge floor systems: Part I"*, M.Sc. Thesis, The University of Texas at Austin, USA

Schneider, C. R. A. and Maddox, S. J. (2003), "Best practice guide on statistical analysis of fatigue data", International Institute of Welding Doc. IIW-XIII-WG1-114-03.

ABOUT THE AUTHOR

Robert Hällmark was born on October 5, 1981, in Kalix in the northern part of Sweden.

He received his master degree in Civil Engineering at LTU in 2006, with a master thesis about low-cycle fatigue of steel piles in integral abutment bridges, as a part of the RFCS-project INTAB. He has ever since been working with composite steel-concrete bridges and steel structures. The first seven years as a bridge designer at Ramboll and the last five years as a steel bridge specialist at the Swedish Transport Administration (Trafikverket). Parallel to these works, Robert has been conducting part-time Ph.D. studies at LTU.

During the Ph.D. studies, Robert has taken part in two European R&D projects. First, in 2008-2011, as Ramboll's representative in the RFCS-project ELEM, about prefabricated steel-composite bridge. Later, in 2015-2018, as a LTU representative and work package leader in the RFCS-project PROLIFE, about prolonging the lifetime of existing steel- and steel-concrete-bridges. Based on the research performed within the ELEM-project, Robert received a Tech. Licentiate degree in 2012. Robert's research has been recognized and has over the years resulted in some awards, among which these are found: *the best Swedish Master Thesis of the year, within the field of Steel Construction (2006), Vattenfall Award for the best Licentiate Thesis of the year at LTU (2013), IABSE Young Engineer Award (2016).*